Investigating the contributions to cell function of the different Swi-Snf complex subunits in *Saccharomyces cerevisiae*

A dissertation presented for the degree of Doctor of Philosophy,

in the Faculty of Science, Trinity College Dublin

By

Hadel Mosfer Aljaeed

2024

The Moyne Institute of Preventive Medicine

Department of Microbiology

School of Genetics and Microbiology

Trinity College Dublin

Declaration

I declare that this thesis has not been submitted as an exercise for a degree at this or any other university and it is entirely my own work, except where it is duly acknowledged in the text.

I agree to deposit this thesis in the University's open-access institutional repository or allow the library to do so on my behalf, subject to Irish Copyright Legislation and Trinity College Library conditions of use and acknowledgement.

I consent to the examiner retaining a copy of the thesis beyond the examining period.

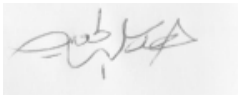

Hadel Aljaeed

Summary

The eukaryotic genome is packaged as a DNA-protein structure known as chromatin. The basic subunit of chromatin is the nucleosome, which contains two copies of each of the core histone proteins H2A, H2B, H3, and H4, around which is wrapped 146 - 147bp of DNA. This structure is generally repressive for processes such as gene transcription that require access to the DNA. However, chromatin is dynamic. ATP-dependent chromatin remodelling complexes can act to open or close this structure to enable or deny access to the DNA as and when required. The first ATP-dependent chromatin remodelling complex discovered was the Swi-Snf complex found in the yeast, *Saccharomyces cerevisiae*. This multi-subunit complex is best characterized as an activator of transcription. However, the precise role of each of the Swi-Snf subunits in transcription is not well understood.

The first goal of the study was to investigate the role of each Swi-Snf complex subunit in cell function by examining the phenotypes in various Swi-Snf subunit mutants. Specifically, I examined *snf2*, *swi3*, *snf5*, *snf6*, *snf11*, *snf12*, *taf14*, and *swp82* deletion mutants in addition to a *snf2K798A* catalytically dead mutant. Unfortunately, I was unable to obtain a *SWI1* mutant to include in my analysis. My repeated gene deletion attempts failed which I hypothesised was due to the *swi1* deletion mutant being either too sick to recover or being inviable. Also, my attempt to create a Swi1p anchor-away strain was not successful. Considering there are reports of *swi1* mutants in the literature, I would suggest that the ability to obtain a viable *swi1* mutant is strain specific and was incompatible with the strain backgrounds I used.

The phenotypic analysis revealed that some Swi-Snf subunit mutations significantly affected doubling time and growth, while others had a minimal impact. For example, the greatest growth defect was found in *snf2* and *snf5* mutant strains. The *snf2* and *snf2K798A* mutants were not always similar and displayed many distinct phenotypes.

When cell morphology was examined, the data revealed that the *snf6* mutant displayed an elongated cell morphology, while *snf2*, *snf2K798A*, and *snf5* strains had a clumpy cell morphology. According to spot test results using different reagents and different temperatures in liquid and solid media, the mutants again showed differences in their response to DNA-damaging reagents and cell wall stress. Together, the phenotypic tests indicated that the different subunits can possess diverse and distinct activities in multiple cellular processes, such as controlling cell size and proliferation, as well as influencing the cellular response to DNA damage.

RNA-Seq analysis was used to compare the transcriptomes of each mutant strain to wt and to each other. Since the Swi-Snf complex functions as a co-activator of gene transcription, I expected most genes in each mutant to be downregulated. Surprisingly, this was not the case. For example, *snf2* mutants, which should completely cripple the remodelling activity of the complex, had a similar number of genes up-regulated as were downregulated. This suggests *SNF2* plays an equal role in the negative regulation of transcription as it does in positively regulating gene transcription. Furthermore, the *swi3* deletion mutant showed almost twice as many genes were upregulated suggesting the major role of *SWI3* is in the repression of transcription. Thus, the data suggests that the Swi-Snf co-activator complex can be considered to equally be a co-repressor of transcription.

The transcriptome data also revealed that even among Swi-Snf subunits within the same module, there were large variations in the number of genes regulated by each subunit, as well as differences in how these functionally related subunits contribute to the transcription of these genes. For example, whereas one subunit might be required for activation of a gene, another subunit could play a role in repression of the same gene. Most strikingly, there was only a minimal overlap (57 genes) in the transcriptomes of *snf2*, *swi3*, *snf6* and *snf5* mutants which, between them, are subunits representative of each of the Swi-Snf submodules. Together, this suggests each subunit can exert widespread distinct regulatory effects upon positive and negative gene

transcription when functioning either within the Swi-Snf complex or, most intriguingly, when functioning outwith the complex.

Analysis of published global sites of occupancy across the genome for the various Swi-Snf subunits revealed that each subunit occupied a distinctly different number of sites. Swi3p occupied the greatest number of sites compared to other subunits (980 sites), whereas Taf14p had the most unique occupancy profile in terms of its presence at sites other than protein coding genes. Interestingly, Snf2p was found located most frequently across gene coding regions compared to its occupancy at promoters. This was surprising, as the best characterized role for Swi-Snf has been in remodelling nucleosomes at gene promoters to enable transcription initiation. This latter data might suggest a primary role for Snf2p dependent chromatin remodelling by Swi-Snf is during transcription elongation. Importantly, there was only a small overlap in the number of sites occupied by all the Swi-Snf subunits analysed. This is in support of Swi-Snf subunits being able to function independently from each other and outwith the confines of the Swi-Snf complex.

Swi-Snf subunit occupancy data was also correlated with the lists of genes up and downregulated in each mutant. The goal was to determine the specific genes that are directly controlled by each Swi-Snf subunit, and to assess whether Swi-Snf subunits could be working independently from each other within or outwith the complex. The data revealed that the correlation between Swi-Snf subunit occupancy and genes shown to be influenced by the particular subunits was poor. This could indicate that the major impact upon transcription is indirect or works over long-range distances. Conversely, the results could be due to limitations of the ChIP technique in fully identifying the sites of protein occupancy, or the sites of occupancy of the subunits are not occupied under the glucose-grown conditions used in this study. Indeed, performing ChIP for the subunits under multiple growth and stress conditions might be needed to identify the full suite of sites occupied by Swi-Snf as its recruitment at certain target sites will be cell signal specific.

The second part of my project examined the interplay between the Swi3p subunit of the Swi-Snf co-activator complex and the Cyc8p subunit of the Tup1-Cyc8 co-repressor complex. This interaction was chosen for analysis because previous unpublished data, which was confirmed in this study, revealed that Cyc8p levels were undetectable by Western blotting in a *swi3* deletion mutant. Importantly, since *CYC8* transcription levels were unaffected in the *swi3* mutant, this suggests that the impact of the *SWI3* gene deletion upon Cyc8p levels was occurring at the level of the Cyc8 protein. Furthermore, the *SWI3* gene was shown to be responsible for repressing almost twice as many genes as it activates, thus implicating Swi3p as having a large role in mediating gene repression.

Firstly, to investigate this potential interplay between *SWI3* and *CYC8* the *swi3* transcriptome was compared to that of the *swi3 cyc8* double mutant. This was to test the prediction that the *swi3* mutant, in which Cyc8p was potentially absent, would have a transcriptome similar to that in a *swi3 cyc8* double mutant. However, the results showed that this was not the case. The data showed that *CYC8* could still negatively influence transcription of genes in the *swi3* mutant suggesting that despite the abundance of Cyc8p in this mutant being below the detection threshold of western blotting, Cyc8p was still present at a level that could influence gene transcription. Secondly, by comparing the transcriptomes of *swi3*, *cyc8* and *swi3 cyc8* mutants, the data revealed that gene repression by *SWI3* could function both independently of *CYC8,* and synergistically with *CYC8*. These findings therefore showed that the Swi3p subunit significantly contributes to the repression of gene transcription via Cyc8p-dependent and independent mechanisms.

Finally, co-immunoprecipitation was used to confirm a direct interaction between Swi3p and Cyc8p. The results also suggested that the Swi3p and Cyc8p interaction might be mediated by Swi3p and Cyc8p whilst these subunits are residing within their respective Swi-Snf and Tup1-Cyc8 complexes.

Overall, these data suggest wide-ranging unique roles for the individual subunits of the Swi-Snf complex that may be functioning when these proteins are residing within or out with the complex. The data also implicates the Swi-Snf co-activator complex as having an almost equal role in mediating gene repression, and that Swi3p plays the greatest role in this negative regulation of transcription. Finally, I have revealed evidence of a direct physical interaction occurring between the Swi-Snf and Tup1-Cyc8 complexes mediated by the Swi3p and Cyc8p subunits. Together, these data oppose the generally accepted consideration of these complexes independently acting as predominant activators or repressors of transcription. Instead, the data might suggest these complexes should be considered as intimate partners which work together to ensure gene transcription is accurately and appropriately positively and negatively regulated in response to the changing environment.

Acknowledgements

I am sincerely thankful to my supervisor Dr. Alastair Fleming for giving me the opportunity to join his lab. I appreciate all your support and advice during my project. I was lucky to be one of your students. I would like to thank the Fleming lab members, Special thanks to Dr. Brenda Lee for all her kindness help, and support. Also, thank you to my lab mates Reham Alnajjar and Zain Baazeem.

A great thanks to the technical and administrative staff in the Moyne. Thank you to Dr. Karsten Hokamp (School of Genetics, Trinity College Dublin) for his help throughout this work. A huge thank you to my recent thesis committee members, Dr. Vincent Kelly, and Dr. Máire Ní Leathlobhair for their suggestions and support.

Thank you to past and current members of the Moyne for their help, and encouragement over the last four years.

I would like to thank all the postgraduate student support members they are very kind and supportive. Special thanks to Martin John McAndrew for his help and support over the past two years.

I would like to most truly thank my country Saudi Arabia, special thanks to King Salman Bin Abdulaziz AL Saud and Crown Prince Mohammad Bin Salman Al Saud for giving me the opportunity to be a PhD student in Ireland. I wish to thank all those whose kindness and support during my journey I shall never forget such as the amazing Saudi team support structure in the Saudi Cultural Bureau in Dublin. Special thanks to Dr. Fahdah Al Shaikh, and Dr. Jnan Al Dehan, Dr. Mohamed Al Saholi, Mr. Youssif Al Sadoon. Without their influence, support, and genuine care I would have most definitely floundered. A great thanks to my master's degree supervisor Professor Mohamed Hani Moubasher (Since college, Cairo University, Egypt), his unquenchable support will always be treasured.

Thank you to My parents Mosfer Al Jaeed, and Fatmah Alotaibi, and my sisters Hanin, Hanouf, Ghadeer, and Raghad, my brother Abdulmohsen. Without their continuous support, it would have been impossible to complete my PhD. But I must give very special acknowledgement to Baba who was and is a constant support of strength, understanding, and love in every way possible to ensure I had every means available and more to achieve my dream.

Very special thanks to my incredible children Sarah and Khaled who have patiently stood by me, understood and kindly waited for my return over the last two years living in Ireland while we loved and virtually hugged each other all the time online. Sarah and Khaled thank you my darlings you are my loving shining light, my greatest achievement in life, you are everything to me.

Conferences

1. Aljaeed HA. and Fleming AB. 2023, (June 1st). Attended DAPI at University College Dublin (UCD) in Ireland.

2. Aljaeed HA. and Fleming AB. 2023, (June 22nd). Investigating the contributions to cell function of the different Swi-Snf complex subunits in *Saccharomyces cerevisiae.* Poster Presentation at the Irish FungalSociety Annual Conference at Dublin College University (DCU) in Ireland.

3. Aljaeed HA. And Fleming AB. 2023, (June 5th – 8th). Attended the PYFF Physiology of Yeast and Filamentous Fungi at (UCC) University Cork College, Ireland.

4. Aljaeed HA. and Fleming AB. 2023, (August 20th – 25th). Investigating the contributions to cell function of the different Swi-Snf complex subunits in *Saccharomyces cerevisiae.* Poster presentation at ICYGMB 31 (International Conference on Yeast Genetic and Molecular Biology) at the Innovation Centre in Florence, Italy.

5. Aljaeed HA. and Fleming AB. 2023, (June 19th – 20th). Investigating the contributions to cell function of the different Swi-Snf complex subunits in *Saccharomyces cerevisiae.* Poster Presentation at the Irish Fungal Society Annual Conference at Queen's University Belfast Ireland.

Table of Contents

List of Figures

List of Tables

Chapter 1

Introduction

1.1 Overview

To understand the mechanism of eukaryotic gene regulation, the yeast *Saccharomyces cerevisiae* has been used as a model organism [1] ,[2]. This single-celled organism has many proteins and pathways common to human cells and has a short doubling time. These characteristics, together with the efficiency with which the yeast's genome can be manipulated, renders it an ideal subject for genetic analysis [3].

In the yeast genome, the DNA is packaged into a structure called chromatin. At the heart of chromatin lie nucleosomes, repeating units composed of histone protein octamers around which 146/147 base pairs of DNA are wrapped [4] ,[5] ,[6]. A key challenge in modern biology involves understanding how this nucleoprotein structure controls the access of genetic information within the DNA.

Chromatin is generally considered repressive to any process that requires access to the DNA such as transcription, replication, recombination, and DNA damage repair [7]. However, chromatin is a dynamic structure which can be 'remodelled' to enable, or deny, access to the underlying DNA as and when required. This so-called 'chromatin remodelling' can be achieved via post-translational modification to the histone proteins themselves or via the action of ATP-dependent chromatin remodeling complexes [8], [9].

Generally, these complexes have the ability to open and close chromatin structure through processes such as nucleosome sliding, nucleosome eviction, and histone exchange. The first chromatin remodelling complex discovered was the yeast SWI-SNF (switch/sucrose-non-fermenting) complex which is generally considered to be an activator of transcription. Subsequent studies found this complex to be evolutionarily conserved.

Conversely, the first global repressor of transcription identified was the Tup1-Cyc8 (Ssn6) co-repressor complex, which also has homologues in higher eukaryotes [10]. Thus, these complexes are archetypes of conserved machinery that can switch genes on and off via their action on chromatin.

This thesis examines the role of the individual subunits of the yeast Swi-Snf complex and reveals a functional and physical link between the Swi-Snf activator and the Tup1-Cyc8 co-repressor.

1.2 Chromatin

The genome of the budding yeast comprises 16 chromosomes and contains approximately 6000 genes [11]. The DNA is packaged within the nucleus in a nucleoprotein structure called chromatin [12]. The nucleosome is the basic building block of chromatin which comprises 146 - 147bp of DNA wrapped around an octamer of histone proteins; two copies each of histones H2A, H2B, H3, and H4 [13](Table 1.1). Histone H1, known as the linker histone, forms an association with the nucleosome core particle. Although the budding yeast form of histone H1 (Hho1p) is believed to play a role in regulating chromatin structure and certain chromatin-related functions, such as DNA double-strand break repair [14]. Together, this structure can fold up on itself to form higher order structures to package the genome within the yeast nucleus (Fig. 1.1).

The nucleosome structure is generally considered to be repressive to any process that needs access to the underlying DNA such as transcription, replication, recombination, and DNA damage repair [12]. However, it is a highly dynamic structure that can be altered, or 'remodeled', to either promote or DNA access to the underlying DNA as and when required.

Two forms of chromatin are found in the eukaryotic genome. Heterochromatin, is densely packed and inhibits gene expression. It increases the stability of the eukaryotic genome and is specifically distributed in yeast [15]. Euchromatin is characterized by its more open state and is permissive for gene expression [16].

The heterochromatin regions in *S. cerevisiae* are mostly found at the telomeres and the silent mating type loci. Genes in these loci are transcriptionally inactivated, or "silenced," as a result of the condensed state of chromatin at these sites [17]. Subtelomeric regions, defined as portions positioned more than 25 Kb from the end of the chromosome, are also regarded as genomic regions which can be subject to limited, or at least highly regulated, transcriptional activity. Genes in these regions often belong to specific gene families, such as stress response genes [17].

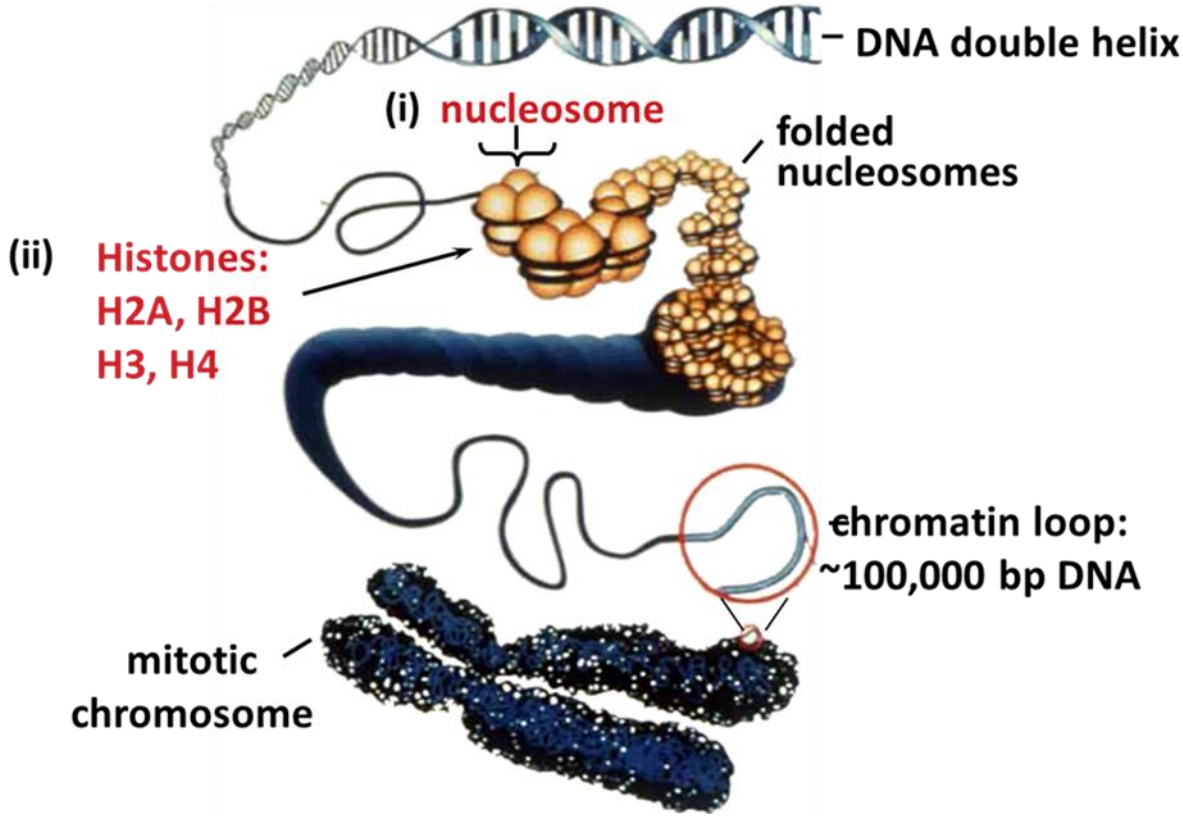

Figure 1. 1: Schematic of the chromatin: (i) Nucleosomes comprise double-stranded DNA wrapped around eight histone proteins. **(ii)** Two each of histone proteins (H2A, H2B, H3, and H4).

1.2.1 The nucleosome

The nucleosome is the basic building block of eukaryotic chromatin. This consists of 147 base pairs of DNA coiled 1.65 rotations around the histone octamer [18], [19](Fig. 1.2). The nucleosome is comprised of a tetramer made up of two copies of each of the H3 and H4 histone proteins, and two heterodimers of H2A-H2B [19], [20]. The region between neighboring nucleosomes is referred to as linker DNA [21].

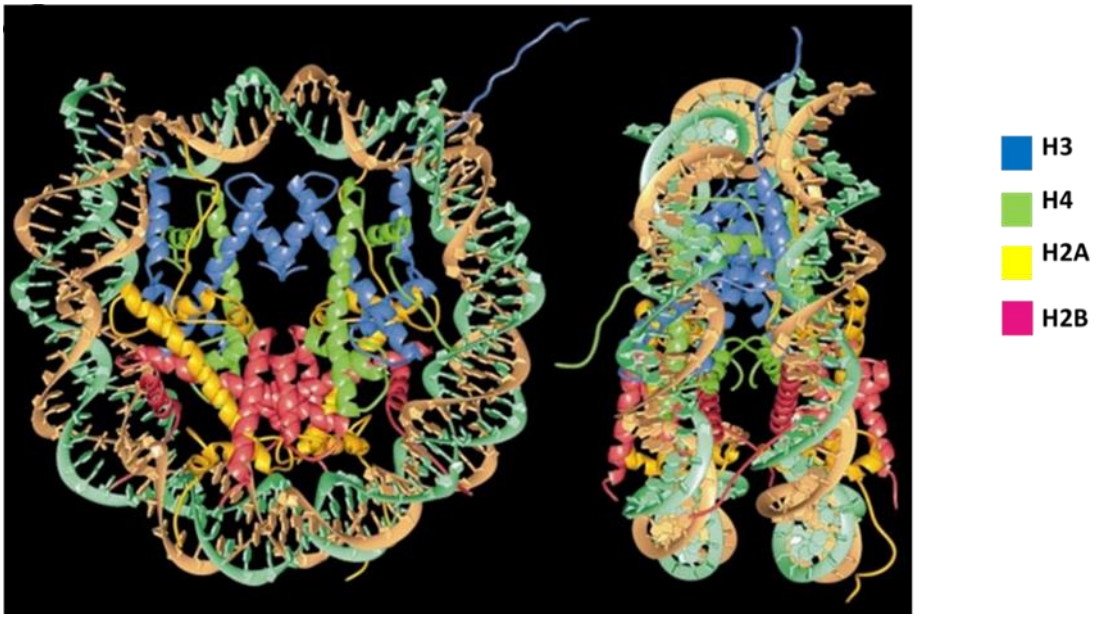

Figure 1. 2: The structure of the core nucleosome. High-resolution crystal structure of the nucleosome [13]. The DNA fiber is wrapped around a tetramer of H3 (blue) and H4 (green), along with two H2A (yellow) and H2B (pink) dimers. Figure adapted from [22].

Within the nucleosome, histones contact the phosphate backbone of DNA every 10.4 base pairs. This means that there are 14 places where histones and DNA touch in the nucleosome, which makes this structure very stable [13].

Properties of the histone proteins				
Histone	Molecular weight (Da)	Number of amino acid residues	Content of basic amino acids (% of total)	
			Lysine	Arginine
H1	21,130	223	29.5	1.3
H2A	13,960	129	10.9	9.3
H2B	13,774	125	16.0	6.4
H3	15,273	135	9.6	13.3
H4	11,236	102	10.8	13.7

Table 1. 1: Table to show properties of the histone proteins. Type (H1, H2A, H2B, H3, and H4), molecular weight (Daltons, Da), number of amino acid residues, and percentage (%) of proteins comprised of lysine and arginine residues are shown.

The four core histones, H2A, H2B, H3, and H4 are small, basic proteins whereby 20% of their amino acids are either Lysine or Arginine residues (Table 1.1) [23]. In *S. cerevisiae*, there are two genes that encode each of the core histones. The core histones have similar structures comprising a C-terminal globular domain and an N-terminal histone tail. The C-terminal region contains the histone fold domain, whereas the N-terminal tails are unstructured and extend outward from the central nucleosome [24].

The histone fold domain (HFD) is a structural motif which facilitates the dimerization of histones, forming the core of the nucleosome around which DNA is wrapped. The HFD is characterized by three alpha helices separated by two loops, creating a handshake motif that allows for the specific pairing of histone proteins [25]. Research has shown that HFD is not only present in eukaryotic histones but also in other proteins across all three domains of life, indicating its fundamental role in cellular processes [25].

Nucleosomes are arranged on DNA in a 'beads on a string' conformation approximately 10 nanometers (nm) in diameter; a structure called the 10 nm fiber [26], [27]. This structure can then fold up on itself to form the 30 nm fiber. Higher order folding can then compact the chromatin further (Fig. 1.1).

1.3 Post-translational modification of histones

Post-translational modifications (PTMs) of the histone proteins occurs predominantly in the N-terminal tails which comprises approximately 25% of the mass of each core histone (Fig. 1.3) [21]. Less frequently, PTMs can also be found in the globular region, and in the C-terminal tails [28]. Post-translational modifications of the histone tails play a crucial role in regulating both transcriptional activation and repression [22]. Post-translational modifications of histones include methylation, ubiquitylation, acetylation, ADP-ribosylation, and sumoylation of arginine (R) or lysine (K) residues and phosphorylation of serine and threonine residues [29], [30](Fig. 1.3).

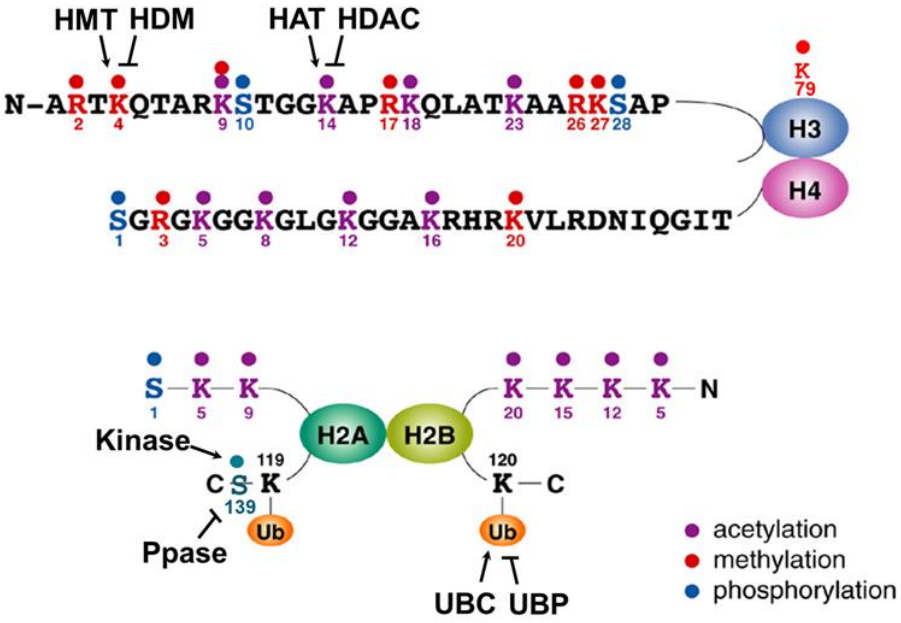

Figure 1. 3: Histones post-translational modifications. Examples of sites of histone acetylation (purple), methylation (red), phosphorylation (green), and ubiquitination (orange) are indicated. Histone methyltransferases (HMTs), histone acetyltransferases (HATs), ubiquitin conjugating enzymes (UBCs), and kinases are the writers that modify histones. Histone demethylases (HDM), histone deacetylases (HDAC), ubiquitin proteases (UBP), and phosphatases (Ppase) are the erasers which can remove the

modifications. The figure was taken from published data and depicts post-translational modifications in human cells, many of which are conserved in yeast cells [31].

Chromatin modifications have diverse impacts on the structure of nucleosomes and can influence several elements of gene regulation, including initiation, elongation, and termination of transcription [28], [32]. These histone modifications are thought to function via the 'histone code hypothesis'.

The histone code hypothesis proposes that 'writers' such as histone acetyltransferases (HATs), histone methyltransferases (HMTs), kinases, and other similar proteins are the enzymes that add the modification to the histones (Fig. 1.4). Specifically modified regions of chromatin act as a signal for other non-chromatin proteins called 'readers' which 10ecognize the sites of modification and bring about a cellular response. 'Erasers' such as histone deacetylases (HDACs) and demethylases (HDMs) then remove the code. [33], [34].

1.3.1 Histone acetylation

The acetylation of histone tails at the N-terminal was discovered in 1964 and is the most extensively studied alteration of histones which has been widely linked to the activation of genes [35].

Histone acetylation most frequently occurs on lysine (K) residues of the N-terminal tails of H3 and H4. Histone acetylation plays an important role in neutralizing the positive charge on the histone tails, thereby impacting the interaction with DNA. Thus, histone acetylation is often associated with chromatin decompaction and transcriptional activation [36], [37](Fig. 1.4).

Histone acetyltransferases (HATs) are the writers that add the acetyl groups to histones. The first HAT described in yeast was Gcn5p which acetylates specific N-terminal lysine residues on histones H2B and H3. Gcn5p serves as the enzymatic component of different complexes, such as SAGA, ADA/SLIK, and ADA, which have been

associated with the control of transcription [38]. Subsequent studies found other HATs with distinct specificities[39] (Table 1.2).

Histone acetylation can be removed by histone deacetylases (HDACs). When histone deacetylase (HDAC) removes the acetyl groups from the lysine side chains, the positive charge on the histone is restored. This results in condensed chromatin, making it more difficult for proteins such as RNA Polymerase II to access the DNA, and leading to decreased gene expression [40].

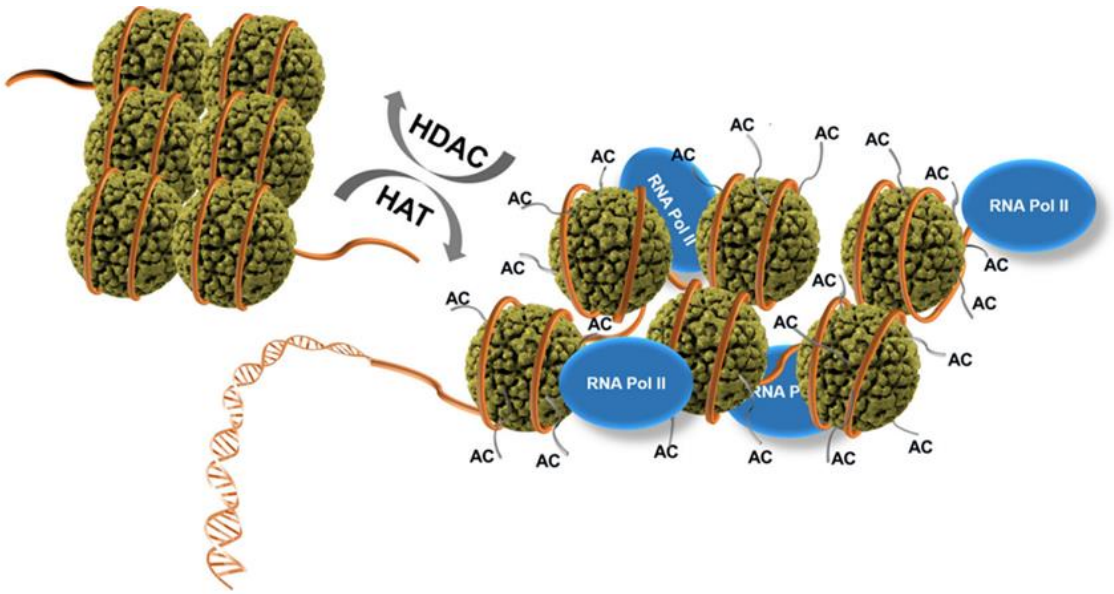

Figure 1. 4: Histone acetylase (HAT) and histone deacetylase (HDAC) activities regulate gene activation and repression. When histone lysine residues undergo acetylation (AC) by a HAT, the chromatin structure opens up, allowing RNA polymerase II (RNA Pol II) to bind. Conversely, an HDAC removes acetyl groups from the histone lysine residues, resulting in a closed chromatin conformation that prevents RNA Pol II binding. Histones are represented as dark green spheres, with DNA wrapped around them depicted as an orange tube. The histone lysine residues are illustrated as thin, short gray tails on the histone spheres. This figure was obtained from published data [40].

Histone	Acetylated Residue	Modification	Modification enzymes	
			HAT(s)	HDAC(s)
H2A	K5 K8	Ac Ac	Esa1 Esa1,Hat1	Rpd3 Rpd3
H2A.Z	K3 K8 K10 K14	Ac Ac Ac Ac	Esa1 Esa1 Esa1 Esa1	
H2B	K11 K16	Ac Ac	Esa1 Gcn5, Esa1	 Rpd3
H3	K4 K9 K14 K18 K23 K56	Me, Ac Ac Ac Ac Ac Ac	Rtt109,Gcn5 Gcn5 Gcn5, Sas3 Gcn5 Gcn5 Rtt109	Rpd3, Hda1 Hos2, Hda1 Hos2, Hda1 Hos2, Hda1 Hos2, Hda1 Hst3, Hst4
H4	K5 K8 K12 K16 K20	Ac Ac Ac Ac Ac	Esa1 Esa1 Esa1 Esa1, Sas2 Esa1, Sas2	Rpd3, Hos2 Rpd3, Hos2 Rpd3, Hos2 Sir2, Hos2, Hst1 Sir2, Hos2, Hst1

Table 1. 2: HATs and HDACs in yeast: A table of acetylated (Ac) and methylated(me) residues in each histone type, and the enzymes responsible for acetylation (HAT(s)) and deacetylation (HDAC(s)). The table was taken from published data [41].

1.3.2 Histone methylation

Histone methylation (me) is another form of histone modification that was discovered in the mid-20th century [42]. Histone methylation, is a process of transfer of methyl groups to the arginine and lysine residues of histones, particularly H3 and H4. The enzymes responsible for this modification are histone methyltransferases (HMTs) (known as “writers”), which add methyl groups, and histone demethylases (HDMs) (known as “erasers”), which remove them (Fig. 1.5) [43], [44]. Histone methylation is critical for chromatin structure and gene expression regulation. Unlike acetylation, methylation does not change the charge of histone tails but influences their interaction with DNA and other proteins.

In yeast, only the lysine (K) residues 4, 36, and 79 of histone H3 can be methylated. Methyltransferases can attach up to three methyl groups to a single lysine residue, resulting in mono-, di-, or tri-methylation patterns [45], [46].

Set1, which is part of an eight-protein complex called COMPASS, adds a methyl group to lysine 4 of histone H3 [47]. H3K4 methylation shows a progressive variation in levels across most active genes. Tri-methylation is concentrated near the promoter region, di-methylation is located at the 5’ end of the gene, and mono-methylation is more abundant further downstream. The degree of methylation is determined by the length of interaction between the Set1 methyltransferase complex and the nucleosome [46], [48]. Set2 methylates lysine 36 (H3K36) of histone H3 and is enriched at the 3’ region of active ORFs [49]. Dot1 (Disruptor of telomeric silencing) adds methyl groups to the H3K79 residue and was initially discovered as a factor involved in the silencing of yeast telomeres [50]. However, H3K79me also plays a role in transcription, progression through the cell cycle, and the cell response to DNA damage [51].

The process of histone methylation is highly conserved throughout a wide range of eukaryotic organisms throughout evolution [46], [52].

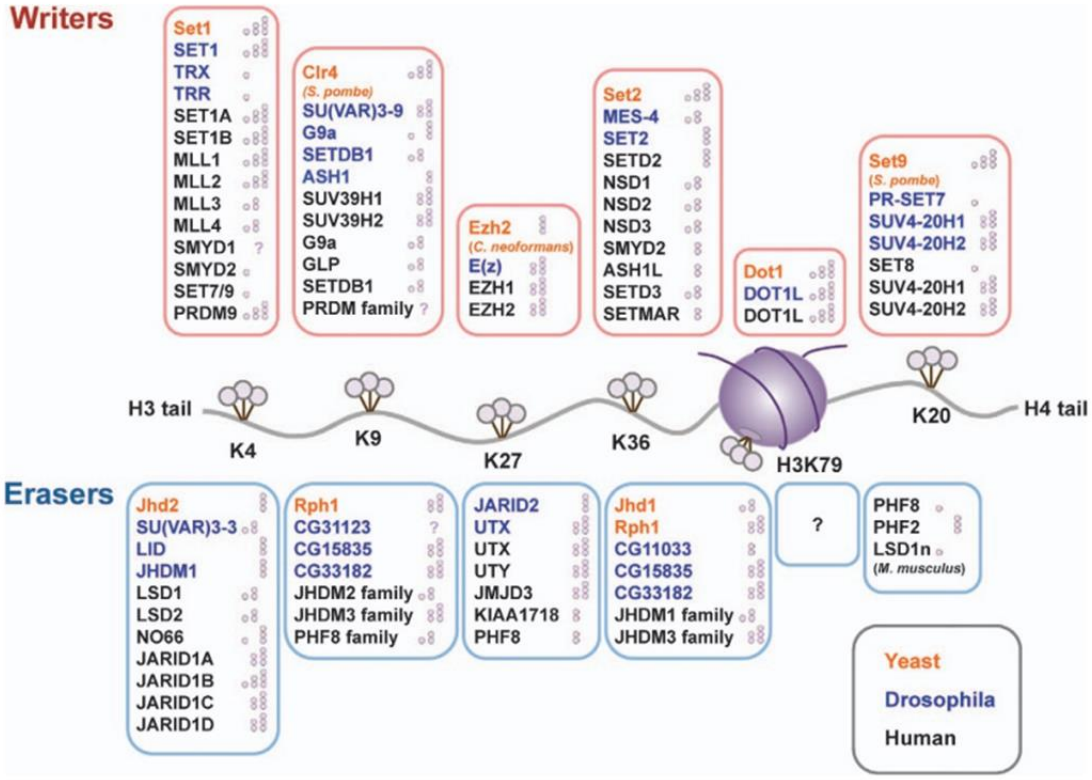

Figure 1. 5: A schematic illustration of a nucleosome that highlights the key histone H3 and H4 lysine methylation sites. The methylation state specificities of the reported writers (methyltransferases) and erasers (demethylases) for each lysine methylation are also shown: single circle me1, double circle me2, triple circle me3. The figure was adapted from published data [44].

1.4 Gene transcription in yeast

Transcription in eukaryotes occurs exclusively within the nucleus [53]. The mechanism of transcription in yeast *S. cerevisiae* is carried out by three RNA polymerases (Pols I, II, and III). Each polymerase exhibits specificity in synthesizing distinct RNA types from DNA.

RNA polymerase I is situated within the nucleolus and consists of 14 subunits and is responsible for synthesizing all of the 'structural' ribosomal RNAs (rRNAs). The rRNA molecules are not translated into protein. Ribosomal RNAs (rRNAs) are integral constituents of the ribosome and play a vital role in the translation process [54], [55]. RNA polymerase II, consisting of 12 subunits, is situated within the nucleus and is responsible for the synthesis of all protein-coding nuclear pre-mRNAs.RNA polymerase II is the primary enzyme that transcribes most eukaryotic genes, including protein-encoding genes that are later translated into proteins, as well as genes for other regulatory RNAs such as microRNAs (miRNAs) and long-coding RNAs (lncRNAs) [56]. RNA polymerase III, containing 17 subunits, catalyzes the synthesis of tRNAs, 5S rRNA, and other non-coding RNAs [57], [58].

Focusing upon RNA pol II transcription, the transcription process is carried out in 3 stages: initiation, elongation, and termination.

1.4.1 Initiation

Initiation is the first step of RNA Pol II transcription which involves the assembly of transcription machinery at the promoter region of a gene (Fig. 1.6). During this stage, transcription factors (TFs) such as TFIIA, TFIIB, TFIID, TFIIE, TFIIF, and TFIIH, together with RNA Pol II that carries the TATA-box-binding protein (TBP), combine to create the pre-initiation complex (PIC). This intricate structure arises before the commencement of transcription at the promoters of protein-coding genes [59]. Initiation occurs in DNA regions at promoters devoid of nucleosomes, often termed the Nucleosome-Free or Depleted Region (NFR or NDR) [60].

Transcription initiation begins when transcription factors recognize and bind to specific sequences in the promoter region of the gene. The core promoter typically contains the TATA box, where the TATA-binding protein (TBP) binds. Once TBP is bound to the TATA box, other general transcription factors (TFs) such as TFIIB, TFIIE, TFIIF, and TFIIH combine to form the pre-initiation complex (PIC). This complex is essential for recruiting RNA polymerase II (RNA Pol II) to the promoter [61]. TFIIH then plays a role in unwinding the DNA around the transcription start site, creating a single-stranded DNA template for RNA synthesis. RNA Pol II can then begin synthesizing the RNA transcript by adding nucleotides complementary to the DNA template strand [62].

Initiation is a highly regulated process and serves as a critical point for controlling gene expression. Various regulatory factors and signals can influence the initiation step, affecting the overall transcription levels of specific genes.

After initiating transcription and synthesizing a short stretch of RNA, RNA Pol II undergoes a transition from initiation to elongation. It clears the promoter region, moving along the DNA template to continue RNA synthesis.

1.4.2 Elongation

The elongation step of transcription involves the process of RNA polymerase II (RNA Pol II) moving along the DNA template and synthesizing a complementary RNA transcript (mRNA) [63].

While elongation occurs, several RNA processing events happen concurrently. These include capping at the 5' end of the RNA, splicing to remove introns (in the case of pre-mRNA), and polyadenylation at the 3' end of the RNA.

The elongation step continues until RNA Pol II reaches a termination signal on the DNA template, at which point transcription ceases.

Elongation is a critical phase of transcription as it not only dictates the production of a full-length RNA molecule but also ensures proper RNA processing for subsequent stages of gene expression.

1.4.3 Termination

Transcription termination marks the end of the transcription process and occurs when RNA polymerase II reaches the end of a gene. Here, RNA polymerase II recognizes specific DNA sequences, such as the polyadenylation signal within the gene. This signal marks the end of the gene and the point where the RNA transcript should be cleaved.

Once RNA polymerase II reaches the termination signal, the RNA transcript undergoes cleavage near the polyadenylation signal. The 3' end of the mRNA is then modified with a poly(A) tail by a polyadenylation complex.

After cleaving the RNA transcript, RNA polymerase II continues transcribing the DNA template for a short distance before dissociating from the DNA. This process is known as transcriptional run-on and is important for proper termination.

The remaining RNA downstream of the cleavage site is usually degraded by the 5' to 3' exonuclease Xrn2 (also known as Rat1). Xrn2 binds to the free 5' end of the remaining RNA and degrades it while chasing RNA polymerase II. Once Xrn2 catches up to the RNA

polymerase, it helps to release RNA polymerase II from the DNA which marks the end of transcription.

Termination in *Saccharomyces cerevisiae* is also a tightly regulated process and is essential for proper gene expression and RNA maturation. This step ensures that transcription stops at the right location and allows for the release of both the newly synthesized RNA and the RNA polymerase II for use in subsequent transcription cycles.

Importantly, the process of transcription in yeast has to cope with the DNA template existing as chromatin.

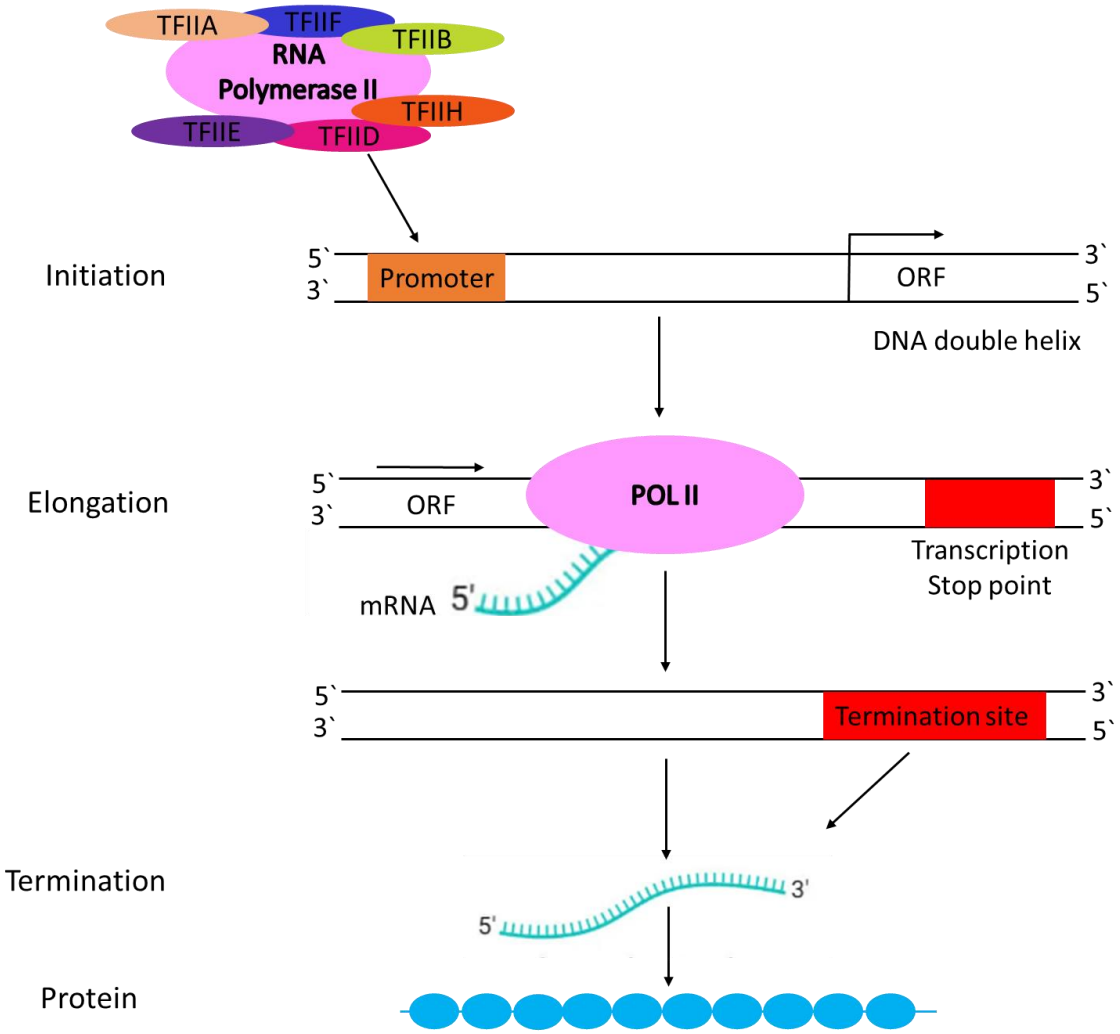

Figure 1. 6: Schematic of RNA pol II transcription. RNA polymerase II (POL II) with transcriptional factors (TFs) makes the pre-initiation complex (PIC) in the nucleus. In the elongation stage, mRNA is transcribed from the DNA template. Termination marks the end of mRNA synthesis and mRNA release.

1.5 ATP-dependent chromatin remodelling

Although chromatin is generally inhibitory to any process that needs access to the DNA, such as transcription, it is a dynamic structure that can be altered, or 'remodelled' to enable or deny access to the DNA. This is crucial for controlling the expression of individual genes[64]. Chromatin remodeling can be achieved by the action of complexes that can utilizes the energy from ATP hydrolysis to reposition or remove nucleosomes [23]. This process affects the accessibility of the DNA to cellular machinery, either making it more or less accessible [4], [23].

The ATP-dependent remodeling complexes are classified into four families, which are defined by their ATPase subunits (Fig. 1.7).

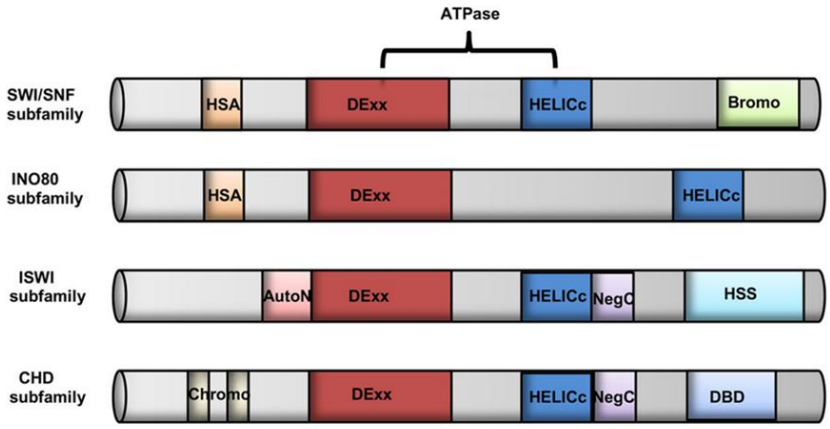

Figure 1. 7: There are four families of ATP-dependent chromatin remodelling complexes. The SWI/SNF family comprises the helicase-SANT-associated domain (HSA) and a bromodomain located at the carboxy-terminal. The INO80 family is characterized by the presence of an HSA domain, which is distinguished by a lengthy insertion located between the two ATPase subdomains. The ISWI family is characterized by the presence of a carboxy-terminal HSS (HAND-SANT-SLIDE) domain, as well as two domains next to the ATPase: AutoN (autoinhibitory N-terminal) and NegC (negative regulator of coupling). The CHD family shares similarities with ISWI remodelers, which include a C-terminal NegC and a domain called DBD that is similar to HSS. However, the CHD family has tandemly-arranged chromodomains [23].

The SWI/SNF (switch/sucrose non-fermentable) and RSC (remodels the structure of chromatin) complexes are members of the SWI/SNF family in budding yeast. The yeast SWI/SNF complex contains 12 subunits and RSC complexes contain 17 subunits [65]. The ATPase subunits of SWI/SNF (Snf2p) and RSC (Sth1p) contain an N-terminal helicase-SANT (HSA) domain and a C-terminal bromodomain. The HSA domain specifically interacts with actin or actin-related protein (ARP) subunits, while bromodomains typically bind to acetylated histone residues and may play a role in targeting of the complex.

The ISWI (imitation switch) family contains an ATPase subunit with a conserved C-terminal HAND-SANT-SLIDE (HSS) domain that binds to the unmodified tail of histone H3 as well as the flanking linker DNA. The ISWI family in *S. cerevisiae* contains 3 ISWI complexes, (ISW1a, ISW1b, and ISW2) each consisting of only two or three subunits [51], [65].

The CHD (chromodomain helicase DNA-binding) family of complexes in yeast is composed solely of an ATPase component. CHD1 possesses a pair of consecutive chromodomains at the beginning of the protein and a SANT-SLIDE domain at the C-terminal which recognizes methylated histone residues [65], [66], [67].

The INO80 (inositol-requiring 80) family is characterized by an ATPase subunit that includes an individual elongated insertion located between the DExx and HELICc lobes, forming a "split" ATPase domain. Additionally, it features an N-terminal HSA domain that bears resemblance to the SWI/SNF family Snf2p subunit. The yeast members of the INO80 family consist of two representatives: INO80, which is composed of 14 subunits, and SWR1, which is composed of 17 subunits [68].

All remodeling complexes are considered to share a common mechanism that involves a histone-anchored ATPase (see Fig. 1.8). This ATPase is responsible for causing directional movement of DNA around a nucleosome. The DNA strand is pushed around the nucleosome while it remains anchored in place by the remodeling complex. Thus, the DNA strand is moved relative to the initial nucleosome position. [69].

This translocation mechanism can result in nucleosome sliding, nucleosome eviction or removal of histones from the nucleosome (Fig. 1.9). Some remodellers are involved in editing nucleosomes by installing or removing histone variants [70]. The INO80 subfamily of remodelers removes a specific histone from a nucleosome and replaces it with either a canonical or variant histone independent of replication.

Common examples of histone editing involve the replacement of canonical H2A or H3 with their related variants, a process facilitated by remodeling complexes such as the yeast SWR1 complex (SWR1C) and the mammalian SRCAP (Snf-2-related CBP activator protein) and p400 [71], [72]. Incorporating histone variants into a single nucleosome or an array of nucleosomes can influence the recruitment, inhibition, or activity of various factors [73].

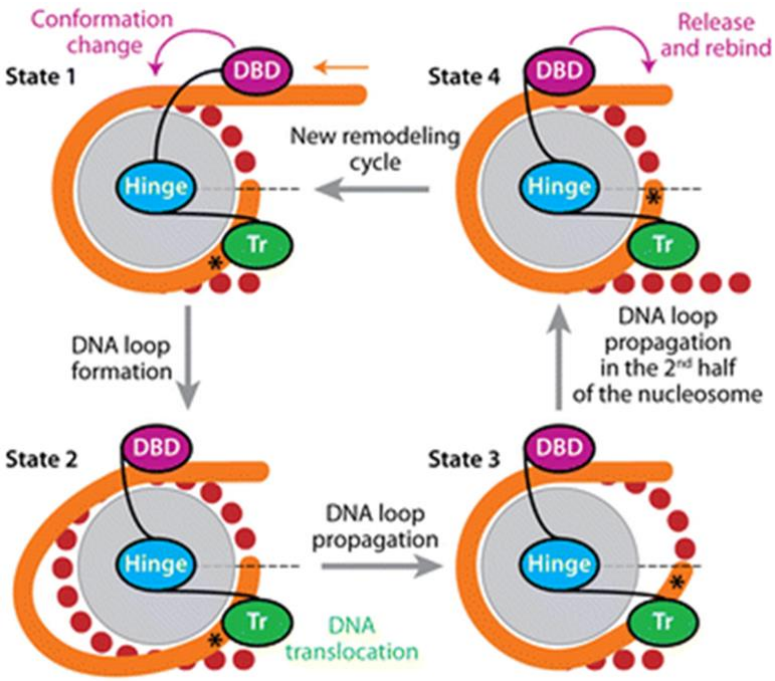

Figure 1. 8: The ATP-dependent chromatin remodelling complex mechanism.

In State 1, the DNA wraps around the histone octamer while the remodelling complex binds and anchors itself to a fixed position on the histone octamer. Simultaneously, the DNA binding domain (DBD) attaches to the linker DNA adjacent to the nucleosome. As the remodelling complex becomes anchored, a conformational change occurs in the translocase domain (Tr), the catalytic component of the complex. This conformational alteration prompts the disintegration of DNA-histone contacts, allowing for the repositioning of the linker DNA along the histone protein surface, thereby establishing new DNA-histone interactions. State 2 illustrates the formation of a loop in the excess DNA resulting from this rearrangement. Moving to State 3, the excess DNA loop is shown passing through the translocase domain (Tr). This step involves the Tr domain actively facilitating the movement of the excess DNA, ensuring its passage without disrupting the overall nucleosome structure. By State 4, histone-DNA contacts have been reestablished across the nucleosome's second half, stabilizing the newly formed configuration. This process results in the effective remodeling of the nucleosome, altering its structure and potentially facilitating access to DNA for various cellular processes [74].

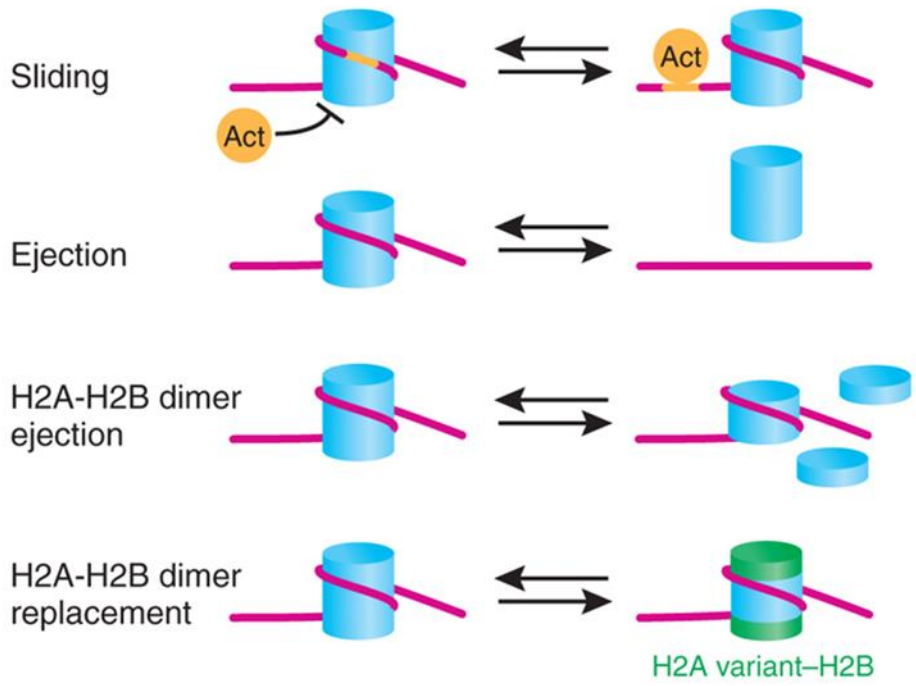

Figure 1. 9: ATP-dependent chromatin remodelers mechanism. ATP-dependent remodelling complexes facilitate the opening of nucleosomal DNA as they can slide, eject or rearrange nucleosomes by evicting H2A-H2B dimers, depending on the complex and the target site. The SWR1 complex is distinctive in its capacity to effectively substitute H2A-H2B dimers with dimers containing a histone H2A variant (Htz1 or H2A.Z). “Act" refers to an activator that has a specific location on the DNA where it can bind [50].

Recruitment to target sites can be via specific DNA sequences or histone modifications that mark the target sites for remodeling. By altering the chromatin structure, these ATP-dependent chromatin remodeling complexes regulate gene expression by controlling the accessibility of DNA to the transcriptional machinery.

ATP-dependent chromatin remodelers are also found in higher eukaryotes where they also play vital roles in regulating gene transcription and cell and tissue development. Not surprisingly, mutations in chromatin remodeling complexes are associated with human diseases, including cancer, and targeting these pathways is evolving as a therapeutic strategy [75].

1.5.1 Chromatin remodelleing complexes are evolutionarily conserved.

Chromatin Remodelers and their role in disease.

Chromatin remodeling complexes, such as SWI/SNF, are evolutionarily conserved complexes important in gene expression regulation across many different species. The fact that chromatin remodelers are evolutionary conserved highlights their critical role in maintaining genome stability and cellular homeostasis. These functions that have been preserved from yeast to humans. Dysregulation of these complexes, driven by mutations, can have profound implications across species, underlying both developmental and disease processes.

Cancer

Chromatin remodeling complexes, particularly SWI/SNF, are strongly linked to cancer. Mutations or loss of function in components of these complexes can impair gene expression regulation, resulting in uncontrolled cell growth and tumorigenesis. For instance, mutations in ARID1A and SMARCB1, key components of the human SWI/SNF complex, are associated with ovarian cancer, renal rhabdoid tumors, and other cancers. Additionally, abnormalities in other SWI/SNF components are observed in about 20% of all human cancers [76].

Neurological Disorders

Dysregulation of chromatin remodeling is also associated with neurodevelopmental disorders. Mutations in genes encoding CHD proteins have been linked to conditions such as CHARGE syndrome, which is characterized by various developmental abnormalities. Furthermore, mutations in ATRX, a component of the SWI/SNF complex, are associated with intellectual disability and ATRX syndrome, which is related to alpha-thalassemia [77].

Developmental Disorders

Several congenital disorders are tied to mutations in chromatin remodeling complexes. For instance, mutations in SMARCA4 (part of SWI/SNF) result in Coffin-Siris syndrome, characterized by developmental delay, intellectual disability, and distinct facial features. Similarly, CHD7 mutations cause CHARGE syndrome, leading to severe developmental and physical abnormalities [78].

Immunological Disorders

In the immune system, chromatin remodeling complexes help regulate the expression of genes involved in immune cell differentiation and function. For example, defects in chromatin remodeling components can lead to immune system dysfunctions or immunodeficiencies [79], [80].

Aging and Degenerative Diseases

Chromatin remodeling also plays a critical role in cellular aging and age-related diseases. Dysregulated chromatin remodeling has been linked to age-associated diseases such as Alzheimer's and Parkinson’s disease, where abnormal gene expression patterns contribute to neurodegeneration [81].

Overall, chromatin remodeling complexes are vital to cellular regulation, and their dysfunction can lead to a wide range of diseases, from cancer to neurological disorders. Understanding the mechanisms of these complexes offers potential for the

development of therapeutic targets for treating chromatin-related diseases when these complexes are aberrant.

1.5.2 The Swi-Snf complex

The SWI/SNF (switching/sucrose non-fermenting) complex was the first chromatin remodelling complex to be discovered and was identified in the yeast *S. cerevisiae.* The SWI/SNF complex was discovered through two independent genetic screens conducted in the early 1980s-90s to explore genes controlling the induction of *SUC2* and the *HO* endonuclease in *Saccharomyces cerevisiae*. These screens led to the identification of the *SWI* (switch) and *SNF* (sucrose non-fermentable) genes via mutants unable to switch mating type and unable to ferment sucrose [82]. Subsequent studies found the gene products of many of these genes resided in a large complex.

The Swi/Snf complex in yeast specifically regulates around 10% of all genes during glucose-grown conditions, and it plays a crucial role in transcription in response to different stress situations [83]. The Swi-Snf complex is highly conserved from yeast cells to human [84].

1.5.2.1 The Swi-Snf complex structure

The Swi-Snf complex in yeast is composed of 12 proteins, with a total molecular weight of around ~2 megadaltons (MDa) [82]. There are 5 modules within the Swi-Snf complex; 1-the Snf2 module which contains Snf2 and Snf11; 2- the Swi3 module containing Swi3, Snf6, and Snf12; 3- the Snf5 submodule which includes Snf5, Taf14, and Swp82, 4- the Swi1 module; and 5- the Arp module which includes Rtt102, Arp7, and Arp9. Of note, the Arp module is shared with the RSC complex in yeast [83](Fig. 1.10).

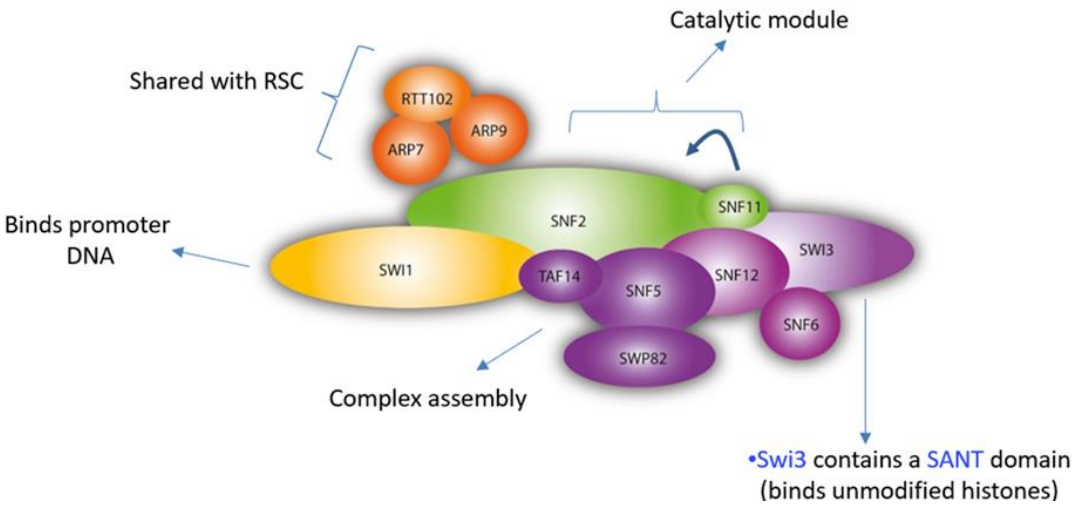

Figure 1. 10: The yeast Swi-Snf complex: sub-units of the Swi-Snf complex are shown in their designated sub-modules. (1) Arp7-Arp9-Rtt102 (orange); Snf11-Snf2 (green); (3) Snf12-Snf6- Swi3 sub module and (4) Taf14-Snf5-Swp82 sub module (purple); (5) Swi1 (yellow). The figure was adapted from published data [83].

The different subunits have been shown to have different functions within the Swi-Snf complex [83], [85](Table 1.3). Snf2p is the central and most crucial subunit of the SWI/SNF complex. It possesses ATPase activity, which is essential for driving the complex chromatin remodeling functions. This subunit hydrolyzes ATP to provide the energy necessary for the complex to alter chromatin structure [83]. Snf5p acts as a scaffold protein, helping to organize and stabilize the complex. It also plays a role in facilitating interactions with other proteins and nucleosomes [86]. Swi3p functions as an adaptor or scaffold protein, mediating the interaction between Snf2p and other complex subunits. It may also contribute to substrate specificity [87]. Similar to Swi3p, Swi1p aids in organizing the complex and promoting interactions between other subunits and the nucleosome [86]. Snf6p is believed to play a role in the complex remodeling activity, possibly influencing its ability to interact with and alter nucleosomes [88].

Subunit	Subunit Function	Size (kDa)	Module
Snf2p	Catalytic subunit (ATPase)	194	Catalytic module
Snf11p	Promotes Snf2 activity	19	
Snf5p	Complex assembly	102.5	Snf5-Swp82- Taf14 module
Taf14p	Not essential for stability, unknown function	274.3	
Swp82p	Not essential for stability, unknown function	82	
Swi3p	Complex assembly	93	Snf6-Snf12-Swi3 module
Snf6p	DNA-binding and complex assembly	37	
Snf12p	Complex stability	73	
Swi1p	DNA binding	148	Swi1 module
Rtt102p	peripheral member	177.9	Arp module
Arp9p	Promotes Snf2 ATPase activity	53	
Arp7p	Promotes Snf2 ATPase activity	54	

Table 1. 3: The yeast Swi-Snf subunits. The 12 protein subunits of the Swi-Snf complex in yeast and their size and function [83], [89].

The ARP module within SWI/SNF plays a significant role in nucleosome binding, primarily through its interaction with extra-nucleosomal DNA. This interaction is pivotal to complex function and underscores the conserved nature of the ARP module, which is present in various chromatin-modifying complexes. It is plausible to propose that the ARP module serves as a universal mechanism for chromatin-remodeling complexes to engage with linker or nucleosomal DNA, thereby initiating nucleosome binding.

By undergoing continuous conformational changes, the ARP module facilitates the engagement of the nucleosome substrate onto the ATPase catalytic core. This process promotes concerted nucleosomal binding, crucial for the remodeling activity of the complex. While not essential for the assembly of remodeler complexes like SWI/SNF or RSC, the ARP module plays a crucial regulatory role in modulating ATPase activity [90], [91].

In summary, the SWI/SNF chromatin remodeling complex plays a crucial role in modulating chromatin structure and gene expression by regulating the accessibility of DNA to transcription factors and other regulatory proteins. The complex uses the energy from ATP hydrolysis to remodel nucleosomes, leading to changes in chromatin organization and gene activity.

1.5.2.2 The Swi-Snf complex in humans and its role in disease

The yeast SWI/SNF complex is essential for controlling gene expression by making gene promoters more accessible for transcription initiation. In humans, there are two analogs of the yeast Swi-Snf complex known as "BRG1- or BRM-associated factors" (BAF or SWI/SNF-A) and "Polybromo-associated BAF" (PBAF or SWI/SNF-B) [92]. The human SWI/SNF complexes have been linked to various diseases, particularly cancer. Indeed, nearly 25% of all cancers have mutations in subunits of the human SWI/SNF complexes, many of which are loss-of-function mutations, suggesting a tumor suppressor role [93]. Mutations in the components of the human SWI/SNF complexes can disrupt normal cellular functions and lead to uncontrolled cell growth and cancer development. For example, research has shown that the SWI/SNF complex interacts with key signaling pathways and transcription factors, including those involved in inflammation and the NF-κB signaling pathway, which are critical for maintaining normal cell functions and preventing diseases [94]. Some example of cancers associated with mutations in the human Swi-Snf complex are Ovarian Clear Cell Carcinomas, Cholangiocarcinomas, Clear Cell Renal Cell Carcinomas, Small Cell Carcinoma of the Ovary, Hypercalcemic Type and Rhabdoid Tumor Predisposition Syndromes [95].

Mutations in human Swi-Snf subunits are also linked to several neurodevelopmental disorders and intellectual disabilities, such as Coffin-Siris syndrome, Nicolaides-Baraitser syndrome, Kleefstra's syndrome spectrum, autism spectrum disorder, and schizophrenia [96].

In summary, as in yeast, the human SWI/SNF complex is also a key player in chromatin remodeling and gene regulation. Its proper function is vital for preventing diseases, and its disruption can lead to various pathologies, especially cancer. Ongoing research continues to uncover the complex's diverse roles in human health and disease, highlighting its potential as a therapeutic target. On that note, SWI/SNF-associated cancers are particularly susceptible to bromodomain inhibitors. Targeting pathways

involving SWI/SNF complexes has become a focus for cancer therapy, with bromodomain inhibitors showing promise as potential therapeutic agents [97].

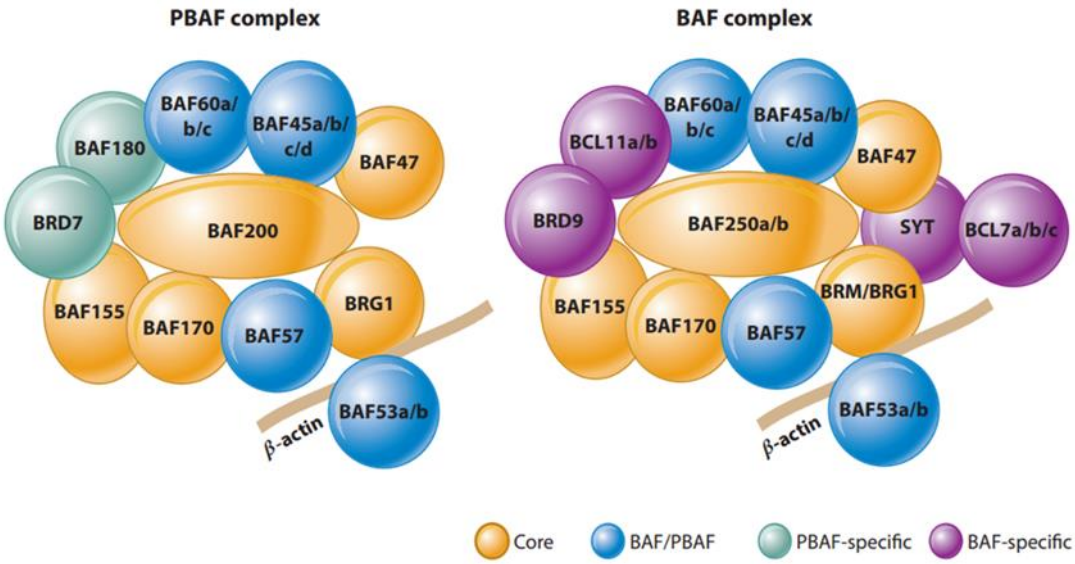

Figure 1. 11: The SWI-SNF complex homologues in human cells. The BAF and PBAF SWI/SNF complexes are depicted [98].

1.5.2.3 The relationship between Swi-Snf and histone post-translational modifications: the histone code hypothesis in action.

The Swi-Snf complex is the most well-studied chromatin remodelling complex which has been shown to play roles in various cellular events such as transcription and DNA damage repair [99]. The acetylation of histones by Gcn5p can impact the activity of the Swi-Snf complex, as the bromodomain within the Swi-Snf complex has an affinity for acetylated histones, which may modulate Swi-Snf complex recruitment and stability [100]. The interplay between Swi-Snf and histone acetylation is important because they both contribute to the regulation of gene expression. The Swi-Snf complex is involved in modification of physical structure of chromatin, making it more or less accessible, whereas Gcn5 modifies histones to either promote or inhibit transcription. Their mutual actions ensure that genes are expressed at the right time and place, which is vital for proper cellular function and response to environmental stimuli. Furthermore, the Swi-Snf complex and Gcn5 have been shown to share a number of target genes, suggesting that they may work together to coordinate the regulation of these genes. This overlapping function is demonstrated by genes such as *SUC2*, *FLO1, HO, PHO5*, and *GAL1*, where both the Swi-Snf complex and Gcn5p histone acetylation activity are implicated in their regulation [101]. Taken together, the Swi-Snf chromatin remodeling complex and the Gcn5p HAT are interrelated in their roles, with each playing a complementary role in modifying chromatin structure and histone marks to activate or inhibit transcription as needed.

The SWI/SNF complex can also influence the activity of COMPASS by altering the accessibility of chromatin. For instance, if the SWI/SNF complex exposes a gene promoter region, COMPASS can methylate H3K4, leading to gene activation. Conversely, if the SWI/SNF complex functions to obscure a gene promoter, Clr4 can methylate H3K9, leading to gene repression. Furthermore, the methylation marks set by COMPASS and Clr4 can also affect the binding and activity of the SWI/SNF complex. For example, the SWI/SNF complex has been shown to have an affinity for chromatin

regions marked by H3K4me3 by COMPASS, which signifies active transcription [102]. The relationship between these complexes is not just sequential but also reciprocal, as they can regulate each others binding and activity on chromatin. This dynamic interaction ensures that genes are expressed at the right time and place, and to the optimum levels, which is vital for proper cellular function and response to environmental stimulation.

1.6 The Tup1-Cyc8 co-repressor complex

The Cyc8–Tup1 complex in *Saccharomyces cerevisiae* is made up of a single Cyc8p (Ssn6p) subunit and four Tup1p subunits, as detailed by Varanasi *et al*. in 1996 [103]. The complex has a size of 1.2 MDa (Fig. 1.12) [103]. Approximately 3% of all *S. cerevisiae* genes can be repressed by Tup1-Cyc8. Mutant strains of this complex have been shown to exhibit various behaviors such as flocculation, slow growth, loss of glucose repression, and inappropriate expression of certain genes [104]. Neither Tup1p nor Cyc8p directly bind to DNA. Instead, several DNA-binding proteins recruit Tup1-Cyc8 to specific gene subsets. As a result, Tup1-Cyc8 influences the transcription of genes regulated by factors such as glucose and oxygen availability, DNA damage, and cell type [1], [10].

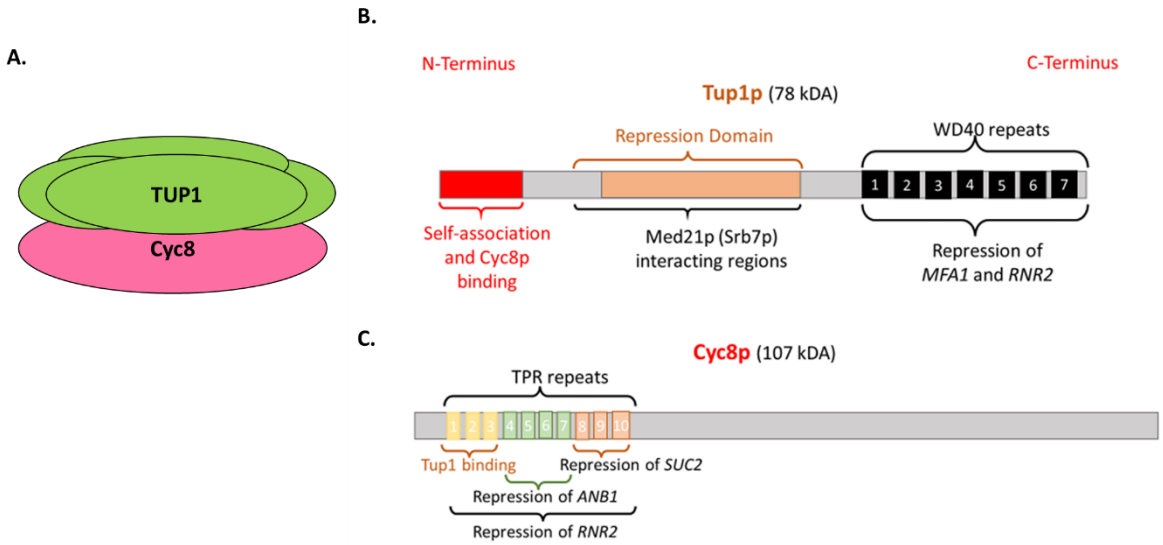

Figure 1. 12: The yeast Tup1-Cyc8 complex. (A) 4 Tup1p subunits (green), accompanied by Cyc8p subunit (pink). **(B)** Schematic illustrating the specific regions correlated with the established functions of Tup1p. The crucial domains responsible for self-association and binding to Cyc8p, along with the repression domain and WD40 repeats, are highlighted. **(C)** This schematic illustrates the TPR motifs positioned at the N-terminus of Cyc8p. The figure in (B, C) was taken from published data [105].

Near its N-terminus, Cyc8p contains ten copies of the 34-amino-acid tetratricopeptide repeat (TPR) motif, with repeats 1–3 being primarily significant for its interaction with Tup1 [106], [107]. At its C-terminal end, Tup1p harbours seven copies of a WD40 sequence domain, also referred to as the β-transducin motif. This domain is essential for repressing certain target genes but not necessary for repression of others, like *SUC2*. The N-terminal residues 1–72 of Tup1p is essential for its interaction with Cyc8p and for self-association. However, this region is not necessary for repression [108].

Tup1p shares homology with the Groucho protein in Drosophila and human TLE corepressors, which are pivotal in the gene regulation of multicellular eukaryotes.

The generalised model for Tup1-Cyc8 complex function suggests that Cyc8p serves as an adaptor protein, facilitating binding with targeting proteins and Tup1p, whereas Tup1p fulfils the repressive function within the complex [108] Certainly, studies have demonstrated that elevating *TUP1* expression alone is adequate to suppress the transcription of Mat-a specific genes [109]. Nevertheless, cells with elevated *TUP1* levels exhibited a flocculant and slow-growth phenotype, indicating that simply increasing *TUP1* expression isn't adequate to suppress all genes regulated by Tup1-Cyc8 [109].

Moreover, evidence indicates that the complex can also participate in gene activation, although this impact is observed at a smaller subset of genes [110], [111].

Various mechanisms have been suggested to elucidate how the Tup1-Cyc8 complex induces gene repression [104] Studies have demonstrated that the complex interacts with and facilitates the presence of hypoacetylated chromatin, leading to gene transcription repression[112], [113]. Other research indicates its role in maintaining a structured arrangement of nucleosomes over gene promoters, to obstruct transcription initiation [114]. Tup1-Cyc8 has also been proposed to interfere with the function of transcription factors and the general transcriptional machinery, thereby directly repressing gene transcription. More recent findings propose its primary

function is to obstruct the activation domains of transcription factors bound to target genes, thereby inhibiting transcription [115].

However, the suggested mechanisms of action are not necessarily mutually exclusive. In fact, it has been demonstrated that complete depression at specific target genes occurred only when multiple repression mechanisms employed by Tup1-Cyc8 were disrupted [116]. Different genes may require distinct mechanisms of action, or combinations thereof, to regulate their transcriptional state in response to environmental fluctuations.

1.7 Antagonistic regulation of gene transcription by the Swi-Snf and Tup1-Cyc8 complexes

The Swi-Snf complex is considered as a coactivator of gene transcription, while the Tup1-Cyc8 complex has been characterised as a general corepressor of gene transcription. Their antagonistic action in regulating gene transcription has been analysed at the well-studied *FLO1* and *SUC2* genes. The *SUC2* gene in *S. cerevisiae* encodes invertase, an enzyme crucial for sucrose utilization [117]. The *FLO1* gene contributes to the production of cell-wall proteins which mediate a cell aggregation phenotype called flocculation. These genes illustrate chromatin-mediated gene regulation, presenting valuable insights into the interplay between these two archetypal regulatory complexes (Fig. 1.13) [118].

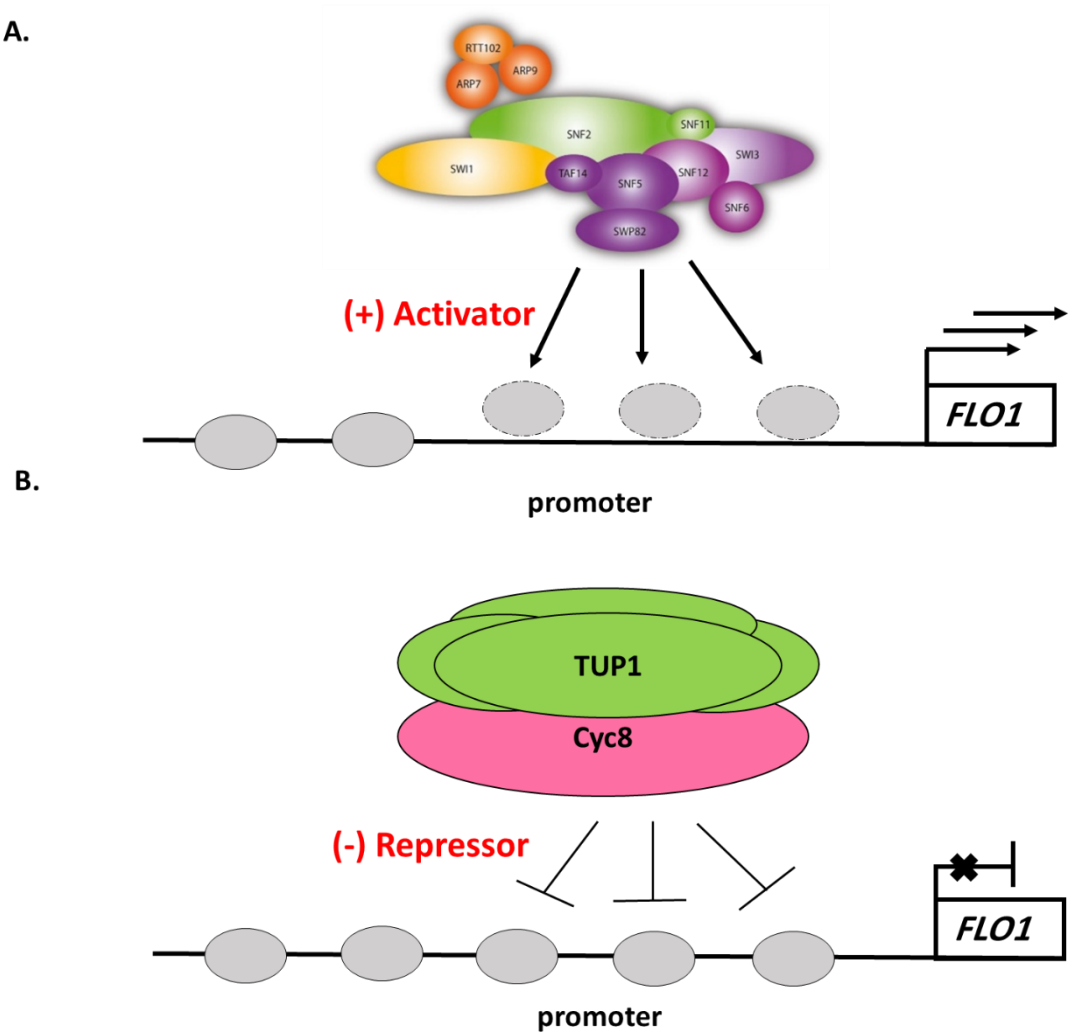

Figure 1. 13: Swi-Snf as an activator and Tup1-Cyc8 (Ssn6) as a repressor of transcription. Schematic to show a gene subject to co-regulation by the Swi-Snf and Tup1-Cyc8 complexes. **(A)** Swi-Snf complex removes the nucleosomes (grey ovals, hatched outline) at the *FLO1* promoter to enable transcription initiation (indicated by arrows and the + sign. Conversely, the Tup1-Cyc8 complex strongly positions nucleosomes (grey ovals, solid outline) at the *FLO1* promoter to repress transcription (indicated by absence of arrows and the – sign [114].

1.8 The objective of this study

- Examine the role of each subunit in cell function and transcription.
- Analyse global Swi-Snf subunit occupancy.
- Compare the global transcriptome data in Swi-Snf subunit mutants with global Swi-Snf subunit occupancy data.
- Investigate the role of Swi-Snf in gene repression.
- Investigate an interplay between the Tup1-Cyc8 and Swi-Snf complexes.

Chapter 2

Materials and Methods

2.1 Yeast strains and growth conditions

Yeast strains used in this study are listed in (Table 2.1). Yeast extract peptone (YEP) broth (1% (w/v) yeast extract, 2% (w/v) peptone, and 2% (w/v) glucose and YEP agar (All Foremedium) were used for growth. Unless otherwise stated cells were grown at 30°C with shaking at 200 rpm. Start to Inoculate 10 ml YEP with a single yeast colony (overnight). This culture was used to inoculate a larger volume of YEP (50ml in a conical flask) the next day, this was left to grow until the desired OD600 was reached (OD_{600} 0.6-0.8 it was considered to be log phase) measured using a spectrophotometer.

Yeast Strains with autotrophic markers were grown in a synthetic complete (SC) medium prepared using 0.19% yeast nitrogen base, 0.059% complete supplement medium, 0.5% (NH4)2SO4, and for solid media 2% agar was added. This media was autoclaved and then glucose was added to a final concentration of 2%, amino acids were then added or omitted as required.

Strain	Genotype	Source	Used for
BY4741 (wt)	*Mat* a *his3Δ1 leu2Δ0 met15Δ0 ura3Δ0*	(Baker Brachmann *et al.*, 1998) [119]	RNA-Seq analysis
snf2	FY2083. *MATa, his3-Δ200, ura3Δ0, trp1-Δ63, lys2Δ0, met15Δ0, snf2::KAN*	F. Winston [120]	RNA-Seq analysis
snf2K798A *(snf2cat)*	FY2084. *MATa, ura30 snf2-798*	F. Winston [120]	RNA-Seq analysis
swi3	*MATa, his3-Δ200, ura3Δ0, trp1-Δ63, lys2Δ0, met15Δ0, swi3::KAN*	ResGen library	RNA-Seq analysis
snf5	*MATa, his3-Δ200, ura3Δ0, trp1-Δ63, lys2Δ0, met15Δ0, snf5::KAN*	ResGen library	RNA-Seq analysis
snf6	*MATa, his3-Δ200, ura3Δ0, trp1-Δ63, lys2Δ0, met15Δ0, snf6::KAN*	ResGen library	RNA-Seq analysis
snf11	*MATa, his3-Δ200, ura3Δ0, trp1-Δ63, lys2Δ0, met15Δ0, snf11::KAN*	ResGen library	Phenotypic tests
snf12	*MATa, his3-Δ200, ura3Δ0, trp1-Δ63, lys2Δ0, met15Δ0, snf12::KAN*	This study	Phenotypic tests
taf14	*MATa, his3-Δ200, ura3Δ0, trp1-Δ63, lys2Δ0, met15Δ0, taf14::KAN*	ResGen library	Phenotypic tests
swp82	*MATa, his3-Δ200, ura3Δ0, trp1-Δ63, lys2Δ0, met15Δ0, swp82::KAN*	ResGen library	Phenotypic tests
swi3 cyc8	MATa, his3-Δ200, ura3Δ0, trp1-Δ63, lys2Δ0, met15Δ0, *swi3::KAN*, *cyc8::URA3*	Fleming Lab	RNA-Seq analysis
cyc8	MATa, his3-Δ200, ura3Δ0, trp1-Δ63, lys2Δ0, met15Δ0, *cyc8::URA3*	Fleming Lab	RNA-Seq analysis

Strain	Genotype	Source	Used for
(YEL044) HHY221	*W303 MATa TOR1-1 fpr1Δ::loxP-LEU2-loxP rpl13a::RPL13A-2×FKBP12-loxP*	(Haruki et al., 2008) [121]	Anchor away
Swi3 Myc	*Mat a*; *his3Δ1*; *leu2Δ0*; *met15Δ0*; *ura3Δ0 SWI3::Kan-9myc*	Fleming Lab	Co-IP experiment
Cyc8 HA	*Mat a*; *his3Δ1*; *leu2Δ0*; *met15Δ0*; *ura3Δ0 CYC8::hphNT1-3HA*	Fleming Lab	Co-IP experiment
Swi3Myc-Cyc8HA	*Mat a; his3Δ1; leu2Δ0; met15Δ0; ura3Δ0 SWI3::Kan-9myc CYC8::hphNT1-3HA*	Fleming Lab	Co-IP experiment

Table 2.1: Yeast strains used in this study

2.2 Growth Curve and Final Cell Density

The YEPD liquid medium was used for growing cells, and ThermoSpectronic (Genesys 10UV) was used to measure OD600. The measurements were taken every 2 hours by combining a 90 µl sample with 10 µl H2O. The final cell density was determined after 24 and 48 hours of growth in YPD using a hemocytometer.

2.3 Microscope images of the yeast cells (cell morphology)

Yeast cells were grown to the mid-log phase in YEPD at 30°C, and then the cells were washed with sterile water. Next, 20 µl of the samples were spotted onto a glass slide and viewed under 100X oil immersion magnification. Leica Application Suite (LAS) software was utilized for capturing and visualizing the images.

2.4 Spot tests

After reaching the mid-exponential stage of growth, a haemocytometer was used to count the cells. The cultures were resuspended in YEP media at 1 X 10^7 cells/ ml and 10-fold serial dilutions were prepared and were spotted (2.5 µl of each sample/spot)

onto YEP agar plates grown for 3 days at 30 °C. The different reagents and different temperatures used are indicated, as appropriate.

2.5 Yeast cell transformation (High-efficiency LiAc transformation)

High-efficiency LiAc transformation procedure was used to transformed the yeast cell based on the protocol[122]A 50 ml culture of YEPD was inoculated to $5x10^6$ cells /ml and and incubated at 30°C, with shaking (200rpm), until a cell density of 2×10^7 was reached (~2 doubling). The cells were resuspended in 1 ml of sterile 100mM Lithium acetate (LiAc) and transferred to a 1.5ml microcentrifuge tube. Cells were pelleted at top speed for 30 seconds and the LiAc was removed. Then, the cells were resuspended in 500 µl of 100 mM LiAc, giving a final cell density of 2×10^9 cells/ml. Then, the suspension was vortexed and divided into 50 µl aliquoted into 1.5 Eppindorfe tubes for each transformation mix. The cells were pelleted and LiAc was removed. The transformation mix was added to each cell pellet. The transformation mix consisted of 240 µl PEG (50% w/ v PEG 3350) polyethylene glycol, 36 µl 1M LiAc, 25 µl of 10 mg/ml single-stranded DNA from salmon testes (Sigma) that had been boiled at 95°C for 5 minutes and then placed on ice and 1 µg DNA. This mixture was increased to 360 µl with Sterile water, and vortexed vigorously for 1 minute. Then, incubated the mix in a water bath at 42°C for 40 minutes. The cells were then centrifuged at 7000 rpm for 30 seconds and the transformation mix was gently removed with a micropipette. The cell pellet was resuspended in 1 ml of sterile water. For transformants involving auxotrophic markers, cells were plated directly onto selective media. For transformations involving antibiotic markers, the cells were incubated in 5 ml of YPD and overnight at 30°C, 200 rpm. The next day the cells were centrifuged for 5 minutes at 453 g, after this step the supernatant was removed and the cells were plated onto the selective media.

2.6 Gene deletions and epitope tagging

The gene deletions and tagging of target genes were carried out by PCR-mediated gene disruption adapted from [123], [124]. The primers (60bp) were constructed for gene deletions including auxotrophic markers. These primers contained 5' 40bp overhangs that were complementary to regions up and downstream of the target open read frame (ORF), as well as 20bp 3' sections that were complementary to a plasmid bearing an auxotrophic marker (Fig 2.1) (Table 2.2). The pRS406 vectors, which include auxotrophic markers, were acquired from EUROSCARF and the published protocol was followed. All gene deletion mutants were confirmed by PCR via the strategy as shown in Fig. 2.2 using confirmation of the *snf12* gene deletion mutant as an example.

Name	Sequence (5’-3’)	Description
ACT1-F	CTGAATTAACAATGGATTCTGG	PCR control
ACT1-R	AGATACCTCTCTTGGATTGAGC	PCR control
URA3con-F	GCAAGGGCTCCCTAGCTACT	Gene deletion
URA3con-R	AATGCGTCTCCCTTGTCATC	Gene deletion
HIS3co-F	GACGACCATCACACCACCACTGA	Gene deletion
HIS3con-R	GATCATTCTTGCCTCGCAGA	Gene deletion
Snf2PRS-F	ATG AAC ATA CCA CAG CGT CAA TTT AGC AAC GAA GAG GTC AGA TTG TAC TGA GAG TGC AC	Gene deletion
Snf2PRS-R	CTA TAC ACT CGC TTC TGT CAT GCT CGA GTC CGC TTC ATC TGG CTG TGC GGT ATT TCA CAC CG	Gene deletion
Swi3con-F	CAG GAT GGC CAA TGA TGT TA	Gene deletion
Swi3con-R	CAA GTC AAG TGA CGC ACC AT	Gene deletion
Snf11con-F	TTG TTT TGC CGG GTA ACA AT	Gene deletion
Snf11con-R	CTG TAC TTG CTC TGC GGG TA	Gene deletion
Snf5-DF-F	AAG TGG AGG CTA AGC ACC AA	Gene deletion
Snf5-DF-R	CTT GTT CCC TCA GCT GGT GT	Gene deletion
Snf6con-F	ATC CAG AAA GGG GAG GCT AA	Gene deletion
Snf6con-R	GCA GTA GCT GCA CAA ATC CA	Gene deletion
SNF12con-F	CGCGGGAAATCCTTCAGGAC	Gene deletion
SNF12con-R	GTGGCCCTCATCTCTACTAC	Gene deletion
Swi1con-F	CGATTACGAAACGACGCCAC	Gene deletion
Swi1con-R	CCAAGATGTGACTTCATGGC	Gene deletion
Taf14con-F	CAC GTC AAG GCT GTA GTG CG	Gene deletion

Taf14con-R	CTA GCA ACC TGG TCC CCT CG	Gene deletion
Swp82con-F	CCG TTC AGA AAG TGG CCC TG	Gene deletion
Swp82con-R	CCA ATT GTG CAC ATG CAT TC	Gene deletion
Swi1-del-pRS-F	CAGATTATTGTTCACCAGGTAATAATCACTGA CTGGCGGCAGATTGTACTGAGAGTGCAC	Gene deletion
Swi1-del-pRS-R	ACTAAAGGCGCTCTTCCGACTGTATTGTTTCCA TAAGGTCCTGTGCGGTATTTCACACCG	Gene deletion
Swi1 AA-F	ACT TTA CAA TTT AAA AAA TGA TAT CCT AAC CAA TTT GGA ACG GAT CCC CGG GTT AAT TAA	Anchor away
Swi1 AA-R	GGA AGA AAT AAG CAG TAA AAG AAT ATT GTT TAA AAA AAT CGC AGA ATT CGA GCT CGT TTA AAC	Anchor away

Table 2. 1: Primers used in strain construction and confirmation in this study.

Plasmid	Selectable marker	Used for	Source
pRS406	URA3	deletion mutant construction	Christianson et al., 1992 [125]
pRS413	HIS3	transformation control	Christianson et al., 1992 [125]
pFA6a-FRB-His3Mx6	HIS3	Anchor away	(Haruki et al., 2008) [121]

Table 2. 2: Plasmids used in this study.

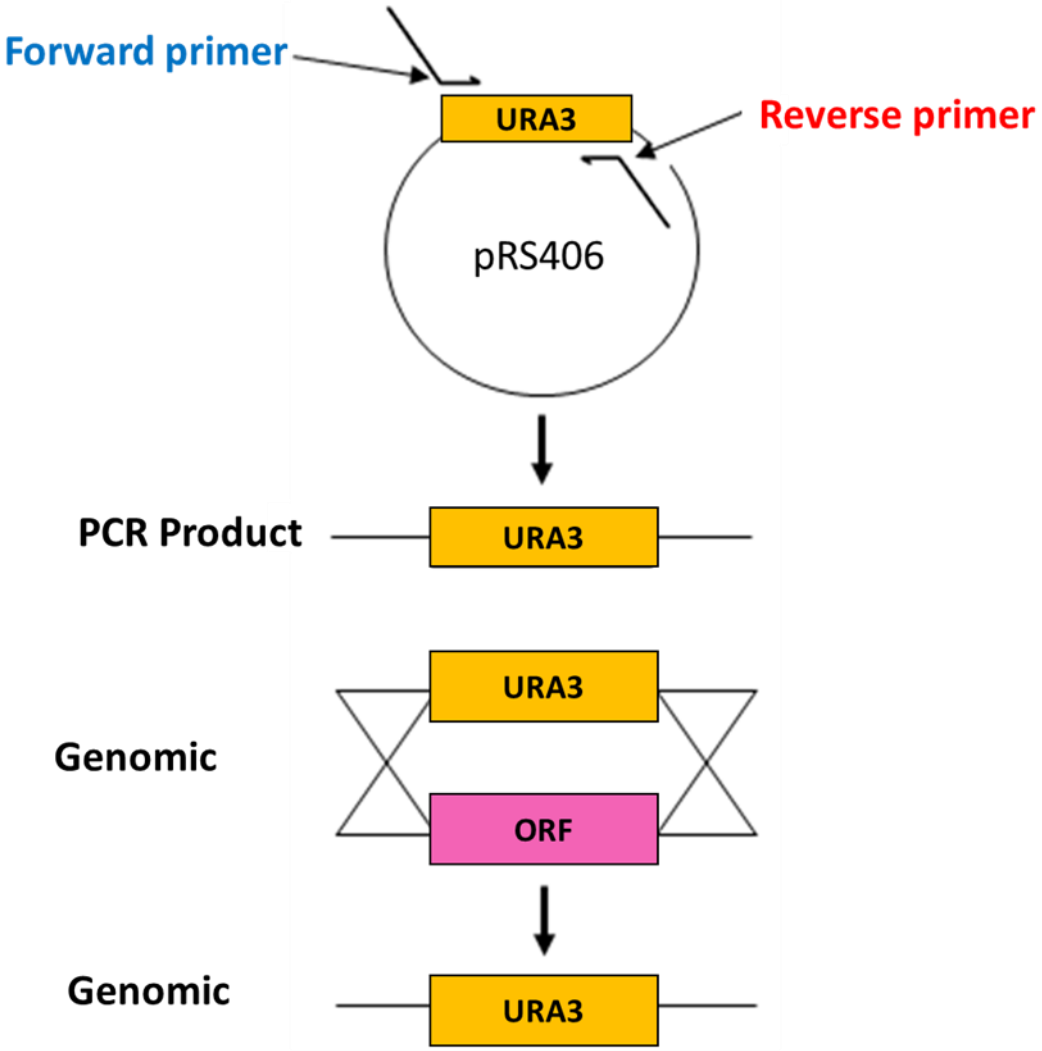

Figure 2. 1: Gene deletion process. Gene deletion fragments were produced by using primers that are complementary to the template plasmid and contained 40bp of DNA sequences that were homologous to the DNA flanking the gene that was selected for removal meaning that the selectable marker was substituted for the target ORF using homologous recombination [119].

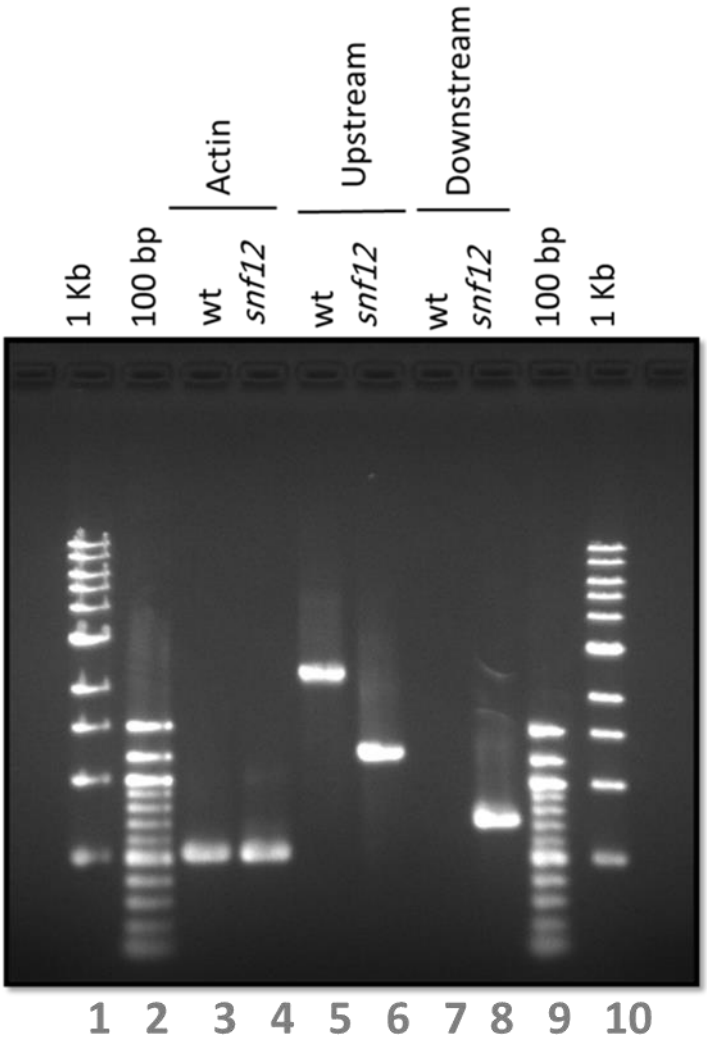

Figure 2. 2: PCR amplification to confirm the *snf12* gene deletion mutant: lane (1) 1Kb marker, lane (2) 100bp marker, lane (3 and 4) wt actin and *snf12* actin, lane (5 and 6) upstream wt and snf12 primers (1136 bp) which is positive in mutant and negative in wt lane (7 and 8), Lane (6) was the wt fragment which is 2210 bp.

2.7 DNA Extraction

To extract the DNA, 10 ml overnight culture was centrifuged at 376 rcf for 5 minutes. The supernatant was discarded and yeast cells were resuspended in 1 ml of water and transferred to a 1.5 ml microcentrifuge tube. Then, the cells were pelleted by centrifugation at 16,363 rcf for 5 minutes and the supernatant was discarded. Pellets were resuspended in 200 µl breaking buffer (2% Triton X-100, 1% SDS, 100mM NaCl, 10mM Tris-Cl [pH8.0], 1mM EDTA [pH8.0]) and 200 µl of 400-600 µm glass beads (Sigma) were used, and 200 µl phenol/chloroform/isoamyl alcohol were added to the suspension and the samples were mixed by vortexing for 3 minutes. 200 µl TE (pH 7.5) was added the samples were mixed and briefly vortexed and centrifuged at 16,363 rcf for 5 minutes. The upper aqueous layer was transferred to a new 1.5 ml microcentrifuge tube and 400 µl of chloroform was added. Then, this was centrifuged at 16,363 rcf for 5 minutes the upper layer was transferred to a new 1.5ml tube and 1ml of 100% ethanol was added. DNA was pelleted by centrifugation at 16,363 rfc for 5 minutes. The supernatant was discarded and the DNA pellet was resuspended in 500 µl 70% ethanol. DNA was pelleted by centrifugation at 16,363 rcf for 5 minutes and the DNA pellet was dried and resuspended in 400 µl TE (pH 7.5) and 25 µg of RNase A. This was incubated at 37°C for 1 hour. DNA was then ethanol precipitated.

2.8 Ethanol Precipitation

The DNA was precipitated by adding 0.4 volume of 4 M Lithium Chloride and 3 volumes of 100% ethanol. This was stored at -20°C for 1 hour. Precipitated DNA was then pelleted by centrifugation at 16,363 rcf for 10 minutes and then resuspended in 500 µl 70% ethanol. The DNA was further pelleted by centrifugation at 16,363 rcf for 5 minutes and the pellet was dried in a heatblock at 37 °C and then resuspended in the desired volume of either nuclease free water or TE buffer, pH 8.0.

2.9 RNA Extraction

The RNA extracted used the Hot Phenol method adapted from Current Protocols [126]. 50 ml cells were grown to the mid-log phase (0.6-0.8 OD600), and then a 5 ml volume of culture was pelleted by centrifugation for 5 minutes at 453 g, the pellet after resuspended into 1 ml of sterile water then transferred to 1.5 ml tube and pelleted by centrifugation, the pellets stored at -80°C (at this stage). The cell pellet was resuspended in 400 ml TES (10 mM Tris-Cl pH=7.5, 10 mM EDTA pH=8, 0.5% w/v SDS) and 400 µl saturated phenol. Then, incubate this at 65°C for 1 hour with occasional vortexing for 15 seconds. Followed by placing the sample on ice for 5 minutes and then centrifuged for 5 minutes at 16,363 g. The upper layer (aqueous layer) was transferred to a new 1.5 ml Eppendorf tube, 400 µl of saturated phenol was added and the sample was vortexed, then centrifuged for 5 minutes at 16,363 g. The aqueous layer was then transferred to a new 1.5 ml Eppendorf tube and 400 µl of chloroform was added and centrifugation at 16,363 g for 5 minutes. The upper aqueous layer then was transferred to a new 1.5 ml Eppendorf tube and 40 µl of sodium acetate (4M, pH=5.3) was added, and then 1 ml of ice-cold 100% v/v ethanol. This mix was stored at -20°C for one hour, then centrifuged for 10 minutes at 16,363 g at 4°C. The pellet was then washed with ice-cold 70% (v/v) ethanol and centrifuged for 5 min at 16,363 g at 4°C. After the pellet was dried resuspended in nuclease free water. The concentration of the RNA samples was measured using a NanoDrop ND-100 spectrophotometer (Thermo Scientific) measured at an absorbance wavelength of 260 nm.

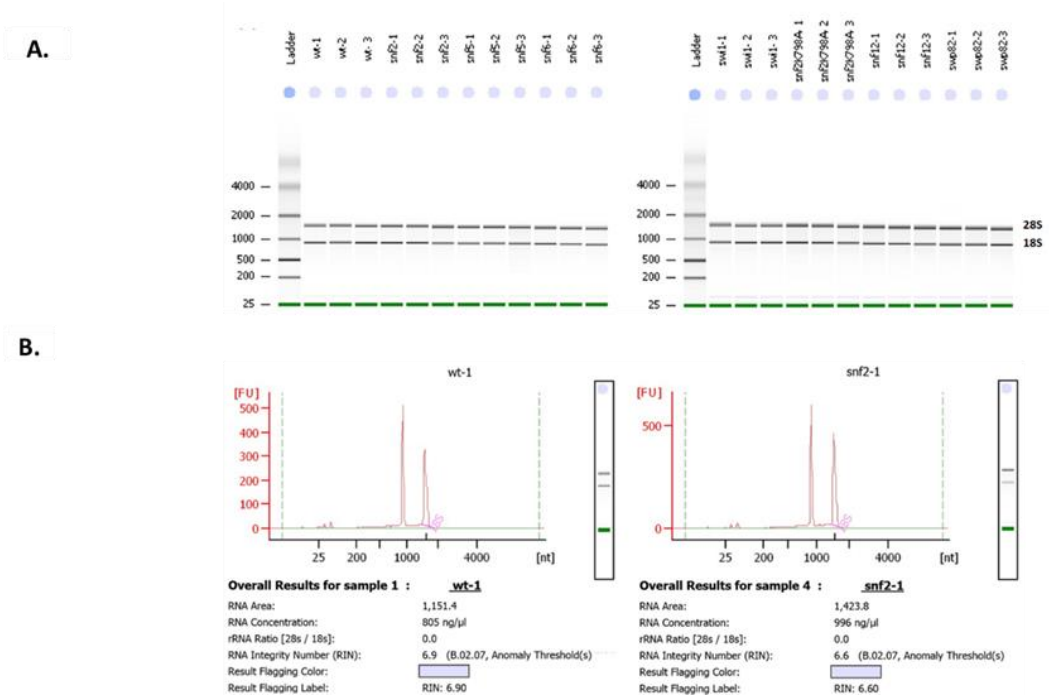

Figure 2. 3: RNA sample preparation for RNA-Seq analysis. (A) RNAnano bioanalyzer image showing the 28S and 18S rRNA bands from total RNA prepared from the samples indicated. **(B)** Chromatograms showing RNA integrity (RIN) using RNAnano bioanalyzer 2100.

2.9.1 Protein extraction

Protein was extracted by using a 20% trichloroacetic acid (TCA) Protocol [127]. Overnight culture were grown in a 50 ml to the mid-log phase OD600 = 0.6-0.8. A cell volume equivalent to 10 OD units was taken and centrifuged at 376 rcf for 5 minutes. The supernatant was discarded, and the pellet was resuspended in 1 ml of 20% trichloroacetic acid (TCA), then transferred to a 1.5 ml microcentrifuge tube, and centrifuged at 16,363 rcf for 1 minute, discarded the supernatant again. The cell pellets were resuspended in 250µl 20% TCA and ~500µl of glass beads (400 600 µm) were added. By using a high-speed benchtop homogenizer the samples were vortexed for thirty seconds, then kept on ice for 1 minute, this step was repeated three times. The cell lysate was transferred to a new 1.5 ml microcentrifuge tube, and then the glass beads were washed using 500 µl 5% TCA. The wash was added to the cell lysate and stored on ice for 3 minutes. Following by centrifuged the cell lysate at 1,363 rcf for 1 minute. The supernatant was discarded, and the pellet was resuspended in 300 µl 1X Laemmli (0.1% 2-mercaptoethanol, 10% glycerol, 2% SDS &63 mM unbuffered Tris-Cl). This was incubated at 95° C for 5 minutes. and then centrifuged for1 minute at 16,363 rcf. The supernatant was then transferred to a new 1.5 ml microcentrifuge tube and stored at -20°C.

2.9.2 Bradford assay

The Bradford assay was performed according to the manufacturer's instructions (Sigma). Bovine serum albumin (BSA) standards of 2, 4, 6, 8, and 10 µg/ ml were prepared, and the protein samples were diluted in H2O. Then the Bradford reagent (Sigma) was added, and Absorbance (A595) was measured using a spectrophotometer. After that, the protein concentration was calculated by comparing absorbance values obtained from a standard curve, then the protein concentration was calculated. The working stocks of protein samples were adjusted to 2 mg/ ml using 1X Laemmli buffer and stored at -20°C.

2.9.3 SDS Polyacrylamide gel electrophoresis (PAGE)

The BioRad Mini cell system was used to prepare 12% (v/v) resolving gel (4 ml of 30% acrylamide, 0.38 M Tris-Cl (pH= 8.8), 0.001% w/v SDS, 0.001 % w/v ammonium persulfate and 0.001% v/v TEMED). 1 ml of isopropanol was added to the resolving gel to allow for polymerization. Then, the isopropanol was discarded and the stacking gel (1.65 ml 30% acrylamide, 78 mM Tris-Cl (pH=6.8), 0.0015 w/v SDS, 0.001% w/v APS and 0.001% v/v TEMED) was poured, and a plastic comb was added (the comb with 10 and 12 well) was used, before loading the protein samples into each well, the samples was boiled for 5 minutes at 95°C, 30 µg of each protein samples was used in each well. The gels were run at 100V for 120 minutes in running buffer (25 mM Tris, 190 mM glycine, 0.1% (w/v) SDS).

2.9.4 Western Blot

Western blotting protocol was adapted from current protocols [128]. The protein was transferred to a polyvinylidene fluoride (PVDF) membrane (Immobilon) in transfer buffer (25 mM Tris, 190 mM glycine, 20% v/v methanol) at 300 mA for 50 minutes with ice surrounding the Bio-rad equipment (Mini trans-blot 153BR). The PVDF membrane was soaked in methanol for 20 seconds and then 2 minutes in water, 2 sponges and 4 pieces of blotting paper were soaked in transfer buffer before useing. After the protein has been transferred to the membrane. The membrane was incubated at room temperature for 1 hour in blocking buffer (5% w/v dried skimmed milk in Tris-buffered saline with 0.05% v/v Tween 20 (Sigma). Following that the membrane was incubated with the primary antibody overnight at 4°C the primary antibody was used (see Table 2.4). The next day the membrane was washed in TBST (Tris-buffered saline, 0.1% Tween 20) for 5 minutes (4 times). Then the membrane was incubated at room temperature for 90 minutes with the secondary antibody in a blocking buffer. After that, Washing the membrane in TBST for 10 minutes only once, and then washed in TBS (Sigma) for 10 minutes (3 times). Echanced chemiluminescent (ECL) Western Blotting Substrate

(Pierce) prepared according to the manufacturers' instructions and the bound antigens were viewed using Imagequant LAS4000 imager.

Antibody	Concentration	Species	Source
β-actin	1:3000	Mouse	Abcam (ab8224)
α-Myc	1:5000	Mouse	Millipore (05-724)
α-Snf2	1:2000	Rabbit	J. Reece
α-Snf5	1:1000	Rabbit	Upstate
α-Swi3	1:1500	Rabbit	J. Reece
α-Cyc8	1:500	Goat	Santa Cruz (SC- 11953)
α-Tup1	1:1000	Goat	Santa Cruz (SC- 11951)

Table 2. 3. Antibodies used in Western Blots: Table to show the antibodies used in Western blots. All antibodies were diluted in 5 % skimmed milk in tris-buffered saline with 0.05% Tween 20 (TBST).

2.10 End-point Polymerase chain reaction (PCR)

The PCR was performed using MyTaq HS (Bioline) DNA polymerase mix according to the instructions provided by the manufacturer. The PCR reaction conditions: 1- Initial denaturation at 95 °C for 1 minute. 2- 30 cycles of denaturation at 95 °C for 15 seconds. 3- annealing for 15 seconds and extension at 72°C for 10 seconds. 4- This was followed by a final extension step for 2 minutes at 72°C. The annealing temperature was determined according to the primers used, the primers were designed using NCBI's BLAST.

2.11 Anchor away

Anchor away technique provides the making of a conditional mutant for any nuclear protein. The protocol used is adapted from the one utilized by Haruki et al [121]. The cells were cultured in a 50 ml solution overnight and the optical density at 600 nm was determined the next day. A sample was taken at Time Zero when the OD600 reached around (0.3 - 0.4) unless specified differently. Rapamycin from Fisher was introduced to the culture at a concentration of 1µg/ml. The culture was then incubated at 200 rpm at 30 °C.

Subsequently, samples were collected at the appropriate time intervals and then processed for RNA extraction or TCA protein.

In order to analyse the impact of loss of Swi1p upon gene transcription, I therefore attempted to prepare a conditional *swi1* mutant using the novel Anchor-Away technique. The protein of interest (Swi1p) is tagged with an FRB epitope (target) and the ribosomal protein RPL13A is tagged with an FKBP12 epitope (anchor). Upon addition of rapamycin, the anchor binds to the target, and the FRB-tagged Swi1p is shuttled out of the cell nucleus, bound to the FKBP12-tagged RPL13A. Following the design of the tagging oligonucleotides, I attempted to tag the Swi1 protein by integrating the tagging allele into the genome. Unfortunately, following repeated attempts and screening of possible positively selected candidates, I was unable to successfully tag the protein.

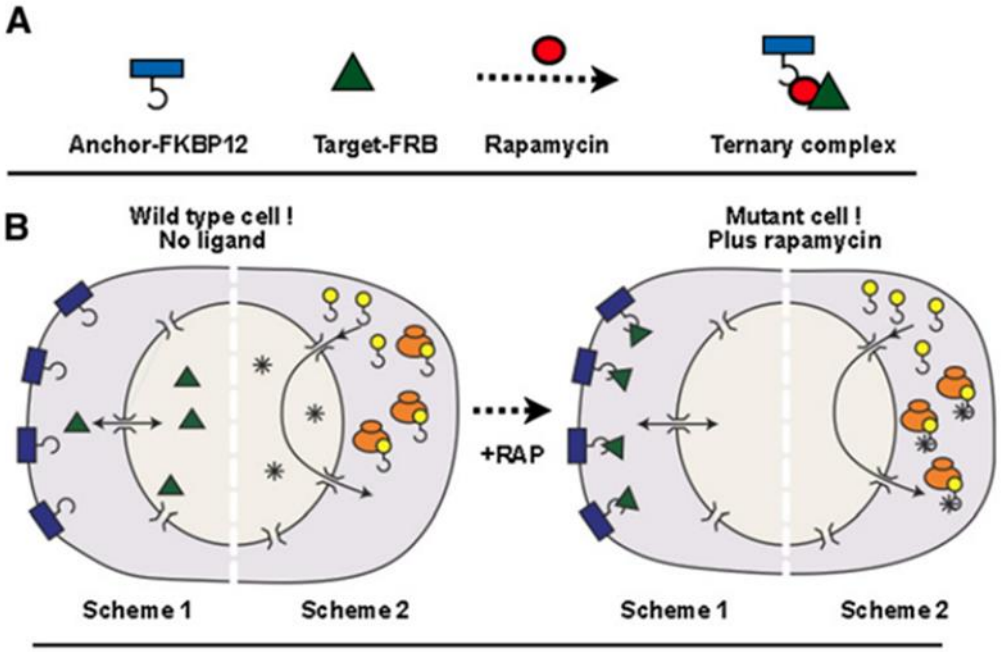

Figure 2. 4: The anchor away technique. Schematic depiction of the anchor away technique [121]. **(A)** The anchor and target C-terminally fused to the FKBP12 and FRB domains, respectively, and the ternary complex formed upon the addition of rapamycin. **(B)** Two main schemes were successfully applied to deplete the nucleus of target proteins.

2.12 Co-immunoprecipitation (Co-IP) of proteins from yeast

The coimmunoprecipitation technique has been examined using the adapted protocol from [129]. A volume of 250 ml of yeast cells was cultured till reaching an optical density (OD600) of ~1 – 2 cells pellet. The cells were then collected by centrifugation and washed once with 1x TBS. For each strain, 1 gram total of the cells was placed in two 2 ml screw-capped tubes with each tube containing (0.5 grams) of the strain. The pellets should be measured (e.g. 0.5 g, 0.46 g), and then the pellet tube should be stored at -80°C until the experiment is ready to begin. The procedure consists of the following steps:

To prepare whole cell lysates: add 0.1 ml of ice-cold, newly made 1x lysis buffer to each 0.1 g of frozen cell pellets. The tubes are placed on ice. Each tube was supplemented with 400 µl of 0.5 mm glass beads. Operate the tubes in a bead-beating apparatus for 45 seconds at a high intensity to achieve homogenization. Chill all tubes on ice for a duration of 5 minutes prior to applying a second 45-second pulse. Once more, position the tubes on the ice surface, repeating this action a total of 7 times. Using a 21-gauge needle, create a small hole in the bottom of each tube. Gently insert each punctured tube into a collecting tube that is the right size, such as a 5-ml polypropylene round-bottom tube. Place the samples in a chilled centrifuge, such as Eppendorf 5702R or Sorvall RC5C, and spin them for 5 minutes at a speed of 200 times the force of gravity (200×g). Delicately mix the liquid that passed through with a pipettor and transfer the entire amount to a 1.7-ml microcentrifuge tube. The effluents from identical strains can be consolidated into a single microcentrifuge tube. Centrifuge the tubes in a chilled microcentrifuge at maximum speed (~20,000×g) for a duration of 5 minutes. Transfer the resultant supernatants into sterile microcentrifuge tubes using a pipette (this is the whole cell lysate tube).

Before starting the normalization step 2µl of the whole lysate was taken in a new 1.5 microcentrifuge tube for each strain (the Input tube).

Normalization of cell lysates: Cell lysates were adjusted by protein concentration to ensure identical amounts of protein were supplied to each IP sample. The Bradford reagent was produced according to the manufacturer's instructions for an assay reagent with an equivalent protein concentration. A 1:20 dilution was prepared for each entire cell lysate obtained in (Step 1) using water. Three cuvettes containing Bradford or protein assay reagent were prepared for each strain. These cuvettes were then filled with diluted lysate, with the amount of lysate increasing in each cuvette. For instance, include 3 microliters, 4 microliters, and 5 microliters. Additionally, prepare empty spaces by combining equal volumes of lysis buffer that has been diluted 1:20 with water. Obtained the optical density (OD595) measurement for each sample. Subsequently, the protein concentration of each sample was determined by averaging the OD595 value. To equalize the concentrations, all samples were adjusted by adding 1× lysis buffer.

Coimmunoprecipitation: involves incubating cell lysates with an antibody and beads to selectively isolate the target protein. To do each immunoprecipitation, extract 30 µl of the 50% slurry of protein A Sepharose (equivalent to 15 µl of densely packed beads) and transfer it to a microcentrifuge tube with low retention properties. Rinse the beads five times in a solution of Lysis Buffer with a concentration of 1×. Using a pipette, carefully mix the entire amount of beads with 1 ml of lysis buffer. After each washing step, rotate the tubes in a microcentrifuge at a speed of 500 times the force of gravity (500×g) for a duration of 1 minute. Then, cautiously extract the wash solution using a pipette. Dissolve the rinsed beads in 210 µl of 1× Lysis Buffer for each IP sample. Follow the supplier's recommendations to determine the correct quantity of antibody to use for each immunoprecipitation. Thoroughly combine the substances by carefully using a pipette. Assign a 1.7-ml microcentrifuge tube with low-retention properties to each immunoprecipitation (IP) sample. Transfer 200 µl of the mixture containing beads and antibodies into each of the tubes that have been labeled. Dispense 500 microliters of whole cell lysate into each immunoprecipitation tube, ensuring that all samples have been

adjusted to the same concentration as outlined in Step 2. Each tube contained a total volume of 700 µl, which consisted of both beads and lysate. Reserve the leftover lysate for the purpose of assessing protein levels, following the instructions provided in the final step of the coimmunoprecipitation section. The entirety of the specimens were collected. The sample was subjected to end-over-end rotation at a temperature of 4 °C for a duration of 2 hours. 2.5µg of antibodies were used per immunoprecipitation (IP).

Wash and elute the immunoprecipitants: Save 50 µl of the supernatant in a new microcentrifuge tube, This is the 'unbound tube' then normalize the unbound tube to 2µg/ml (unbound tube use in western blot lane).

Centrifuge the samples in a microcentrifuge at 500xg, 4 °C for 2 min the acceleration due to gravity, at a temperature of 4 degrees Celsius, for a duration of 2 minutes. Carefully extract as much of the liquid portion as feasible using a pipette. Reserve 50 µl of the liquid remaining after centrifugation and combine it with 50 µl of 2× sample buffer (supernatant without bound substances). Store small portions at a temperature of -20 °C and examine using Western blotting to evaluate the effectiveness of immunoprecipitation (Western blotting procedure). Each tube was treated with 1 ice-cold of wash buffer that had been chilled. Agitate and reconstitute all the beads by gently flipping each tube multiple times. The beads have been completely re-suspended in the wash buffer. Centrifuge all tubes at a speed at 500xg for 1 min the force of gravity (500×g) for a duration of 1 minute in a microcentrifuge maintained at a temperature of 4 °C. Subsequently, carefully extract the liquid portion above the sediment using a pipette. Wash once more. Next, 1 ml of wash buffer was introduced into each tube. Using a precision pipette, the beads were gently mixed and then transferred to a new 1.7-ml low-retention tube that had been cooled. Centrifuge all tubes at a speed of 500xg the force of gravity (500×g) for a duration of 1 minute in a microcentrifuge maintained at a temperature of 4 °C. Please perform an additional washing cycle. Subsequently, Rotate the tubes once more for a short period of time. A P20 pipette was utilized

to eliminate any surplus wash buffer. To elute, add 30 µl of 1× Laemmli buffer to each tube and briefly vortex. Position all tubes on a heat block set at a temperature of 65 °C, and allow them to incubate for a duration of 10 minutes. Agitate each tube in a swirling motion for a duration of 30 seconds. Centrifuge the samples in a microcentrifuge at the maximum speed of about 20,000xg the force of gravity (20,000×g) for a duration of 1 minute. Extract 30 microliters from each tube using a pipette and transfer it to a new 1.7-milliliter tube. These samples are the ones that were obtained through elution in the immunoprecipitation process. (The IP tube).

Analysis of immunoprecipitations: The immunoprecipitated proteins are separated by SDS-PAGE and then analyzed by Western blotting the antibodies were used (see Table 2.2) The 'Input' and (Unbound supernatant), IP samples are included to assess immunoprecipitation efficiency.

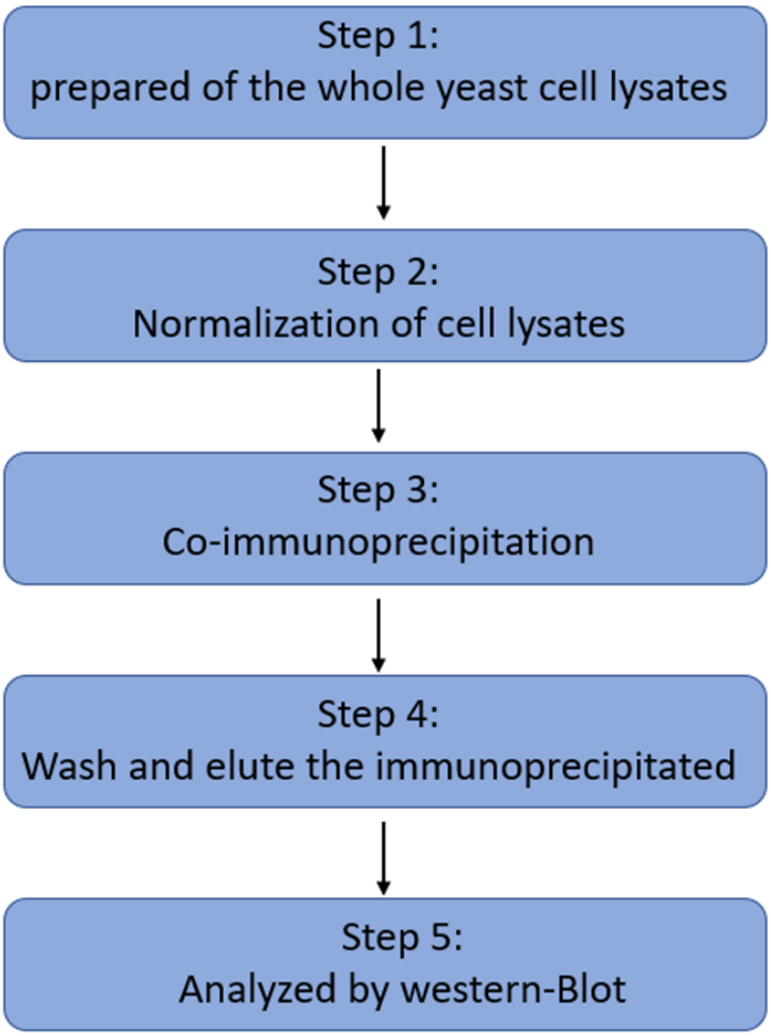

Figure 2. 5: Flowchart of the Co-IP protocol procedure [129].

2.13 Statistical analysis of experiments

GraphPad Prism 10 was used for statistical analysis. The statistical significance of a result was assessed using the One-Way or Two-Way ANOVA (as appropriate). The result was deemed statistically significant with a p-value of ($p<0.05$).

2.14 Bioinformatic analysis

2.14.1 RNA-Seq data

The RNA-Seq analysis was performed by Eurofins, who used Illumina HiSeq, and Illumina NovaSeq (NovaSeq 6000 S4 PE150 XP) (Table 2.5).

Dataset	**Sequencing Company**	**Sequencing Platform**	**Source**
wt, *snf2Δ*, *snf2K798A, swi3Δ, cyc8Δ* strains	Eurofins Genomics (Germany)	Illumina HiSeq	Published data [105], [130]
wt, *snf5Δ, snf6Δ* strains	Eurofins Genomics (Germany)	Illumina NovaSeq (NovaSeq 6000 S4 PE150 XP)	This study
wt, *swi3 cyc8* strains	Eurofins Genomics (Germany)	Illumina NovaSeq (NovaSeq 6000 S4 PE150 XP)	This study

Table 2. 4: Summary of genomics companies and sequencing platforms used for RNA-Seq.

2.14.2 Gene Ontology Analysis

The gene ontology analyses were carried out using: 1- *Saccharomyces cerevisiae* database (SGD), 2- panther gene ontology website, and 3- metascape website. The result is then presented by Prism GraphPad and Microsoft Excel.

2.14.3 Venn diagrams

The Venn diagrams were carried out using FunRich software, and the DeepVenn website.

2.14.4 Heatmaps

1- Heatmap2 R gplot packaging was used to generate the Heatmap figures for RNA-Seq analysis to see the differences in gene expression. 2- The gene ontology Heatmaps were performed using Metascape.

2.15 ChIP-exo data analysis

The data of the ChIP-exo was taken from Rossi *et. al*., [131]. Then the result was analysed with the same software as the RNA-Seq analysis for the gene ontology and Venn diagrams.

Chapter 3

Investigating phenotypic differences in Swi-Snf subunit Mutants

3.1. Introduction

The yeast Swi-Snf chromatin remodeling complex was the first example of an ATP-dependent chromatin remodeler discovered [132]. The Swi-Snf ATP-dependent chromatin remodeling complex plays a key role in regulating transcription in yeast and is thought to regulate 10% of all genes [133], [134], [135]. Much of what is known about Swi-Snf activity has come from analysis of *snf2* deletion mutants. However, less is known about the role of the other Swi-Snf subunits functioning both within and potentially out with the Swi-Snf complex.

I therefore analysed the phenotypes of different strains of yeast that were each deficient for a particular Swi-Snf subunit including mutants containing *snf2*, *swi3*, *snf5*, *snf6*, *snf11*, and *snf12* gene deletions. In addition, a catalytically dead *snf2* mutant strain (*snf2K798A*) was analysed. This strain contains a Snf2 protein that is ATPase deficient due to a lysine to alanine amino acid substitution at position 798. Importantly, although the *snf2K798A* mutant is catalytically dead, the Swi-Snf complex is expected to remain structurally intact [83]. This is in contrast to a *SNF2* gene deletion mutant where studies have suggested that, in the absence of Snf2p, the complex falls apart [83]. Mutants of subunits of the Swi-Snf ARP module, comprising Arp7p, Arp9p, and Rtt102p, were not included in this analysis since these subunits are shared between RSC and SWI/SNF [136].

The goal of this project was to examine the role of each subunit in Swi-Snf complex cell function and transcription by systematically examining the phenotypes and transcription profiles in subunit deletion mutants. Consequently, in this chapter, I have analysed the phenotypes of the different Swi-Snf subunit mutants in an initial attempt to gain insight into each subunits function.

3.2. Results

3.2.1 Construction and confirmation of Swi-Snf subunit mutants

The Swi-Snf subunit mutants used for this study were either obtained from the Yeast Gene Deletion library or were constructed by PCR-mediated gene deletion as part of this study (Table 2.1). All gene deletions were confirmed by PCR analysis prior to use, as described in Materials and Methods.

Since the *swi1* deletion mutant was not available within the yeast gene deletion library, I made several attempts to construct this gene deletion mutant in this study. However, I was unable to obtain a *SWI1* gene deletion using conventional PCR-mediated gene deletion techniques [137]. I therefore attempted to prepare a conditional mutant of *SWI1* using the anchor away technique [121]. This technique involves tagging the target protein, in this case Swi1p, with a tag which enables the rapid removal of the protein from the nucleus. However, yet again, I was unable to prepare such a Swi1p conditional mutant. Thus, it was not possible in this study to analyse a *SWI1* deficient mutant.

3.2.2 Measuring the doubling time

To initially investigate the effect of the mutation in each strain upon cell growth and proliferation, I measured the doubling time for each Swi-Snf subunit mutant and compared it to wt (Fig. 3.1). The data showed that the *snf11* and *snf12* mutant strains showed no difference in doubling time compared to wt, taking about 90 min to double. Conversely, *snf2* and *snf5* had the longest doubling times of about 500 min. The *snf2K798A*, *swi3*, *snf6,* and *taf14* mutants all showed significantly longer doubling times than wt, each with a doubling time of more than 300 min.

Overall, the data show that some mutations caused substantial alterations in doubling time, while others had minimal effects. Thus, the different Swi-Snf subunit mutants can have different impacts upon cell growth, suggesting distinct and varying roles for the subunits in yeast cell function.

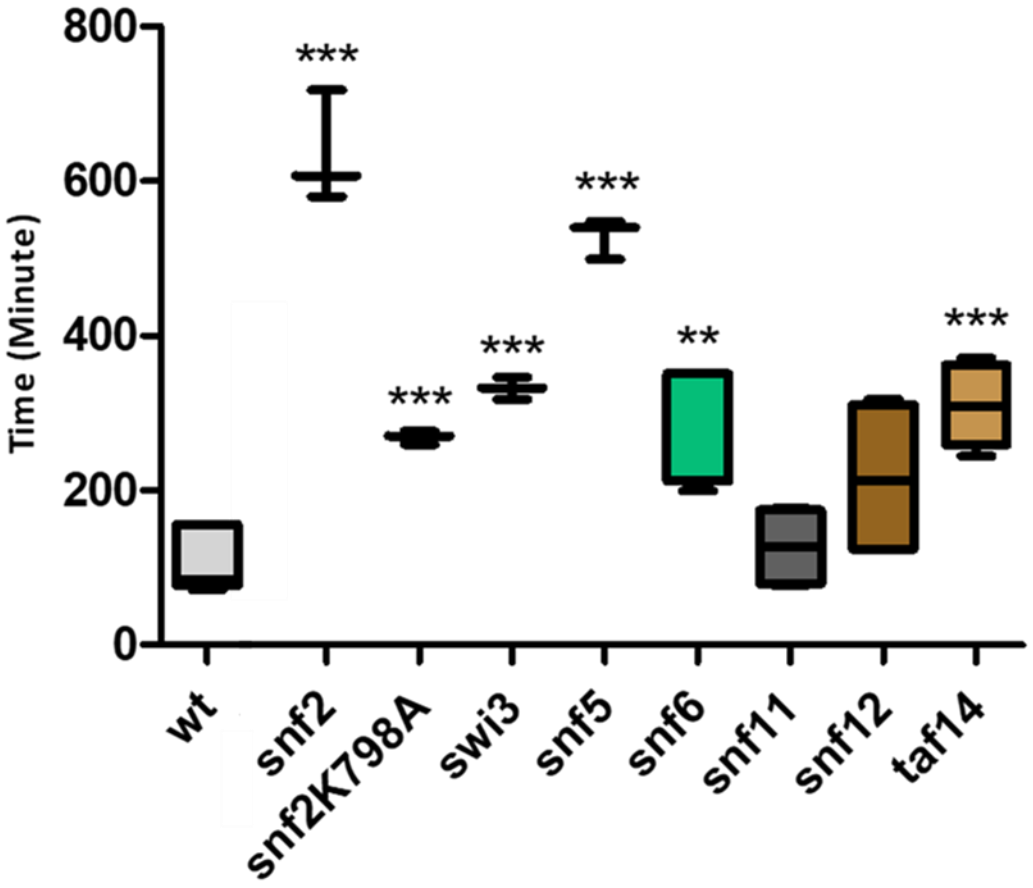

Figure 3. 1: Comparison of the doubling time of wt and each mutant of the Swi-Snf complex: Doubling time measurement compared with wt (BY4741). Cells were grown in YPD and OD_{600} was measured over time. T-test determines significance from at least three biological replicates (* p = 0.05, ** p = 0.01, *** p = 0.005).

3.2.3 Analysis of Swi-Snf subunit mutant growth during exponential phase

Next, I monitored the growth of mutant strains throughout exponential phase when grown in liquid media containing glucose (Fig. 3.2). However, in this analysis, I only examined the *snf2*, *swi3*, *snf5,* and *snf6* mutant strains which, between them, represent mutants from each of the Swi-Snf specific subcomplexes (see Fig. 1.10).

The results revealed that the *snf6* mutant showed no initial defect in growth compared to wt, but then showed a reduced growth rate and achieved a much lower final OD than wt. The *snf2* and *snf5* mutants showed a longer lag phase before reaching the exponential phase after which the maximum ODs they achieved were half that of wt. The *swi3* mutant showed the poorest growth on YPD; this strain showed the greatest delay before rapid growth started and achieved the lowest final optical density.

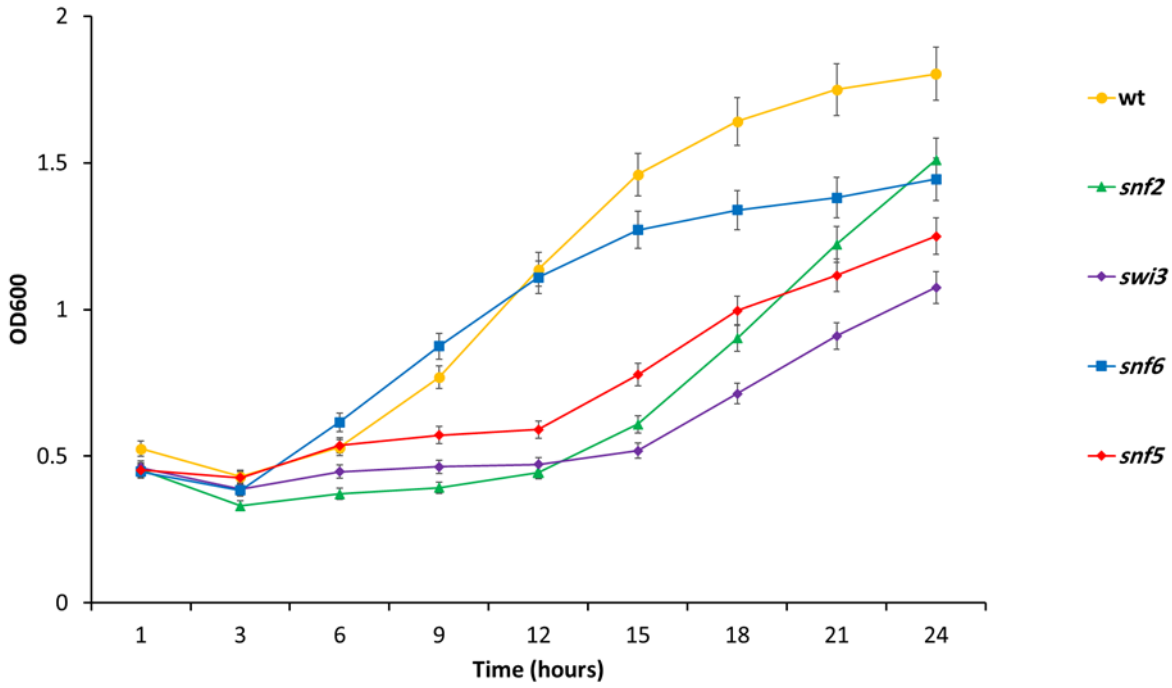

Figure 3. 2: Analysing growth of Swi-Snf mutants throughout exponential phase. Wild type (wt) and the Swi-Snf subunit mutants indicated were grown at 30°C for 24 hours in YEPD and OD_{600} readings were taken at regular intervals. Cells were inoculated to the same starting cell density and the increase in OD_{600} reading over the time course is shown. The experiment was performed in triplicate.

3.2.4 Examination of cell morphology

The Swi-Snf mutants were examined under the microscope to reveal diverse cell morphologies (Fig. 3.3). Compared to wt cells, the *snf2* and *snf2K798A* mutants appeared as small clumps. These clumps were not dispersed by the addition of EDTA suggesting this cell aggregation was not due to flocculation (data not shown) [138]. This clumpy cell phenotype was also observed in *snf5* cells, whilst *swi3* cells looked similar to wt cells. The *snf6* cells showed a high frequency of elongated cells, a phenotype also apparent in the *snf11* mutant, but to a lesser extent. The *taf14* and *swp82* mutants showed a large cell morphology. Thus, the different subunit mutants displayed an array of distinct and striking cell morphologies.

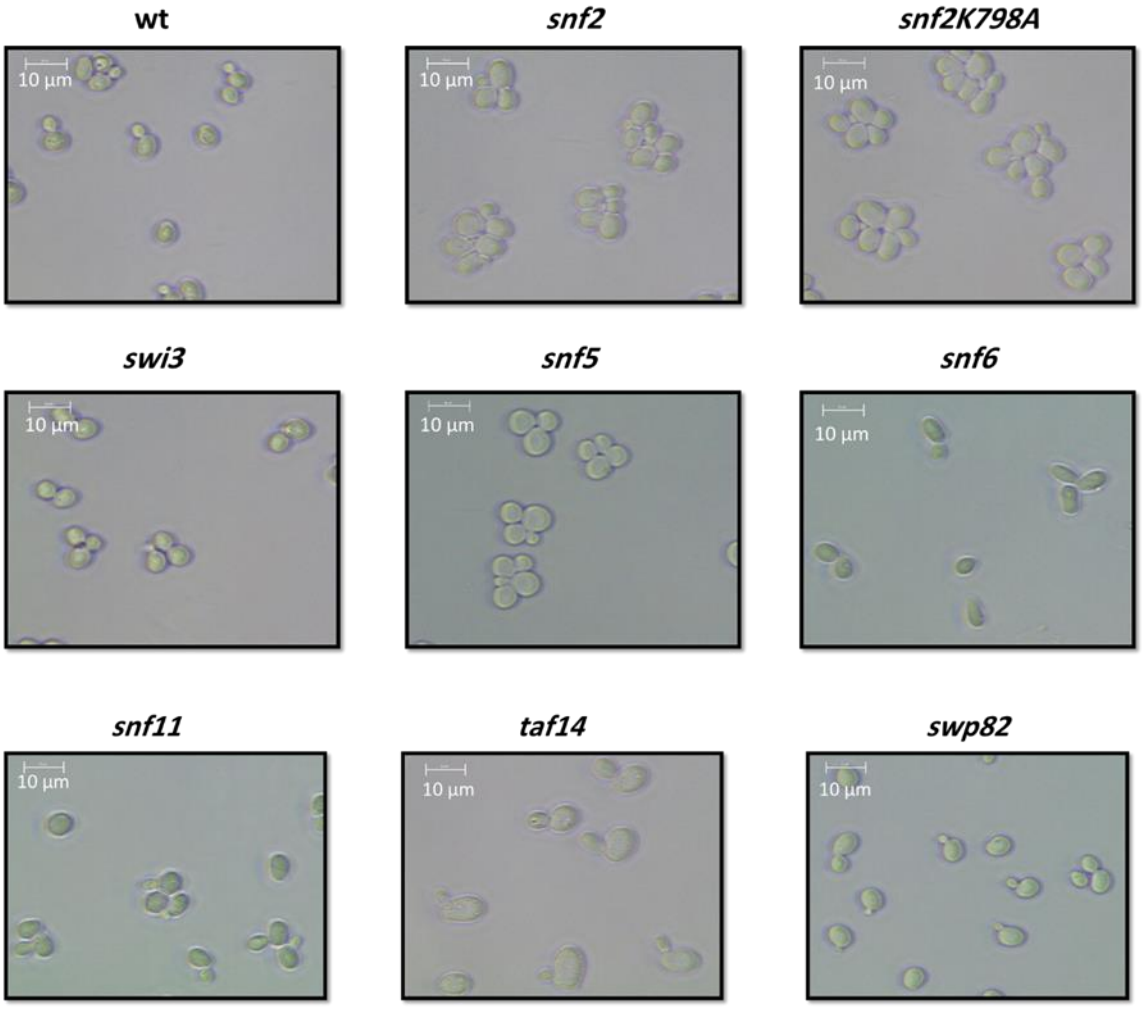

Figure 3. 3: Swi-Snf mutant cell morphology. The different Swi-Snf mutant strains indicated were grown on YPD, and cells from exponentially growing cultures were examined under the microscope. Microscopy was performed under 100X oil immersion magnification. The white scale bar represents 10µm. Images shown are representative of morphologies most frequently observed from at least three biological replicates.

3.2.5 Spot test analysis

3.2.5.1 Measuring temperature sensitivity

The ability of the mutants to grow at different temperatures was measured by spot tests on which the mutants were grown at both high and low temperatures; specifically cells were grown on agar plates incubated at 15ºC, 37ºC, and 42ºC and compared to the optimal growth at 30°C. Cells were normalised to an equal cell density and serial dilutions were prepared from which aliquots were spotted onto YPD plates which were then incubated at the different temperatures shown (Fig. 3.4). At a low temperature of 15ºC, *snf2* and *snf6* appeared to have slightly reduced growth compared to the wt and to their own growth at 30°C (B). When the mutants grew at high temperatures (37ºC and 42ºC) only the *snf5* and *taf14* mutants showed a sensitivity to the higher temperatures. Thus, only specific Swi-Snf subunit mutants showed sensitivity when stressed by temperature, with the *taf14* mutant showing the greatest sensitivity to high and low temperatures.

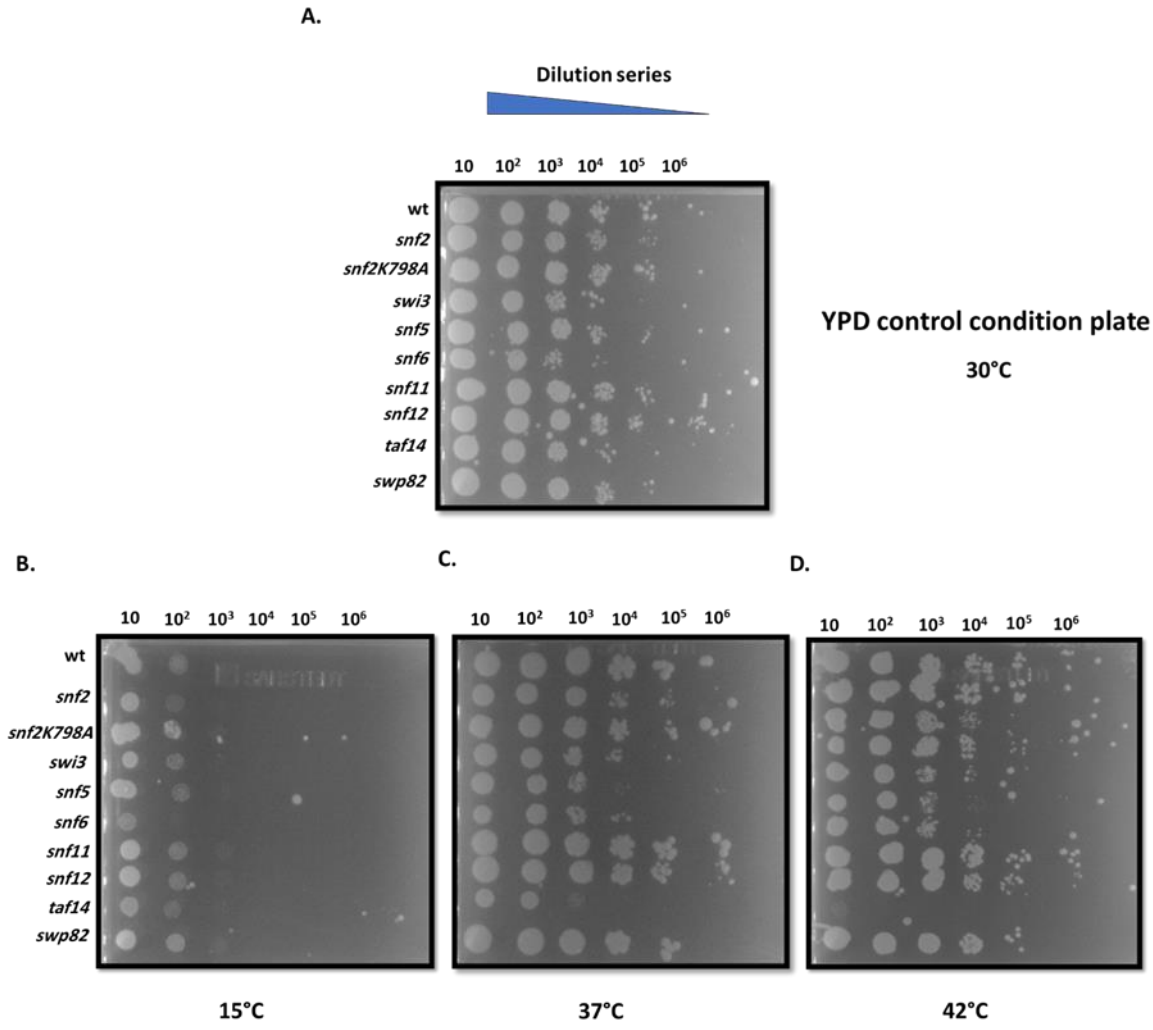

Figure 3. 4: Testing temperature sensitivity. Strains were spotted onto plates containing glucose (YEPD) and incubated at either. **(A)** Control plate for growth on solid media at 30°C **(B)** Growth at 15°C **(C)** 37°C and **(D)** 42°C as indicated. All strains were grown in different temperatures to a mid-exponential phase of growth, and cell numbers were normalised to 1 X 107 cells/ ml prior to dilution. A 10-fold serial dilution was then prepared and 2.5 µl of each sample was then spotted onto agar plates. All plate images were taken after 3 days of growth. Images shown are representative of results of the experiment having been performed in triplicate.

3.2.5.2 Analysis of fermentation ability during growth on solid media containing different carbon sources

Next, I examined the various Swi-Snf mutants for their ability to perform fermentation when grown on solid media containing different carbon sources (Fig. 3.5). For this experiment equal numbers of cells were spotted onto YEP plates containing either glucose, galactose, or raffinose and with Antimycin A (Anti A). Antimycin A was used as a drug to block respiration thereby allowing us to examine the ability of the cells to metabolise solely via fermentation [139]. When cells were challenged to undergo fermentation when grown on galactose, the *snf11,* and *snf12* mutants showed no difference in their ability to grow on the galactose plate as compared to wt. The *snf6*, *taf14,* and *swp82* mutants showed a mild growth retardation on the galactose plates (Fig. 3.5B). Conversely, the *snf2*, *snf2K798A, snf5*, and *swi3* deletion strains showed the most severe growth defect.

When the experiment was repeated on raffinose-containing plates, only the *snf2*, *swi3 snf5,* and *snf6* mutants showed a growth defect. Thus, more Swi-Snf mutants show an inability to ferment galactose, whilst the *snf2* deletion mutant shows the greatest defect in galactose and raffinose fermentation (Fig. 3.5C).

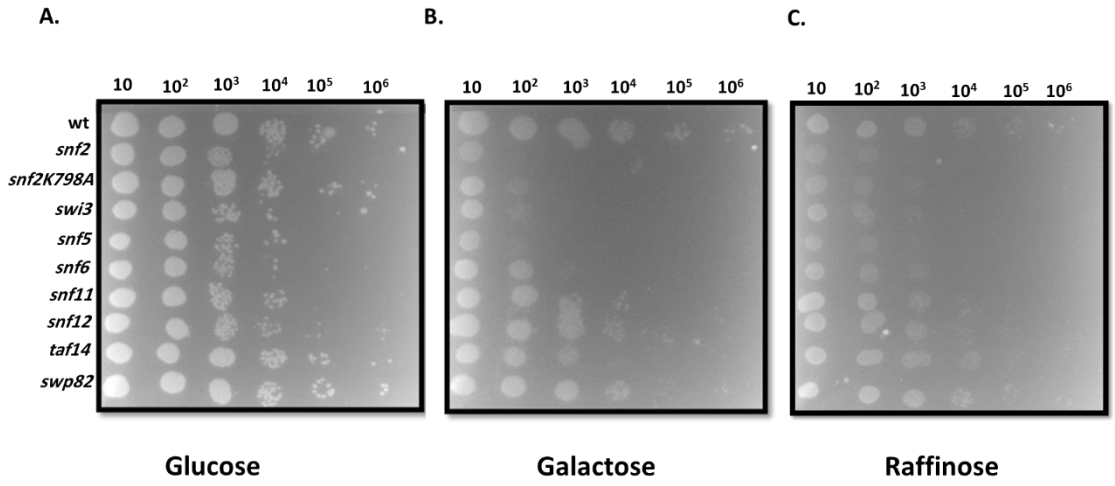

Figure 3. 5: Growth on different carbon sources. Spot tests of yeast cells from each of the strains indicated were plated as 10-fold serial dilutions starting from 1 x 10^7 cells/ml to a mid-log phase of growth. **(A)** Strains were spotted onto YP-Dextrose (YP-Glu) and **(B)** YP-Galactose (YPGal). **(C)** YP-Raffinose (YP-Raf) with antimycin A as an electron transport inhibitor. 2.5 µl of culture were spotted on the plates and photographed following 48 h of growth at 30 ^{o}C. Images shown are representative of results of the experiment having been performed in triplicate.

3.2.5.3 Analysing Swi-Snf mutants for DNA damage sensitivity

The Swi-Snf complex was initially identified as a transcriptional activator that enhances gene transcription [83]. However, studies have revealed it also plays a role in DNA damage repair pathways [140]. We therefore tested the various Swi-Snf mutants for their response to DNA damaging reagents methyl methane sulfonate (MMS) and hydroxyurea (HU). MMS causes DNA fragmentation due to base mispairing and inhibition of DNA replication [141]. HU acts to inhibit the enzyme ribonucleotide reductase to reduce dNTPs levels which inhibits DNA synthesis and replication [142].

When cells were challenged with MMS, most of the Swi-Snf mutants were sensitive in the presence of this reagent, with the *snf6* mutant showing the greatest sensitivity. Interestingly however, both *snf2* mutants, and the *snf5* mutant, were not sensitive to this drug (Fig. 3.6A).

When the experiment was repeated using HU, the Swi-Snf mutants showed a much more diverse growth response to the presence of this reagent. Whereas *snf11* and *swp82* mutants showed no sensitivity to HU, *snf2* and *snf6* mutants were extremely sensitive to HU. *swi3, snf5*, *snf12,* and *taf14* mutants showed an intermediate sensitivity to HU. Interestingly, although the *snf2K798A* mutant did show a sensitivity to HU, this sensitivity was significantly less than that observed in the *snf2* deletion mutant where growth was severely inhibited compared to wt (Fig. 3.6B).

Together, these data show mutants in the different subunits of Swi-Snf show varying responses to the presence of DNA damage-inducing agents, suggesting distinct roles for the sub-units in the DNA damage response.

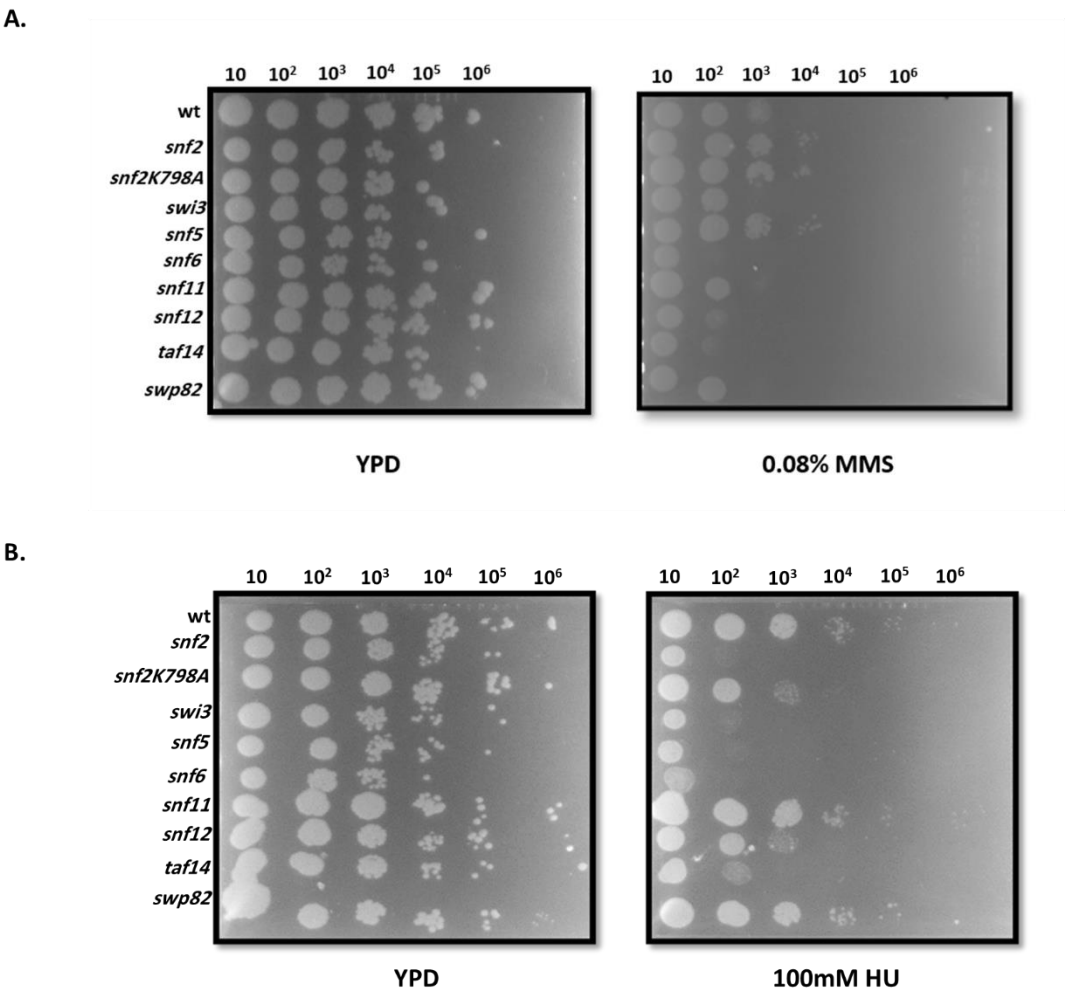

Figure 3. 6: Testing cell sensitivity to DNA damaging reagent MMS and HU. YPD containing different concentrations of **(A)** (MMS), **(B)** (HU). Cells (2.5µl) from each of the strains indicated were plated as 10-fold serial dilutions onto plates with different concentrations of MMS and HU. Images shown are representative of results of the experiment having been performed in triplicate.

3.2.5.4 Analysing Swi-Snf mutants for cell wall stress

Here, I investigated the Swi-Snf mutants for their response to cell wall stress by exposing cells to caffeine (Fig. 3.7). Caffeine has pleiotropic effects on yeast but is commonly used to evaluate the function of the Mpk1p-mediated cell wall integrity pathway and thus assess resistance of yeast to cell wall stress [143], [144].

The results showed that in *snf2* and *snf6* mutants, growth on caffeine was abolished. However, interestingly, the other mutants were less sensitive to caffeine than the wt.

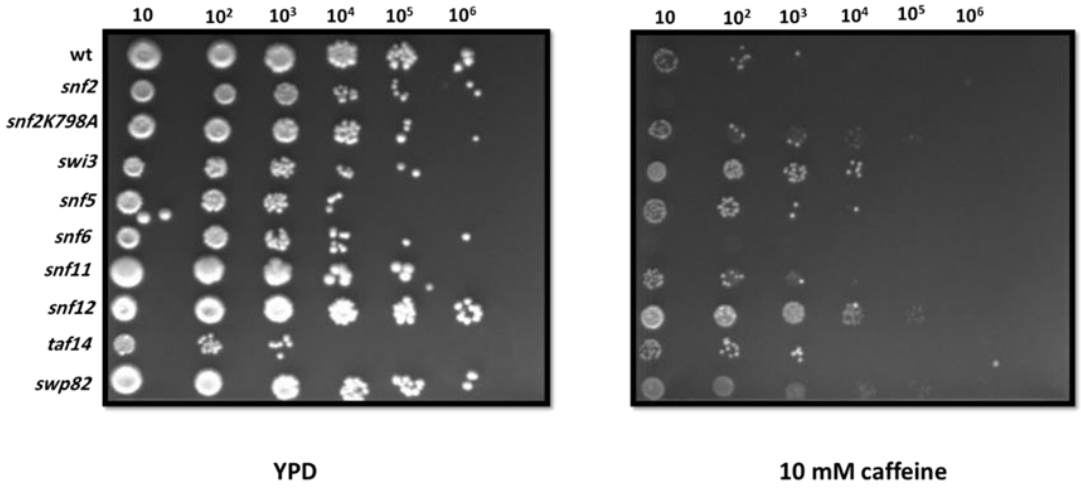

Figure 3. 7: Testing the cell sensitivity to caffeine. Strains were spotted onto plates containing caffeine. The control plate measured for growth on solid YPD media at 30°C, whilst the test plate contained 10mM of caffeine. All strains were grown to a mid-exponential phase of growth, and cell numbers were normalised to 1 x 10^7 cells/ml prior to dilution. A 10-fold serial dilution was prepared and 2.5 µl of each sample was then spotted onto agar plates. All plate images were taken after 3 days of growth. Images shown are representative of results of the experiment having been performed in triplicate.

3.2.5.5 Analysing Swi-Snf mutants for osmotic sensitivity

I next measured the sensitivity of selected mutant strains to osmotic stress by testing their ability to grow in the presence of sodium chloride (NaCl). The yeast cells indicated were grown until the exponential phase in YPD, normalised to an equal cell density, and serial dilutions were prepared from which equal volumes were spotted onto YPD containing NaCl (Fig.3.8). The result showed that the *snf2* and *snf5* mutant strains showed greater sensitivity to growth in the presence of NaCl compared to the wt and the other mutants.

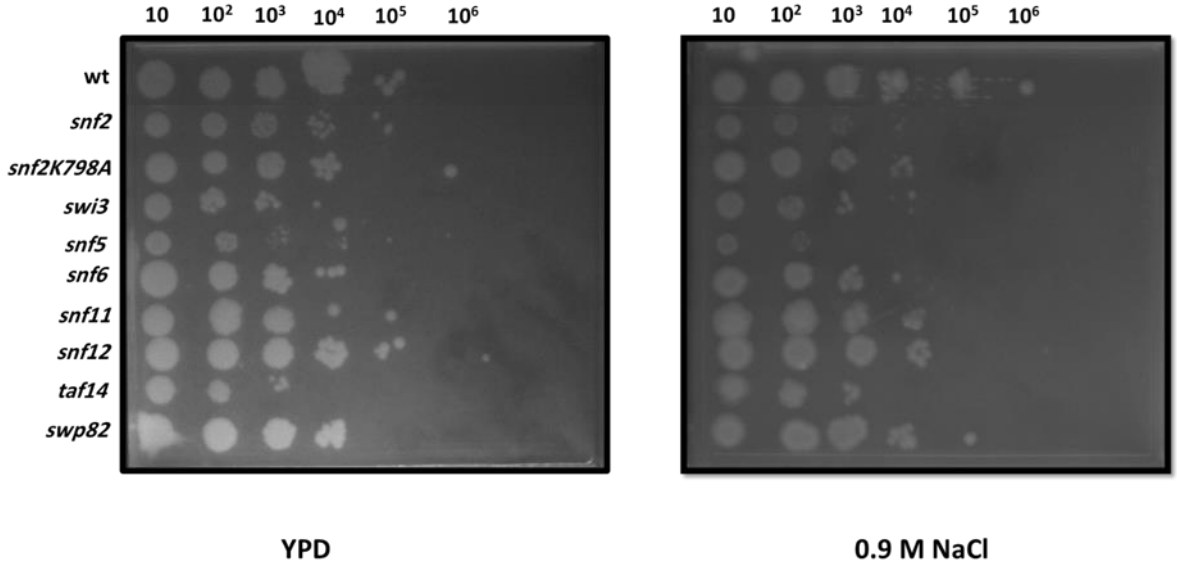

Figure 3. 8: Testing cell sensitivity to osmotic stress. Strains were spotted onto plates containing NaCl. The control plate for growth was YPD only at 30°C. The test plate contained 0.9M NaCl. All strains were grown to a mid-exponential phase of growth, and cell numbers were normalised to 1 X 107 cells/ ml prior to dilution. A 10-fold serial dilution was prepared and 2.5 µl of each sample was then spotted onto agar plates. All plate images were taken after 3 days of growth. Images shown are representative of results of the experiment having been performed in triplicate.

Main findings

- A *swi1* mutant is potentially inviable.
- *snf2* and *snf5* have the greatest growth defects.
- *snf5*, *snf2*, and *snf2K798A* mutants have a clumpy cell morphology.
- *snf6* cells display an elongated cell morphology.
- *taf14* mutants have a large cell morphology.
- *taf14* is temperature sensitive for growth at high and low temperatures.
- The different mutants show large differences in their response to DNA damage reagents.
- The *snf2* and *snf2K798A* mutants are not always similar and display many distinct phenotypes.

Discussion

The Swi-Snf complex was the first ATP-dependent remodelling complex discovered that played a critical role in gene expression by altering the structure of chromatin, making it more accessible to transcription factors and other regulatory proteins [132].

Although the Snf2p subunit has been well characterized, the roles of the other Swi-Snf subunits are not fully understood.

The first aim of my study was to compare the phenotypes of each Swi-Snf subunit mutant to determine whether they had different phenotypes which might indicate if they have different roles or not. The prediction would be that if the subunits only functioned to support Swi-Snf complex activity, then all of the subunit mutant phenotypes should be similar.

Unfortunately, I was unable to obtain a *SWI1* mutant to include in my analysis. My repeated gene deletion attempts failed which I hypothesised was due to the *swi1* deletion mutant being either too sick to recover or was inviable. The literature about *swi1* mutants is ambiguous; some studies suggest *swi1* mutants are not viable, whilst

other studies have used *swi1* mutants [145]. I would propose that in my strain background, a *swi1* mutant is not viable.

Interestingly, my attempt to create a Swi1p anchor-away strain was also not successful. This technique involves adding a C-terminal tag to Swi1p to enable the rapid protein depletion from the nucleus following the addition of rapamycin to cultures [121]. This is a well-established and frequently used technique to create conditional mutants in yeast. I would propose that the C-terminal tagging cripples the Swi1p protein function resulting in cell death. Thus, I could not obtain a tagged Swi1p strain due to the successfully tagged proteins potentially causing cell death in the strain background used.

When I measured doubling time in the suite of mutants I did have, the data revealed that *snf11* and *snf12* showed no significant difference in doubling time compared to wt, indicating a minimal impact on growth in these mutants. However, the *snf2K798A, swi3*, *snf6*, and *taf14* mutants took significantly longer to double than wt suggesting a substantial effect on growth in these mutants. The longest doubling time was found in the *snf2* and *snf5* mutants, pointing to crucial roles for *SNF2* and *SNF5* in maintaining normal growth (see Fig. 3.1).

These findings suggest that while some mutations in SWI/SNF subunits cause substantial alterations in doubling time and thus growth characteristics, others have minimal effects. This highlights the importance of specific subunits in regulating the complex's function and the growth of yeast cells.

It is interesting to note that the *SNF2* gene deletion mutant and the Snf2p catalytic mutant had markedly different growth defects. Furthermore, the *snf2* and *snf2K798A* mutants also showed markedly different responses to HU, caffeine, and NaCl stress. This is surprising as both mutants should have a Swi-Snf complex non-functional for Swi-Snf activity due to the absence of an active Snf2p ATPase-containing subunit. However, it has been suggested that a *snf2* deletion mutant destabilizes the Swi-Snf complex [83]. Thus, the fact that the *snf2* deletion mutant has the greatest defect

compared to the catalytic mutant is consistent with an unstable Swi-Snf complex in the *snf2* deletion mutant which would lead to greater defects. Furthermore, this result suggests that the inactive yet potentially intact Swi-Snf complex found containing the *snf2* catalytic mutant retains some residual Swi-Snf activity that is independent of its ATPase activity.

When I examined the cell morphology of the mutants under the microscope, a wide range of differing morphologies was revealed. The *snf2* mutant, and the *snf5* mutant, appeared as small clumps of between 4-5 cells. As this phenotype was not due to flocculation, this could suggest a role for these subunits in the cell wall remodelling required for successful cell separation (Fig. 3.3).

The *snf6* mutants also showed a striking elongated cell morphology again suggesting a defective cell wall in these mutants. In support of this, the *snf6* mutant was the most sensitive to caffeine which is used as a test for cell wall sensitivity to stress.

Also of note, the *taf14* mutant showed a large cell phenotype suggesting a role for this subunit in regulating cell size. This could suggest a role for the Taf14p subunit in the regulation of the cell cycle, regulation of the cell wall, or downregulation of protein synthesis. Further experiments would be needed to test this. The *taf14* mutant was also the only mutant that exhibited an increased sensitivity to growth at high and low temperatures. Interestingly though, despite these strong and unique phenotypes, the *taf14* mutant showed an almost wt growth pattern when grown on YPD under 'regular' conditions. Thus, although the data suggest that the Taf14p subunit has roles in cell size regulation and responding to temp stress, loss of Taf14p was not detrimental to regular growth.

When exposed to HU, which causes DNA damage, many of the mutants showed high sensitivity. However, the most interesting result here was that *swp82*, *snf11*, and *snf12* mutants showed only minor sensitivity to this reagent (Fig 3.6B). Together, this suggests that although many of the Swi-Snf subunits contribute to an important role for Swi-Snf in responding to DNA damage, the Swp82p, Snf11p, and Snf12p subunits do

not seem to play a large role in this response. Furthermore, the fact that the *snf2* deletion mutant is very sensitive to HU, whilst the *snf2K798A* mutant is not, suggests the ATPase activity of the complex does not play the most critical part in the Swi-Snf complexes response to this drug and the presumable impact this drug has in causing DNA damage. This is at odds with the role Swi-Snf is thought to play in DNA damage repair where it has been proposed to remodel nucleosomes around a DNA double strand break (DSB) to enable repair; a role similar to that shown by INO80, which does need the ATPase activity.

Overall, these simple experiments suggest that the different subunits can have wide-ranging and often unique roles in multiple cell functions including regulating cell size and growth and how the cells respond to DNA damage.

Chapter 4

Investigating global gene transcription in Swi-Snf subunit mutants

4.1 Introduction

Swi-Snf is an ATP-dependent chromatin remodelling complex that is required for the activation of up to 10% of all the genes in *S. cerevisiae* [146]. The *HO* and *SUC2* genes are the most well-characterized genes controlled by Swi-Snf [118],[114] [147]. In the previous chapter, I identified the phenotypic differences in the Swi-Snf subunit mutants compared to the wt.

Here, I planned to identify the genes under transcriptional regulation of selected Swi-Snf subunits by comparing the global RNA transcriptome data of selected subunit mutants with each other, and versus wt. Specifically, RNA Seq was used to examine the transcriptomes of the following mutant strains; *snf2*Δ, *swi3*Δ, *snf5*Δ, *snf6*Δ and a *snf2K798A* mutant strain containing a single amino acid (lysine to alanine) substitution at position 798. This mutation is catalytically dead for ATPase activity and is therefore inactive for Swi-Snf chromatin remodelling activity [148]. It has been proposed that many of the deletion mutants, including the *snf2*, *snf5*, *snf6*, and *snf12* deletion cause the Swi-Snf complex to dissociate [83]. The *snf2K798A* mutant on the other hand, would be predicted to remain part of an intact, yet inactive, Swi-Snf complex [149]. Thus, we were particularly interested to compare the *snf2* and *snf2K798A* mutants in which we would expect to see different transcriptional consequences.

The four deletion mutants described above (*snf2*Δ, *swi3*Δ, *snf5*Δ, *snf6*Δ) were chosen for use in this analysis as the data from Chapter 3 suggested that these mutants had the greatest impact on cellular phenotypes and represent mutations of subunits within each of the proposed modules of the Swi-Snf complex. Interestingly, my repeated attempts to make a *swi1* gene deletion mutant were unsuccessful suggesting that this mutant was either too sick to recover following the deletion attempt or was not viable.

This RNA-Seq analysis should reveal the number of genes down and upregulated by each subunit thereby defining each subunits' role in regulating gene transcription.

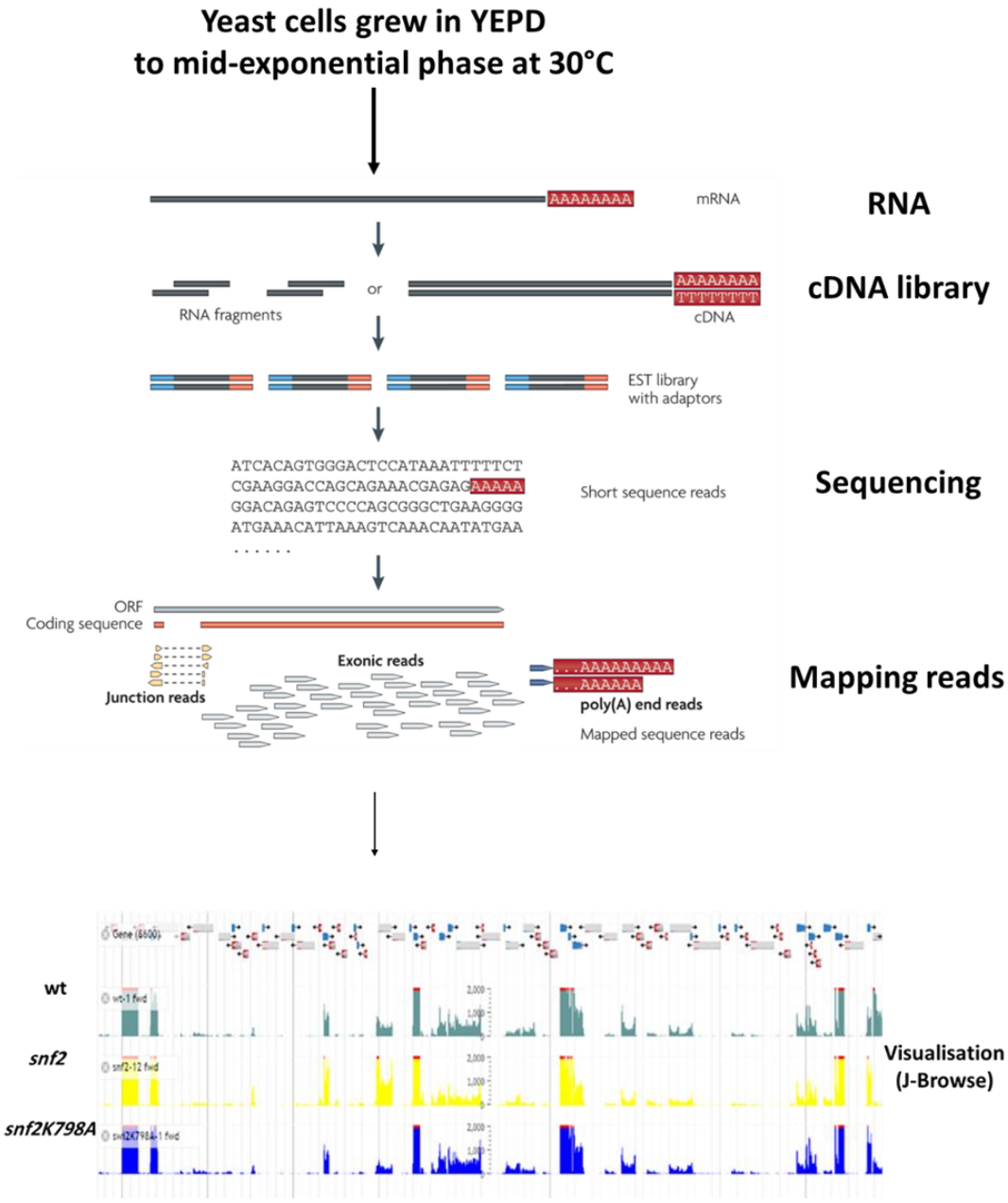

Figure 4. 1: Pipeline for RNA Sequencing analysis. A schematic showing the principal steps involved in using RNA -Seq technology to identify global gene transcription levels. This process begins with the isolation of total RNA from yeast cells grown to mid log phase at 30°C, preparation of cDNA, sequencing of cDNA, mapping of sequencing reads to the genome, visualization of reads on a genome browser, and analysis of data to reveal differential gene transcription profiles. The figure was adapted from [150].

4.2 Results

4.2.1 RNA-Seq data quality control

A schematic to show the overall pipeline for the RNA-seq analysis is shown in Fig. 4.1. Total RNA was extracted from wt and each mutant and the quality of RNA was analysed and confirmed as being of good quality prior to sending for sequencing (see Materials and methods Fig. 2.3). Following sequencing, I checked the quality of the resultant triplicate RNA-Seq data for each strain by plotting the normalized counts of each biological replicate against each other to give an R^2 plot (Fig. 4.2). As can be seen, the R^2 value for each comparison was between 0.8 and 1.0, suggesting the reproducibility of each triplicate data set was good for all mutants.

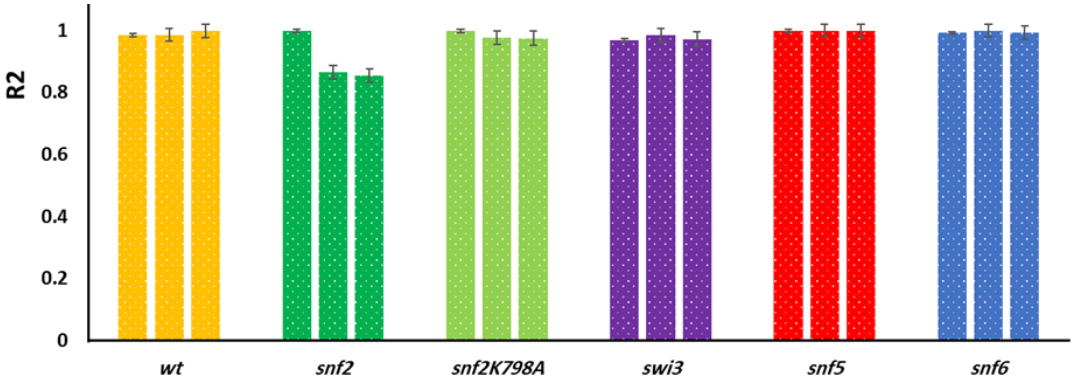

Figure 4. 2: High correlation between biological replicates. Graph depicting the compiled Pearson R^2 values obtained from plotting the normalised counts of each sample against each other. Three biological replicates were performed for each strain.

4.2.2 Gene transcription profiles in the Swi-Snf mutants

The first step in my analysis was to identify the genes that were at least twofold down- or upregulated in each of the mutant strains compared to wt (log2>1 or Log2<-1, FDR of <0.05). Downregulated genes in a mutant would indicate a positive (activating) role for that particular subunit at those genes, whilst upregulated genes would suggest a negative (repressing) role for that subunit at such genes (Fig. 4.3).

The RNA seq analysis revealed that in a *snf2* deletion mutant 348 genes were downregulated more than twofold compared to wt, and there were 307 genes at least twofold upregulated. In the *snf2K798A* catalytic null mutant 349 genes were down-regulated and 264 genes were up-regulated. In the *swi3* mutant there were 300 genes downregulated and 584 genes were upregulated. In the *snf5* mutant there were 215 genes downregulated and 214 genes upregulated. Finally, in *snf6* there were 271 genes downregulated and 86 genes upregulated.

Thus, there were significant differences in the numbers of genes up and downregulated in each of the mutants. The *snf2* and *snf2K798A* mutants had similar numbers of genes down and upregulated, whilst the *swi3* mutant showed the most genes which were upregulated (584 genes). This suggests that the Swi3p subunit has the greatest negative influence upon gene transcription while *SNF2* plays the greatest role in positively regulating gene transcription.

Importantly, overall, these data suggest a significant role for the Swi-Snf co-activator complex in negatively regulating gene transcription, with the Swi3p subunit being most heavily implicated in the negative regulation of transcription and the Snf6p subunit playing the least role in negative regulation of transcription. This is contrary to our understanding of the Swi-Snf complex functioning predominantly as an activator of gene transcription.

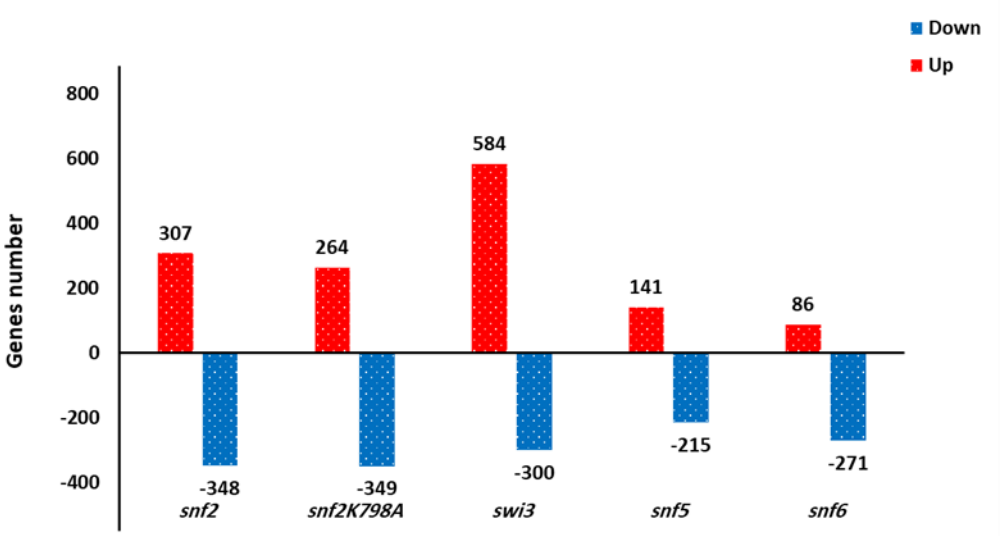

Figure 4. 3: Number of genes up- and downregulated more than 2-fold in each Swi-Snf subunit mutant compared to wt (P Values<0.05). Blue colour indicates genes downregulated (Down); red colour reflects the number of genes upregulated (Up).

4.2.3 Visualisation of RNA seq data to show differential gene expression in each mutant

I next visualized the genes which were up and downregulated more than two-fold in the *snf2*, *snf2K798A*, *swi3*, *snf5*, and *snf6* mutant compared to wt to gain insight into any general trends in the RNA-seq data. A heat map was generated of the top 100 genes down and upregulated in each mutant strain to show the differential levels of transcription in each mutant (Fig.4.4). Each row represents a gene, and each column represents a mutant. The results showed that the *snf2* deletion mutant and the *snf2K798A* catalytic mutant had similar looking transcriptomes. The profiles of the transcriptomes in the *snf5* and *snf6* mutants were also very similar to each other. Interestingly however, the *swi3* mutant profile was the most distinctly different transcription profile from all of the other mutants. Thus, the *swi3* mutant seems to have the most unique transcriptome of the Swi-Snf subunit mutants tested compared to wt.

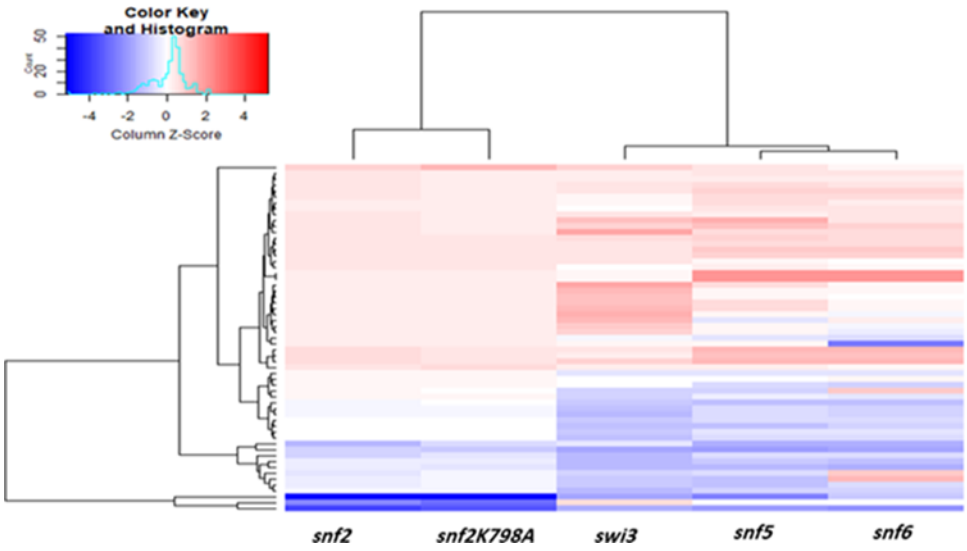

Figure 4. 4: Visualisation of differential gene transcription in Swi-Snf sub-unit mutants. A cluster heat map in which rows represent 100 genes down and up-regulated, columns represent mutants. The blue colour reflects down-regulated genes and red colour reflect up-regulated genes. (>2-fold and FDR of <0.05). Heatmap2 R gplot packaging was used to generate this figure.

4.2.4 Comparing a *snf2* deletion mutant with a *snf2K798A* catalytic mutant

4.2.4.1 Comparing the downregulated genes in a *snf2* deletion mutant with a *snf2K798A* catalytic mutant

The main aim of this chapter was to investigate the differences in the transcriptome data in the Swi-Snf complex subunit mutants to determine whether each subunit might have distinct roles. I first analysed the *snf2* mutants because *SNF2* encodes the ATPase subunit of Swi-Snf which is the catalytic heart of the complex and should potentially be the most important subunit.

The previous results of the heatmap in Fig. 4.4 showed that there was a high similarity between the genes which were significantly up- or downregulated in the *snf2* deletion mutant and the *snf2K798A* catalytic mutant. This was surprising as we expected more of a difference considering the *snf2* mutation has been proposed to disrupt the Swi-Snf complex structure and activity, whilst the complex was expected to be inactive in the *snf2K798A* mutant, yet the complex should remain structurally intact [83].

Therefore, I decided to take a more detailed look at the RNA-Seq data for these two strains to examine if there were more subtle differences between the genes regulated in each Snf2p deficient mutant.

Since the Swi-Snf complex is best characterised as a co-activator of transcription, I began by looking at the differences in downregulated genes in the *snf2* deletion mutant and the *snf2K798A* catalytic mutant compared to wt. The genes downregulated in each mutant could be considered to be under the positive control of Snf2p in wt.

As described previously, in the *snf2* deletion mutant, there were 348 genes downregulated compared to wt, whilst in the *snf2K798A* mutant, there were 349 genes downregulated (Fig. 4.3). These are the genes considered to be activated by Snf2p. Thus, the *snf2* and *snf2K798A* mutants negatively affect a similar number of genes.
Analysis showed that there was a large overlap in the genes downregulated in these mutants (Fig. 4.5A). By comparing the average transcription level of the overlapping

genes, the result showed no significant difference in the transcription levels of the 325 genes downregulated in two mutants (Fig. 4.5B). Similarly, there was no difference in the average transcriptional levels of the genes uniquely downregulated in *snf2* (23 genes) and *snf2K798A* (24 genes). Examples of genes downregulated in both mutants, in *snf2* only, and in *snf2K798A* only, are shown in Fig. 4.5C, D and E, respectively.

Thus, the *snf2* deletion mutant and the *snf2K798A* mutant influence a similar number of genes, and the impact on transcription of the common and uniquely downregulated genes was similar in the two mutants.

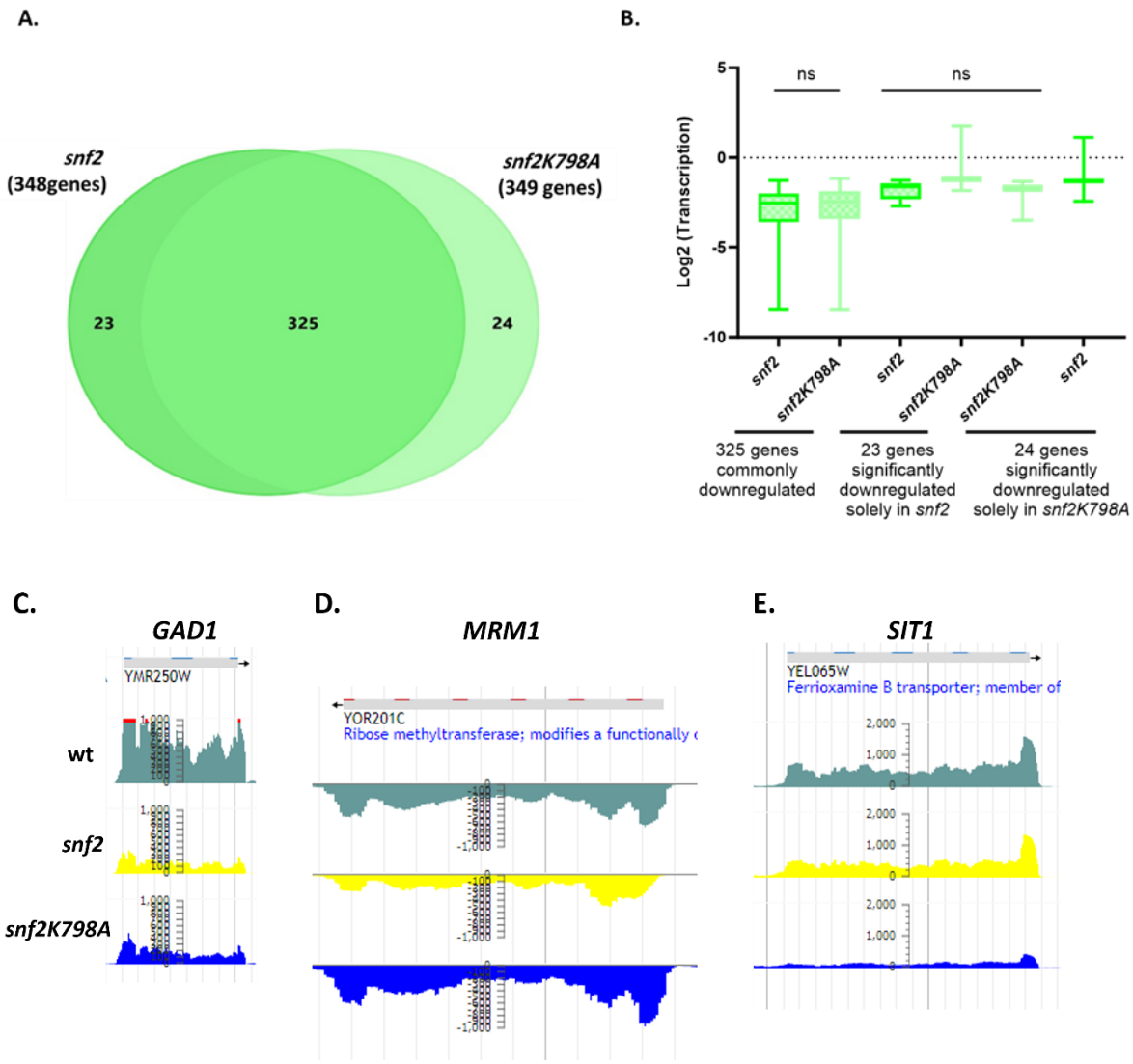

Figure 4. 5: (A) Venn diagram to identify the genes shared and uniquely down-regulated in the *snf2* and, *snf2K798A* mutant strains. **(B)** Box plot to show the average fold changes of the down-regulated genes relative to wt. **(C)** J-browse image to show transcription level examples of shared genes in *snf2* and *snf2K798A GAD1*. **(D)** J-browse image to show transcription level example of genes significantly solely downregulated in *snf2* (*MRM1)*. **(E)** J-browse image to show transcription level example of genes significantly solely downregulated in *snf2K798A* (*SIT1)*.

4.2.4.2 Gene ontology analysis of genes downregulated in the *snf2* and *snf2K798A* mutants

To identify if the genes downregulated in the *snf2* and *snf2K798A* mutants had specific functions, gene ontology analysis was used.

Firstly, I looked at the 325 genes commonly downregulated in the two mutants. In the molecular function category, 27 genes play a role in transporter activity, 71 genes played a role in catalytic activity, and 28 genes were involved in DNA binding (Fig. 4.6A). Examples of these genes include *ARC15* which encodes the protein that binds to actin to form the cytoskeleton of the cell [151], and *USV1* which encodes a DNA-binding transcription factor activity that modulates the transcription of specific gene sets transcribed by RNA polymerase II [152] (Fig. 4.6B). *TUF1* encodes a transcription factor containing the homeobox domain. It is usually involved in the control of gene expression during morphogenesis and development [153].

When I looked at the biological process term, most of the commonly downregulated genes (89) were involved in the cellular process and 60 genes played a critical role in the metabolic process. Examples of these genes were *MNP1* which encodes a protein that comprises part of the ribosome, and *GAD1* which encodes a decarboxylation enzyme [14].

In the cellular component, there were 101 genes involved in cellular anatomical entity and 26 genes involved in protein-containing complexes. Examples of these genes include *VTC3*, encoding a vacuolar transporter chaperone [154], and *HXT6* which encodes a glucose transporter protein [155] (Fig 4.6B).

Of the 23 genes solely downregulated in *snf2,* there were 6 genes that played a role in cellular component terms (Fig. 4.6C). Examples of these genes include *GPD1* and *PST2* which encodes enzymes that catalyzes redox reactions [156] (Fig. 4.6D). Interestingly, where the *MRM1* gene is uniquely downregulated in the *snf2* deletion mutant, this gene is upregulated in the *snf2K798A* mutant [157] (Fig. 4.5D and Fig. 4.6D).

When the analysis was repeated with the 24 genes solely downregulated in the *snf2K798A* strain, the results showed 5 genes involved in catalytic activity, such as *FRE7* which encodes an oxidoreductase enzyme (Fig. 4.6F) [158]. In the biological process category, there were 4 genes involved in homeostatic processes like *ISU2* which encodes a cytoplasmic protein that binds to nascent or unfolded polypeptides and ensures correct protein folding or transport (Fig. 4.6 F) [159].

Overall, these results showed that Snf2p is required for the activation of a wide range of genes and that there were no significant differences in gene ontology of the genes uniquely downregulated in the *snf2* and *snf2K798A* mutants.

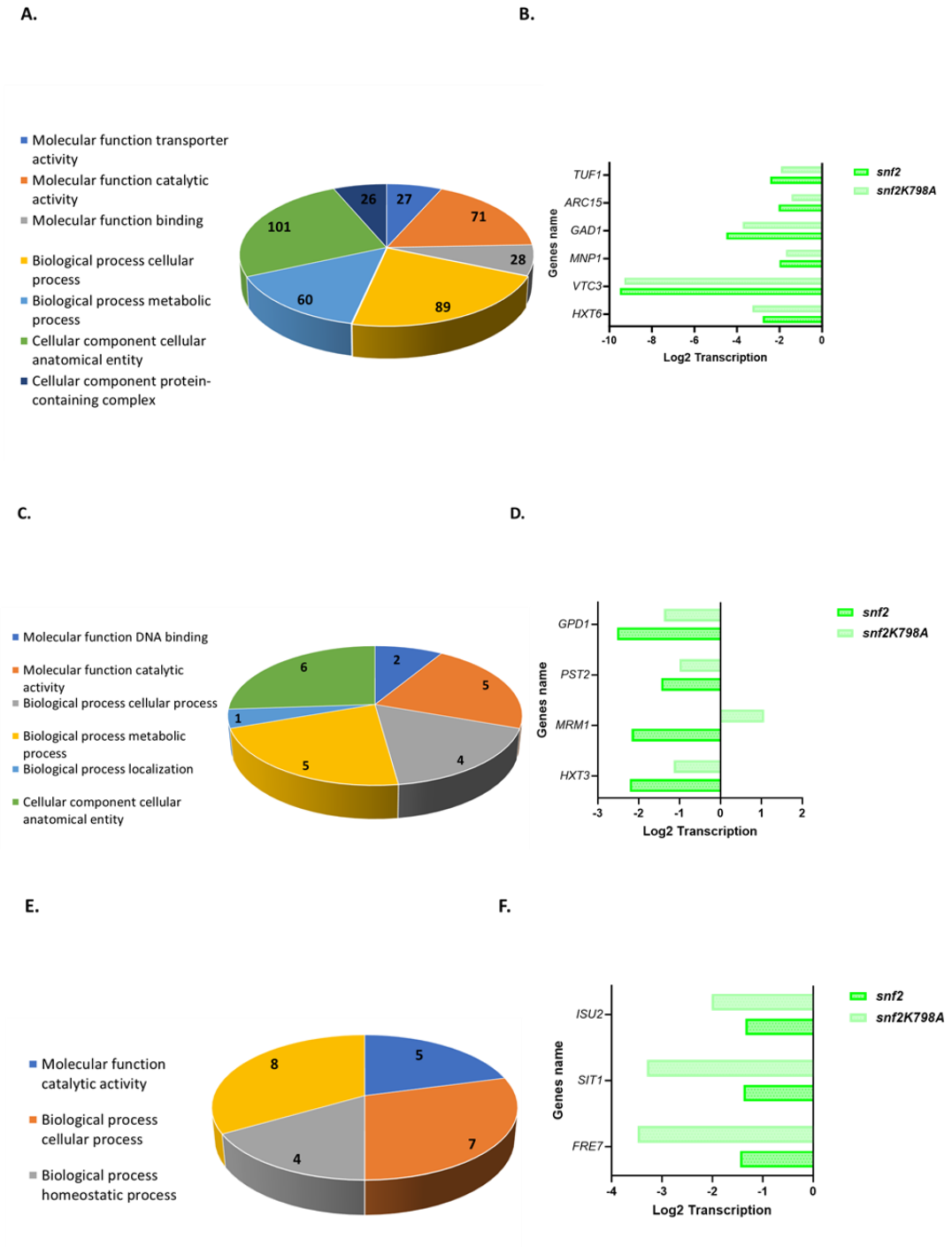

Figure 4. 6: Gene ontology analysis of genes downregulated in the *snf2* and *snf2K798A* mutants. (A) Gene ontology of the commonly downregulated genes in two mutants (325 genes). **(B)** Examples of these genes and their fold changes relative to wt. **(C)** gene ontology of the genes significantly downregulated only in the *snf2* deletion mutant

strain (24 genes). **(D)** Examples of these genes and their fold changes relative to wt. **(E)** gene ontology of the genes significantly downregulated only in *snf2K798A* (23 genes). **(F)** Examples of these genes and their fold changes relative to wt.

4.2.4.3 Analysing the genes upregulated in a *snf2* deletion mutant and a *snf2K798A* catalytic mutant

I next compared the upregulated genes in the *snf2* and *snf2K798A* mutants. These are the gene cohorts at which *SNF2* can be seen to be acting as a repressor of gene transcription. There were 307 genes upregulated in the *snf2* mutant, and 264 genes upregulated in the *snf2K798A* (Fig. 4.7A). The Venn diagram revealed that there was a large overlap in the genes upregulated in these mutants (244 genes).

When the average transcription levels of the 244 overlapping genes were compared, the data showed there was no significant difference in the transcription level of the 244 genes upregulated in each mutant, (Fig.4.7B), with the *snf2* mutant showing a similar change in average transcription upregulation as was seen in the *snf2K798A* mutant. Similarly, when I compared the average transcription levels of those genes solely upregulated in the *snf2* and *snf2K798A* mutants, both mutants again showed the same level of upregulation. Examples of genes upregulated in both mutants, in *snf2* only, and in *snf2K798A* only, are shown in Fig. 4.7C, D and E, respectively.

Therefore, the *snf2* deletion mutant and *snf2K798A* mutant upregulate a similar number of genes and have a similar influence upon the upregulation of these genes.

It is worth noting that although Swi-Snf is generally considered an activator of transcription, the transcriptome data from the *snf2* and *snf2K798A* mutants shows that *SNF2* has a repressive role of an almost equally large number of genes as it activates.

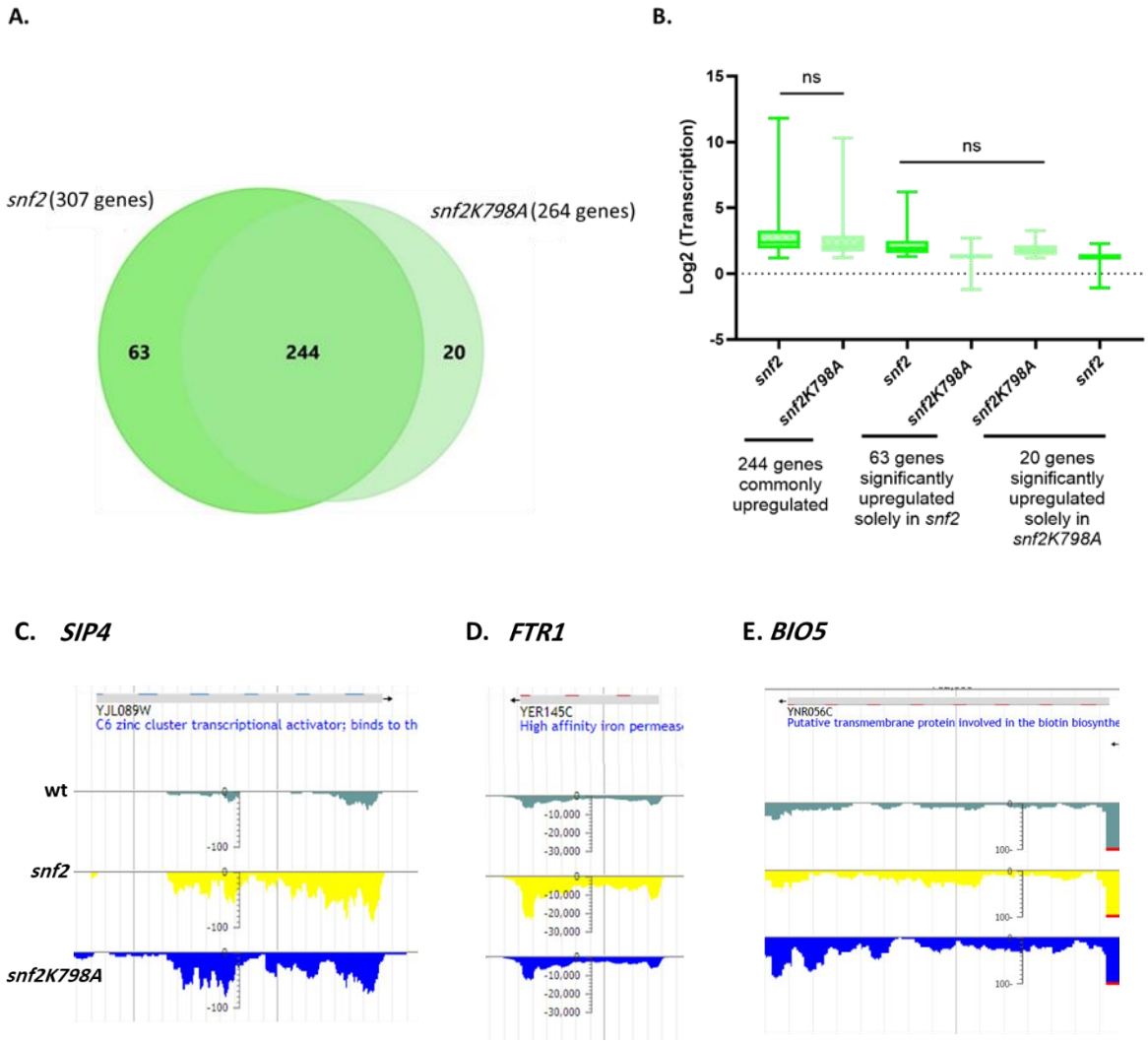

Figure 4. 7: (A) Venn diagram to identify the genes shared and uniquely upregulated in the *snf2* and *snf2K798A* mutant strains. **(B)** Box plot to show the average fold changes of the different classes of upregulated genes. **(C)** J-browse image example to show the transcription level of genes up in *snf2* and *snf2K798A (SIP4)*. **(D)** J-browse image to show transcription level example of genes significantly solely upregulated in *snf2 (FTR1)*. **(E)** J-browse image to show transcription level example of genes significantly solely upregulated in *snf2K798A (BIO5).*

4.2.4.4 Comparing the gene ontology difference in the *snf2* and *snf2K798A* upregulated genes

Next, I analysed the gene ontology of the genes upregulated in both mutants. Firstly, I looked at the shared genes that were upregulated in both mutants (244 genes) (Fig. 4.8A). The result showed that there were genes involved in ubiquitylation including the *RIM8* gene which encodes a ubiquitin-protein ligase [160], and *SIP4* which encodes a transcription factor [161] (Fig. 4.8B).

Amongst the 63 genes solely upregulated in the *snf2* mutant, the *FTR1* encodes a high-affinity iron permease, [162], and the *EDS1* gene encodes a putative zinc cluster protein predicted to be a transcription factor [163] (Fig. 4.8 C, D).

When I looked at the 20 genes upregulated solely in the *snf2K798A* mutant, (Fig. 4.8 E) the data showed that *RIM4, a* gene involved in RNA splicing, was upregulated [164] (Fig. 4.8E, F).

Taken together, there was a similar impact on gene transcription in the *snf2* and *snf2K798A* mutants, despite the expected collapse of the Swi-Snf complex structure reported to occur specifically in the *snf2* deletion mutant.

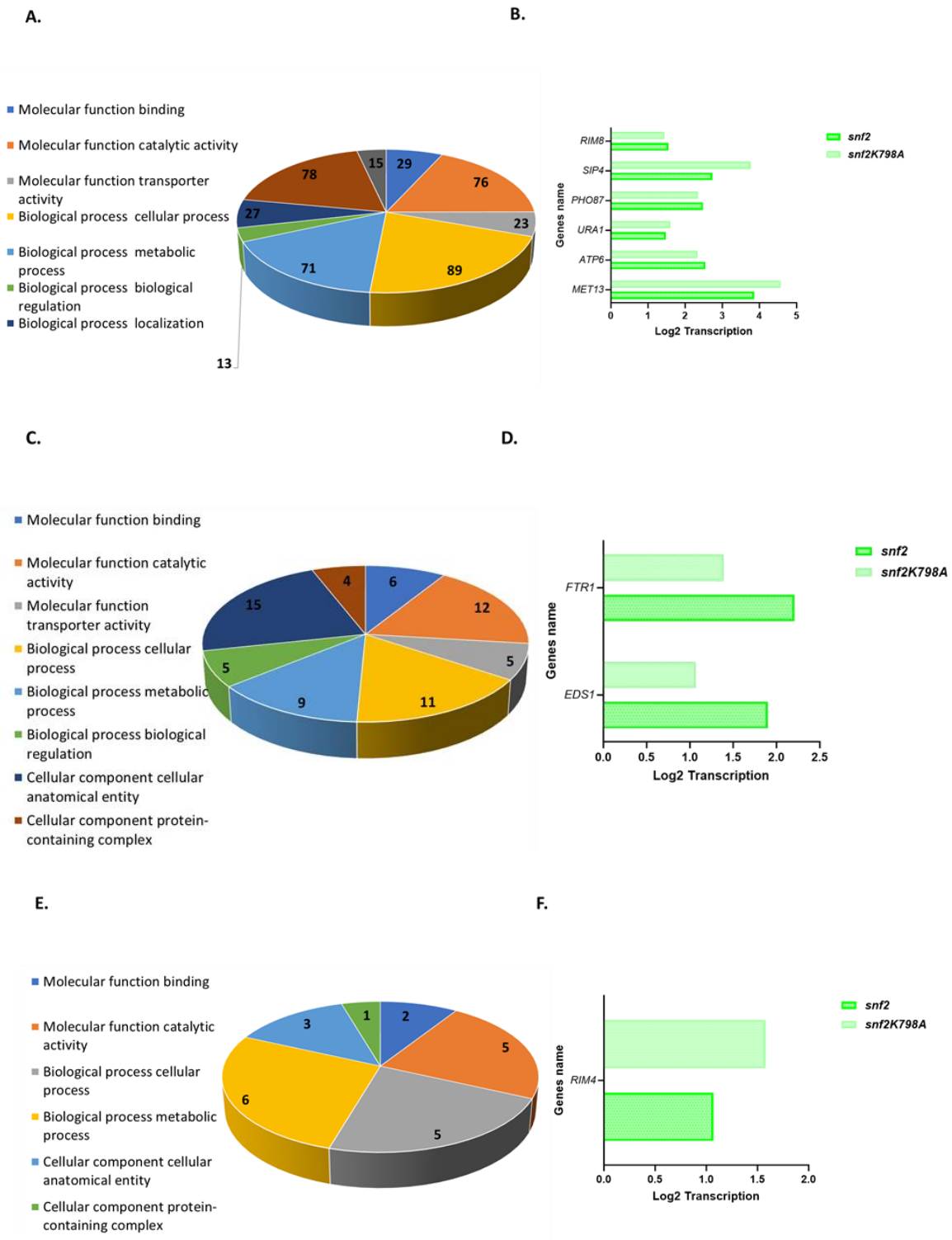

Figure 4. 8: Gene ontology analysis of the genes upregulated in the *snf2* and *snf2K798A* mutants. (A) gene ontology of the commonly upregulated genes in two mutants (244 genes). **(B)** Examples of these genes and their fold changes relative to wt.

(C) gene ontology of the genes solely upregulated in the *snf2* mutant strain (63 genes) **(D)** Examples of these genes and their fold changes relative to wt. **(E)** genes ontology of the genes solely upregulated in the *snf2K798A* (20 genes). **(F)** Examples of these genes and their fold changes relative to wt.

4.2.5 Comparing each Swi-Snf subunit mutant with the *snf2* mutant

The Snf2p subunit is the catalytic heart of the Swi-Snf complex, making it arguably the most important Swi-Snf subunit [83]. I therefore compared the genes down- and upregulated in each of the Swi-Snf subunit mutants with the genes down- and upregulated in the *snf2* deletion mutant.

4.2.5.1 Comparing genes downregulated in *snf2* and *snf5* deletion mutants

I first investigated the number of genes whose transcription was downregulated relative to wt in the *snf5* mutant compared to those downregulated in the *snf2* deletion mutant (Fig. 4.9A). The *snf5* mutant showed 215 genes were downregulated, whilst the *snf2* mutant showed 348 were downregulated. The data showed 124 of these genes overlapped between the two mutants, whilst 224 were uniquely downregulated in *snf2*, and 91 genes were uniquely downregulated in *snf5*.

The next step was to examine whether or not there were differences in the average levels of transcription of the genes downregulated in the *snf2* and *snf5* mutants (Fig. 4.9B). This would offer insight into the contribution of each subunit to the regulation of gene transcription. Analysis of the 124 genes commonly down regulated in both mutants revealed that these genes were downregulated the most in the *snf2* mutant. Of the genes uniquely downregulated in the *snf2* (224 genes) and *snf5* mutants (91 genes), the genes downregulated in the *snf2* mutant were downregulated to the greatest extent. Thus, loss of *SNF2* has the greatest negative impact upon gene transcription than loss of *SNF5*.

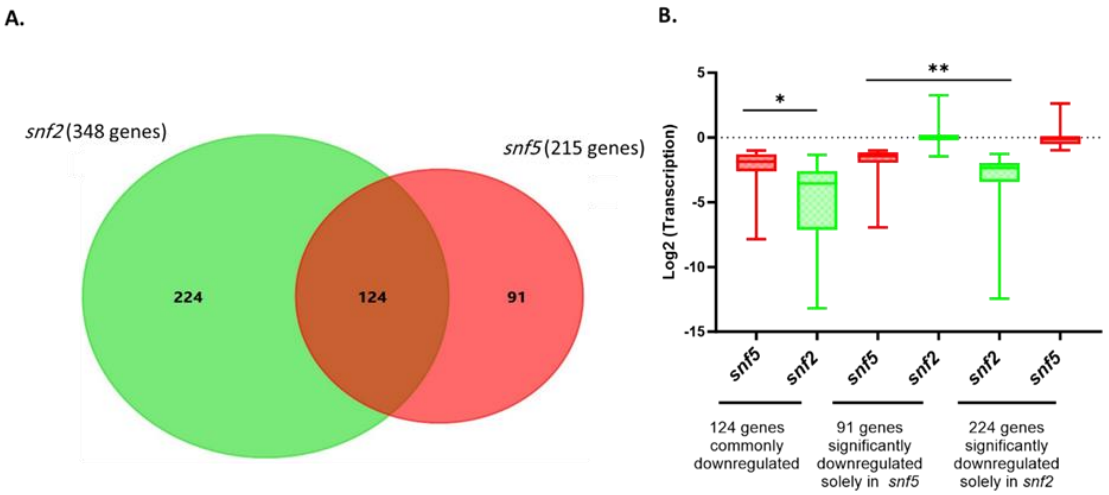

Figure 4. 9: (A) Venn diagram to identify the genes shared and uniquely down-regulated in the *snf2* and, *snf5* mutant strain. **(B)** Box plot to show the fold changes of the down-regulated genes.

Interestingly, when I examined a scatter plot the genes solely downregulated in the *snf5* deletion mutant (91 genes) there were several of these genes that were upregulated more than 2-fold in the *snf2* deletion mutant (Fig.4.10A). Examples of these genes include *SUC2* and *FLO9* (Fig.4.10B). This result suggests that at these genes, *SNF5* has a positive effect upon their transcription, whilst *SNF2* works as a repressor of transcription.

Similarly, when I analysed the genes that were solely downregulated in the *snf2* mutant (224 genes), there were a number of these genes that were upregulated more than 2-fold in the *snf5* mutant (Fig. 4.10C). This result suggests that at these genes, *SNF2* has a positive effect upon their transcription, whilst *SNF5* works as a repressor of transcription. Examples of these genes include *ALD3* and *CTT1* (Fig. 4.10D).

In summary, these data suggest that the Snf2p and Snf5p subunits of the Swi-Snf complex can play distinct roles in the regulation of gene transcription and, at some genes, the *snf2* and *snf5* mutants have opposing impacts upon transcription.

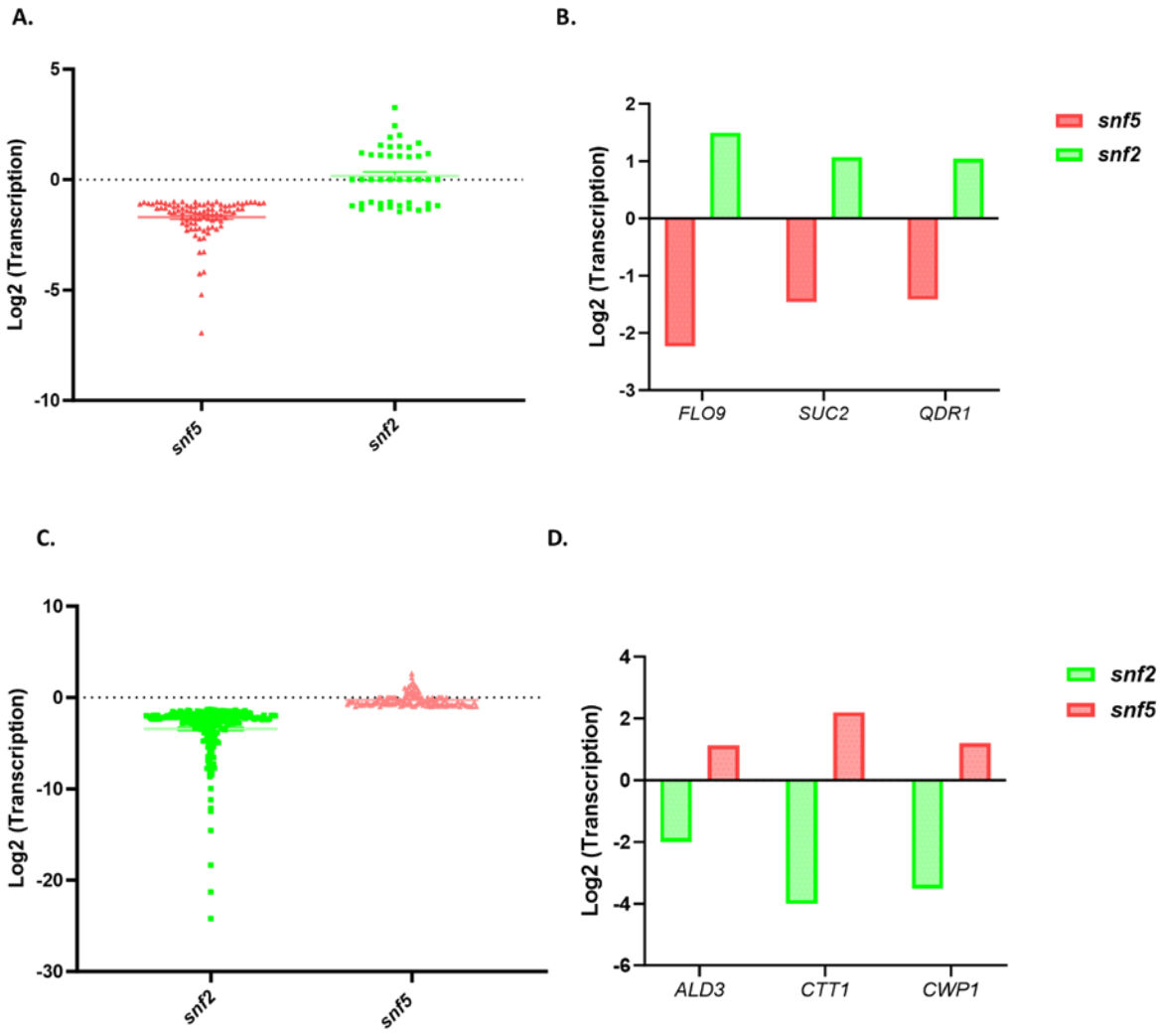

Figure 4. 10: (A) scatter plot of the 91 genes significantly downregulated solely in a *snf5* mutant strain. **(B)** Examples of the genes shown in A and their fold changes relative to wt. **(C)** scatter plot of the 224 genes significantly downregulated solely in a *snf2* mutant strain. **(D)** Examples of the genes shown in C and their fold changes relative to wt.

4.2.5.2 Gene ontology of the genes uniquely downregulated in *snf5* compared to *snf2*

Next, gene ontology analysis of the 91 genes significantly downregulated solely in the *snf5* mutant were analysed. The result revealed *SUC2* and *IMA1* in the molecular function GO category (Fig. 4.11 A, B).

In the cellular component GO category, 21 genes played a role in the cell periphery, the broad region around and including the plasma membrane of a cell, which included the Flocculin-encoding *FLO9* gene[165].

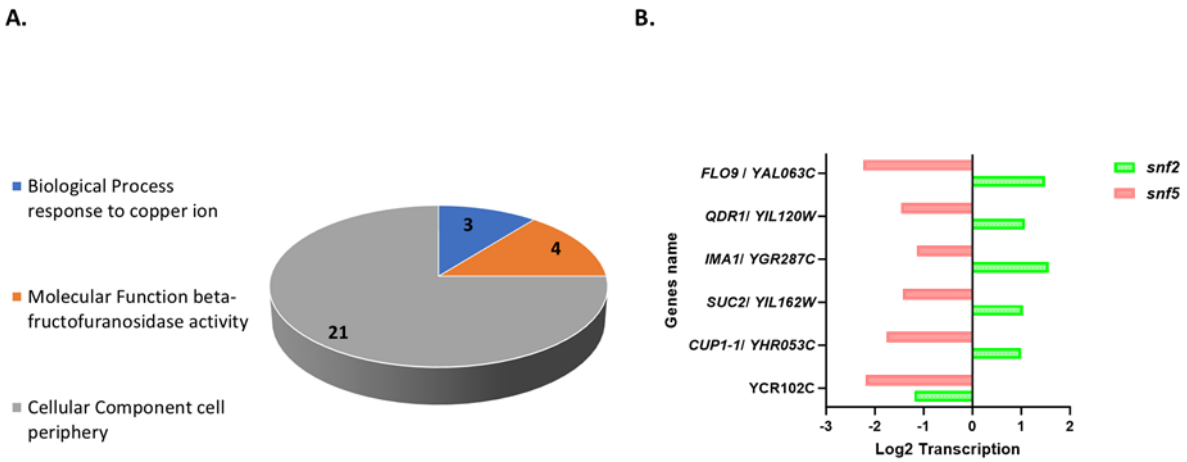

Figure 4. 11: Gene ontology analysis of the genes solely downregulated in *snf5*. (A) Gene ontology of the genes downregulated solely in *snf5*. **(B)** Examples of these genes and their fold changes relative to wt in *snf2* and *snf5*.

4.2.5.3 Comparing genes upregulated in *snf2* and *snf5* deletion mutants

I next compared the genes upregulated in the *snf2* and *snf5* mutant strains (Fig. 4.12A). These genes represent those genes in wt at which *SNF2* and *SNF5* are exerting a repressive role. There were 141 genes upregulated in the *snf5* mutant and 307 genes upregulated in a *snf2* mutant. The result showed only 73 of these upregulated genes were shared between both mutants. 234 genes were uniquely upregulated in the *snf2* mutant, while 68 genes were uniquely upregulated in the *snf5* strain. Therefore, the Snf2p subunit has a much greater influence upon gene repression, in terms of the number of genes upregulated in its absence, compared to the Snf5p subunit.

When I examined the average upregulation of the different gene cohorts in the *snf2* and *snf5* mutants, the data showed that loss of *snf2* caused the greatest gene de-repression compared to loss of *SNF5* at both the uniquely *snf5* upregulated genes and the commonly upregulated genes (Fig. 4.12B).

Thus, Snf2p plays a greater role in gene repression than the Snf5p subunit. Together, this shows that Snf2p not only positively and negatively regulates more genes than Snf5p, it also shows that Snf2p negatively influences these genes more strongly than Snf5p.

Upon further analysis of the genes uniquely upregulated in the *snf5* mutant using a scatter plot, there were some of these genes which were downregulated in the *snf2* mutant (Fig. 4.13A). Examples of these genes included *HSP12* and *IRC15* (Fig. 4.13B). Thus, at these genes in wt, *SNF5* plays a negative role in transcription, whilst *SNF2* plays a positive role. Conversely, within those genes uniquely upregulated in the *snf2* mutant, there were some of these genes which were downregulated in the *snf5* mutant (Fig. 4.13 C, D). Here, *SNF2* is playing a negative role while *SNF5* plays a positive role.

This is more evidence of the different Swi-Snf subunit genes having antagonistic influences on the transcription of the same target genes.

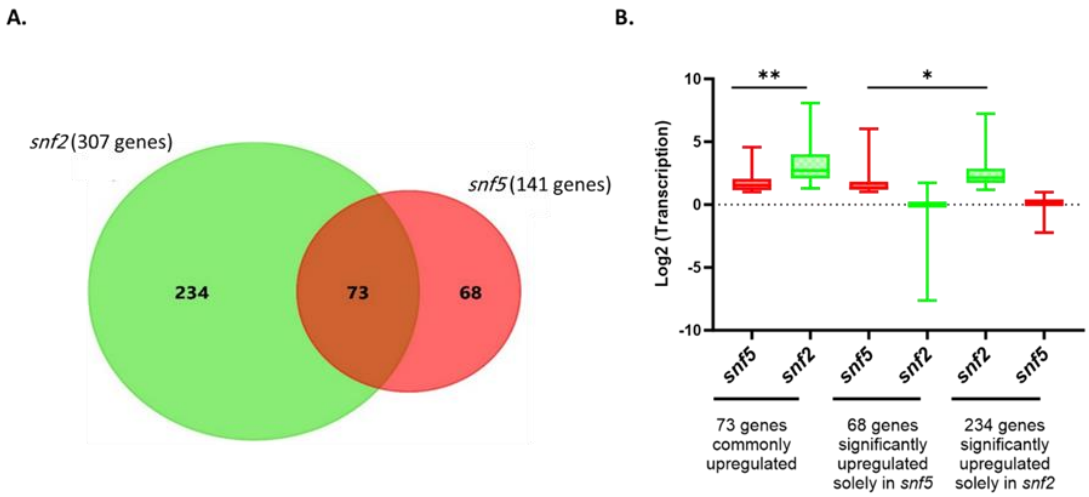

Figure 4. 12: (A) Venn diagram to identify the genes shared and uniquely upregulated in the *snf2* and *snf5* mutants compared to wt. **(B)** Box plot to show the fold changes of the upregulated genes.

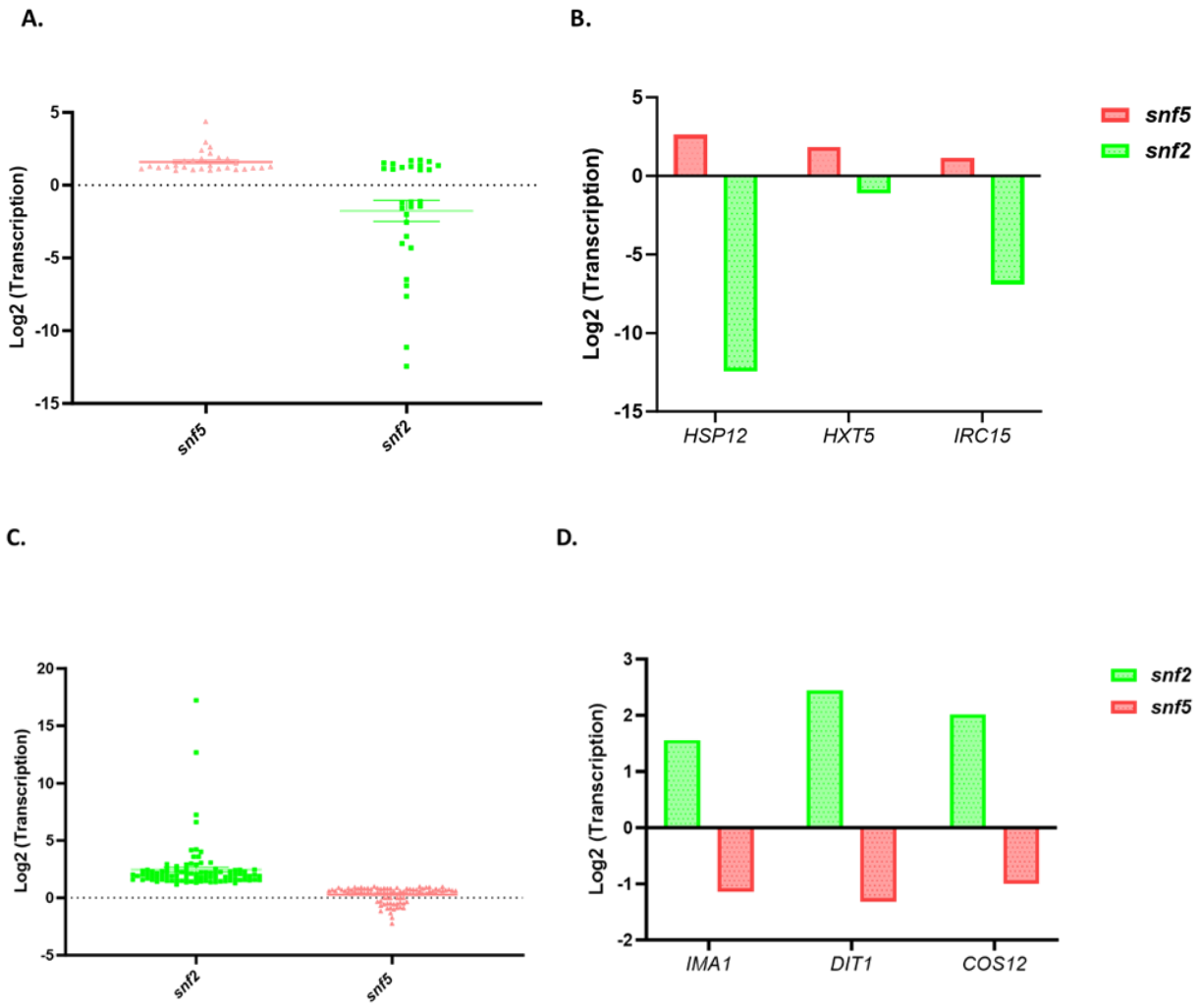

Figure 4. 13: (A) Scatter plot of the genes significantly upregulated solely in a *snf5* mutant strain. (**B)** Examples of these genes and their fold changes relative to wt. **(C)** scatter plot of the genes significantly upregulated solely in a *snf2* mutant strain. **(D)** Examples of these genes and their fold changes relative to wt.

4.2.5.4 Gene ontology of genes uniquely upregulated in *snf5* compared to *snf2*

The gene ontology analysis of the genes upregulated solely in a *snf5* mutant (68 genes) showed that *SPS2* and *DON1* genes were included in the biological process GO term (Fig. 4.14 A, B). In the molecular function GO category, 16.2% of these genes, like *GRE2,* played a role in oxidoreductase activity. The *ALD3* gene was representative of a gene found in the cellular component category.

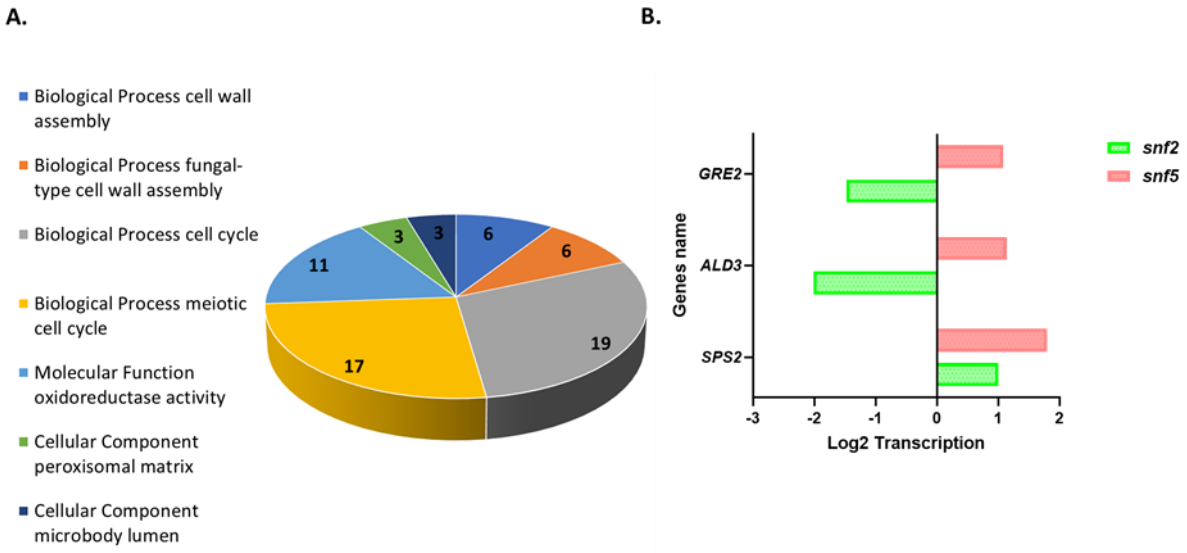

Figure 4. 14: Gene ontology analysis of genes upregulated in the *snf5* mutant. **(A)** gene ontology of the genes significantly upregulated solely in *snf5*. **(B)** Examples of these genes and their fold changes relative to wt.

4.2.6 Comparing genes downregulated in a *snf6* deletion mutant with genes downregulated in a *snf2* mutant

I next compared the genes downregulated in a *snf6* mutant with those genes down regulated in a *snf2* mutant (Fig 4.15A). The analysis revealed there were 271 genes downregulated in *snf6* compared to 348 in *snf2*. One hundred and fifty-five genes overlapped between the *snf2* and *snf6* mutants, whereas the number of genes uniquely downregulated in *snf2* was 193, while 116 genes were uniquely downregulated in *snf6*.

I next examined the average transcription levels of the commonly downregulated genes and the uniquely downregulated genes in the *snf2* and *snf6* strains (Fig. 4.15B). Overall, the results showed that for the downregulated genes, those genes downregulated in the *snf2* mutant were consistently downregulated to a greater extent than those genes downregulated in the *snf6* mutant.

Thus, again, the data suggests that loss of Snf2p has a greater influence upon the levels of target gene activation than loss of the Snf6p subunit.

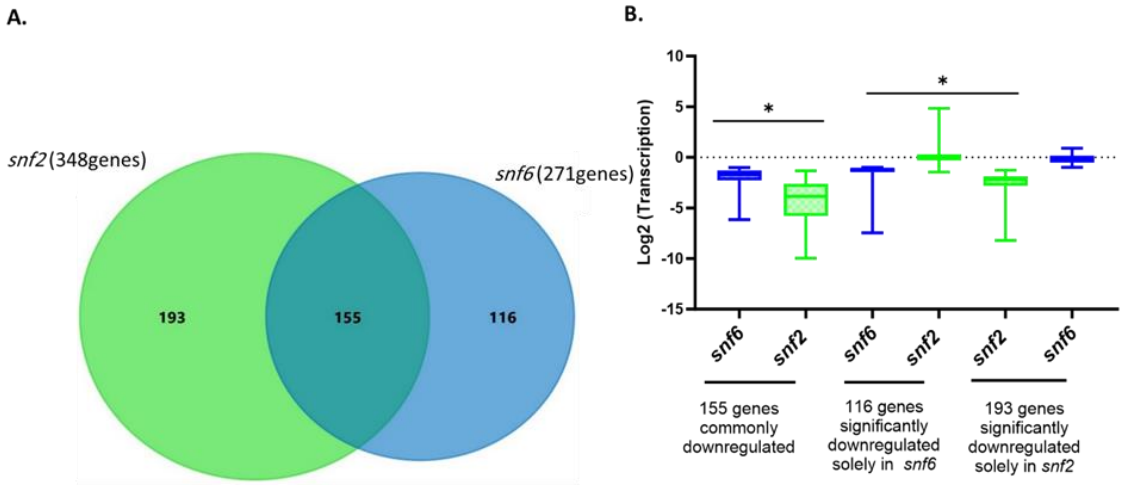

Figure 4. 15: (A) Venn diagram to identify the genes shared and uniquely downregulated in the *snf2* and *snf6* mutant strains. **(B)** Box plot to show the fold changes of the down-regulated genes.

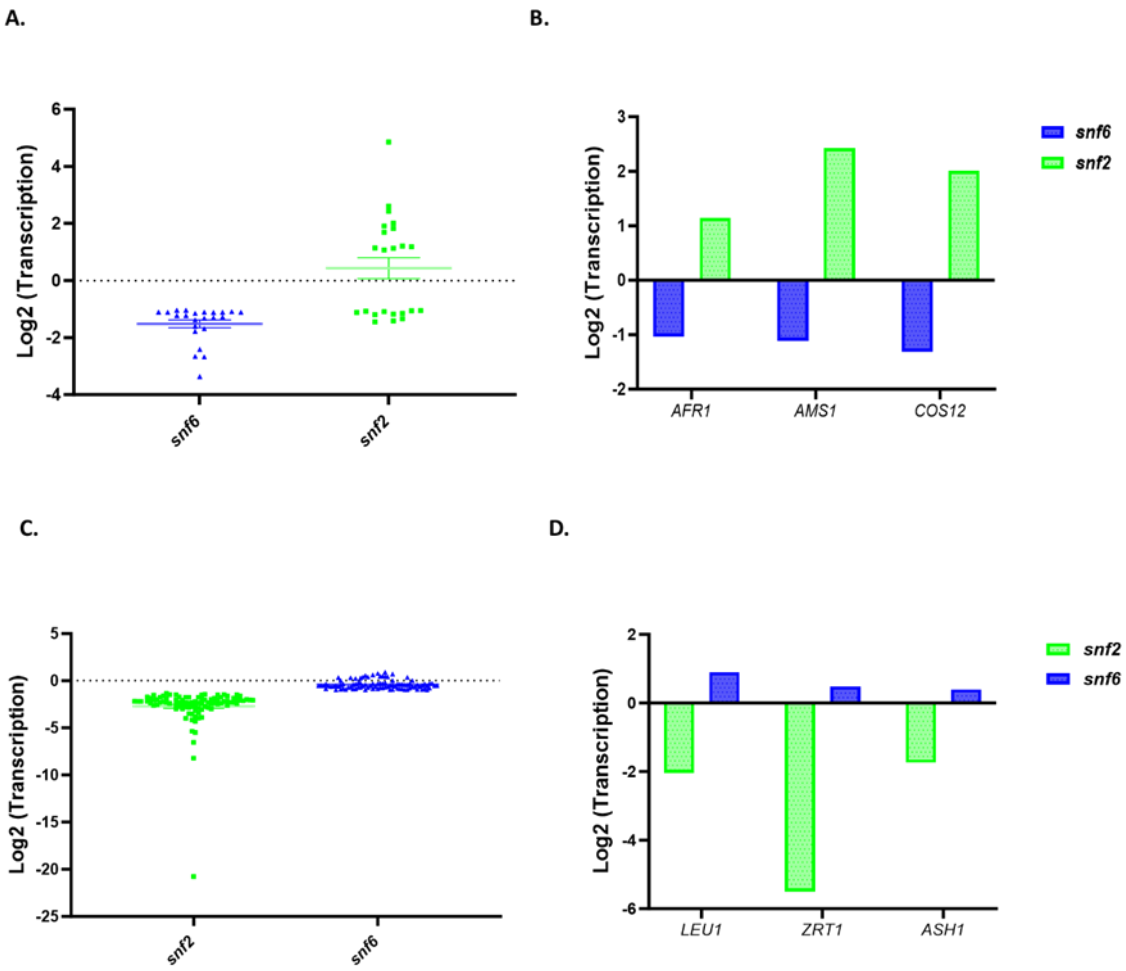

Figure 4. 16: (A) Scatter plot of the genes significantly downregulated solely in a *snf6* mutant strain (116 genes). **(B)** Examples of these genes and their fold changes relative to wt. **(C)** Scatter plot of the genes significantly downregulated solely in a *snf2* mutant strain (193 genes). **(D)** Examples of these genes and their fold changes relative to wt.

Upon further analysis of the genes uniquely downregulated in the *snf6* mutant, there were some of these genes which were upregulated in the *snf2* mutant (Fig. 4.16A). Examples of these genes included *AFR1* and *AMS1* (Fig. 4.16B). Thus, at these genes in wt, *SNF6* plays a positive role in transcription, whilst *SNF2* plays a negative role. Conversely, within those genes downregulated in the *snf2* mutant, none of these genes were significantly more than 2-fold upregulated in the *snf6* mutant (4.16 C, D).

Therefore, at these genes, *SNF2* is playing an exclusive positive role, while *SNF6* plays no role in their regulation.

This is more evidence of the different SWI-SNF subunit genes having antagonistic influences on the same target genes, which highlights that the different Swi-Snf subunits can have distinctly different roles upon target gene transcription.

4.2.6.1 Analysing the gene ontology of the *snf6* uniquely downregulated genes

I next performed GO analysis on the 116 genes uniquely downregulated in the *snf6* mutant. The result revealed 30 genes included in the plasma membrane cellular component category including the *HXT5*, *QDR2* and *PDR11* genes (Fig. 4.17A); 27 genes were found within the organonitrogen compound catabolic process category, such as *AMS1* (Fig. 4.17B), and 19 genes were found within the response to stress category including the *AFR1* gene which encodes a protein required for pheromone-induced projection (shmoo) formation[166].

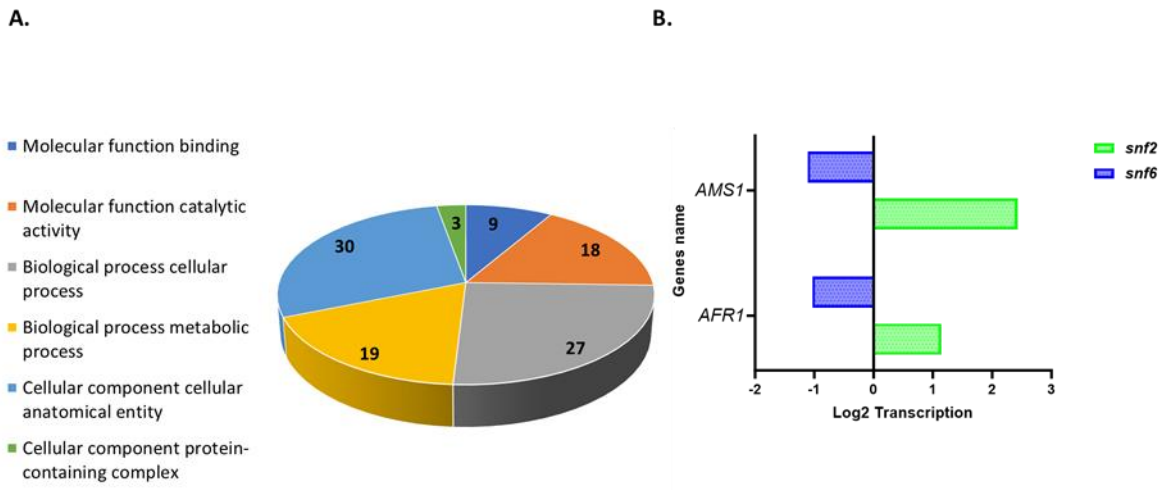

Figure 4. 17: Gene ontology analysis of the 116 genes solely downregulated in the *snf6* mutant. **(A)** Gene ontology of the genes solely downregulated in *snf6* (116 genes). **(B)** Examples of these genes and their fold changes relative to wt.

4.2.6.2 Comparing genes upregulated in *snf6* and *snf2* deletion mutants

There were 86 genes upregulated in the *snf6* mutant, of which 62 of these genes were shared with the *snf2* mutant. Only 24 genes were uniquely upregulated in the *snf6* mutant (Fig. 4.18A).

When I examined the genes uniquely upregulated in these mutants, the genes upregulated in the *snf2* mutant were consistently upregulated the most compared to the genes upregulated in the *snf6* mutant (Fig. 4.18B).

Thus, the impact of the loss of *SNF6* upon target gene repression is less than that due to the loss of the Snf2p subunit suggesting Snf2p contributes more to gene repression than Snf6p.

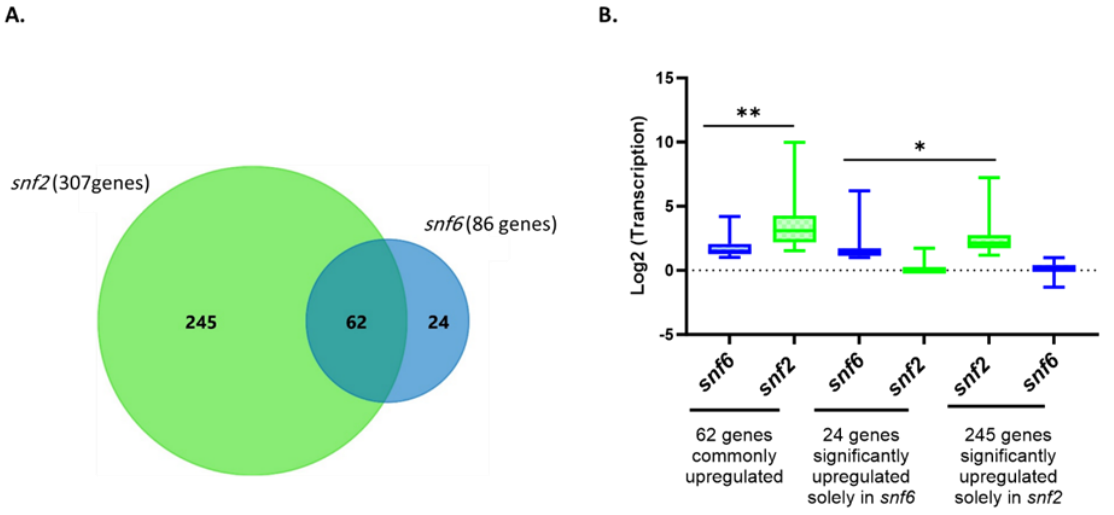

Figure 4. 18: (A) Venn diagram to identify the genes shared and uniquely upregulated in the *snf2* and *snf6* mutant. **(B)** Box plot to show the fold changes of the up-regulated genes.

When I examined the genes solely upregulated in the *snf2* mutant, there was evidence that some of these genes were significantly downregulated in the *snf6* mutant (Fig. 4.19A). Examples of these genes are *RGM1* and *COS12* (Fig. 4.19B). This suggests that these genes are subject to negative regulation by *SNF2* and are positively regulated by *SNF6*. This is again evidence of the different Swi-Snf subunits having antagonistic influences upon common target gene transcription.

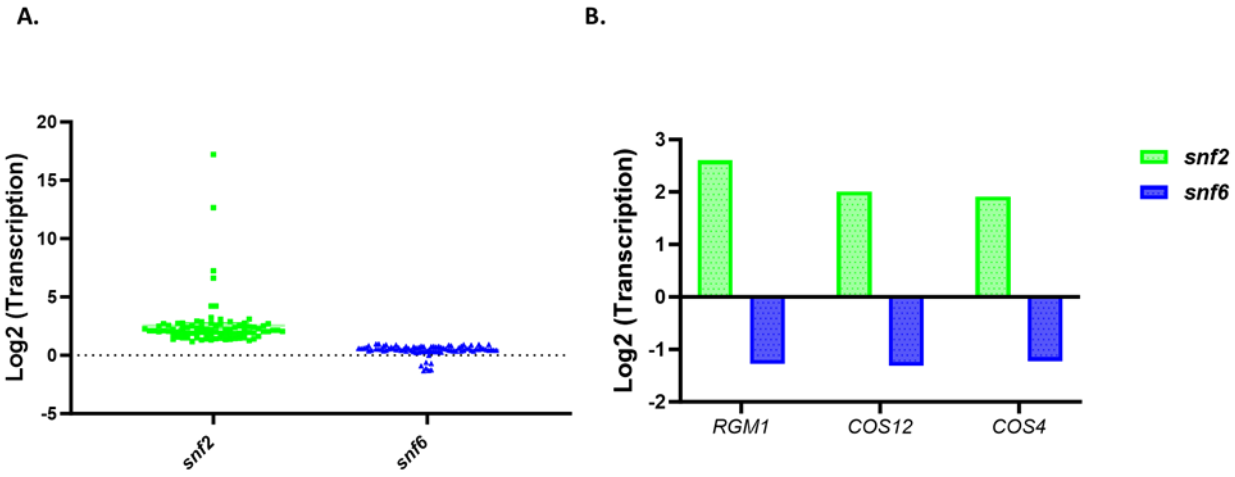

Figure 4. 19: (A) Scatter plot of the genes significantly upregulated solely in a *snf2* mutant strain with transcription in the *snf6* mutant **(B)** Examples of these genes and their fold changes relative to wt.

4.2.6.3 Gene ontology of the genes uniquely upregulated in *snf6* compared to *snf2*

I next analysed the gene ontology of the 24 genes solely upregulated in the *snf6* mutant (Fig. 4.20). There were 9 genes listed within the 'cellular component' term; *CDA1*, *HXT10*, *SPS1*, *ADH2*, *RAD59*, *FEB1*, *DSE4*, *YRF1-3*, and *YRF1-7*. In the 'molecular function' term, the result showed that 6 genes were included in the catalytic activity category. These genes included *ALD6* and *FBP1*. In the 'biological process category', there were 2 genes included; *RAD59* and *FBP1*.

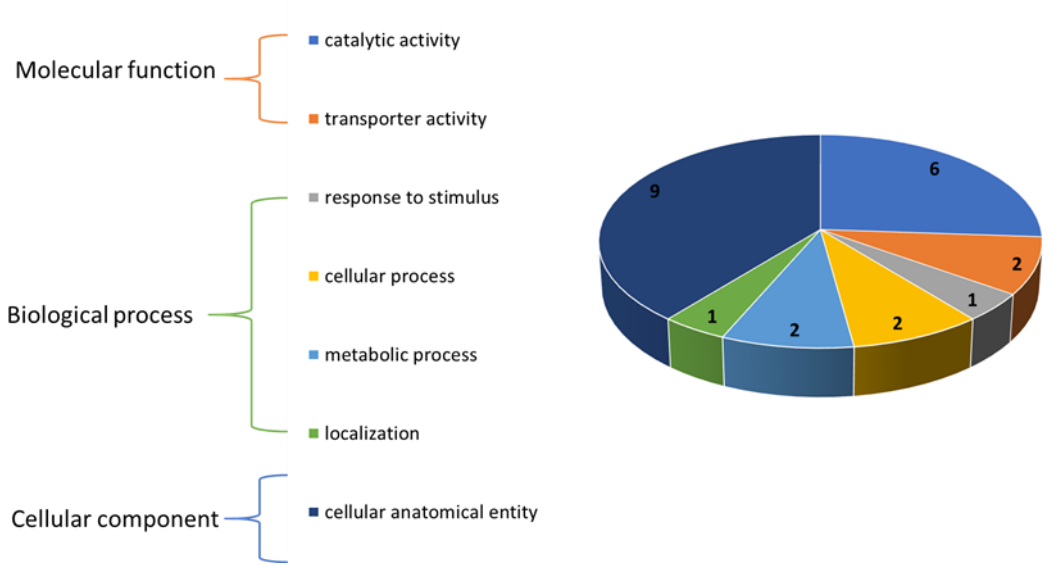

Figure 4. 20: Gene ontology analysis of the genes significantly upregulated solely in the *snf6* mutant compared to the *snf2* mutant.

4.2.7 Comparing the genes downregulated in a *snf2* and *swi3* mutant

Finally, I compared the genes downregulated in the *swi3* mutant with the downregulated genes in the *snf2* mutant (Fig. 4.21A). Here, there were 300 downregulated genes in the *swi3* mutant compared to the 348 genes downregulated in the *snf2* mutant. The Venn diagram revealed a cohort of 116 genes that were downregulated in both mutants, whilst 232 genes were uniquely downregulated in *snf2*, and 184 genes were uniquely downregulated in the *swi3* mutant.

When I compared the average fold downregulation of the shared and uniquely regulated genes in the *swi3* mutant versus the *snf2* mutants, the results showed that, in all cases, the level of difference was greatest in the *snf2* mutant compared to the level of downregulation in the *swi3* mutant (Fig. 4.21B). This was consistent with what was previously seen when comparing the *snf2* mutant with the other subunit mutants and suggests that *SNF2* always contributes the most to target gene activation. Examples of genes downregulated in both mutants, in *snf2* only, and in *swi3* only, are shown in Fig. 4.21C, D and E, respectively.

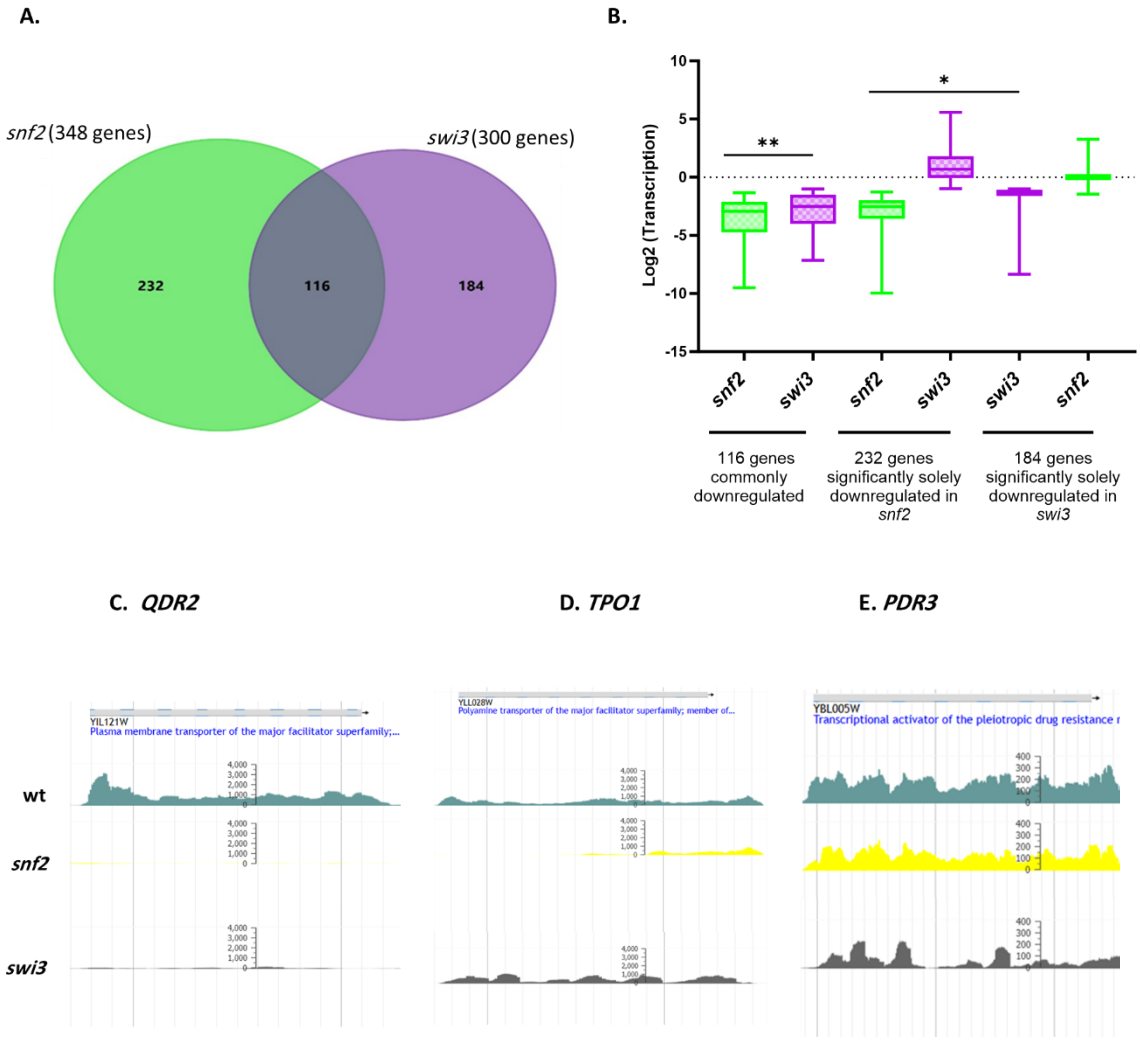

Figure 4. 21: (A) Venn diagram of the genes shared and uniquely downregulated in the *snf2* and *swi3* mutant strains. **(B)** Box plot to show the fold changes of the down-regulated genes. **(C)** J-browse image to show transcription levels of an example of a shared gene downregulated in *snf2* and *swi3* (*QDR2)*. **(D)** J-browse image to show transcription level example of genes solely downregulated in *snf2 (TPO1)*. **(E)** J-browse image to show transcription level example of genes solely downregulated in *swi3* (*PDR3*).

Further analysis of the 184 genes solely downregulated in the *swi3* mutant showed that many of these genes were significantly upregulated in the *snf2* mutant (Fig. 4.22A). This suggests antagonistic regulatory roles for *SWI3* and *SNF2* at these genes such that some of these genes subject to unique positive regulation via *SWI3* are subject to repression by *SNF2*. Examples of these genes are *TIS11* (Fig. 4.22B) and *DIP5* (Fig. 4.22C).

Conversely, of the 232 genes uniquely downregulated in the *snf2* mutant, a large number of these genes (161 genes) were de-repressed (upregulated) more than 2-fold in the *swi3* mutant (Fig. 4.22D). Thus, at these genes, *SNF2* is acting as an activator whilst *SWI3* is acting as a repressor of transcription. An example of one of these genes is *HXT6* (Fig. 4.22E, F).

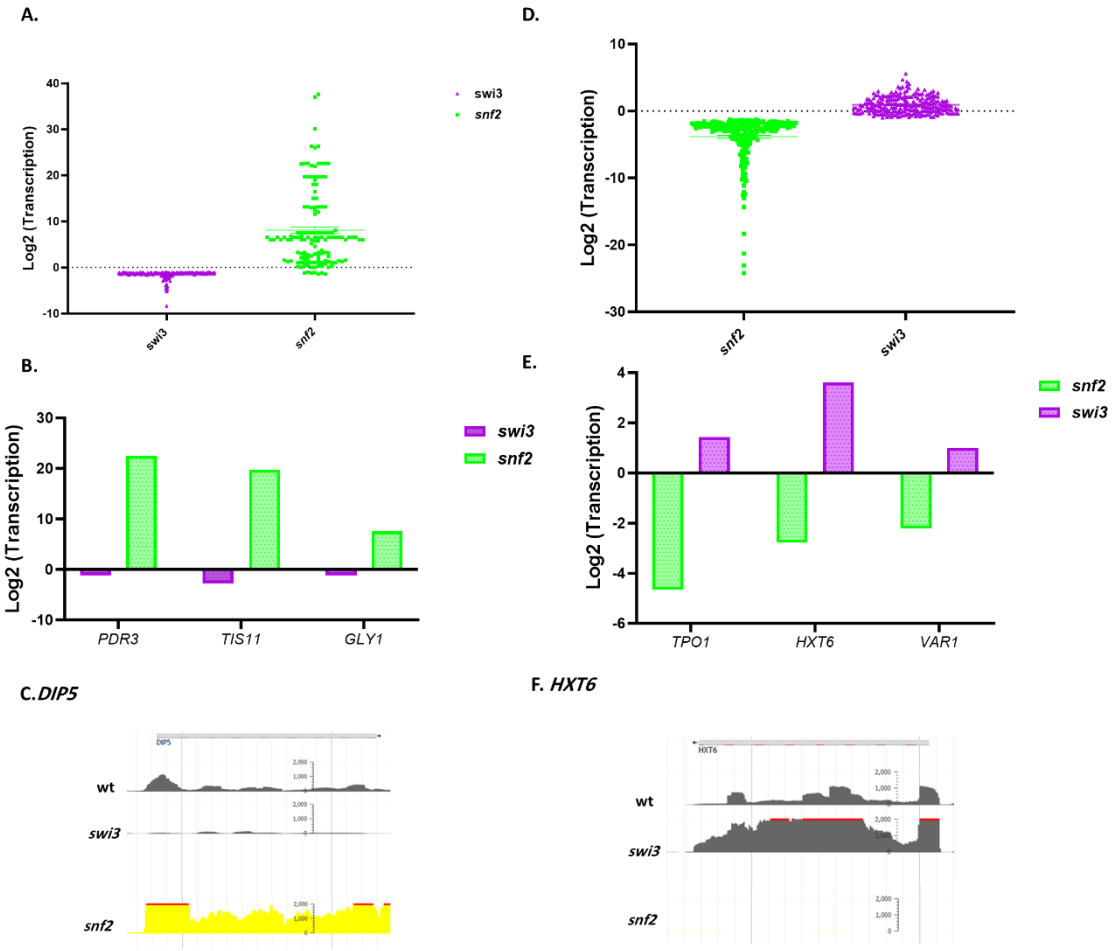

Figure 4. 22: (A) Scatter plot of the (184 genes) significantly downregulated solely in a *swi3* mutant strain and their transcription in the *snf2* mutant. **(B)** Examples of these genes and their fold changes relative to wt. **(C)** J browse example of a gene upregulated in *snf2* and downregulated in *swi3* (*DIP5*). **(D)** Scatter plot of the 232 genes downregulated solely in a *snf2* mutant strain and their transcription in a *swi3* mutant. **(E)** Examples of these genes and their fold changes relative to wt. **(F)** J browse example of a gene upregulated in *swi3* and downregulated in *snf2* (*HXT6*).

4.2.7.1 Gene ontology of the genes uniquely downregulated in *swi3* compared to *snf2*

I next performed GO analysis on the 184 genes significantly solely downregulated in the *swi3* mutant (Fig. 4.23A). In the cellular component category, there were 74 genes which included *DBP2* and *DBP8*, which are involved in the unwinding of a DNA or RNA helix [167]. In the biological process, there were 42 genes involved in the metabolic process, while there were 63 genes included in the cellular component. An example of these genes is the *URA1* gene which encodes the enzyme dihydroorotate dehydrogenase. This enzyme is involved in the *de novo* synthesis of pyrimidine nucleotides, which are essential building blocks for DNA and RNA [168]. The data also showed 33 genes involved in catalytic activity (Fig. 4.23A). Examples of these genes were *FRE1* and *FRE2*, the products of which catalyse the oxidation-reduction of metal ions [158]. There were also 27 genes involved in DNA binding (*NEW1*, *TIF6*).

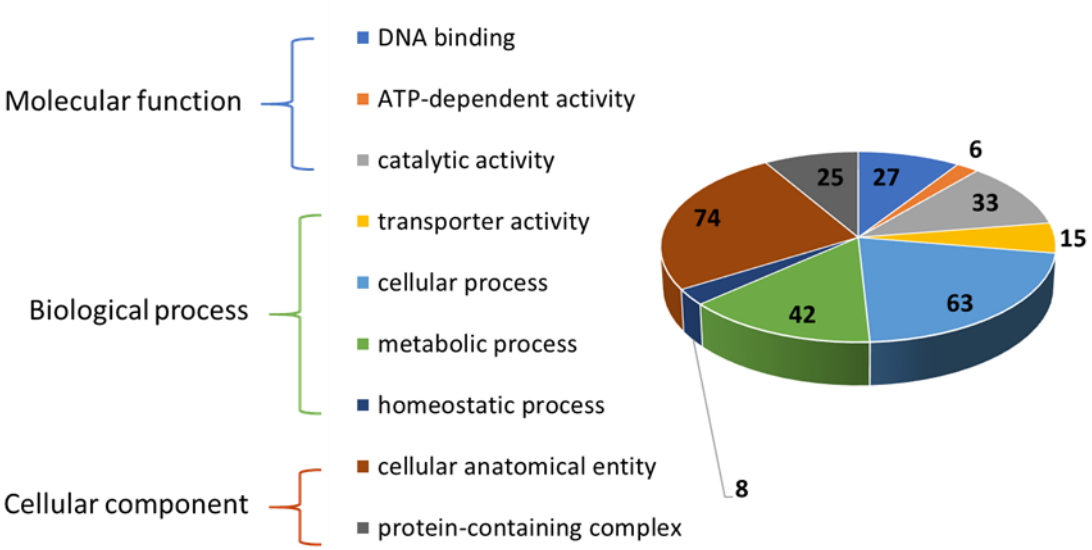

Figure 4. 23: Gene ontology analysis of genes significantly downregulated solely in the *swi3* mutant. Gene ontology of the genes significantly downregulated solely in the *swi3* mutant (184 genes).

4.2.7.2 Comparing the genes upregulated in a *swi3* mutant with those in a *snf2* mutant

The Venn diagram of genes upregulated in the *snf2* and *swi3* strains revealed 148 genes were upregulated in both mutants. Strikingly however, although 232 genes were upregulated only in the *snf2* mutant, almost twice as many genes (436) were uniquely upregulated in the *swi3* mutant (Fig 4.24A). This shows that the Swi3p subunit plays a much greater role in gene repression than Snf2p or any of the other Swi-Snf subunits analysed here.

When I compared the average fold upregulation of the shared and uniquely regulated genes in the *swi3* mutant versus the *snf2* mutants, the results showed that the level of difference was greatest in the *snf2* mutant compared to the level of upregulated in the *swi3* mutant. This was consistent with what was previously seen when comparing the *snf2* mutant with the other subunit mutants in that the Snf2p subunit always contributed the most to target gene activation or repression (Fig 4.24B).

Examples of genes upregulated in both mutants, in *swi3* only, and in *snf2* only, are shown in Fig. 4.24C, D, and E, respectively.

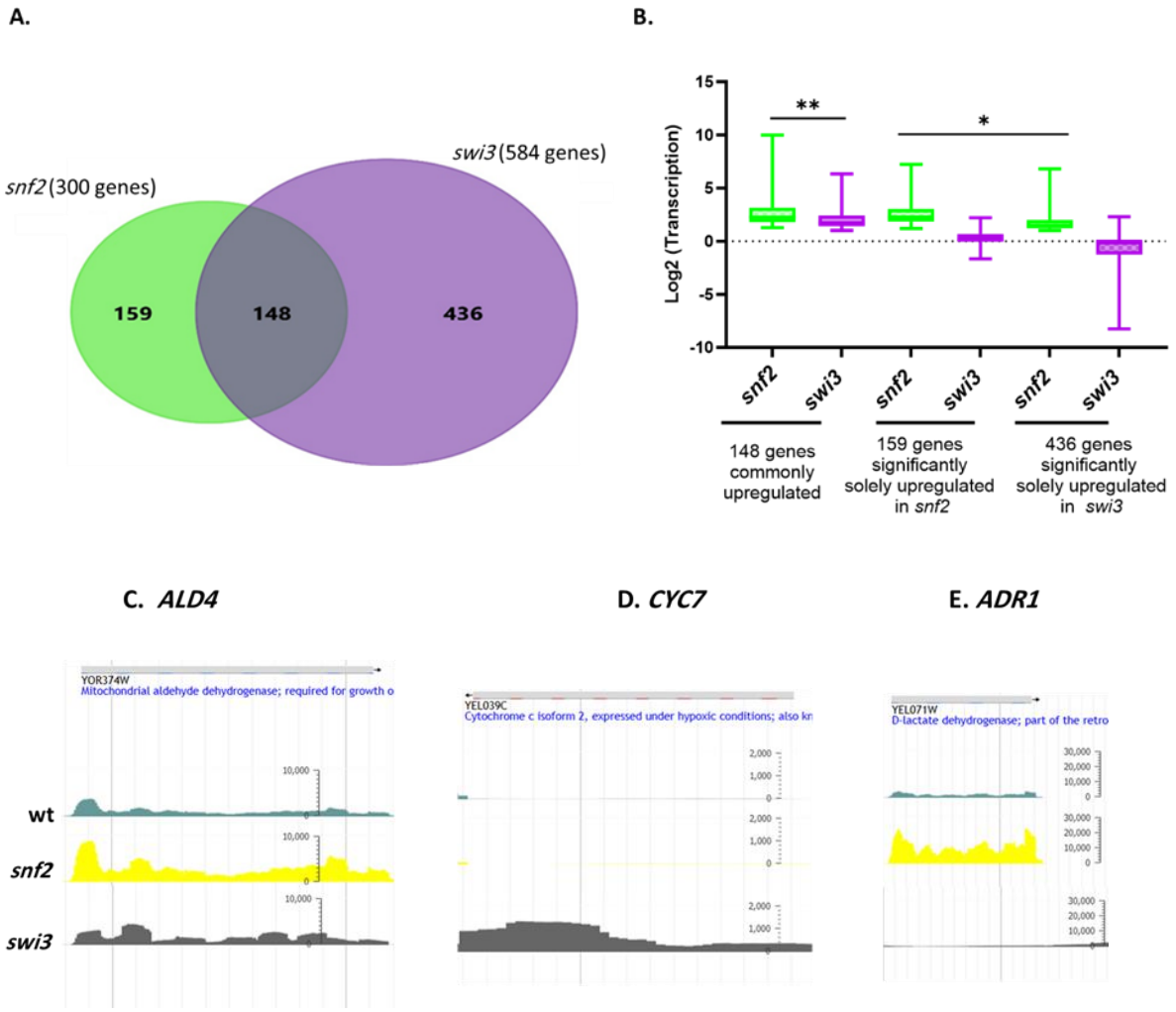

Figure 4. 24: (A) Venn diagram to identify the genes shared and uniquely upregulated in the *snf2*, and *swi3* mutant. **(B)** Box plot to show the fold changes of the upregulated genes. **(C)** J-browse image to show transcription level examples of shared genes upregulated in *snf2* and *swi3, ALD4*. **(D)** J-browse image to show transcription level example of genes significantly solely upregulated in *swi3, CYC7*. **(E)** J-browse image to show transcription level example of genes significantly solely upregulated in *snf2, ADR1*.

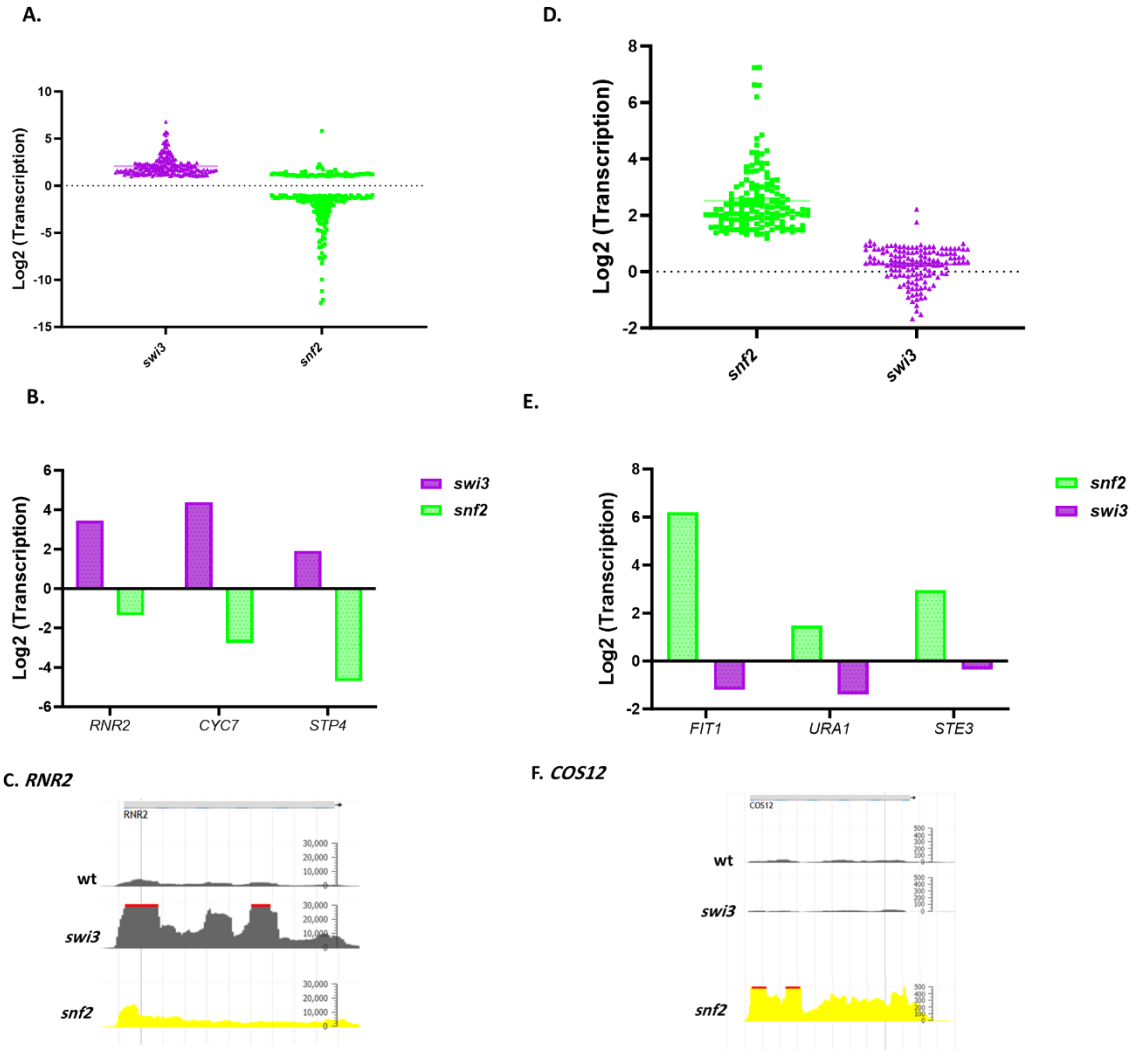

Figure 4. 25: (A) Scatter plot of the 436 genes significantly upregulated solely in a *swi3* mutant strain and their transcription in the *snf2* mutant. **(B)** Examples of these genes and their fold changes relative to wt. **(C)** J browse example of a gene upregulated in *swi3* and downregulated in *snf2* mutant (*RNR2*). **(D)** Scatter plot of the 159 genes significantly upregulated solely in a *snf2* mutant strain and their transcription in the *swi3* mutant. **(E)** Examples of these genes and their fold changes relative to wt. **(F)** J browse example of a gene downregulated in *swi3* mutant and upregulated in *snf2* (*COS12*).

When I examined the 436 genes solely upregulated in the *swi3* mutant and looked at the transcription of these genes in the *snf2* mutant, some genes were shown to be significantly downregulated in the *snf2* mutant (Fig. 4. 25A). Examples of these genes were *RNR2* and *CYC7* (Fig. 4.25B, C). This suggests that at some of the genes subject to negative regulation by *SWI3*, they can be positively regulated by *SNF2*, again demonstrating antagonistic regulation of target genes by different subunits of the Swi-Snf complex.

Conversely, examination of those genes uniquely upregulated in the *snf2* mutant, showed a large proportion of these genes were downregulated in the *swi3* mutant (Fig. 4.25C). This again suggests an antagonistic role for Snf2p and Swi3p in regulation of transcription of these genes. Examples of these genes include *FIT1* (Fig. 4.25E) and *COS12* (Fig. 4.25F).

4.2.7.3 Gene ontology analysis of the genes uniquely upregulated in the *swi3* mutant compared to the *snf2* mutant

The GO analysis of the genes solely upregulated in the *swi3* mutant compared to the *snf2* mutant, showed genes within the molecular function and biological process category like the *ANB1* and *ATP16* genes (Fig. 4.26A). The *ATP16* gene plays a role in the synthesis of ATP from ADP and phosphate by the transfer of protons from one side of a membrane to the other (Fig. 4.26B) [169].

Also, the *ALP1* gene plays a role in molecular function and biological process whereby its gene product enables the transfer of amino acids across the cell membrane (Fig. 4.26B) [170].

A.

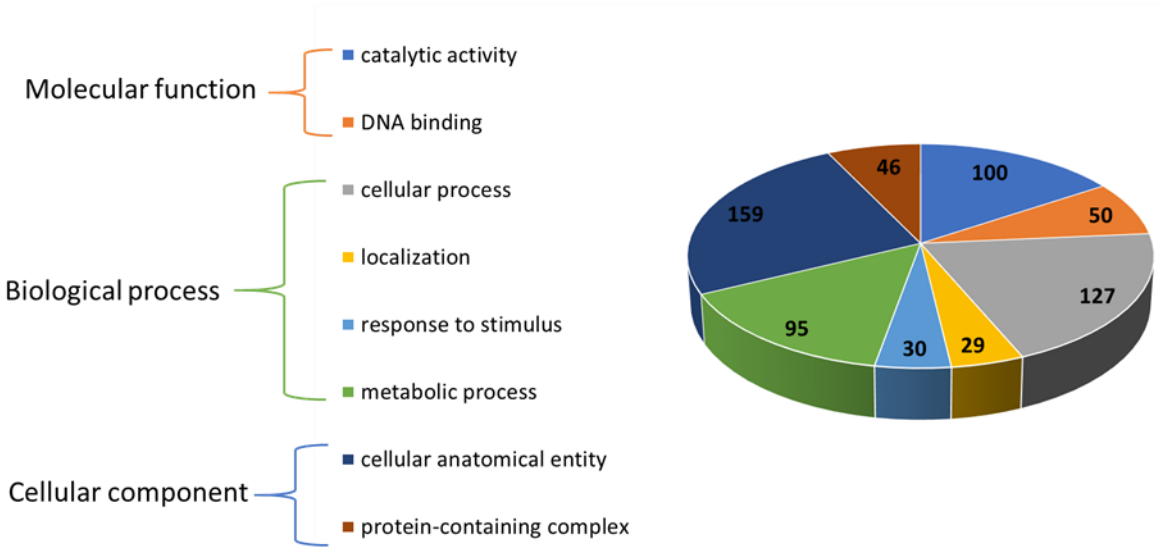

B.

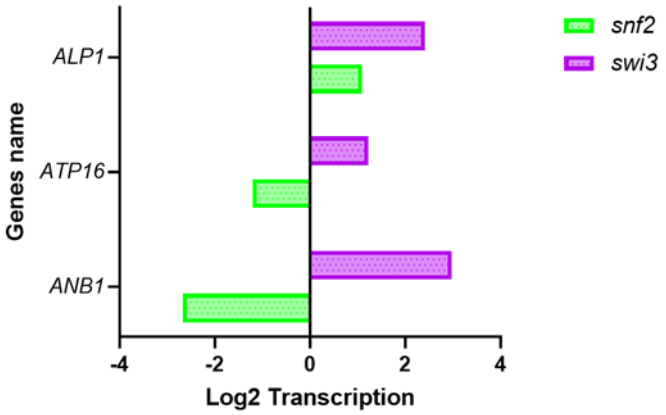

Figure 4. 26: Gene ontology analysis of the genes significantly upregulated solely in the *swi3* mutant. (A) gene ontology of genes solely significantly upregulated in *swi3* (436 genes). **(B)** Examples of these genes and their fold changes relative to wt.

4.2.8 Comparing transcription profiles of Swi-Snf subunit mutants found within the same Swi-Snf complex module

The Swi-Snf complex has been proposed to be comprised of 5 modules: (1) the Arp module, made of Arp7p, Arp9p, and Rtt102p; (2) the catalytic module, containing Snf2p and Snf11p; (3) the Snf6-Snf12-Swi3 module; (4) the Snf5-Swp82-Taf14 sub-module; and (5) the Swi1p module.

4.2.8.1 Visualisation of differential gene expression in the *swi3* and *snf6* mutants

I next looked at the differences in gene transcription between mutants of Swi-Snf subunits found within the same module. The prediction would be that the transcription profiles of subunits found within the same modules would be similar to each other. I therefore first compared the transcription profiles of *swi3* and *snf6* subunit mutants, which are two subunits found in the same module of the Swi-Snf complex (Fig. 4.27). However, the plot of a heat map of the total number of genes up and downregulated in the *snf6* and *swi3* mutants (1241 genes) suggested significant differences in their transcription profiles (Fig. 4.27).

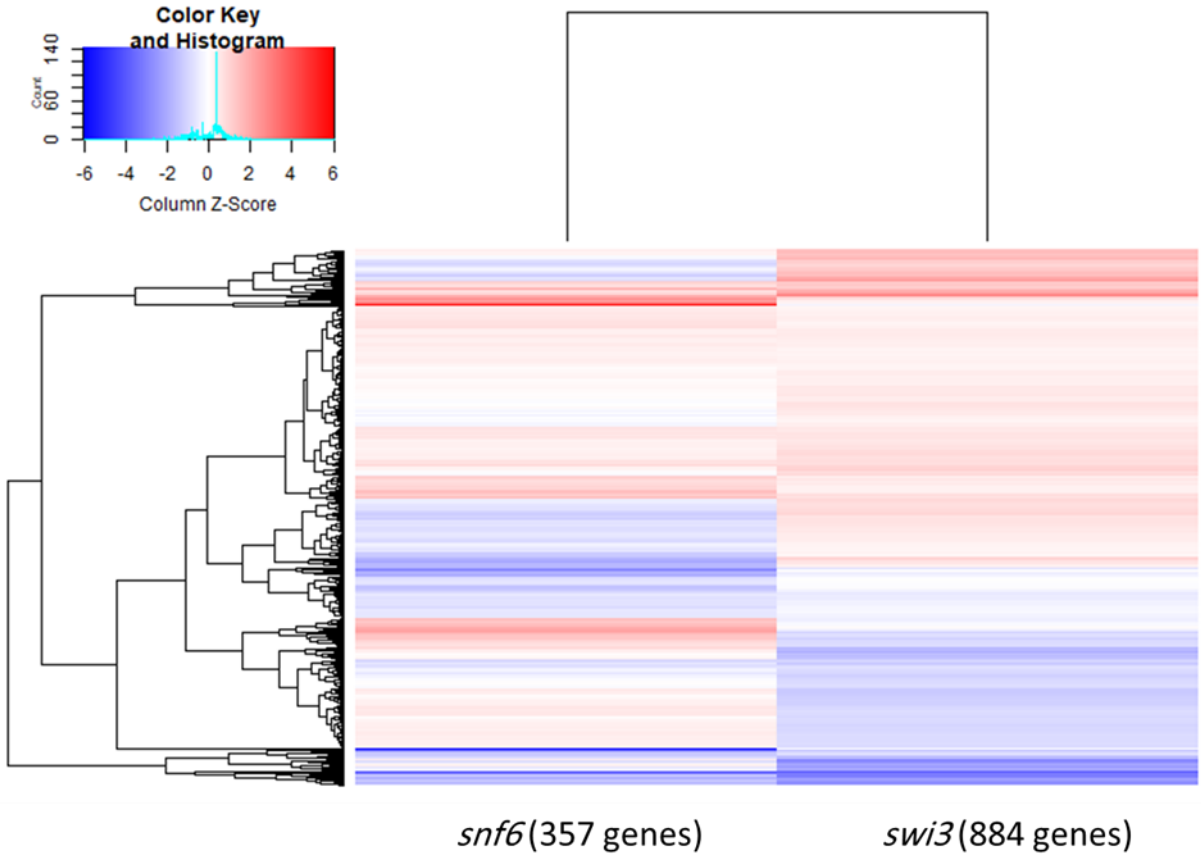

Figure 4. 27: Visualisation of differential gene transcription in the *swi3* and *snf6* mutant. A cluster heat map of all genes up and downregulated in the *snf6* and *swi3* mutants compared to wt, in which rows represent genes, columns represent mutants. The blue colour reflects down-regulated genes and red colour reflect up-regulated genes (>2-fold andFDR of <0.05). Heatmap2 R gplot packaging was used to generate this figure.

4.2.8.2 Comparing the genes downregulated in *swi3* and *snf6* mutants

When I looked at the differences in the genes downregulated in the *swi3* and *snf6* mutant strains in more detail, I found that there were 300 genes more than two-fold downregulated in the *swi3* mutant compared to wt, whereas 271 genes were downregulated in the *snf6* mutant. However, the data showed only 69 of these genes were overlapping; 231 genes were uniquely downregulated in the *swi3* mutant, while 202 genes were uniquely downregulated in the *snf6* mutant (Fig 4.28A).

This surprising result shows that even those Swi-Snf subunits residing within the same sub-modules showed dramatic differences in the numbers of genes under their influence.

I next examined the differences in the transcription levels for the genes commonly and uniquely downregulated in these mutants. The results showed that for the commonly down-regulated genes, the average difference in transcription was greatest in the *swi3* mutant (Fig 4.28B).

Overall, these data suggest that even for Swi-Snf subunits found within the same module, there are differences between the numbers of genes the subunits regulate, and differences in the contribution of these apparently functionally related subunits to the transcription of these genes.

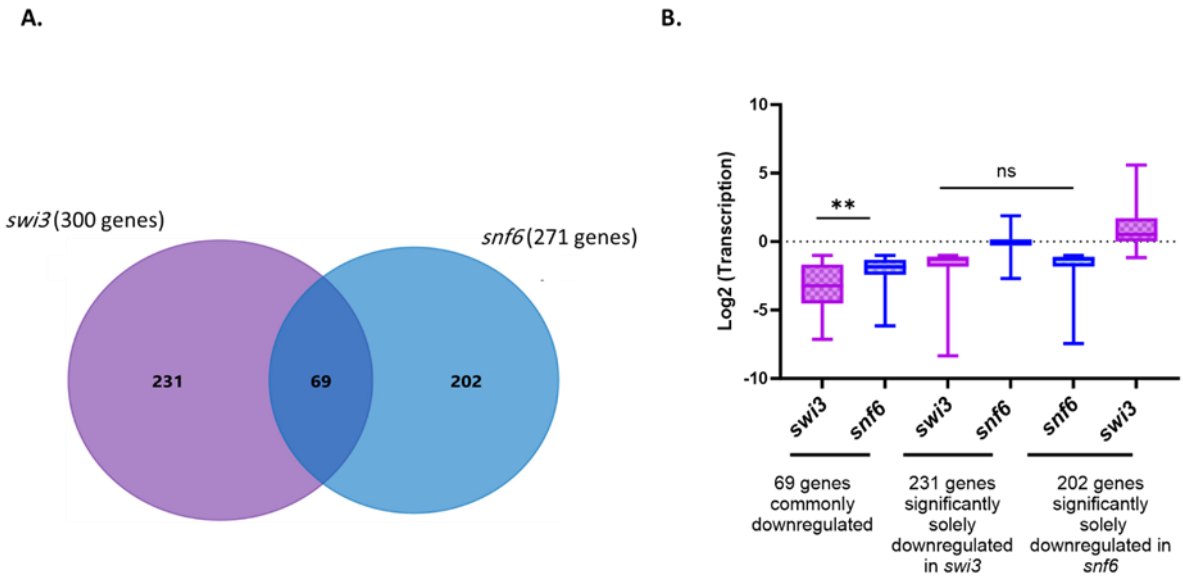

Figure 4. 28: (A) Venn diagram to identify the genes shared and uniquely down-regulated in the *swi3*, and *snf6* mutants. **(B)** Box plot to show the fold changes of the down-regulated genes.

4.2.8.3 Comparing the genes upregulated in *swi3* and *snf6* mutant

When I examined the genes upregulated in the *swi3* and *snf6* mutants, there were 584 genes upregulated in a *swi3* mutant and only 86 genes upregulated in the *snf6* mutant. Only a small set of 43 genes were upregulated in both mutants (Fig. 4.29A).

However, for those 43 genes upregulated in both the mutants, no significant difference in transcription changes could be seen between the *swi3* and *snf6* mutants (Fig 4.29B).

This result shows a major role of *SWI3* is in the repression of genes and shows that even within the context of the Swi3-Snf6 submodule, Swi3p is uniquely dominant in contributing to this negative regulatory role. This result is at odds with the generally accepted role of the Swi-Snf complex as predominantly functioning as a co-activator of transcription.

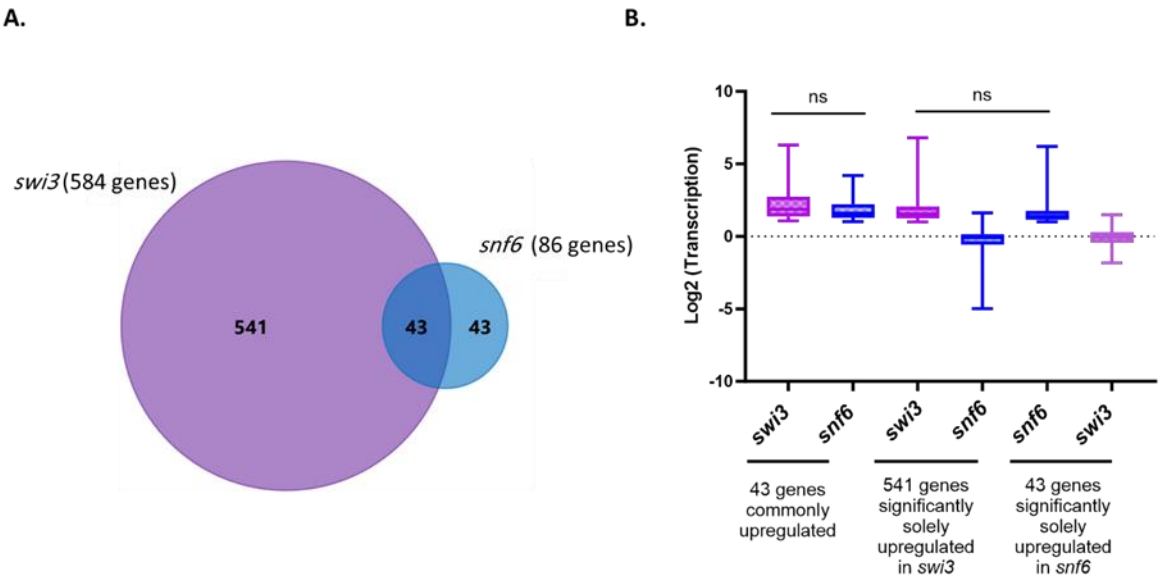

Figure 4. 29: (A) Venn diagram to identify the genes shared and uniquely up-regulated in the *swi3*, and *snf6* mutant. **(B)** Box plot to show the fold changes of the up-regulated genes.

4.2.9 Comparing the transcription profiles of the total number of genes downregulated in each of the Swi-Snf subunit mutants

In the previous analyses I selectively compared the transcription profiles of individual Swi-Snf subunit mutants to each other. In most of the cases, except when comparing the *snf2* gene deletion mutant with the *snf2K798A* mutant, the data suggests widespread differences in the numbers of genes regulated by each subunit mutant, and their influence upon transcription levels of target genes. This result suggests distinct roles in gene regulation for the different subunits of the complex as opposed to the complex acting as a single unit to regulate transcription.

In this section, I have compared the total number of genes downregulated in each Swi-Snf subunit deletion mutant to each other to see more clearly if there is, or is not, a large overlap in the activation roles of the different Swi-Snf subunits.

A Venn diagram was prepared of the total number of genes downregulated in each Swi-Snf subunit deletion mutant (Fig.4.30). However, for clarity, I omitted the *snf2K798A* mutant from the comparison, as I had previously shown that the *snf2* and *snf2K798A* mutants have similar transcription profiles.

Importantly, the downregulated genes should reflect the genes where each subunit typically has a positive (activating) role in the regulation of their transcription. As the subunits are all components of the Swi-Snf complex, which is considered to function predominantly as a co-activator of gene transcription, a high overlap in these downregulated genes would be predicted.

However, only 57 genes were commonly downregulated in each of the Swi-Snf subunit mutants. This information confirms that different cohorts of genes are regulated by the distinct activities of the specific Swi-Snf subunits.

The 57 genes commonly downregulated in each Swi-Snf subunit mutant include genes of diverse roles (Fig. 4.31). However, interestingly, 20 of the 57 genes commonly downregulated in each of the Swi-Snf subunit mutants encoded retrotransposons. This suggests a large proportion (35%) of genes subject to common activation by the Swi-Snf subunits shown here, encode mobile genetic elements.

In summary, there was only minimal overlap in the number of genes subject to common activation of transcription by the Swi-Snf subunits suggesting each subunit plays a largely distinct role in the positive regulation of gene transcription.

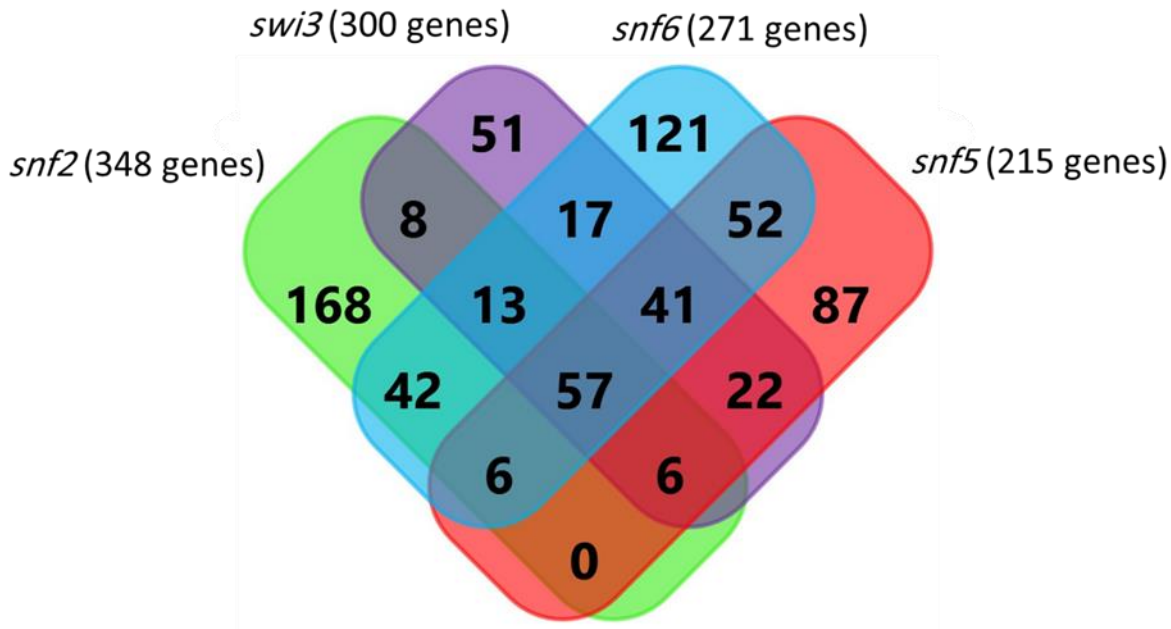

Figure 4. 30: Swi-Snf down-regulated genes. A Venn diagram to identify the shared and uniquely downregulated genes (at least 2-fold change down) in the *snf2*, *swi3*, *snf5*, and *snf6* mutants.

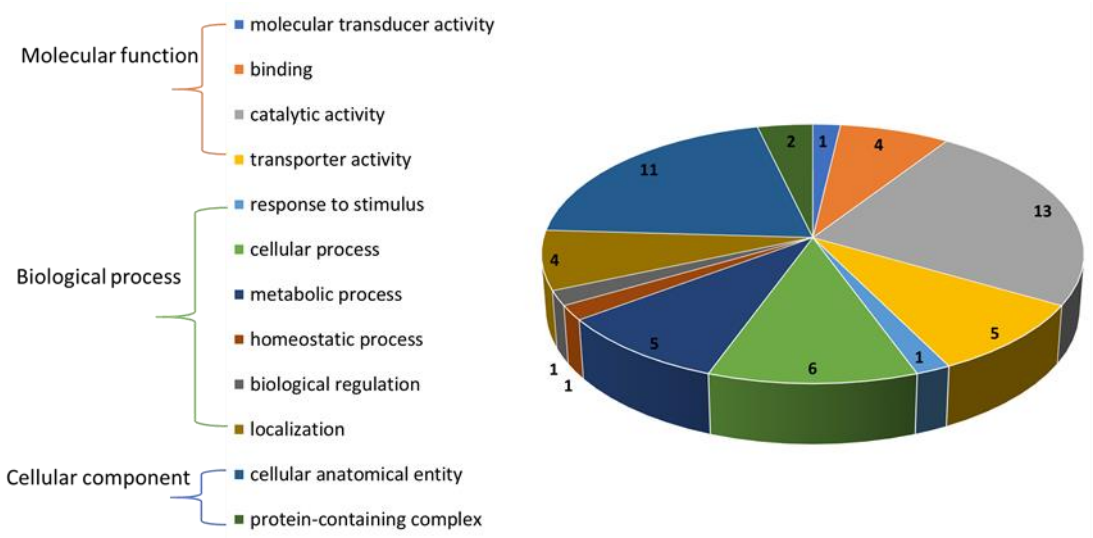

Figure 4. 31: GO analysis of the 57 genes commonly downregulated in the *snf2*, *swi3*, *snf5*, and *snf6* mutant strains.

4.2.9.1 Comparing the transcription levels of the genes commonly downregulated in the Swi-Snf subunit mutants

Next, I compared the average fold downregulation of the 57 genes commonly downregulated in each of the Swi-Snf subunit mutants (Fig. 4.32A). This was done to determine if the impact on transcription of these genes in each mutant was similar or if it differed.

The data showed that, on average, the genes in the *snf2* mutant were downregulated to the greatest extent. The *swi3* mutant showed the next greatest average extent of downregulation followed by the *snf5* mutant. On average, the genes downregulated in the *snf6* mutant were downregulated the least compared to wt.

Thus, the different mutants downregulated the commonly downregulated genes to a different extent, suggesting distinct contributions to active transcription of the same target genes by the different subunits.

When I looked at the 57 genes commonly downregulated in all mutants individually, the data showed more clearly the significant differences in each mutant and highlighted that the *snf2* gene deletion had the greatest negative impact upon gene activation (Fig. 4.32A). Indeed, the large decrease in *CAR2* and *AGA1* gene transcription in the *snf2* mutant compared to the decrease in transcription of these genes in the other mutants can clearly be seen (Fig. 4.32B) [171].

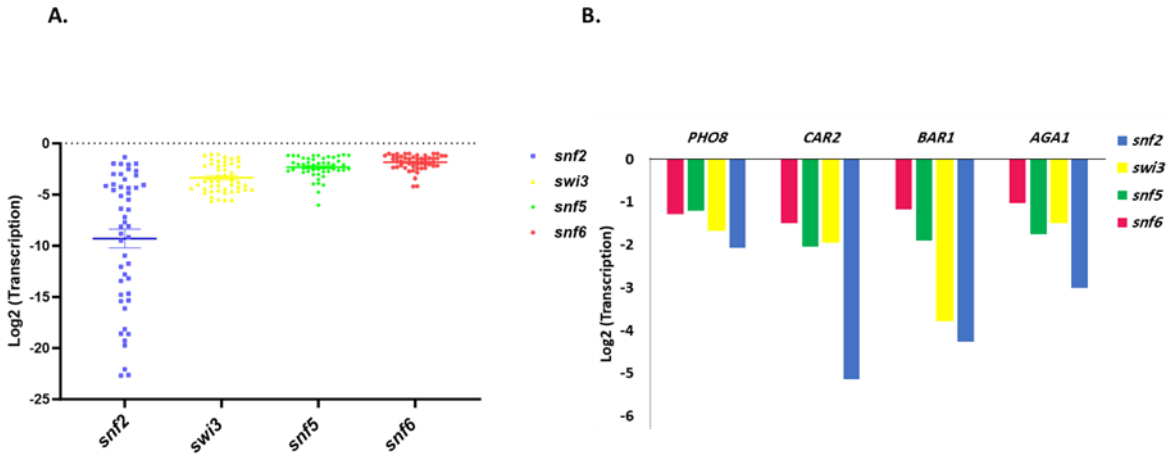

Figure 4. 32: Transcription levels of the 57 genes commonly downregulated in each Swi-Snf subunit. **(A)** Scatter plot to show the average transcription fold changes of the 57 genes down-regulated genes in each mutant compared to wt. **(B)** Examples of these genes and their fold change in transcription relative to wt. One-way ANOVA was used for the statistical analysis.

4.2.9.2 Gene ontology analysis of the total number of genes down-regulated in Swi-Snf mutants compared to wt

Finally, I analysed the gene ontology for the total number of genes downregulated in each of the mutant strains compared to wt (Fig. 4.33). This was done to give an overall picture of the contribution of the different Swi-Snf subunits to gene activation and cell function. The result confirms that the *snf2* and *snf2K798A* mutants have very similar profiles, which was expected as there was high similarity in the numbers of genes downregulated in both mutant strains compared to wt. One difference in the gene

ontology analysis between these mutants was that the *snf2K798A* has a function in the molecular function term, Oxidoreductase activity, which was not found for the *snf2* deletion mutant. The heat map also suggests that the *snf6* mutant profile is not too dissimilar to that of both *snf2* mutants.

The most significant GO term commonly associated with all the downregulated genes in each of the mutants was in the 'DNA integration' category. Examples of genes associated with this GO term were the *PHO* gene family which includes *PHO3*, *PHO5*, *PHO11*, *PHO12*, and *PHO84* as mentioned previously.

On the other hand, the most distinctly different GO terms were associated with the genes downregulated in the *snf5* and *swi3* mutants, with the *swi3* mutant showing the most unique GO profile of the downregulated genes.

Overall, this data reflected the differences in gene function of the genes negatively impacted by mutation in each Swi-Snf subunit, with the biggest difference between the mutants revealed by the GO analysis being evident in the *swi3* mutant.

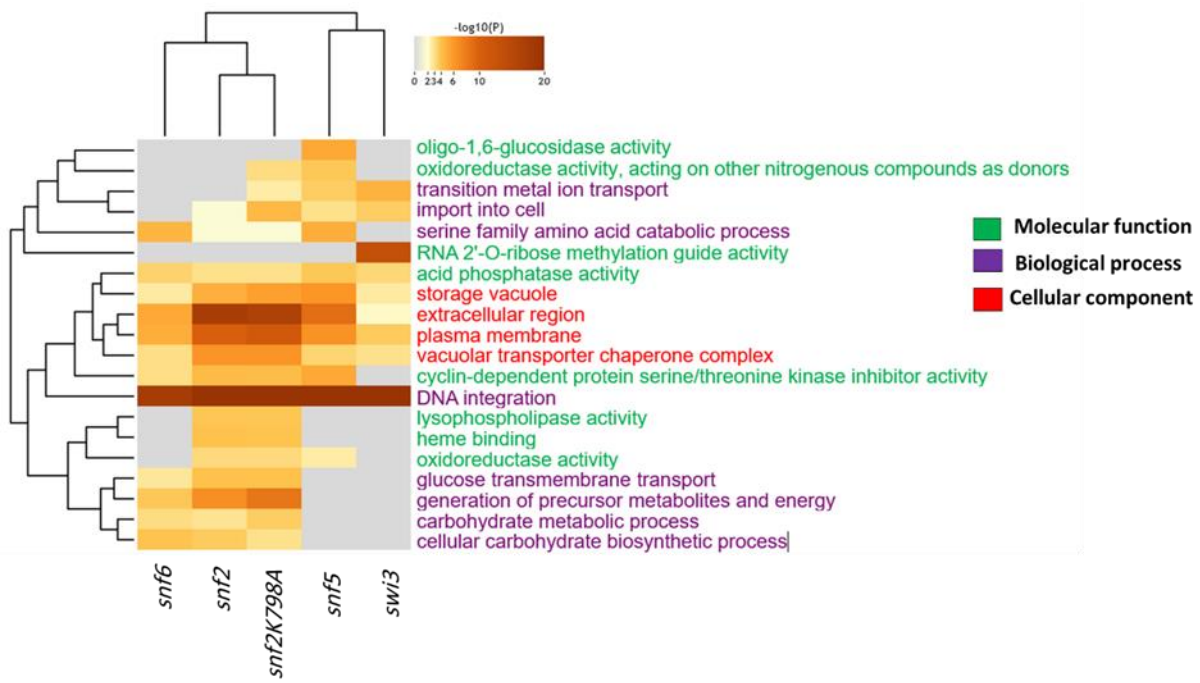

Figure 4. 33: Gene ontology analysis of all genes significantly downregulated in each mutant strain compared to wt. Heat map generated using metascape website for the total number of genes downregulated in the mutants indicated. Each column represents a mutant strain and each row represents a significant GO term. The colour scale indicates the statistical significance of the enrichment of genes assigned to each GO term, darker orange colours indicate more statistically significant. The GO terms are separated into three categories; Molecular Function, Biological Process and Cellular components.

4.2.9.3 Comparing the transcription profiles of the total number of genes upregulated in each of the Swi-Snf subunit mutants

In my final analysis, I repeated the previous analysis upon the total number of genes upregulated in each Swi-Snf subunit deletion mutants (Fig. 4.34). These genes should reflect those genes wherein each subunit has a negative (repressive) role in transcription regulation. In this case, only 35 genes were upregulated and overlapped in all Swi-Snf subunits. Thus, there was again only a minimal overlap in the genes subject to common negative regulation by the Swi-Snf subunits suggesting each subunit plays a largely distinct role in the repression of gene transcription.

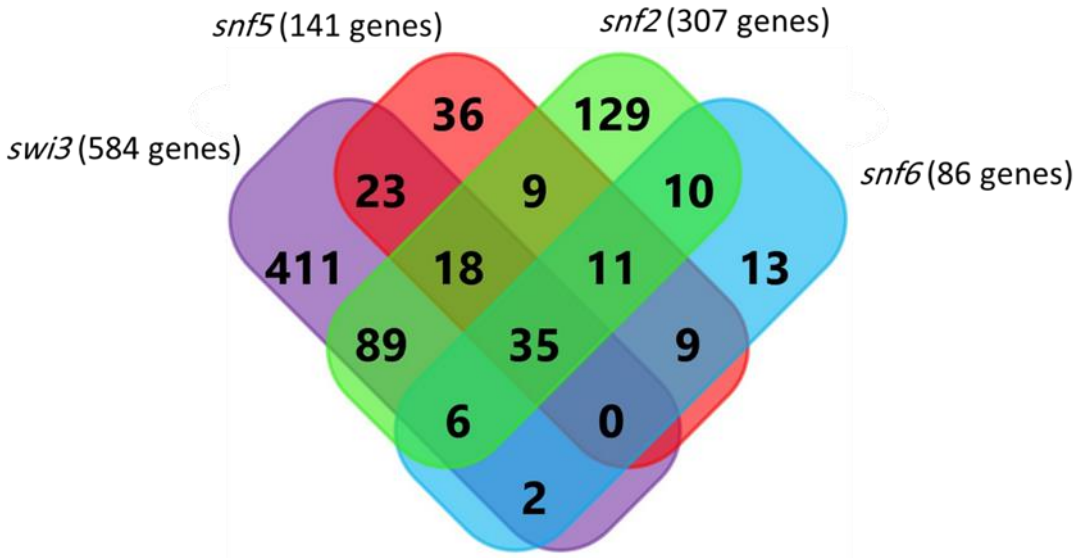

Figure 4. 34: Swi-Snf upregulated genes. A Venn diagram to identify the shared and uniquely upregulated genes (at least 2-fold change down) in the *snf2*, *swi3*, *snf5*, and *snf6* mutants.

4.2.9.4 Comparing the transcription levels of the genes commonly upregulated in all of the Swi-Snf subunit mutants

I then examined the average level of transcription of the 35 genes commonly upregulated in each Swi-Snf mutant (Fig. 4.35A). The results showed that the *snf2* deletion mutant again had the greatest average level of gene upregulation of these commonly upregulated genes. Examples of the commonly upregulated genes at which *SNF2* was playing the greatest role in repression in wt were *AAC1* and *STR3* (Fig. 4.35B).

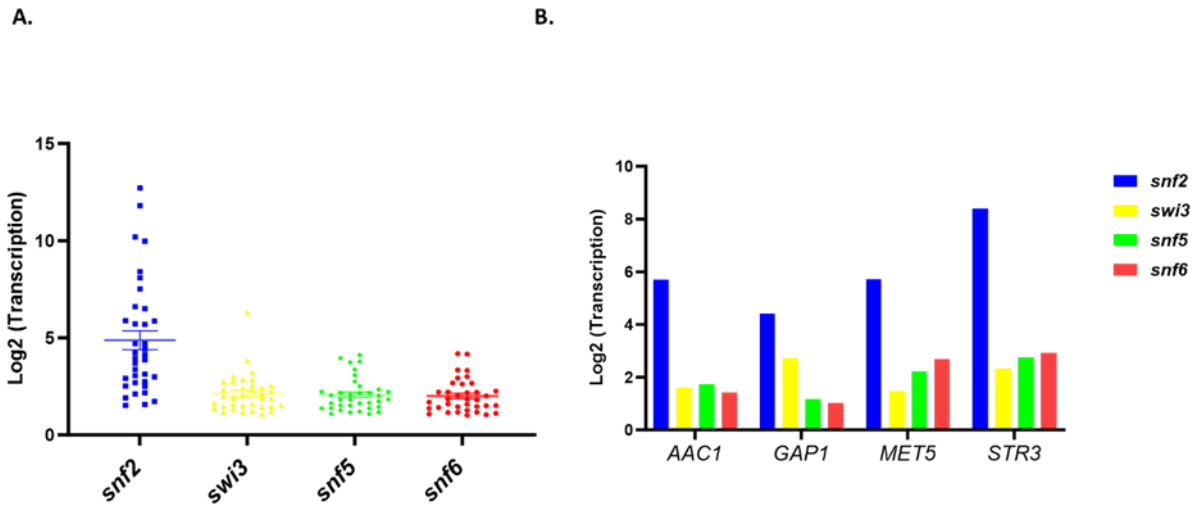

Figure 4. 35: The transcription levels in each Swi-Snf subunit. **(A)** Scatter plot to show the average transcription fold changes of the 35 genes upregulated in each mutant compared to wt. **(B)** Examples of these genes and their fold-change in transcription relative to wt. One-way ANOVA was used for the statistical analysis.

4.2.9.5 Gene ontology analysis of the total number of genes upregulated in each Swi-Snf subunit mutant

Finally, I examined the gene ontology of the total number of genes up-regulated in each subunit mutant of the Swi-Snf complex (Fig. 4.36). The heatmap shown visualizes the complete gene ontology of all the genes upregulated genes in each mutant. As before, the analysis showed a similar profile for the *snf2* deletion and *snf2K798A* catalytic mutants.

Interestingly, the GO profile of the genes upregulated in the *snf5* mutant strain was most similar to that of the genes upregulated in the *snf6* mutant strain, (Fig 4.36, compare column 4 and 5).

However, the most striking result was that the genes upregulated in the *swi3* mutant strain had the most unique GO profile (Fig 4.36, column 1). Here, it could be seen that genes involved in trehalose metabolism and the response to external and abiotic stimuli were uniquely upregulated in the *swi3* mutant.

Overall, these data show a significant and diverse role for the different Swi-Snf subunits in negatively regulating target gene transcription and show that the *SWI3* subunit gene plays the most distinctly diverse role in gene repression compared to the other Swi-Snf subunits.

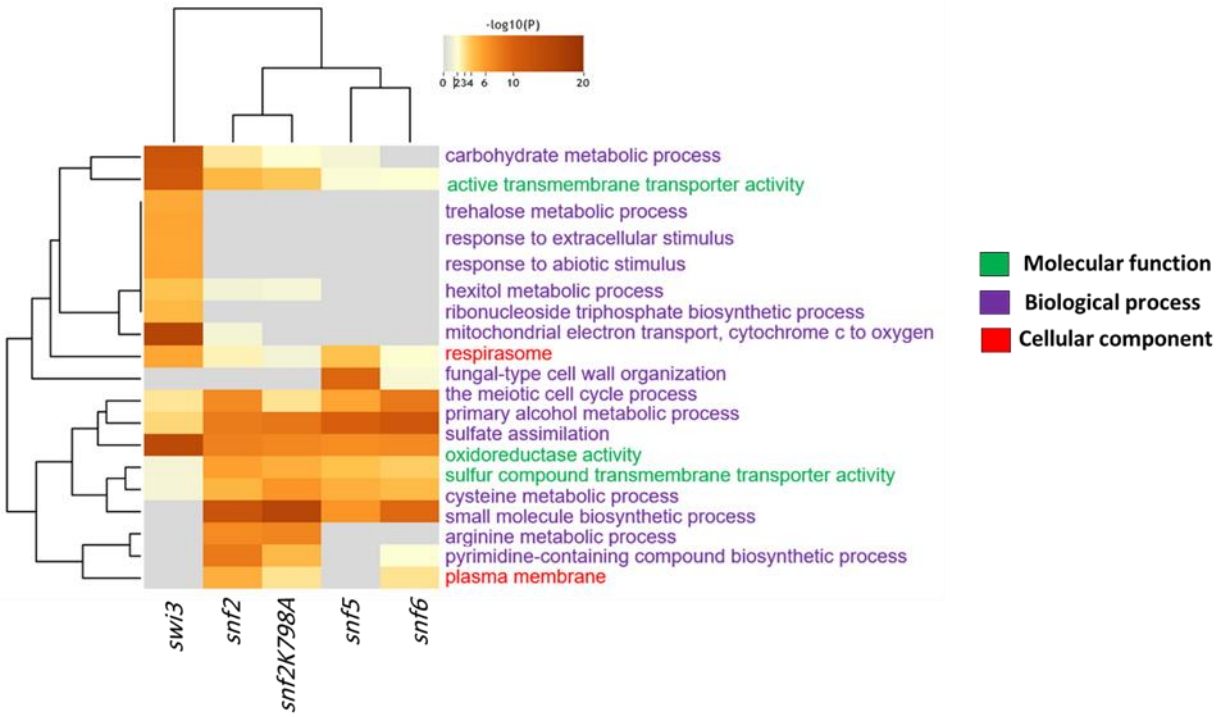

Figure 4. 36: Gene ontology analysis of all genes upregulated more than 2-fold in the Swi-Snf mutant strains. Heat map generated using metascape website. Each Colum represent a mutant strain and each row represents a significant GO term the colour scale indicates the statistical significance of the enrichment of genes assigned to each GO term, darker orange colours indicate more statistically significant. The GO terms are separated into three categories; Molecular Function, Biological Process and Cellular components.

Summary of main findings

- The *snf2*, *snf5*, *swi3,* and *snf6* deletion mutants have different transcriptomes, regulating unique sets of genes, suggesting distinct roles for each subunit upon regulation of gene transcription.
- The *snf2* deletion and *snf2K798A* catalytic mutants have very similar transcriptomes.
- The overlap of genes commonly up or downregulated by the Swi-Snf subunits is small.
- A large proportion of the genes commonly downregulated in *snf2*, *snf5*, *swi3,* and *snf6* deletion mutants encode retrotransposons.
- Significant numbers of genes were upregulated in the Swi-Snf subunit mutants tested suggesting a large role for the Swi-Snf subunits in gene repression.
- *SWI3* plays the largest role in gene repression.
- The different subunits can regulate some target genes antagonistically.
- Even for Swi-Snf subunits found within the same module, there were differences between the numbers of genes the subunits regulate, and differences in the contribution of these apparently functionally related subunits to the transcription of these genes.

Discussion

In this chapter, I analysed the transcriptomes of multiple Swi-Snf complex subunit mutants in yeast. The high correlation between biological replicates suggested good reproducibility for all mutants (Fig. 4.2).

The analysis identified genes that were at least twofold down- or upregulated in the mutants compared to wild type (wt). Downregulated genes suggest a positive regulatory role for the subunit, while upregulated genes indicate a negative regulatory role. The *snf2* and *snf2K798A* mutants showed similar numbers of down- and upregulated genes, while the *swi3* mutant had the most upregulated genes, indicating a significant role for *SWI3* in the negative regulation of gene transcription (see Fig. 4.3) [172], [120]. A heat map of the top 100 genes down and up-regulated in each mutant was generated to observe general trends. The *snf2* deletion mutant and the *snf2K798A* catalytic mutant had similar transcriptomes, while the *swi3* mutant displayed a distinct transcription profile, suggesting unique regulatory mechanisms for *SWI3* (Fig. 4.4).

A detailed comparison of the downregulated genes in the *snf2* deletion mutant and the *snf2K798A* catalytic mutant revealed a large overlap, with no significant difference in transcription levels. This finding challenges the expected differences between the mutants due to the reported disruption of the Swi-Snf complex expected in the *snf2* deletion mutant, which was not expected to occur in the catalytically dead *snf2K798A* mutant [173]. This result might suggest that the Swi-Snf complex may also be disrupted in the *snf2K798A* mutant potentially suggesting that Snf2p ATPase activity is essential for Swi-Snf complex integrity. Interaction studies between the Swi-Snf subunits in the *snf2* deletion mutant and the *snf2K798A* mutant would need to be performed to investigate and confirm this possibility.

Gene ontology analysis was performed to understand the functions of downregulated genes. Commonly downregulated genes were involved in metabolism, transporter activity, catalytic activity, and DNA binding, indicating that Snf2p is essential for the activation of a broad range of genes. The result showing an enrichment of *SNF2* activated genes involved in metabolism is in line with a recent study that has shown Swi-Snf mediates gene regulation through metabolic control, indicating a broader regulatory role for Swi-Snf than was previously appreciated (Fig. 4.7) [174].

Interestingly, the transcriptome data also revealed that *SNF2* can act as a repressor of a cohort of genes as large as that subject to positive regulation by *SNF2*. Indeed, there was upregulation of 307 genes in the *snf2* mutant and 264 genes in the *snf2K798A* mutant; again with a significant overlap of 244 genes between the two. This finding adds a new dimension to our understanding of *SNF2* role in gene regulation, presenting evidence that contradicts the widely held belief that Swi-Snf predominantly functions as a transcription activator.

The gene ontology analysis further underscores the involvement of these genes in regulating critical biological processes such as ubiquitylation and transcription regulation. Notably, genes like *RIM8* and *SIP4* were upregulated in both mutants, while *FTR1* and *EDS1* were uniquely upregulated in the *snf2* mutant. This aligns with the established understanding that protein ubiquitylation plays a pivotal role in regulating various cellular processes, including transcription (Fig. 4.8) [175], [176].

Moreover, the study identifies distinct genes that are uniquely upregulated in each mutant, such as *RIM4* in the *snf2K798A* mutant, which is linked to RNA splicing. This finding highlights the subtle differences in the genetic consequences of the two mutations and echoes the complexity of transcription regulation by *SNF2*, as it can influence a range of nuclear processes beyond the scope of its traditional activator role.

The exploration of the Swi-Snf complex has established the Snf2p subunit as the catalytic core, essential for gene transcription regulation [83]. Prior studies have underscored the critical role of Snf2p, positioning it as a key component within the Swi-Snf complex [177]. This research extends the understanding by comparing gene regulation between *snf2* mutants and other Swi-Snf subunit mutants, with an initial focus on the *snf5* mutant.

Analysis of downregulated genes in both *snf2* and *snf5* mutants showed an overlap of 124 genes. However, the *snf2* mutant uniquely downregulated 224 genes, while the *snf5* mutant affected 91 unique genes, indicating a more substantial impact on gene transcription by *SNF2* loss (see Fig. 4.9). In contrast, the study also assessed genes upregulated in the absence of these subunits. The *snf2* mutant had an upregulation of 307 genes, 234 of which were unique, whereas the *snf5* mutant saw 141 genes upregulated, with 68 unique to it (Fig. 4.12). This suggests a broader role for *SNF2* in gene repression compared to *SNF5*.

The findings also revealed that Snf2p and Snf5p subunits may have distinct and sometimes opposing roles in gene transcription regulation. For example, some genes downregulated in the *snf5* mutant were upregulated in the *snf2* mutant, and vice-versa, highlighting these subunits can have antagonistic effects on expression of the same target gene.

These results highlight the individual contributions of Snf2p and Snf5p to gene transcription regulation, accentuating the complex nature of the Swi-Snf function in gene expression. It suggests there are intricate dynamics occurring among the different Swi-Snf subunits which shape the transcriptional landscape [178].

The comparative analysis of *snf6* and *snf2* deletion mutants in the context of SWI-SNF subunit gene regulation has illuminated their distinct contributions to gene transcription. The study found that *snf2* deletion resulted in a more substantial downregulation of genes, with 348 genes affected compared to 271 in the *snf6* mutant, and an overlap of 155 genes between the two (Fig. 4.15). Furthermore, on average, the

genes were downregulated to a greater extent in the *snf2* mutant than those downregulated in the *snf6* mutant. This highlights the more dominant role of Snf2p in gene activation, aligning with previous findings that highlight the critical function of Snf2p as the ATP-dependent motor in chromatin remodelling [177].

This trend was consistent with the upregulated genes, where the *snf6* mutant had 86 genes upregulated, 62 of which were also upregulated in the *snf2* mutant (Fig. 4.18). However, only 24 genes were uniquely upregulated in the *snf6* mutant, suggesting a more pronounced role for Snf2p in gene repression.

The study also revealed antagonistic effects of *SNF2* and *SNF6* at target genes. For example, some genes upregulated in the *snf6* mutant were downregulated in the *snf2* mutant and vice versa. This finding emphasizes the intricate interplay between different Swi-Snf subunits and their unique impacts on gene transcription [179]. These insights contribute significantly to our understanding of the molecular mechanisms by which the SWI-SNF complex governs gene regulation.

The study of gene expression regulation by *swi3* and *snf2* mutants has revealed a nuanced landscape of antagonistic and cooperative interactions. In the results obtained, we found that 300 genes were downregulated in the *swi3* mutant, while 348 were downregulated in the *snf2* mutant, with a significant overlap of 116 genes (Fig. 4.21). This suggests a shared regulatory influence between these subunits for gene activation. However, the unique downregulation of 232 genes in *snf2* and 184 in *swi3* points to distinct roles in gene regulation for these two subunits. The extent of downregulation was more pronounced in the *snf2* mutant, indicating a more substantial role of Snf2p in gene activation, a finding that is consistent with previous results and published research [83].

Interestingly, genes such as *PDR3* and *TIS11*, which were uniquely downregulated in the *swi3* mutant, were found to be upregulated in the *snf2* mutant, suggesting an antagonistic regulatory mechanism where *SWI3* acts as an activator and *SNF2* as a repressor (Fig.4.22) [180].

Conversely, the upregulation profile was markedly different between the two mutants, with 436 genes uniquely upregulated in the *swi3* mutant, underscoring a more significant role for Swi3p in gene repression compared to Snf2p (Fig. 4.24). The genes exclusively upregulated in the *swi3* mutant were implicated in molecular functions and biological processes essential for ATP synthesis and amino acid transport, with *ANB1* and *ATP16* being key players. These findings demonstrate the complex interplay between *SWI3* and *SNF2*, highlighting both cooperative and antagonistic interactions that contribute to the functional diversity of the Swi-Snf complex subunits in both positively and negatively regulating gene transcription.

In the analysis, I compared the transcription profiles of *swi3* and *snf6* mutants, constituents of the Snf6-Snf12-Swi3 module. Notably, our results differed from expectations, revealing significant differences in their transcription profiles, which aligns with the idea that subunits within the same module can exert distinct regulatory effects, as suggested by previous studies [174], [181].

Examination of downregulated genes in these mutants uncovered that only a fraction overlapped, indicating that even closely associated subunits can target different gene sets. This finding is consistent with the concept that Swi-Snf subunits have unique regulatory signatures, as supported by the work of Church *et al*. (2023) [174], who found that mutations in Swi-Snf components could lead to widespread transcriptional changes [174]. Furthermore, our data revealed that *swi3* mutants exhibited a higher number of upregulated genes compared to *snf6* mutants, suggesting a dominant role of *SWI3* in gene repression functioning independent even of its own submodule components.

This large repressive role for *SWI3* challenges the traditional view of the Swi-Snf complex as merely a co-activator of transcription and resonates with the broader implications of the Swi-Snf role in gene regulation identified in prior research [174], [181].

When I compared all genes up and down regulated in each of the *snf2*, *swi3*, *snf5* and *snf6* mutants, there was only a minimal overlap in gene regulation across these Swi-Snf subunit mutants. This reinforces the individuality of each subunit's role in gene transcription, a concept that has been gradually unveiled by the scientific community, and which needs more investigation. Indeed, this suggests the different Swi-Snf subunits can act independently within or without the Swi-Snf complex.

Building upon the findings in existing literature, our gene ontology analysis combines past and present research to shed light on the Swi-Snf complex intricate role in gene regulation. The analysis highlights a striking resemblance between the *snf2* and *snf2K798A* mutants, mirroring the findings of Euskirchen et al. (2011) who first illuminated the broad spectrum of biological processes influenced by the Swi-Snf complex, including gene expression and nuclear organization [181]. The close numbers of genes downregulated in these strains compared to wild type (wt) resonates with the functional parallels previously noted but is inconsistent with the expected differences in Swi-Snf complex integrity proposed to occur.

Of note, the *snf2K798A* mutant transcriptome revealed a distinct role in oxidoreductase activity, a trait not shared with the *snf2* deletion mutant. This unique function aligns with the observations by Church *et al.* (2023)[174]. who explored the Swi-Snf complex role in metabolic gene transcription and its broader implications for metabolic control. The *snf2K798A* mutations specific impact within the cell may be a new piece in the puzzle of Swi-Snf regulatory capabilities that will need further investigation.

The most significant GO term associated with downregulated genes across all mutants is DNA integration, particularly involving the *PHO* gene family. This finding aligns with the conserved mechanisms affected by Swi-Snf subunit mutations, as suggested by the comprehensive review of the complex role in breast cancer, which highlighted the genetic alterations in Swi-Snf subunits and their association with cancer progression [182]. The *snf5* and *swi3* mutants present markedly different GO terms for their

downregulated genes, with the *swi3* mutant exhibiting the most distinct profile. This divergence reflects the individualized roles of these subunits in gene regulation, a concept that has been progressively uncovered by the scientific community and is supported by this study [181].

Among the Swi-Snf subunits, although *SWI3* repressed the most number of genes, the *SNF2* deletion mutant exhibited the greatest average level of gene upregulation. This suggests that *SWI3* and *SNF2* play the most significant roles in the repression of genes in wild-type strains.

The gene ontology analysis has revealed the unique profile of genes upregulated in the *swi3* mutant strain. Notably, genes involved in trehalose metabolism and response to external and abiotic stimuli were uniquely upregulated in this mutant, indicating a specialized function of *SWI3* in gene repression. This aligns with the findings of Euskirchen et al. (2011), who highlighted the diverse regulatory functions of *SWI3* within the Swi-Snf complex [181]. The gene ontology profiles of the *snf5* and *snf6* mutant strains revealed similarities, suggesting a closer functional relationship between these two subunits in terms of gene regulation. This is consistent with the observations made by Euskirchen et al. (2011), who first mapped the intricate interactions within the Swi-Snf complex, revealing the nuanced interplay between its various components [181].

In summary, this study explored the transcriptional regulation by Swi-Snf complex subunits to reveal the subunits can have complex roles in mediating both positive and negative gene regulation. The *snf2* and *snf2K798A* mutants affected a similar number of genes, challenging the expected differences, and confirming Snf2p's essential role in activating a broad range of genes. The research highlights a major role for Swi-Snf subunits in repressing gene transcription and presents evidence that *SNF2* can act to repress as many genes as it activates and that the major role for Swi3p is in target gene repression. This contradicts the belief that Swi-Snf functions predominantly as a co-activator of transcription.

Overall, the findings highlight the Swi-Snf complex has a much broader regulatory role, with specific subunits having distinct and sometimes opposing effects on gene expression, emphasizing the intricate dynamics among different Swi-Snf subunits in shaping the transcriptional landscape. The study contributes to our understanding of the molecular mechanisms by which the SWI-SNF complex governs gene regulation, highlighting the complex interplay between different subunits.

Future research will be needed to investigate the distinct effects of each subunit to enable a full understanding of the Swi-Snf complex and its regulatory mechanisms of action.

Chapter 5

Analysing global Swi-Snf subunit occupancy

5.1 Introduction

In the previous chapter, I identified the differences in transcriptome data of the various Swi-Snf subunit mutant strains. The RNA-Seq data suggested that only a small set of genes were commonly down and upregulated in the *snf2*, *swi3*, *snf5*, and *snf6* mutant strains. This suggests possible independent roles for the Swi-Snf subunits functioning either within or out with the Swi-Snf complex.

I therefore decided to analyse published data sets showing the global occupancy profiles of selected Swi-Snf subunits. I also wanted to correlate the Swi-Snf subunit occupancy data with the lists of genes up and downregulated in each mutant analysed in chapter 4. The aim was to identify those genes directly regulated by each Swi-Snf subunit either acting on its own or functioning within the complex.

To perform this analysis, previously published Swi-Snf subunit occupancy profiles were used that were generated using the ChIP-exo technique (Fig. 5.1) [131]. Chromatin immunoprecipitation (ChIP) combined with high-throughput sequencing (Seq) techniques have revolutionized our ability to study protein-DNA interactions on a genomic scale. Among these methods, ChIP-exo stands out as a powerful tool for precisely mapping protein binding sites at single-nucleotide resolution [183].

Traditional ChIP-Seq methods can suffer from limitations such as low resolution and high background noise, making it challenging to pinpoint the exact location of protein binding sites. In ChIP-exo, after immunoprecipitation of protein-DNA complexes, exonucleases are used to digest DNA fragments protruding from the protein binding sites, resulting in defined endpoints that accurately mark the protein-DNA interaction sites [184]. This exonuclease digestion step significantly reduces background noise and enhances the resolution of the binding site identification.

By analyzing the ChIP-exo data, I aimed to quantify the number of protein binding sites associated with each Swi-Snf subunit across the yeast genome. This analysis should provide insight into the spatial distribution and abundance of individual Swi-Snf subunits, and the Swi-Snf complex, shedding light on the genomic regions where the complex, and individual subunits, exert their regulatory functions.

In summary, in this chapter, I compared the Swi-Snf subunit binding sites with the RNA-Seq data described in Chapter 4. The aim was that this integrative approach should provide a deeper understanding of the molecular mechanisms underlying Swi-Snf-mediated transcriptional regulation and its impact on cellular function in yeast [131].

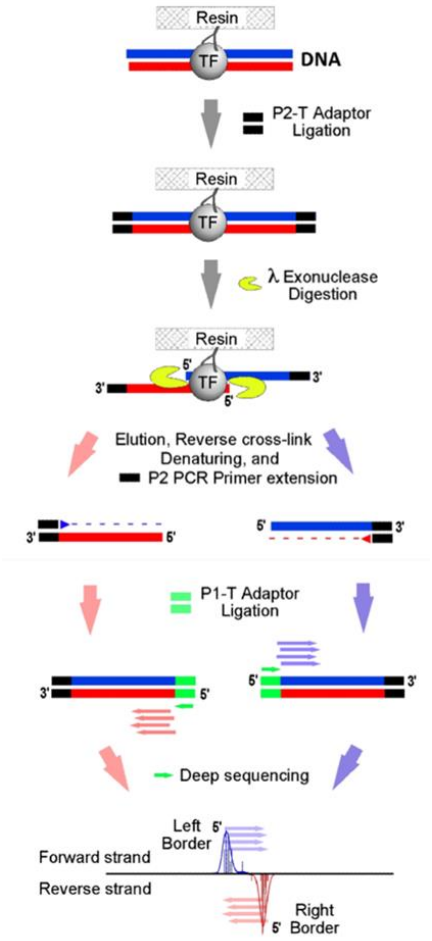

Figure 5. 1: The ChIP-exo technique. Following chromatin immunoprecipitation (ChIP), the 3' sonicated ends are distinguished from the eventual exonuclease-treated 5' end by ligating a P2-T adaptor to the ChIP DNA while it remains bound to the resin, preceding exonuclease digestion. Subsequent 5' to 3' exonuclease trimming, up to the site of cross-linking, selectively eliminates the P2-T adaptor sequence attached at the 5' end of each DNA strand. Upon cross-link reversal, the eluted single-stranded DNA is rendered double-stranded through P2 PCR primer extension. Subsequently, a P1-T adaptor is ligated to the exonuclease-treated end. The resulting library undergoes high-throughput sequencing. By aligning the 5' ends of the resulting sequencing tags to the reference genome, the exonuclease barrier is identified, thereby pinpointing the precise site of protein-DNA cross-linking. This figure was taken from published data [185].

5.2 Results

5.2.1 Investigating the total number of peaks of Swi-Snf subunit occupancy across the genome

First, I counted the total number of binding sites across the genome for the Snf2p, Swi3p, Snf6p, Snf11p, Taf14p, and Swi1p subunits. The prediction would be that if the subunits only functioned within the Swi-Snf complex, each subunit would be found at the same number of sites.

However, the data showed differences in the total number of sites occupied by each subunit (Table 5.1). Swi3p occupied the most sites (980), followed by Snf6p (775 sites), Swi1p (604 sites), Snf2p (544 sites), Taf14p (349 sites) and with Snf11p showing the least number of sites of occupancy (297 sites).

Further analysis of these sites of occupancy revealed how many actual protein-coding genes (open reading frames, ORFs) were associated with each Swi-Snf subunit. Here, the number of genes associated with each subunit largely reflected the total number of sites of occupancy described previously, with the Swi3p subunit being associated with the highest number of ORFs (486), and the Snf11p subunit being associated with the least number of ORFs (154).

Other features associated with the Swi-Snf subunit peaks were also analysed, such as CUTs (cryptic unstable transcripts), SUTs (Stable unannotated transcripts), and XUTs (sensitive unstable transcripts), to give insight into if any of the subunits were specifically enriched at certain chromosomal features. However, again, the sites of occupancy at these features largely reflected the total number of sites of occupancy of each subunit. Interestingly, a disproportionately high number of small nuclear RNA encoding sequences (snRs) were enriched for Snf2p (33) and Taf14p (21) occupancy.

Swi-Snf subunit	Total number of occupancy sites	ORFs	CUTs	SUTs	XUTs	snR	ACS	ncRNA	tRNA	long terminal repeat	Orphan TFIIB peak	centromere	ARS
Snf2p	544	252	45	34	64	33	10	2	1	1	102	0	0
Swi3p	980	486	77	91	160	9	7	3	2	2	143	0	0
Snf6p	775	369	61	75	135	11	4	3	2	3	110	1	1
Snf11p	297	154	23	25	51	0	0	1	0	0	43	0	0
Swi1p	604	282	49	64	108	0	2	3	1	3	91	0	1
Taf14p	349	193	24	19	18	21	2	2	0	1	69	0	0

Table 5. 1: Global Swi-Snf subunit occupancy profiles as determined by ChIP-exo [131]. The data shows the number of sites of occupancy for the indicated Swi-Snf subunit at the following genomic features: 1. the total number of sites; 2. **ORFs** (Open reading frames: regions of DNA that have the potential to be translated into proteins); 3. **CUTs** (Cryptic unstable transcripts are short RNA transcripts that arise from non-coding regions of the genome); 4. **SUTs** (Stable unannotated transcripts); 5. **XUTs** (sensitive unstable transcripts); 6. **snR (**small nuclear RNAs)*;* 7. **ACS** (specific DNA sequence recognized by the origin recognition complex (ORC); 8. **ncRNA** (Non-coding RNAs); 9. **tRNAs** (transfer RNAs); 10. **long terminal repeat** (LTRs of retrotransposons or retroviruses)*;* 11. **Orphan TFIIB peaks** (a peak of TFIIB (Transcription Factor IIB) binding that does not coincide with annotated transcription start sites (TSS) or known gene promoters); 12. **Centromere** (peaks located near or within centromeric regions); 13. **ARS type** (peaks associated with autonomously replicating sequences (ARSs).

5.2.2 Comparing the occupancy sites of the Swi-Snf subunits

Next, I compared the total number of sites of occupancy of each Swi-Snf subunit to determine the amount of overlap between the sites of occupancy of each Swi-Snf subunit (Fig. 5.2A). It would be predicted that if the subunits only functioned as part of the Swi-Snf complex, then the occupancy profiles of each subunit should fully overlap.

However, when the total sites of occupancy of each Swi-Snf subunit were compared, the Venn diagram revealed only a small overlap in the sites commonly occupied by each subunit (Fig. 5.2A). Indeed, there were only 15 common sites at which all the Swi-Snf subunits were found. However, the Venn diagram did indicate a high degree of overlap between the Swi3p, Snf6p, and Swi1p sites of occupancy. Furthermore, the Snf11p and Snf2p sites overlapped strongly. Conversely, the Taf14p subunit showed the lowest overlap with the other subunit sites of occupancy.

I next compared the peaks of the Swi-Snf subunits that had been found specifically associated with open reading frames (ORFs) (Fig.5.2B). Interestingly, the Venn diagram showed a similar profile to that seen when looking at the total sites of subunit occupancy (Fig. 5.2A). Here, there were only 9 common sites at which each subunit could be found. These 9 genes at which each of the Swi-Snf subunits can be found are shown in Table 5.2. Examples of these genes include *ZEO1*, involved in the plasma membrane, and *CCW12* which is a cell wall protein.

Together, this shows that there is only a small overlap in the sites of occupancy of each of the subunits suggesting each subunit can occupy a significant number of specific sites independently of each other and/or as part of a truncated Swi-Snf complex.

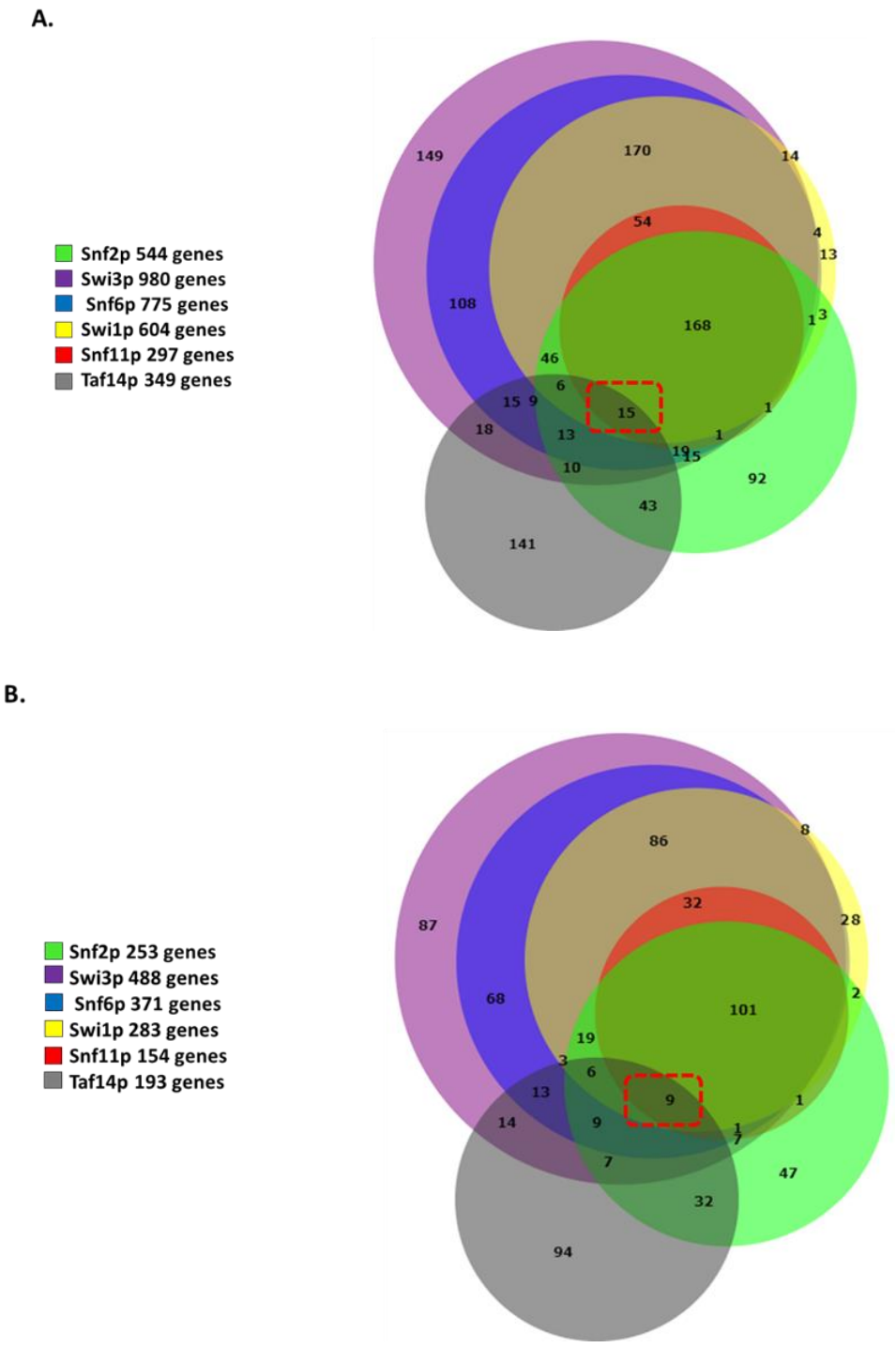

Figure 5. 2: Comparing Swi-Snf occupancy sites. (A) Venn diagram to show the total number of occupancy sites for Snf2p, Swi3p, Snf6p, Swi1p, Snf11p, and Taf14p. **(B)** Venn diagram to show the number of genes (ORFs) occupied by Snf2p, Swi3p, Snf6p, Swi1p, Snf11p, and Taf14p.

Gene	Description of protein
GCN4	bZIP transcriptional activator of amino acid biosynthetic genes
CCW12	Cell wall mannoprotein
YEL008W	Uncharacterized protein
YDR524C-B	Uncharacterized protein
ZEO1	Peripheral membrane protein of the plasma membrane
SER3	phosphoglycerate dehydrogenase and -3 alpha-ketoglutarate reductase
API2	Uncharacterized protein
PHO84	High-affinity inorganic phosphate (Pi) transporter
PGK1	3-phosphoglycerate kinase

Table 5. 2: Table of the 9 genes (ORFs) showing a common site of occupancy for Snf2p, Swi3p, Snf6p, Swi1p, Snf11p, Taf14p.

5.2.3 Comparing the genes associated with Snf2p, Swi3p, Snf6p and Swi1p ocupancy

I next compared the occupancy sites at ORFs associated only with the Snf2p, Swi3p, Snf6p, and Swi1p subunits (see Fig. 5.3). I chose to compare these subunits as, between them, these proteins represent the three submodules that are distinct from the Taf14p-containing module (Snf5-Taf14-Swp82). I chose to omit the Taf14p subunit from this analysis as Taf14p showed a particularly distinct occupancy profile from the other subunits (see Fig. 5.2) that might have obscured a larger overlap in sites of occupancy for the other Swi-Snf subunits.

Indeed, the result of this more focussed occupancy analysis showed that when the ORF-specific sites of occupancy for these subunits were compared, a much larger overlap of 135 genes was revealed. This confirms that the Taf14p subunit has the most unique occupancy profile, and reveals a broader overlap of subunits representative of the other Swi-Snf modules. Conversely, the data still suggests that each of the Swi-Snf subunits can bind a significant number of unique sites independently from each other.

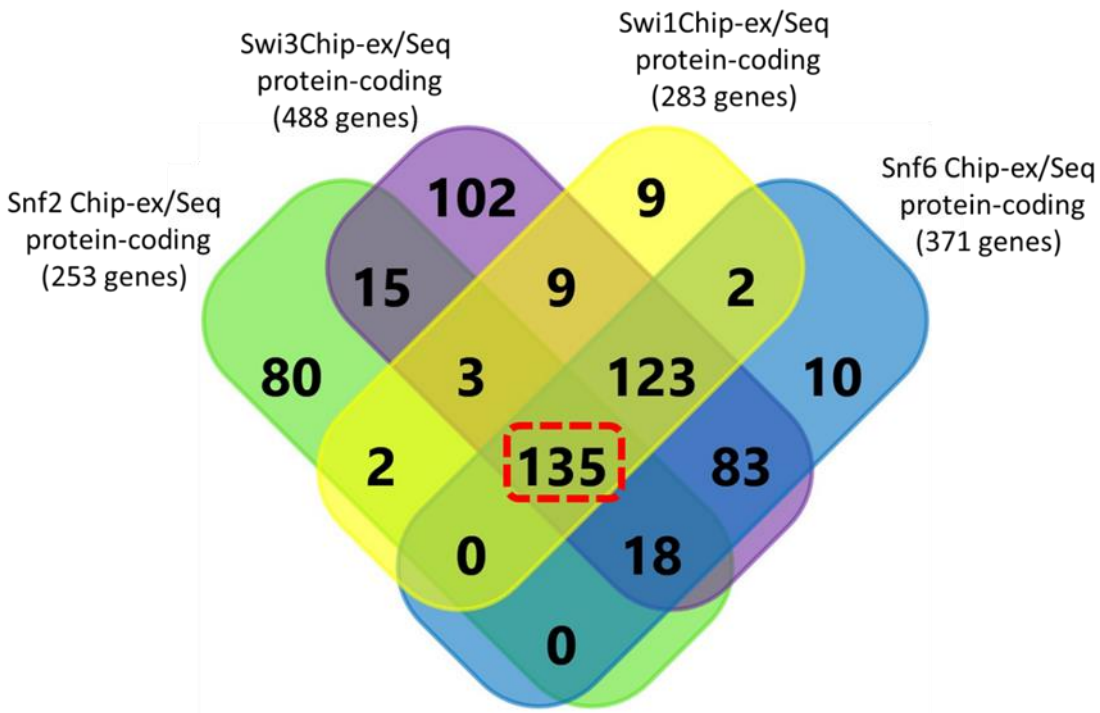

Figure 5. 3: Swi-Snf occupancy sites associated with ORFs. Venn diagram to show the shared peaks of occcupancy of Snf2p, Swi3p, Snf6p, and Swi1p.

5.2.4 Distribution of Snf2p, Swi3p, and Snf6p occupancy across open reading frames (ORFs)

The main aim of this chapter was to correlate Swi-Snf subunit occupancy with the genes up and downregulated in each corresponding Swi-Snf subunit mutant. This should reveal those genes which are directly regulated by each subunit. However, to perform this analysis, I could only examine the Snf2p, Swi3p, and Snf6p occupancy data sets, as I only had both ChIP occupancy data and RNA-seq data for these subunits.

Before attempting the correlation of the ChIP data with the genes shown to be regulated by each subunit, as determined from the RNA-seq analysis in each mutant, I first examined the subunit occupancy patterns at the genes at which these proteins were found. Specifically, I wanted to determine where the peaks of each protein were found at each gene at which they had been mapped as it was evident that peaks of

occupancy could be found at either gene promoters or in the ORFs themselves. For example, at the *SER3* gene, the peak of Swi3p was found in the promoter, whereas the peak of Snf2p at the *UTR5* gene was found across the ORF (Fig 5.4 A and B, respectively).

The results revealed that of the 253 genes (ORFs) allocated with a site of Snf2p occupancy, the majority of these Snf2p sites (175) mapped across the ORF, whilst only 78 Snf2p sites mapped to the gene promoter (Table 5.3). For the 488 sites of Swi3p associated with ORFs, and for the 371 ORF-associated Snf6p sites, there was an almost even split of these sites being found at the promoter or across the ORF. Very few Swi-Snf subunits were found in the downstream intergenic regions. Together, these data show that a significant number of the Swi-Snf subunits were found within ORFs which is inconsistent with the generally accepted model for Swi-Snf to be functioning to remodel nucleosomes at gene promoters [131].

The ORF occupancy data showing the Swi-Snf subunits located at different regions allows for an assessment of the regulatory roles played by these proteins and suggests the different subunits might act at different stages of the transcriptional process at distinct genes. Thus, this approach has not only revealed the spatial dynamics of Swi-Snf subunit interactions with gene regions, but also offers insights into the potential functional significance of these interactions in the regulation of gene expression.

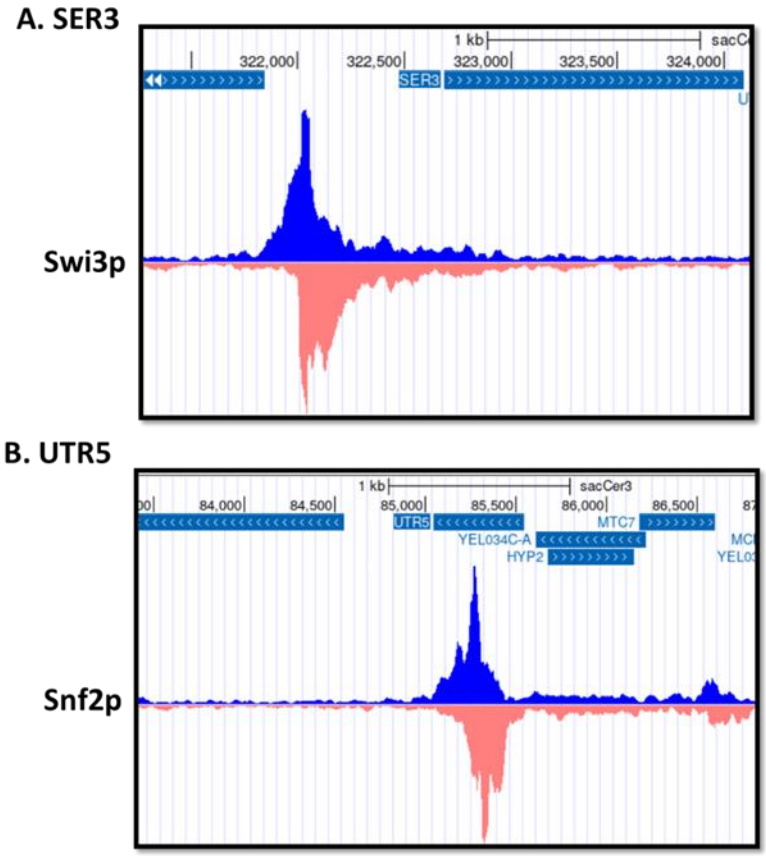

Figure 5. 4: Swi-Snf subunit occupancy profiles at genes can vary: J-browse screen-shot to show. (A) an example of a peak of Swi3p occupancy at a gene (*SER3*) promoter and **(B)** an example of a peak of Snf2p occupancy across a gene coding region (the *UTR5* ORF).

	Site of Occupancy			
Swi-Snf subunit	**Total Occupancy at ORFs**	**Promoter**	**ORF**	**Downstream Intergenic regions**
Snf2p	253	78	175	-
Swi3p	488	234	246	8
Snf6p	371	186	179	6

Table 5. 3: Distribution of Snf2p, Swi3p, and Snf6p occupancy sites at gene regions (ORFs). The number of Snf2p, Swi3p, and Snf6p peak positions found within promoters, open reading frames (ORFs), or downstream intergenic regions is indicated.

5.2.5 Comparing the total number of sites of occupancy of selected Swi-Snf subunits

Next, I compared the total number of peaks in the Swi-Snf occupancy data to determine the extent of the overlap of occupancy for Snf2p, Swi3p, and Snf6p (Fig. 5.5A). The data revealed an overlap in occupancy of Snf2p, Swi3p, and Snf6p at 270 sites, suggesting a relatively strong association between these Swi-Snf subunits. Interestingly, the largest overlap in occupancy was between the Swi3p and Snf6p subunits suggesting a closer functional relationship, or a more extensive crosstalk, between these two subunits.

Conversely, the Swi3p subunit was found at 184 unique sites and the Snf2p subunit was found at 139 unique sites. However, the Snf6p subunit was only found at 30 unique sites. This suggests that the Snf2p and Swi3p subunits might have the most significant independent roles out with the Swi-Snf complex.

I next repeated the occupancy comparison for these subunits, but this time focussed only on their sites of occupancy mapped to ORFs and tRNAs (Fig. 5.5B). Overall, the results of occupancy for these subunits at ORFs and tRNAs looked similar to what was seen when the total sites of occupancy were compared (compare Fig. 5.4 B and A). The Venn diagram revealed that 153 ORFs and tRNAs were commonly occupied by Snf2p, Swi3p, and Snf6p, indicating these genes as a core set of genes targeted by all three components of the Swi-Snf complex (Fig. 5.5B).

Swi3p and Snf6p were found together at the largest number of genes (206 genes), again suggesting a close functional relationship or coordinated regulation of gene expression by these two components.

Conversely, only a small set of genes were occupied only by Snf2p and Swi3p (18 peaks), indicating potentially more specific, or less frequent interactions, between these two components.

In conclusion, this analysis provides insights into the regulatory landscape of Swi-Snf occupancy at protein-coding regions and tRNAs, suggesting both shared and distinct regulatory roles of the Swi-Snf subunits in regulating gene expression. The different overlaps in subunit occupancy from the different comparisons underscores the complexity and dynamic nature of subunit interactions within the Swi-Snf complex.

A.

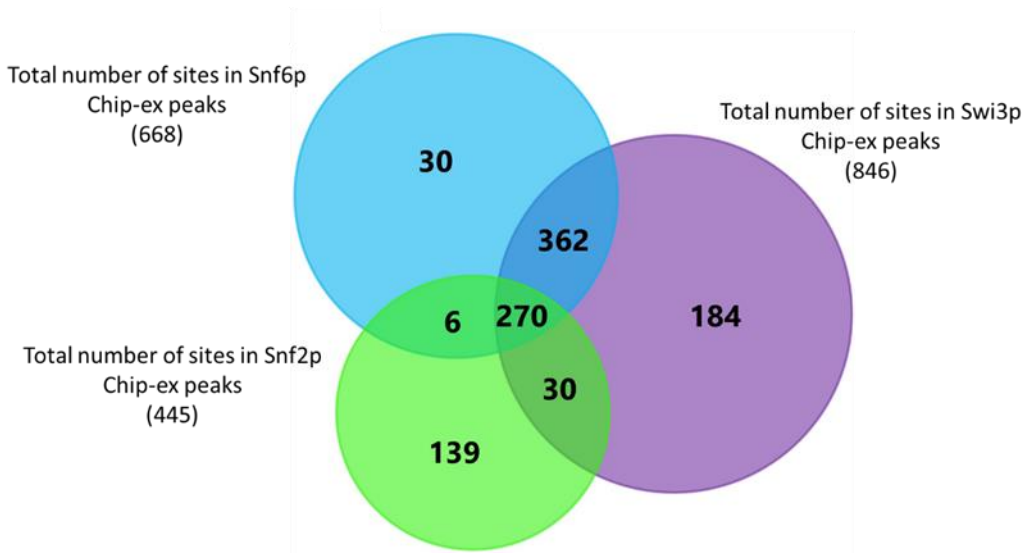

B.

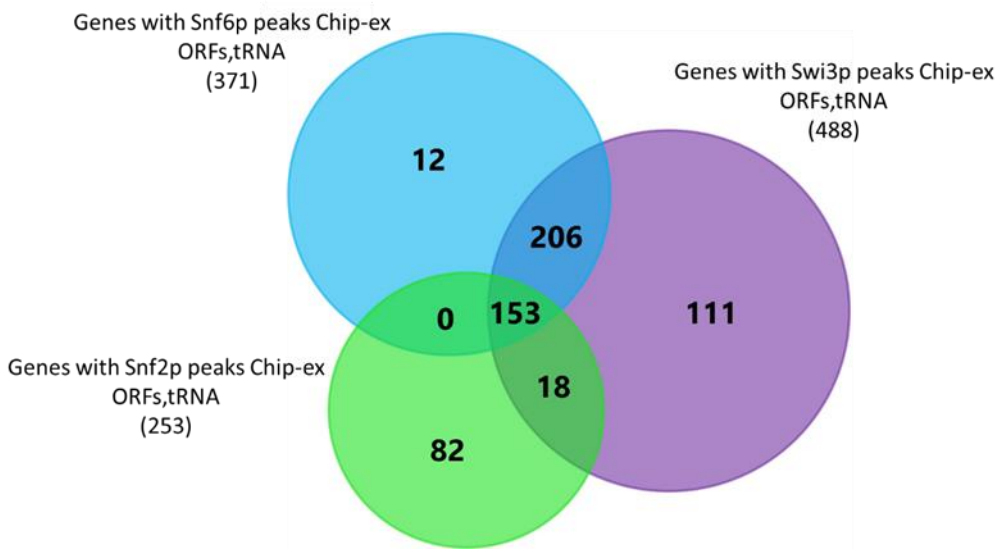

Figure 5. 5: Swi-Snf occupancy sites. (A) Venn diagram to show the total number of peaks of Snf2p (445), Swi3p (846), and Snf6p (668). **(B)** Venn diagram to show the number of peaks of Snf2p (253), Swi3p (488), and Snf6p (371) located at protein-coding (ORF) and tRNA sites only.

5.2.6 Correlating Swi-Snf subunit occupancy with subunit-specific transcription profiles

The previous analysis of Snf2p, Swi3p, and Snf6p occupancy revealed an overlap in occupancy of these proteins at 153 genes (and tRNAs) (Fig. 5.5B). Interestingly, the analysis of the RNA-Seq data in the *snf2*, *swi3,* and *snf6* mutants revealed a cohort of 157 genes that were commonly up or down-regulated in the mutants (Fig. 5.6), suggesting these genes are subject to co-regulation by these three subunits. I therefore compared the list of 153 genes commonly occupied by Snf2p, Swi3p, and Snf6p with the list of genes whose transcription was significantly up or downregulated in the *snf2*, *swi3,* and *snf6* mutants (Fig. 5.7). The prediction would be that if these genes were subject to direct regulation by the Snf2p, Swi3p, and Snf6p subunits, these two data sets should fully overlap. However, as can be seen from (Fig. 5.7), this was not the case; only 9 genes were commonly featured in the two data sets. Thus, the data does suggest that these 9 genes are subject to direct regulation by Snf2p, Swi3p, and Snf6p. An example of one of these genes is *CWP2* (Fig. 5.8).

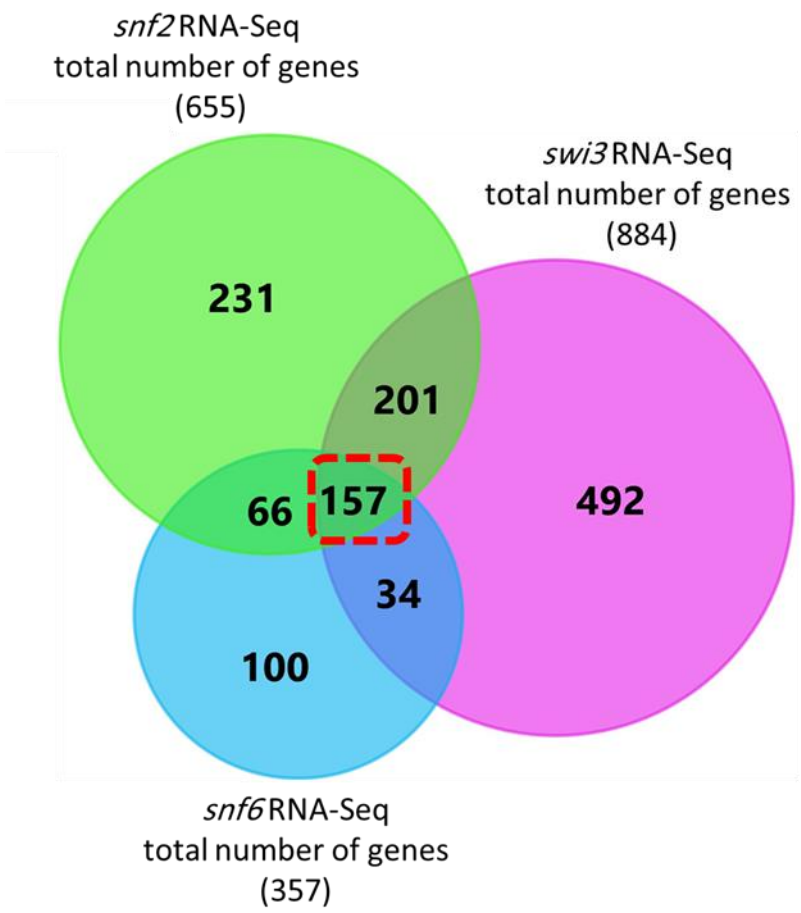

Figure 5. 6: Comparison of the genes down and up-regulated in the *snf2*, *swi3,* and *snf6* mutant strains. Venn diagram to identify the genes commonly down and up-regulated in a *snf2*, *swi3,* and *snf6* mutant.

Investigation of these 9 'directly commonly regulated' genes showed that 2 genes were involved in secondary active transmembrane transporter activity (*AAC1*, *PHO84*), 4 genes were categorized within the biological process GO profile (*PUT4*, *ROX1*, *HMS2*, *YER158C*), *CWP2* was a fungal cell wall gene, and there were two genes of unknown function (Fig. 5.9A). Interestingly when the transcription fold changes relative to wt of the 9 genes in each mutant were plotted, it could be seen that the genes showed distinct changes in transcription in the different mutants (Fig. 5.9B). Thus, even though the data suggests that these 9 commonly regulated genes were subject to direct

regulation by Snf2p, Swi3p, and Snf6p, presumably acting together, each subunit can have a different influence upon the transcription of these genes. For example, at the potentially Snf2p, Swi3p, and Snf6p co-occupied *CWP2* gene, the data suggests that although Snf2p and Snf6p exert a positive effect upon transcription, Swi3p influences the gene negatively to downregulate this genes transcription (Fig. 5.9).

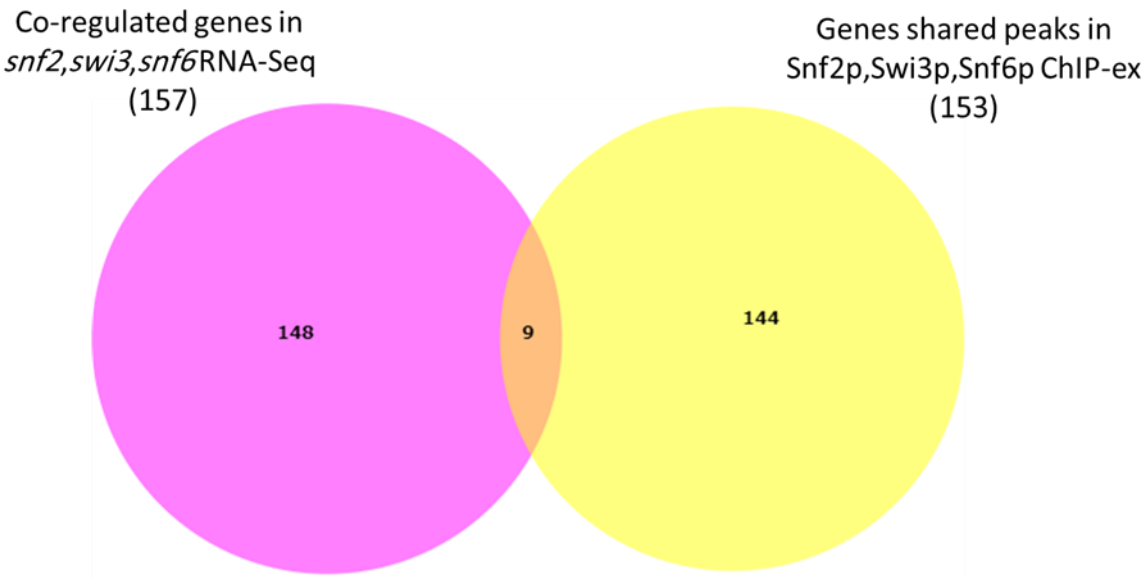

Figure 5. 7: Comparing the genes commonly regulated by *SNF2*, *SWI3,* and *SNF6* with the genes showing co-occupancy of Snf2p, Swi3p, and Snf6p. Venn diagram of the 153 genes showing common Snf2p, Swi3p, and Snf6p occupancy with the 157 genes that are commonly up and down-regulated in the *snf2*, *swi3,* and *snf6* mutants. The 9 genes which overlap can be considered to be 'directly commonly regulated' by Snf2p, Swi3p and Snf6p.

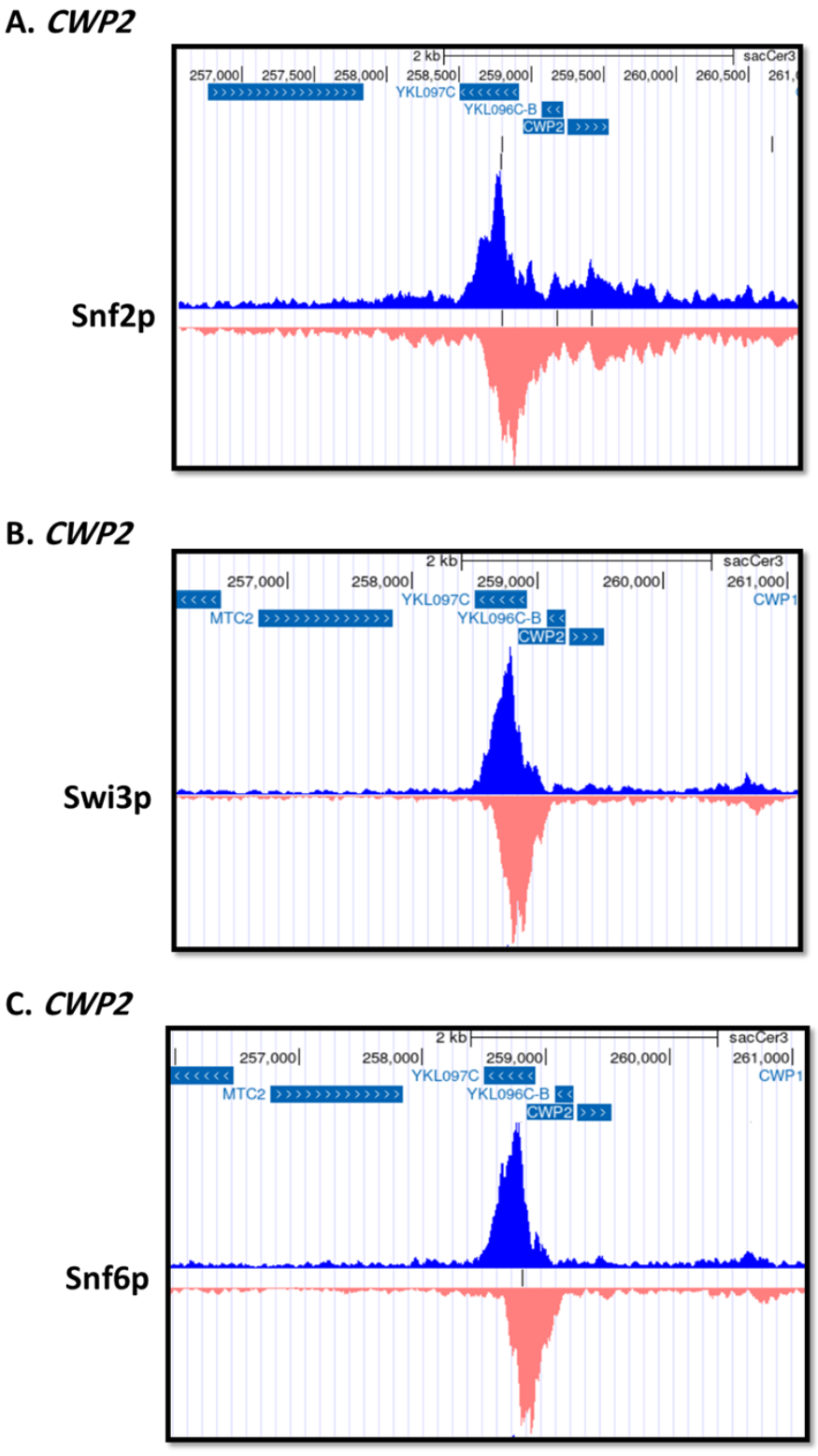

Figure 5. 8: J browse screenshots of the peaks of Snf2p, Swi3p, and Snf6p at *CWP2*.

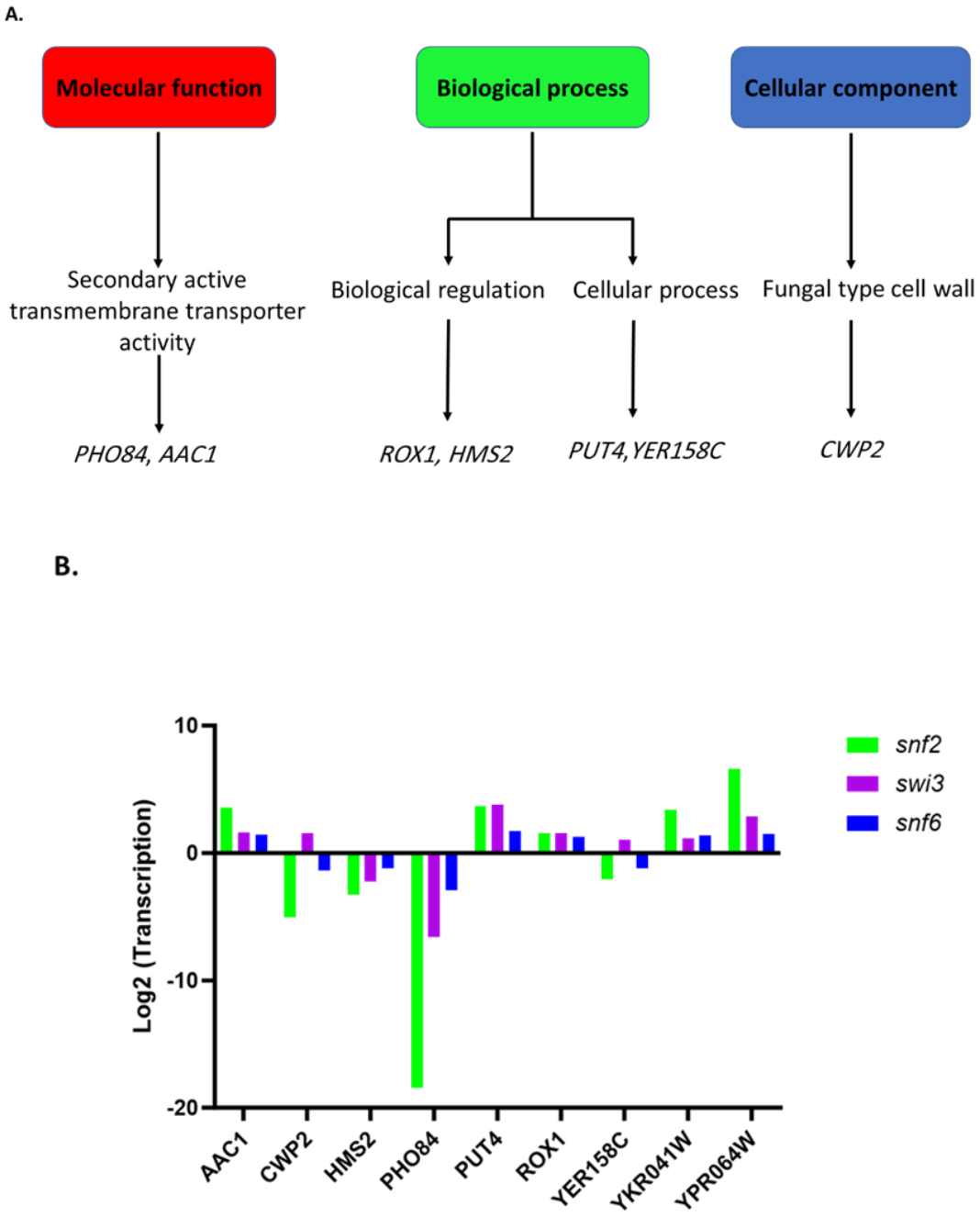

Figure 5. 9: Comparing the genes commonly regulated by *SNF2*, *SWI3*, and *SNF6* with the genes showing co-occupancy of Snf2p, Swi3p, and Snf6p. **(A)** Gene ontology of the commonly regulated and directly occupied genes (9 genes). **(B)** Comparing the transcription level of (9 genes) in the *snf2*, *swi3*, and *snf6* mutant strains.

5.2.7 Correlating Snf2p occupancy with the transcription profile in a *snf2* deletion mutant

The previous analyses revealed a minimal overlap of the sites co-occupied by Snf2p, Swi3p and Snf6p with the genes commonly up and down-regulated in all three mutants. This suggested the individual subunits can uniquely regulate genes when either functioning together or on their own. I therefore next compared the gene occupancy of the individual Swi-Snf subunits with the transcriptomes uncovered in each individual subunit mutant. The aim was to see how well these data sets correlated which might indicate the extent to which the genes up and down regulated in each subunit mutant are directly regulated by that subunit.

I first correlated Snf2p gene (and tRNA) occupancy with the 253 genes downregulated in the *snf2* deletion mutant. These 253 genes would represent genes subject to activation by Snf2p. The Venn diagram showed that 32 of the genes downregulated in the *snf2* mutant genes had a peak of Snf2p associated with them (Fig. 5.10A). Conversely, of the 307 genes upregulated in a *snf2* mutant, 31 of these genes had an associated Snf2p peak. These data suggest that 12.6% of the genes we had identified as being subject to activation by Snf2p might be directly regulated, and 10.1% of genes subject to negative regulation by *SNF2* are directly regulated (Fig. 5.10B).

Gene ontology analysis of the genes directly activated by Snf2p or negatively regulated by Snf2p revealed cohorts containing a diverse array of functions (Fig. 5.11).

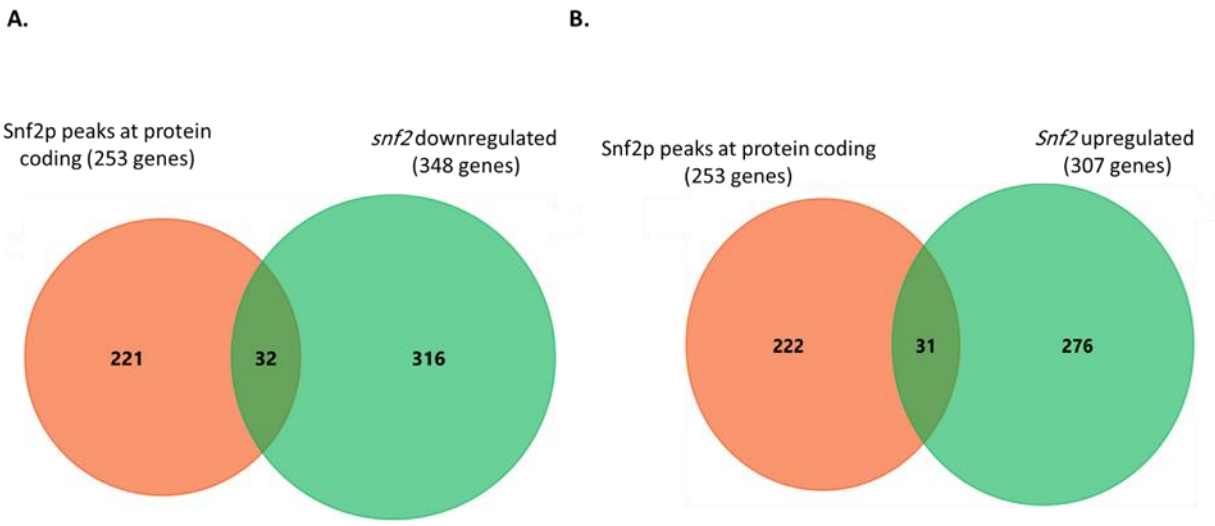

Figure 5. 10: Correlating Snf2p occupancy with genes down and upregulated in a *snf2* mutant. (A) correlation of Snf2p occupancy with genes downregulated in a *snf2* mutant. **(B)** correlation of Snf2p occupancy with genes upregulated in a *snf2* mutant.

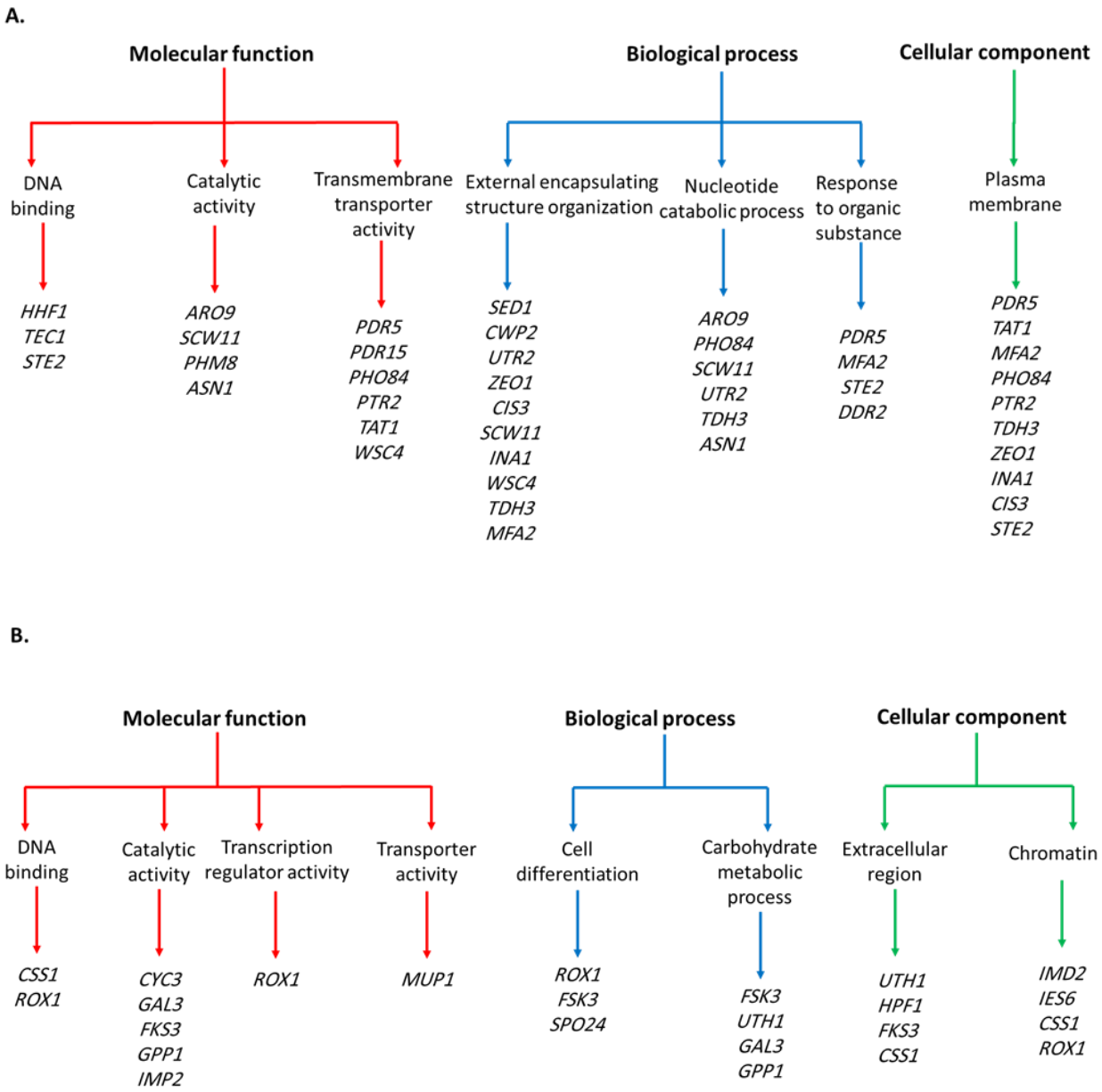

Figure 5. 11: Gene ontology analysis of the genes directly regulated by Snf2p. (A) Gene ontology of the 32 genes downregulated in a *snf2* mutant strain which are also occupied by Snf2p. **(B)** Gene ontology of the 31 genes upregulated in a *snf2* mutant which are also occupied by Snf2p.

5.2.8 Correlating Swi3p occupancy with the transcription profile in a *swi3* deletion mutant

Here, I compared the total number of genes more than 2-fold down-regulated in a *swi3* deletion mutant (300 genes) with Swi3p peaks at protein coding genes (487 genes). The Venn diagram revealed that 41 of the genes downregulated in the *swi3* mutant contained a peak of Swi3p (Fig. 5.12A). Thus, 13.7% of the genes subject to Swi3p activation could be directly regulated by Swi3p.

When I compared the 584 genes upregulated in a *swi3* mutant with the 487 genes containing a peak of Swi3p, 90 of these upregulated genes were found to contain a peak of Swi3p (Fig. 5.12B). Thus, 15.4% of the genes subject to negative regulation by Swi3p could be considered as being directly regulated.

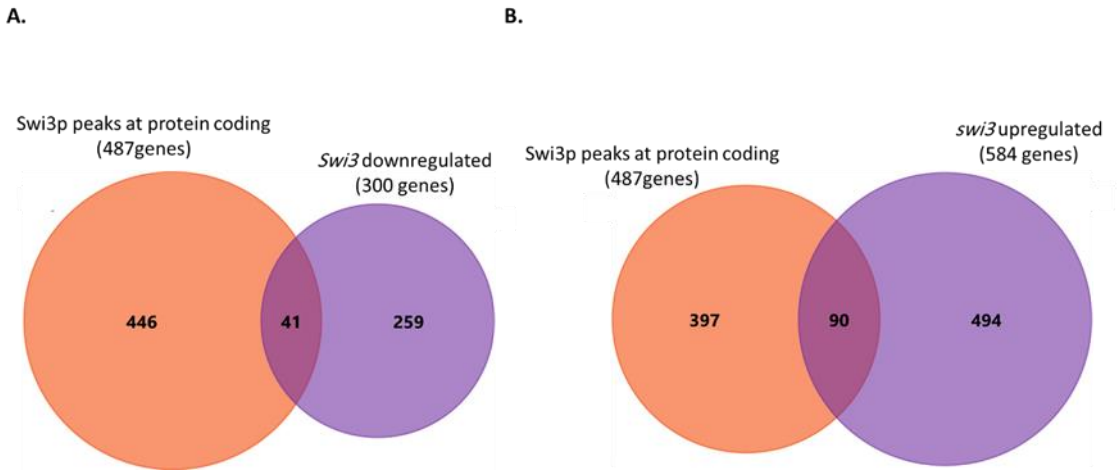

Figure 5. 12: Correlating Swi3p occupancy with genes down and upregulated in a *swi3* mutant. (A) correlation of Swi3p occupancy with genes downregulated in a *swi3* mutant. **(B)** correlation of Swi3p occupancy with genes upregulated in a *swi3* mutant.

When I analysed the gene ontology of the 41 genes downregulated in *swi3* which contained a peak of Swi3p, a broad range of genes were apparent (Fig. 5.13A). Similarly, the Go analyses of the 90 upregulated genes that contained a peak of Swi3p showed a

broad range of gene functions, with no obvious enrichment of genes of a particular function (Fig. 5.13B).

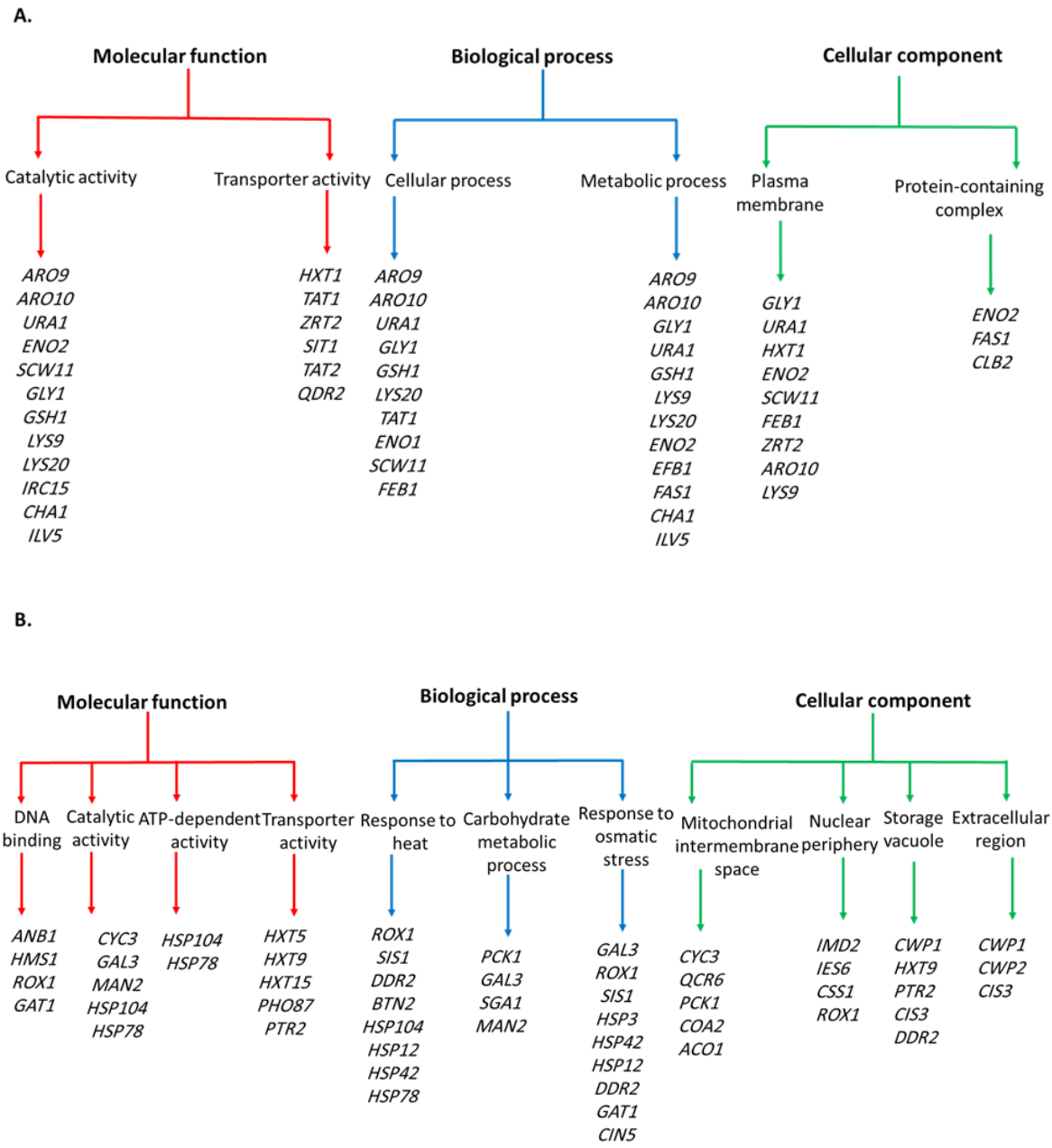

Figure 5. 13: Gene ontology analysis of the genes directly regulated by Swi3p. (A) Gene ontology of the commonly downregulated genes in a *swi3* mutant strain with Swi3p overlapped genes (41 genes). **(B)** Gene ontology of the commonly upregulated genes in a *swi3* mutant strain with Swi3p overlapped genes (90 genes).

5.2.9 Correlating Snf6p occupancy with the transcription profile in a *snf6* deletion mutant

A Venn diagram of the 271 genes downregulated in a *snf6* deletion mutant with the 370 genes occupied by Snf6p, revealed that 29 of the downregulated genes contained a peak of Snf6p (Fig. 5.14A). This suggests that 10.7% of the genes activated by *SNF6* might be directly regulated by Snf6p.

A comparison of the 86 genes upregulated in the *snf6* deletion mutant with 370 genes containing a peak of Snf6p, showed that only 10 of the upregulated genes contained a peak of Snf6p (Fig. 5.14B). Thus, only 2.7% of the genes subject to repression by *SNF6* appear to be directly regulated by Snf6p. Go analysis of the genes apparently directly positively and negatively regulated by Snf6p showed no obvious enrichment of genes of any particular function (Fig. 5.15A and B).

Overall, the data suggests that the correlation of Swi-Snf subunit occupancy with the genes under control of each subunit, as shown via the mutant transcriptomes, is poor. This might suggest a large contribution to Swi-Snf activity occurs indirectly via other proteins or might reflect the inability of current ChIP techniques to uncover all Swi-Snf subunit binding sites.

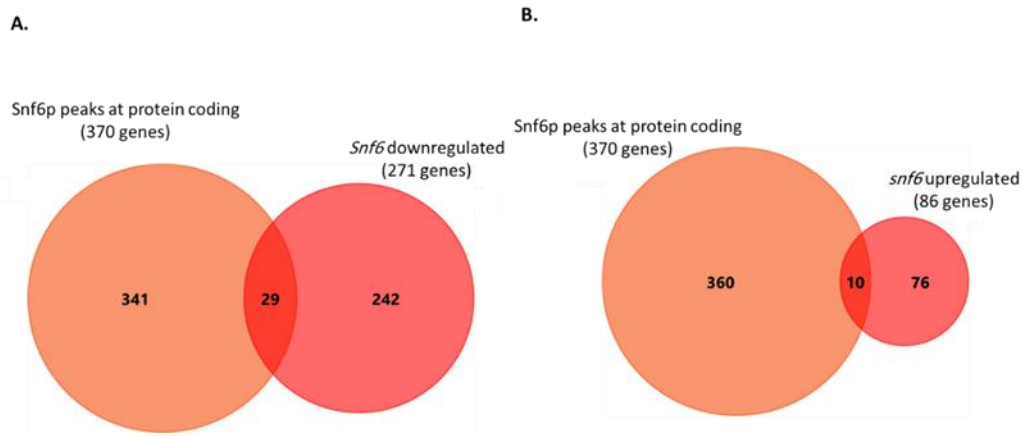

Figure 5. 14: Correlating Snf6p occupancy with genes down and upregulated in a *snf6* mutant. (A) correlation of Snf6p occupancy with genes downregulated in a *snf6* mutant. **(B)** correlation of Snf6p occupancy with genes upregulated in a *snf6* mutant.

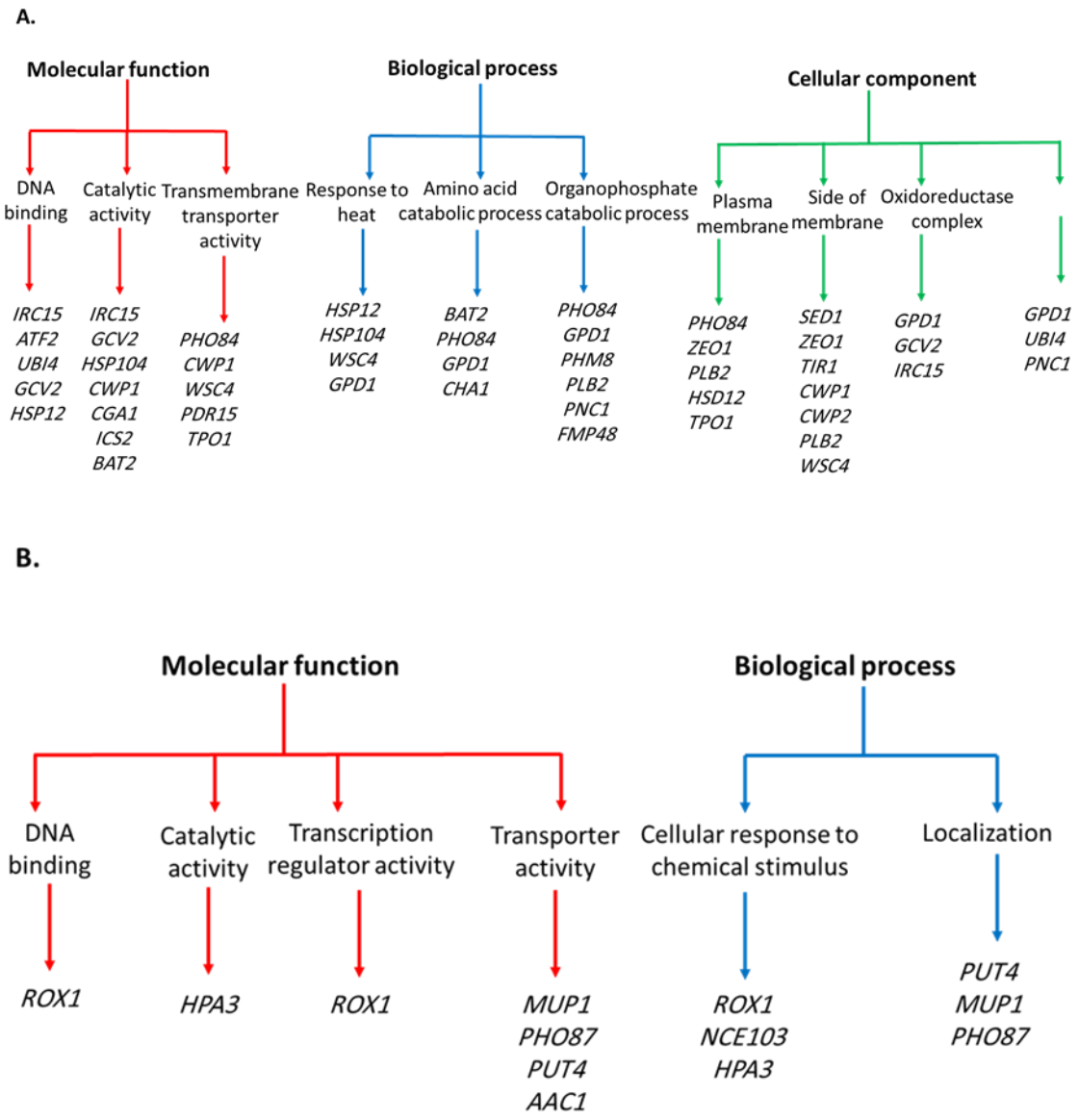

Figure 5. 15: Gene ontology analysis of the overlapped genes at least 2-fold down and up-regulated in a *snf6* gene deletion mutant with Snf6p overlapped genes. (A) Gene ontology of the commonly downregulated genes in a *snf6* mutant strain with Snf6p overlapped genes (29 genes). **(B)** Gene ontology of the commonly upregulated genes in a *snf6* mutant strain with Snf6p overlapped (10 gene).

Summary of main findings for the Swi-Snf subunits analysed

- only a small overlap of sites/genes are occupied by all Swi-Snf subunits.
- Subunits can occupy a large number of unique sites.
- Subunits can be found at gene promoters and across ORFs.
- Swi3p and Snf6p occupy a more similar cohort of genes, which is distinct from the cohort occupied by Snf2p.
- Taf14p shows the most distinct occupancy profile.
- Even where multiple subunit occupancy correlates with genes commonly influenced in the same subunit mutants, (e.g. at *CWP2*), the different subunits can influence these 'directly commonly regulated' genes differently.
- The correlation of individual Swi-Snf subunit occupancy with the genes under control of each subunit is poor.

Discussion

In this study a comprehensive analysis of Swi-Snf subunit occupancy across the genome was performed. The intricate dynamics of chromatin remodeling and its implications for gene regulation was assessed. The Swi-Snf complex, known for its role in nucleosome remodeling, is composed of various subunits, each possibly contributing distinctively to the complex's function. The investigation reveals a subtle background of subunit occupancy, challenging the perception that these subunits operate solely within a single complex.

The results showed that Swi-Snf subunits have diverse genomic occupancy, suggesting roles beyond their established collective function in the complex. Swi3p's prominent presence at 980 sites compared to only 297 sites of occupancy for Snf11p emphasizes this diversity. The analysis of each subunits occupancy and gene regulation profiles emphasizes the subunits individual contributions to gene expression. Specifically, Snf2p and Taf14p show the most significant role in snRNA transcription regulation [186]. Furthermore, the distinct distribution of subunits across cryptic, stable, and sensitive

transcripts suggests a unique genomic presence of the various subunits. These findings, building on previous work by Smith et al. 2003 [187], provide deeper insights into the Swi-Snf complex functions in nucleosome remodelling and gene expression.

The finding that all Swi-Snf subunits co-occupy merely 15 sites suggests that Swi-Snf subunits operate with a high degree of independence. The substantial overlap among Swi3p, Snf6p, and Swi1p, along with Snf11p and Snf2p occupancy sites, indicates intricate subunit interactions and relationships [188]. The minimal overlap of Taf14p with other subunits reinforces the idea of specialized functions for each subunit. Past studies have also highlighted the Swi-Snf subunits varied roles in chromatin remodeling, essential for transcription, replication, and DNA repair [188].

The SWI/SNF complex has been extensively studied for its role in modulating chromatin structure and its implications in cancer and other health-related anomalies [182]. The variability in the composition of the SWI/SNF complex, including intra-species isoforms and inter-species homologs, adds another layer of complexity to its function and regulation [189] In the context of cancer, mutations in the SWI/SNF complex have been associated with various malignancies, including breast cancer, where approximately 30% of tumors have genetic alterations in one or more SWI/SNF subunits [190]. The results shown here in yeast, highlight the importance of understanding the individual and collective roles of Swi-Snf subunits in chromatin remodeling and their potential impact on gene regulation and disease pathogenesis.

The occupancy sites at ORFs linked with Snf2p, Swi3p, Snf6p, and Swi1p subunits display a notable overlap of 135 genes, consistent with broader subunit overlap excluding Taf14p. The distinct occupancy profile of Taf14p suggests a unique regulatory role compared to other subunits, while the observed overlap corroborates the crucial role of the SWI/SNF complex in gene regulation by facilitating chromatin transition for transcription factor access [188]. The distinct occupancy profiles of the SWI/SNF subunits suggest a level of specificity in their binding to chromatin, which may be

influenced by the variability of the subunits within the complex [191]. This specificity is crucial for the regulation of gene expression and is essential for processes such as cell maintenance and response to stress. The data also supports the notion that individual SWI/SNF subunits can independently bind to a significant number of unique sites, which is indicative of their diverse and unique roles in chromatin remodelling and gene regulation [190].

The result depicting the Snf2p, Swi3p, and Snf6p occupancy across ORFs offers insight into the Swi-Snf complex gene regulatory role; notably, the Snf2p prevalence within ORFs challenges the conventional view of Swi-Snf primary function at gene promoters, aligning with recent research indicating a broader role in gene expression regulation beyond promoter regions [190]. Indeed, the data supports a dominant role for Snf2p in chromatin remodelling across gene bodies to enable transcription elongation as opposed to remodelling at promoters to enable initiation. Moreover, the limited occurrence of Swi-Snf subunits in downstream intergenic regions corroborates Ghia et al.'s (2011) findings of preferential binding to coding and promoter regions, crucial for transcription initiation and elongation [179]. Thus, the spatial dynamics of subunit interactions revealed here provide insights into their functional significance, with distinct occupancy profiles suggesting varied subunit roles across different transcriptional stages and genes [192]. This is particularly evident in the case of the *SER3* and *UTR5* genes, where the peaks of Swi3p and Snf2p occupancy were found in the promoter and across the ORF, respectively (Fig. 5.4).

The substantial overlap of 270 sites of occupancy between the Snf2p, Swi3p, and Snf6p subunits indicates coordinated regulation of gene expression by these three subunits acting within an intact Swi-Snf complex (Fig. 5.5A). The marked overlap between Swi3p and Snf6p occupancy at 206 genes suggests a close functional relationship or crosstalk crucial for regulating specific gene sets between these subunits, supporting Xiaofang's (2007) observations of synergistic effects on gene regulation [193]. Unique occupancy sites for Swi3p (184 sites) and Snf2p (139 sites) suggest independent roles outside the

Swi-Snf complex, supported by Ghia et al.'s (2011) work on individual subunits' independent chromatin binding and gene expression influence [179]. Venn diagram analysis highlights the complexity and dynamic nature of subunit interactions, with the core set of 153 ORFs and tRNAs commonly occupied by Snf2p, Swi3p, and Snf6p suggesting a shared regulatory mechanism across these genes, enhancing our understanding of Swi-Snf complex functionality [194].

The overlap of Snf2p, Swi3p, and Snf6p subunit occupancy with transcriptional profiles in *snf2*, *swi3*, and *snf6* mutants revealed just 9 genes as being 'directly commonly regulated' by these three subunits. These genes, ranging from transmembrane transport (*AAC1*, *PHO84*) to cell wall composition (*CWP2*), highlights the complex's diverse roles in cellular physiology, corroborating previous research highlighting its involvement in wide-ranging biological processes [194], [195]. The varied transcriptional responses across mutant strains reveal antagonistic subunit effects on gene expression.

The correlation between single subunit occupancy and those subunits mutant transcriptional profiles was always poor. For example, analysis of Snf2p gene occupancy in relation to the *snf2* mutant transcriptome revealed only 12.6% of down-regulated genes were directly activated by Snf2p, and only 10.1% of up-regulated genes were directly repressed by Snf2p. Similarly, the data suggested only 13.7% of genes down-regulated in *swi3* were likely to be directly activated by Swi3p, while only 15.4% of up-regulated genes displayed Swi3p peaks, indicative of a direct repressive role by Swi3p. These findings suggest the subunits, and potentially Swi-Snf, are either acting mostly via indirect means or suggest that the ChIP-exo technique is still not fully efficient at revealing true subunit occupancy. The poor correlation between Swi-Snf subunit occupancy and gene expression changes in the subunit mutants could also be explained by the subunits having extensive yet selective regulatory control over specific genes in varied cellular contexts, or in response to environmental cues not signaled in the growth conditions used for the experiments performed here.

Thus, improvements in technology to identify and quantify protein: DNA interactions, coupled with experiments to analyse gene transcription profiles and subunit occupancy from cells grown under multiple different conditions, might give greater insight into the true occupancy and activity profiles of each subunit, and the Swi-Snf complex, in the future.

Chapter 6

Investigating the interplay between the Swi-Snf co-activator complex and the Tup1-Cyc8 co-repressor complex

6.1 Introduction

The yeast Swi-Snf complex was the first ATP-dependent chromatin remodelling complex which could activate global gene transcription that was discovered [132]. The yeast Tup1-Cyc8 complex was the first global repressor of gene transcription discovered [196]. Thus, these complexes are archetypes of conserved machinery required to switch gene transcription on and off. Previous research in the lab identified a set of 102 genes that were antagonistically regulated by the Tup1-Cyc8 complex acting as a repressor and the Swi-Snf complex acting as an activator [130]. A well-studied example of one of these antagonistically regulated genes is *FLO1* [114] (Fig. 6.1).

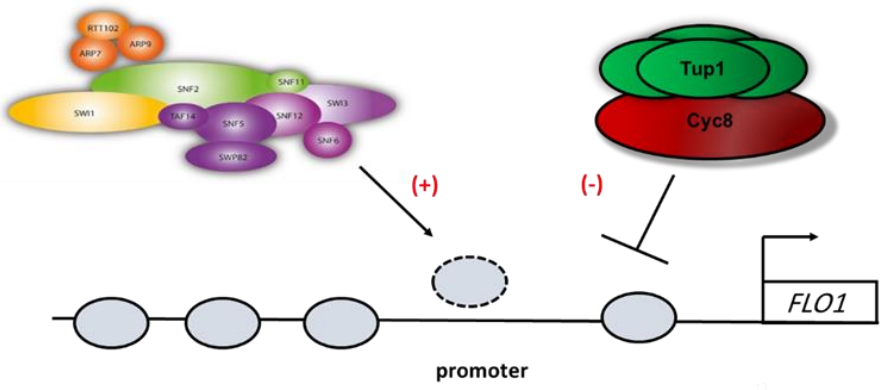

Figure 6. 1: A link between the Swi-Snf and Tup1-Cyc8 complexes: Schematic to illustrate antagonistic gene regulation by the Tup1-Cyc8 and Swi-Snf complexes. In wt cells, the inactive *FLO1* promoter contains a Tup1-Cyc8 dependent array of strongly positioned, hypoacetyated nucleosomes (grey ovals/solid outline) which blocks gene transcription (-). In the absence of Tup1-Cyc8, Swi-Snf becomes enriched at the *FLO1* promoter, evicts nucleosomes (grey ovals/hatched outline), and the *FLO1* gene is activated (+).

6.2 Results

Previous work in our lab suggested that Cyc8 protein levels were abolished in a *swi3* mutant [130]. I repeated the analysis and have shown that this result is reproducible (Fig. 6.2). Cyc8p was undetectable by Western blot analysis in the *swi3* mutant (Fig.6.2A). Conversely, the results showed that Swi3 protein levels were present in a *cyc8* mutant, although at reduced levels compared to that seen in wt (Fig.6.2B). Thus, Cyc8p levels are dependent upon *SWI3*. However, Swi3p levels are not dependent upon *CYC8*. This suggests some sort of interplay between *SWI3* and *CYC8* and predicts that a *swi3* mutant, in which Cyc8p is also absent, should have a similar transcriptome to a *swi3 cyc8* double mutant.

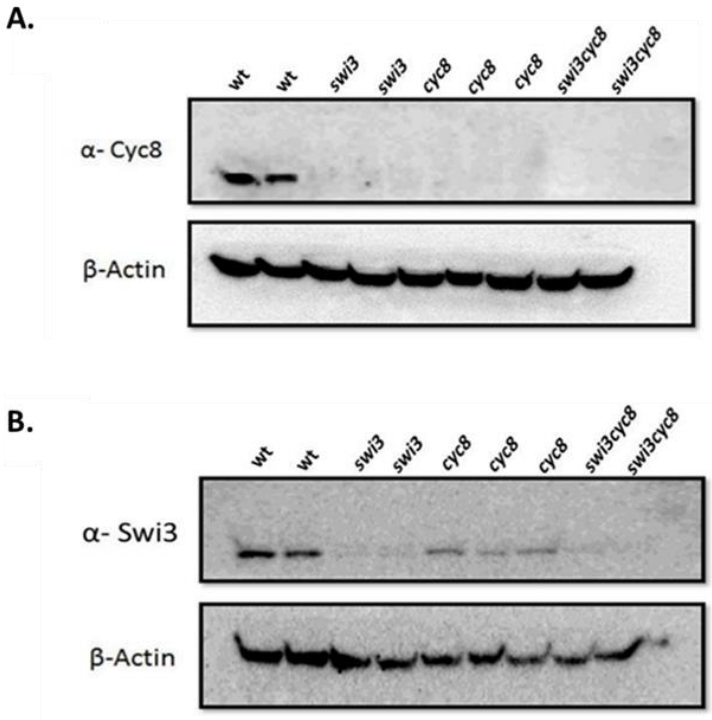

Figure 6. 2: Western Blot analysis of TCA extracted proteins from the log phase cells of wt, *cyc8, swi3*, and *swi3 cyc8* mutant strains. Antibodies were specific to **(A)** Cyc8p and **(B)** Swi3p. β-Actin was used as a loading control. wt, *swi3*, and *swi3 cyc8* strains were loaded duplicate and the *cyc8* mutant strain was loaded in triplicate.

I therefore, used RNA-Seq to compare the transcriptome of a *swi3* single mutant with the transcriptome of a *swi3 cyc8* double mutant strain to confirm if a *swi3* mutant strain should be considered to be most like a *swi3 cyc8* mutant strain, at least at the transcriptional level. If this is the case, it would help explain why the *swi3* gene deletion mutant's transcription profile is the most unique of the Swi-Snf subunit mutants, in that it shows the greatest number of up-regulated (i.e. de-repressed) genes.

6.2.1 RNA Seq analysis in a *swi3 cyc8* double mutant and a *swi3* single mutant

RNA-seq was performed on wt, *swi3*, and the *swi3 cyc8* double mutant. I first checked the quality of the triplicate RNA-Seq data by plotting the data sets against each other to give an R^2 plot (Fig. 6.3). The reproducibility of each triplicate data set was good.

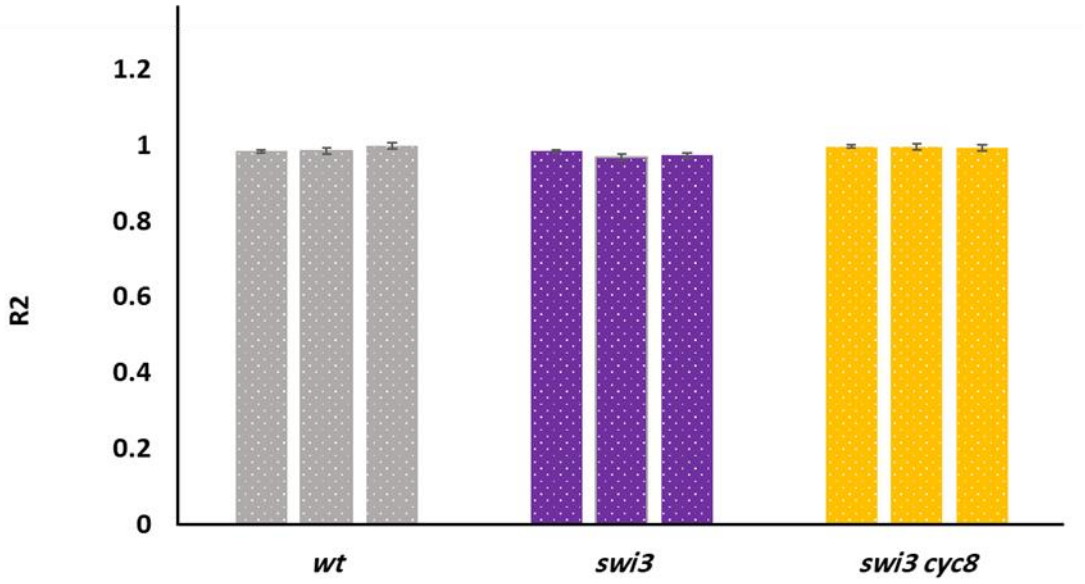

Figure 6. 3: High correlation between biological replicates. Graph depicting the compiled Pearson R^2 values obtained from plotting the normalised counts of each sample in wt, *swi3,* and *swi3 cyc8* against each other. The RNA-seq data from the wt and *swi3* mutant was the same as that analysed in Chapter 4, whereas the *swi3 cyc8* RNA-seq data was obtained for this chapter.

6.2.2 Transcription of *CYC8* is unaffected in a *swi3* mutant

Considering that Swi3p is a component of the Swi-Snf global activator of transcription, the most likely explanation for the lack of Cyc8p in a *swi3* mutant was that *CYC8* transcription would be abolished in the *swi3* mutant. However, as can be seen, *CYC8* mRNA levels in the *swi3* mutant were the same as in the wild type (Fig. 6.4A). Therefore, the decreased Cyc8p levels in the *swi3* mutant were not due to decreased *CYC8* transcription in this strain, where Swi-Snf activity is compromised. I also confirmed that SWI3 transcription levels in the cyc8 mutant were the same as wt levels (Fig. 6.4B).

Thus, there is no evidence to support a role for Swi3p in regulating *CYC8* transcription or for Cyc8p in regulating *SWI3* transcription.

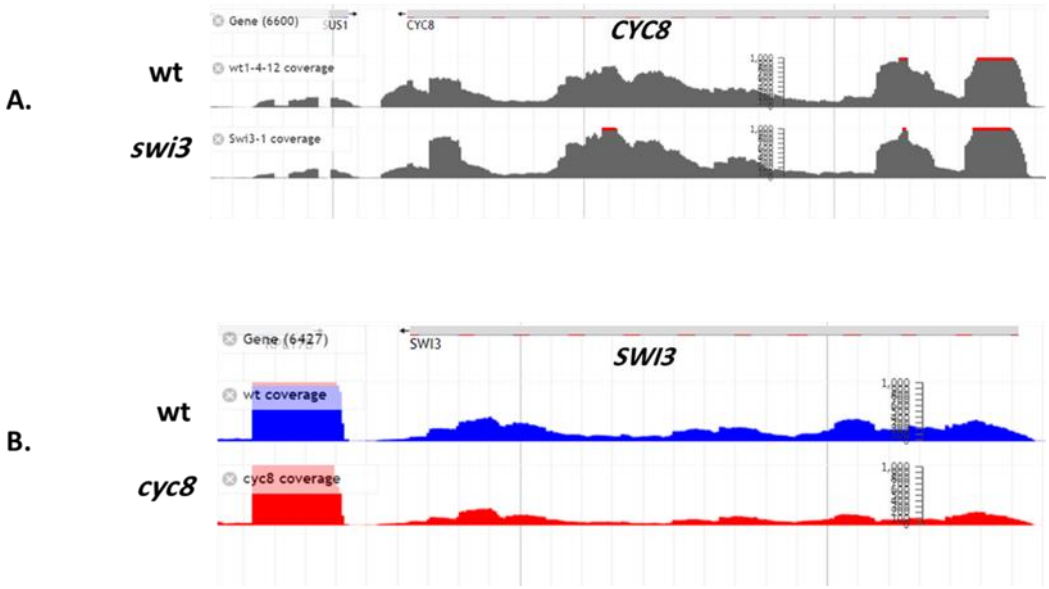

Figure 6. 4: (A) RNA-Seq data (JBrowse) to show *CYC8* transcription in wt and a *swi3* mutant strain. **(B)** RNA-Seq data (JBrowse) to show *SWI3* transcription in wt and a *cyc8* mutant strain.

6.2.3 Differential gene expression in a *swi3* and *swi3 cyc8* mutant

I next wanted to determine if a *swi3* mutant transcriptome was similar to a *swi3 cyc8* double mutant transcriptome, as would be predicted considering that Cyc8p is apparently absent in the *swi3* single mutant.

I first identified the number of genes which were up and downregulated more than 2-fold compared to wt in the *swi3* single mutant and the *swi3 cyc8* double mutant (Fig.6.5A). The results showed 884 genes were up and downregulated in the *swi3* mutant and 686 genes were up and downregulated in the *swi3 cyc8* mutant, compared to wt. A heat map was generated from the total number of genes down and up-regulated in each strain (1570 genes) to visualise the differential levels of transcription in the *swi3* and *swi3 cyc8* strains (Fig. 6.5B). However, contrary to the prediction, the results showed considerable differences in the *swi3* profile compared to the *swi3 cyc8* profile.

Furthermore, when I compared the total number of genes up and downregulated in each mutant, an overlap of only 354 genes was revealed (Fig. 6.5C). Thus, initial analysis suggests that the *swi3* single mutant is not so similar to a *swi3 cyc8* double mutant in terms of global transcription.

A.

	Number of genes up-regulated	Number of genes downregulated	Total number of genes (up and down)
swi3	584	-300	884
swi3 cyc8	438	-248	686

B.

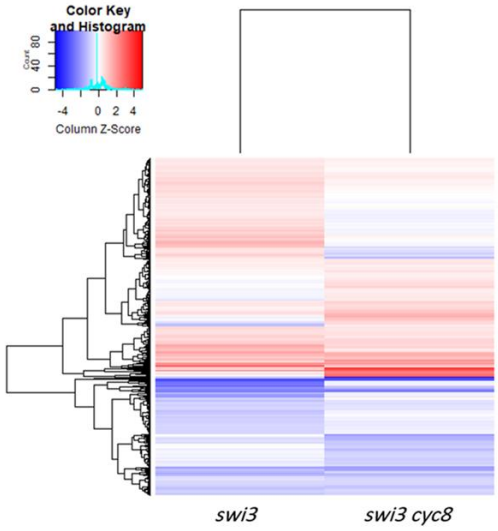

C.

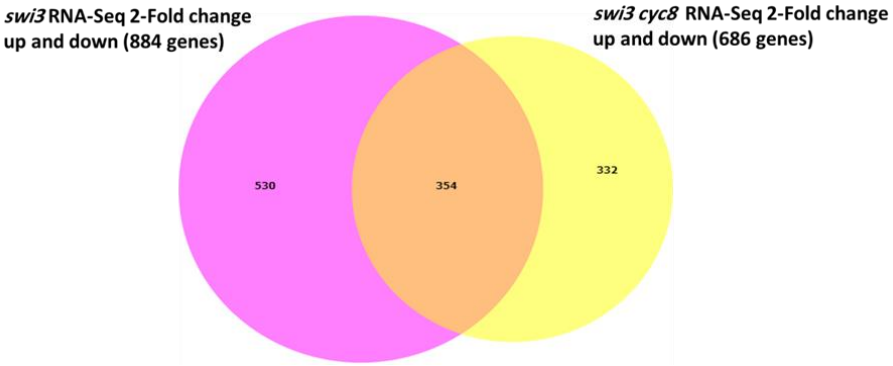

Figure 6. 5: Differential gene transcription in the *swi3*, and *swi3 cyc8* mutant. (A) Table of the total number of genes down and up-regulated in the *swi3* and *swi3 cyc8*. **(B)** A cluster heat map in which rows represent genes, and columns represent mutants. The blue colour reflects downregulated genes and the red colour reflects up-regulated genes. the foldchange (>2-fold and FDR of <0.05). Heatmap2 R gplot packaging was used to generate this figure. **(C)** Venn diagram to show the total number of genes up and down-regulated in the two mutants.

6.2.4 Comparing the genes down and up-regulated in the *swi3* and *swi3 cyc8* mutant

6.2.4.1 Comparing the genes down-regulated in the *swi3* and *swi3 cyc8* mutant

I began by comparing the numbers of genes downregulated relative to wt in the *swi3* single and the *swi3 cyc8* double mutant (Fig.6.6). For this analysis, I only considered genes that were at least two-fold downregulated in the *swi3* (300) and *swi3 cyc8* (248) mutant strains compared to wt (Log_2<-1, FDR of <0.05). These downregulated genes should reflect those genes at which Swi3p and Cyc8p are acting as activators to promote transcription.

A Venn diagram showed that 105 genes were downregulated in both the *swi3* and *swi3 cyc8* mutant strains, whilst 195 genes were solely down-regulated in the *swi3* mutant and 143 genes were uniquely downregulated in the *swi3 cyc8* mutant (Fig. 6.6). This indicates that there are considerable differences in gene regulation between a *swi3* single mutant, which is also depleted for Cyc8p, and a *swi3 cyc8* double mutant strain. Thus, although a similar number of genes were down-regulated in the two mutants, these gene cohorts in the two mutants differ significantly.

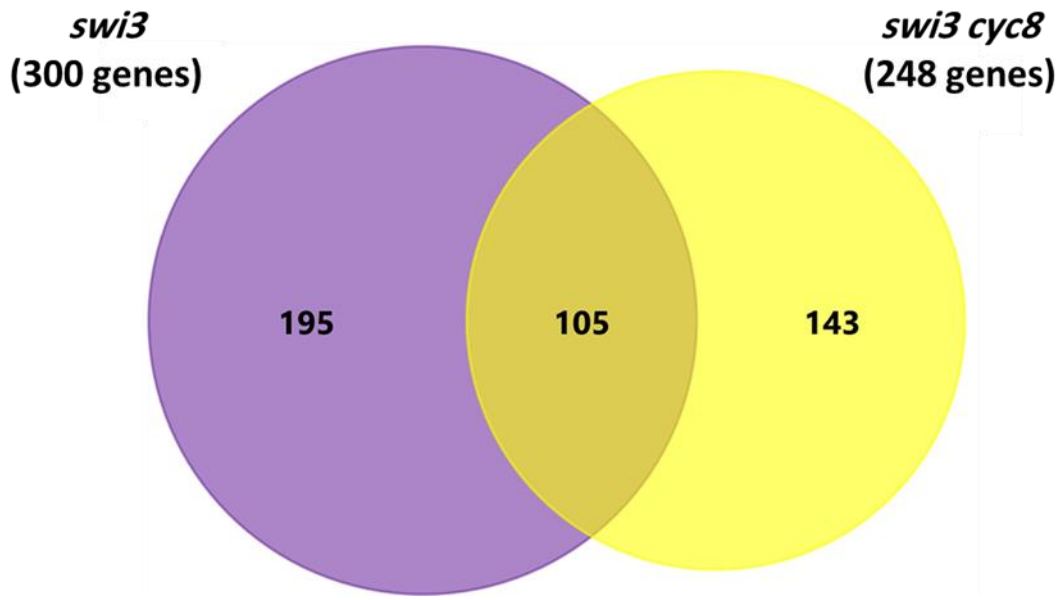

Figure 6. 6: Venn diagram to identify the genes shared and uniquely downregulated in the *swi3* and *swi3 cyc8* mutant strains.

6.2.4.2 Comparing the transcription levels of *swi3* and *swi3 cyc8* down-regulated genes

Next, I compared the average levels of the genes downregulated in the *swi3* and *swi3 cyc8* mutant strains (Fig. 6.7). The results showed there was no significant difference in the average level of downregulation of the 105 overlapping genes in the *swi3* and *swi3 cyc8* mutants.

I then compared the average transcription level of the 195 genes solely downregulated in the *swi3* single mutant with average transcription levels of the 143 genes solely downregulated in the *swi3 cyc8* double mutant. The result again showed no significant difference between the transcription levels of these genes in the two mutants.

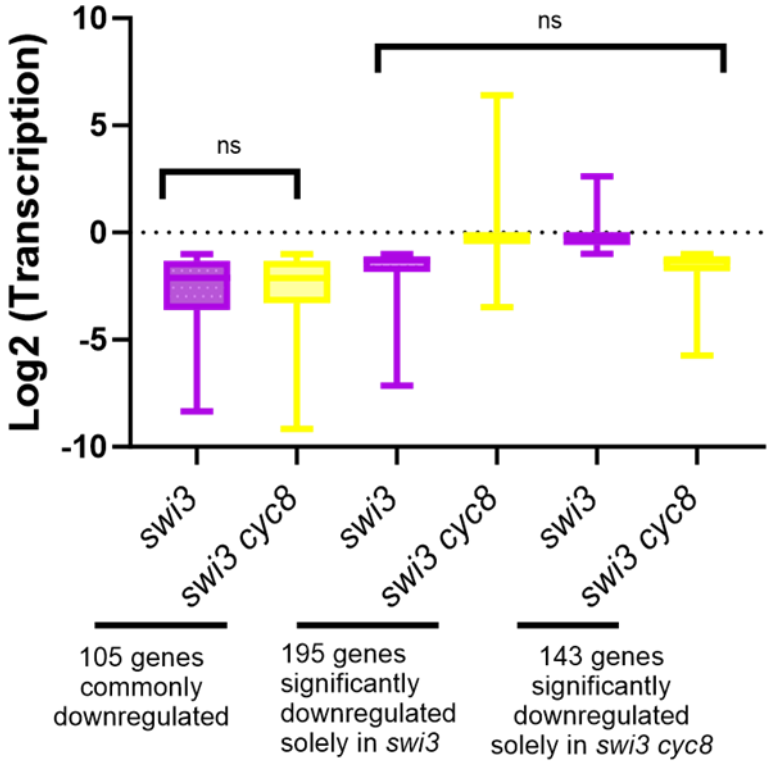

Figure 6. 7: The transcription level in the *swi3* and *swi3 cyc8* mutants. Box plot to show the fold changes of the downregulated genes in the *swi3* and *swi3 cyc8* mutants.

Interestingly, from the 195 genes downregulated solely in the *swi3* mutant strain there were 86 of these genes which were upregulated more than 2-fold in the *swi3 cyc8* mutant (Fig. 6.8A). Examples of these genes include *PHO11* and *PHO89* (Fig. 6.8B).

This result indicates that although these 195 genes are subject to positive regulation by Swi3p, additional deletion of *CYC8* in combination with the *SWI3* deletion, leads to upregulation of 86 of these genes. This suggests that *CYC8* is having a negative impact upon the regulation of these *SWI3*-dependent genes in the *swi3* mutant even though Cyc8p is not detectable by western blotting. This could indicate that Cyc8p may be present at a low concentration in the *swi3* mutant strain where it can repress transcription of this set of 86 genes. Conversely, in the *swi3 cyc8* double mutant, where

there is no Cyc8p at all, these 86 genes are not repressed and are therefore upregulated (Fig. 6.8A).

I next compared the average levels of transcription of the 143 genes downregulated solely in the *swi3 cyc8* mutant strain with the levels of transcription of the same set of genes in the *swi3* single mutant (Fig. 6.8C). The results showed that there was a set of 59 of these genes that were upregulated in the *swi3* single mutant strain (Fig. 6.8C). Examples of these genes were *EGO4* and *BTN2* (Fig. 6.8D). This indicates that of the 143 genes solely down-regulated in the *swi3 cyc8* double mutant, this set of 59 genes are subject to negative regulation by *SWI3* and positive regulation by *CYC8*.

Thus, these data suggest that in a *swi3* mutant strain, Cyc8p, at a low concentration, may be able to positively regulate these genes. However, in the double mutant strain, with the complete absence of Cyc8p, these genes cannot be activated and show downregulation compared to wt.

Together, this striking data suggests that in a *swi3* mutant, where Cyc8p cannot be detected by western blot analysis, there may still be a low concentration of Cyc8p that can positively and negatively influence target gene transcription. This would explain why the *swi3* single mutant and the *swi3 cyc8* double mutant strain are not as similar, in terms of gene transcription, as would be predicted from the Cyc8p western blot result shown in (Fig. 6.2). Alternatively, these results could be due to an indirect effect in the absence of *CYC8*.

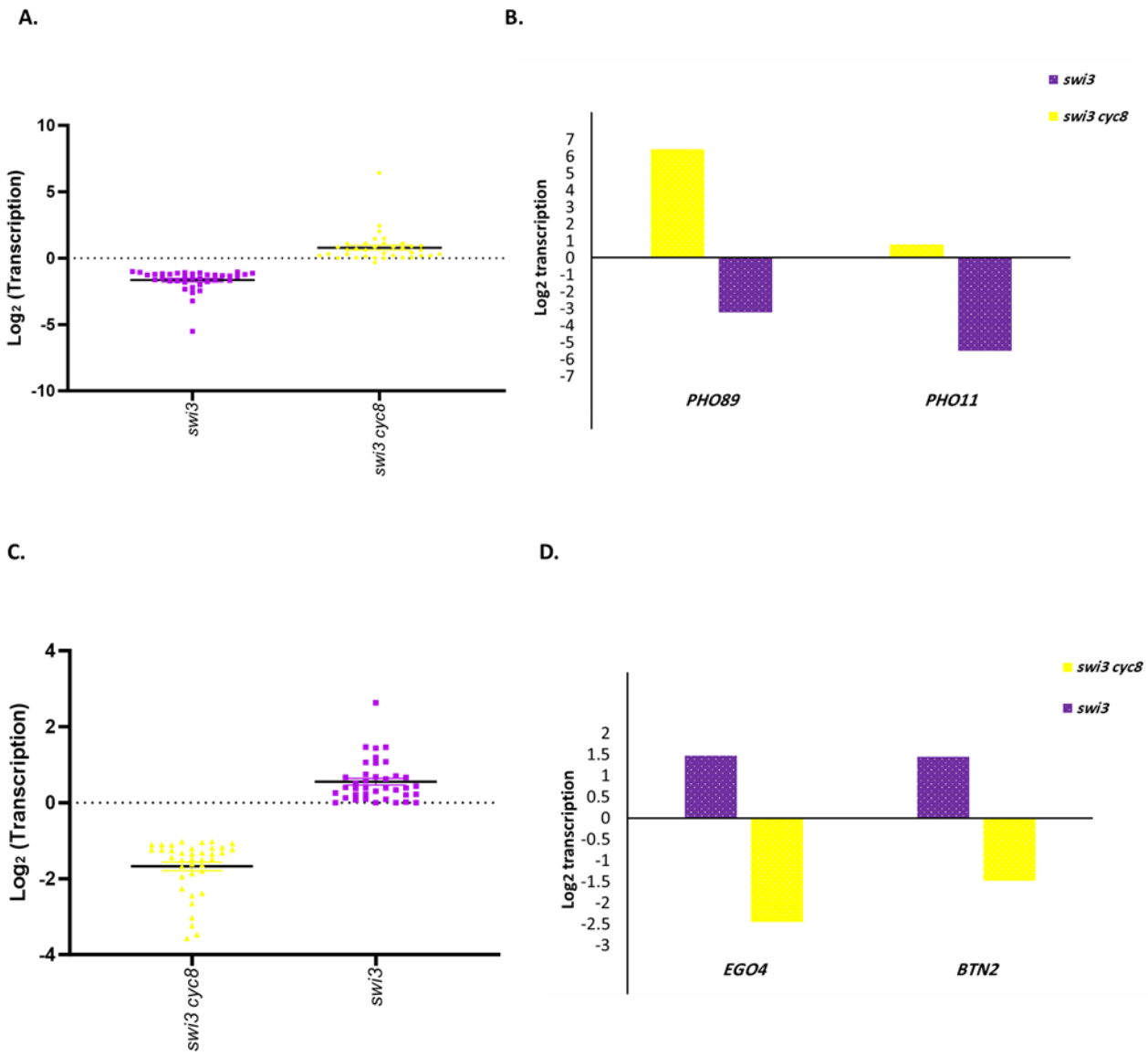

Figure 6. 8: (A) Scatter plot showing the Log2 fold changes for 86 genes of the 195 genes solely down-regulated in a *swi3* single mutant, that were up-regulated in the *swi3 cyc8* double mutant. **(B)** Example for genes there was upregulated fold change from the 195 genes solely regulated by *swi3*. **(C)** Scatter plot showing the Log2 fold changes for 59 genes of the 143 genes downregulated solely in a *swi3 cyc8* that were upregulated in the *swi3* single mutant. **(D)** Examples of the 59 genes downregulated in the *swi3 cyc8* mutant.

6.2.4.3 Gene ontology analysis of genes downregulated in the *swi3* and *swi3 cyc8* mutants

To identify if the genes downregulated in the *swi3* and *swi3 cyc8* mutant strain had specific functions, the Metascape website was used for gene ontology analysis (https://metascape.org). Of the 105 downregulated genes that overlapped in both the *swi3* and *swi3 cyc8* mutants, there were genes enriched that played a role in DNA integration, and genes that were involved in the plasma membrane. Examples of genes involved in DNA integration were *PHO3* and *PHO81*, which encode an acid phosphatase and a cyclin-dependent kinase inhibitor, respectively, both involved in phosphate metabolism [197] [198]. Examples of the genes involved in the plasma membrane included *HXT1*, which encodes a glucose transporter[199], and *FRE2*, which is involved in metal ion uptake [200] (Fig. 6.9).

GO analysis of the 195 genes solely downregulated in the *swi3* mutant revealed that genes were enriched that played a role in DNA integration and rRNA processing (Fig. 6.9). Examples of these genes included *PDR3* which encodes a transcription factor that is induced in response to DNA stress [201].

Finally, analysis of the 143 genes downregulated solely in the *swi3 cyc8* mutant revealed an enrichment of genes involved in the fungal cell wall and urea metabolism (Fig. 6.9). These genes included *AGA2*, which is involved in cell adhesion [202], *CRR1* which is required for spore wall assembly [203], and *BIT61* which encodes a subunit of the TORC2 complex which governs global metabolism and growth [204].

Together, this data shows that the *swi3* and *swi3 cyc8* mutants have different impacts on global gene transcription suggesting distinct roles for *SWI3* and *CYC8* in promoting gene activation.

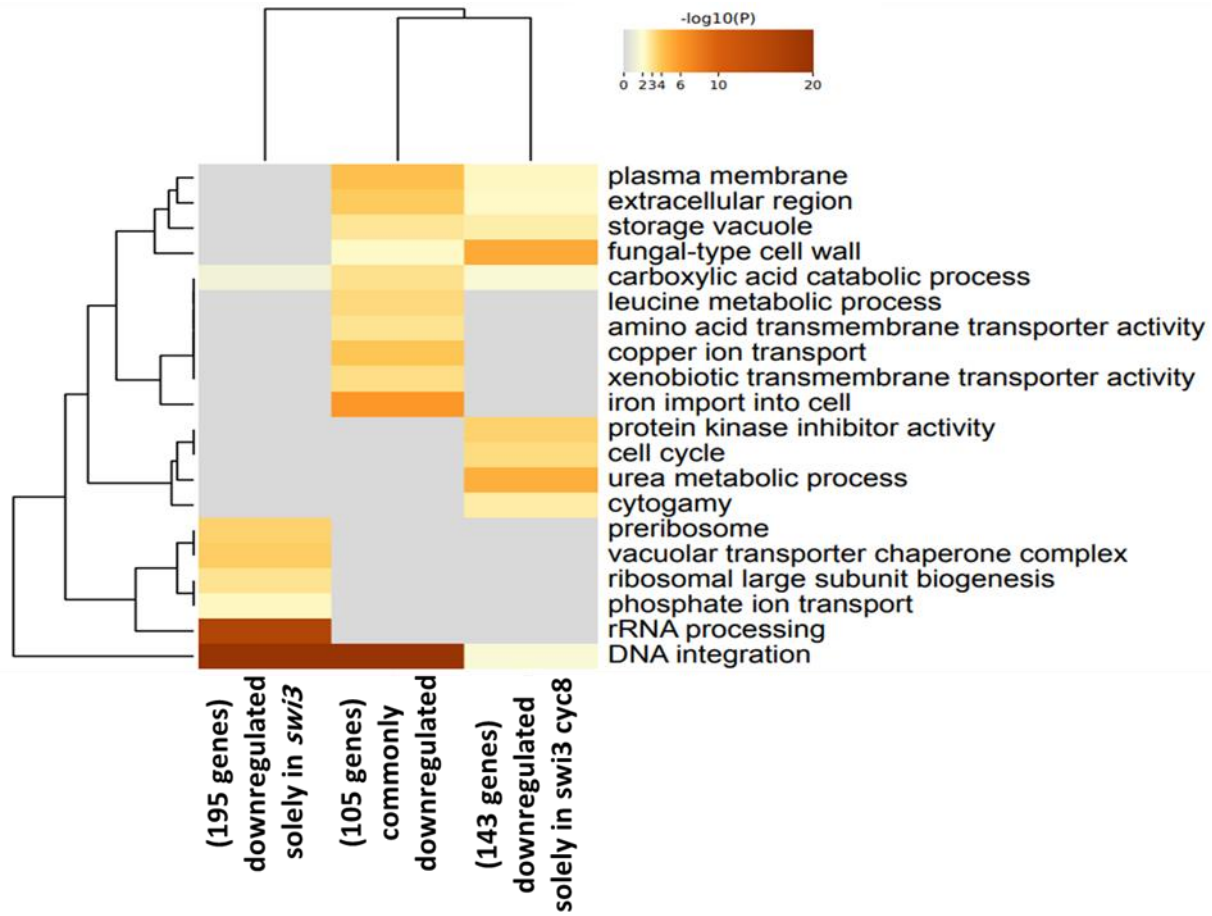

Figure 6. 9: Gene ontology analysis of downregulated genes in the *swi3*, *swi3 cyc8* mutant strain. Heat map generated using metascape website. Colored by p-values dark red indicates significant, orange indicates less significant than the red color, and gray color indicates no functions in those genes. **The first column** represents the Go profile for the 195 genes solely downregulated in the *swi3* mutant. **The second column** represents the Go profile for the 105 genes commonly downregulated in both the *swi3* and *swi3 cyc8* mutants. **The last column** represents the Go profile for the 143 genes downregulated only in the *swi3 cyc8* mutant.

6.2.4.4 Comparison of the genes up-regulated in the *swi3* and *swi3 cyc8* mutants

Next, I compared the genes upregulated in the *swi3* and *swi3 cyc8* mutants. These genes should reflect those genes at which Swi3p and Cyc8p are acting as a repressors of gene transcription. Here, there were 584 genes upregulated more than 2-fold compared to wt in the *swi3* mutant and 438 upregulated in the *swi3 cyc8* mutant (Fig. 6.5A).

A Venn diagram of the genes upregulated in the *swi3* and *swi3 cyc8* mutant strains revealed a cohort of 254 genes that were upregulated in both mutants (shared genes), whilst 330 genes were significantly upregulated only in the *swi3* mutant, and 184 genes were upregulated solely in the *swi3 cyc8* mutant (Fig.6.10).

Overall, the results revealed that the *swi3* and *swi3 cyc8* mutants showed distinct differences in the numbers of genes subject to negative regulation. Furthermore, these data confirm that the dominant impact of *SWI3* upon gene transcription is repressive, and not positive, which is opposite to what would be predicted from the fact that Swi3p is a subunit of the Swi-Snf coactivator complex.

Figure 6. 10: Venn diagram to identify the genes shared and upregulated solely in the *swi3* and *swi3 cyc8* mutant strains.

6.2.4.5 Comparing the transcription levels of *swi3* and *swi3 cyc8* up-regulated genes

Next, I compared the average levels of transcription of the genes upregulated in the *swi3* and *swi3 cyc8* mutant strains (Fig. 6.11). The results showed that there was no significant difference in the average levels of upregulation of the 254 overlapping genes.

I then looked at the genes significantly upregulated only in the *swi3* mutant strain (330 genes) compared to the genes significantly upregulated only in the *swi3 cyc8* mutant strain (184 genes). Here, the average level of transcription upregulation in the *swi3 cyc8* mutant was significantly higher than that in the *swi3* single mutan

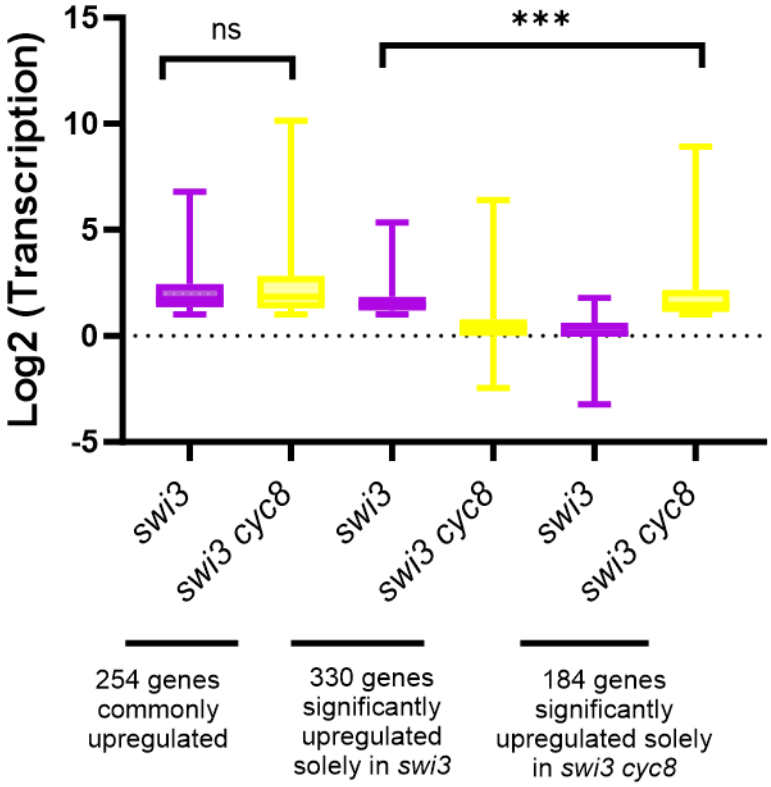

Figure 6. 11: The transcription level in the *swi3* and *swi3 cyc8* mutants. Box plot to show the fold changes of the upregulated genes in the *swi3* and *swi3 cyc8* mutants.

Importantly, of the 330 genes upregulated solely in the *swi3* mutant, 63 of these genes were downregulated in the *swi3 cyc8* mutant strain (Fig. 6.12A). This result again suggests that the de-repression in the *swi3* mutant is *CYC8* dependent and raises the possibility of a role for Cyc8p acting to promote gene transcription whilst at very low levels in the *swi3* mutant. Examples of these genes included *SPG4*, which is involved in resistance to high temperatures during the stationary phase [205], and *EMP46* which is an endoplasmic reticulum associated protein (Fig. 6.12B) [206].

Similarly, when I looked at the 184 genes solely upregulated in the *swi3 cyc8* mutant, there were 37 genes downregulated, or off, in the *swi3* mutant (Fig. 6.12C). This suggests that *CYC8* is having a negative role upon transcription of these 37 genes in the *swi3* mutant which, if this effect is at the protein level, suggests Cyc8p is present at low (undetectable) levels in the *swi3* mutant where it can still contribute to gene repression at these genes. Examples of these genes included *FIT1,* which is a cell wall protein [207], and *PDC5,* which encodes a key enzyme required for ethanol fermentation [208] (Fig. 6.12D).

In summary, the results indicate that *CYC8* can influence some gene transcription in the *swi3* mutant despite Cyc8p levels being undetectable by western blotting in the *swi3* mutant.

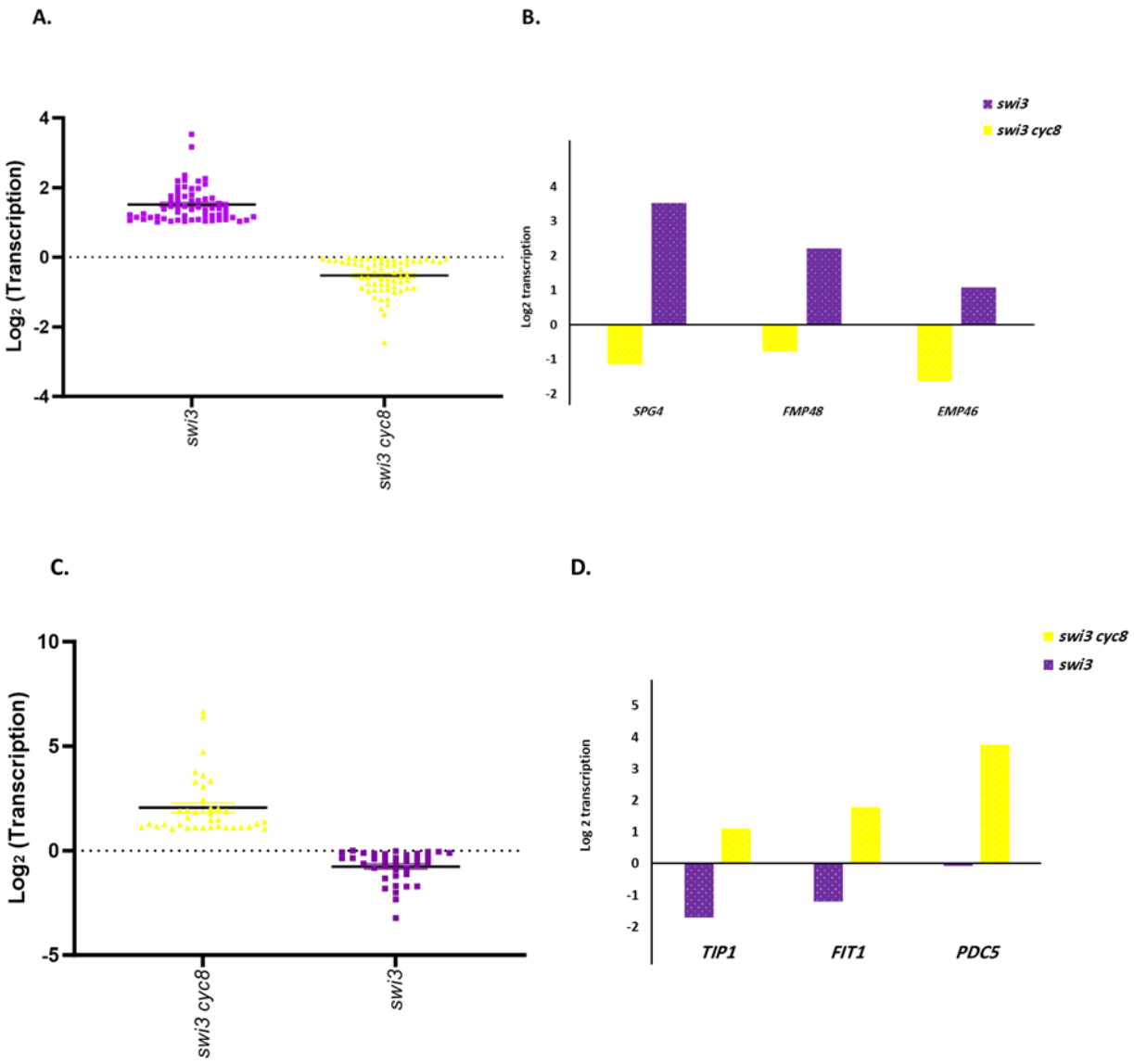

Figure 6. 12: (A) Scatter plot showing the Log2 fold changes for 63 genes from 330 genes solely in a *swi3* single mutant **(B)** An example for genes there was downregulated fold change from the 330 genes solely regulated by *swi3*. **(C)** Scatter plot showing the Log2 fold changes for 37 genes from 148 genes solely in a *swi3 cyc8*. **(D)** An example of genes there were downregulated from the 148 genes solely regulated by *swi3 cyc8*.

6.2.4.6 Gene ontology analysis of genes upregulated in the *swi3* and *swi3 cyc8* mutants

Next, gene ontology was used to analyse the 254 genes commonly upregulated in the *swi3* and *swi3 cyc8* mutant strains. A high number of these genes were shown to be involved in oxidoreductase activity, such as *BNA2,* which is involved in the *de novo* biosynthesis of NAD^+ [209] (Fig. 6.13).

When I looked at the 330 genes solely upregulated in the *swi3* mutant strain, there was enrichment of genes involved in the respirasome and carbohydrate metabolism such as *CYC1*, which encodes cytochrome c [210], and *SUC2* which encodes invertase, respectively [211](Fig. 6.13).

Similarly, when I looked at the 184 genes solely upregulated in the *swi3 cyc8* mutant, I found genes involved in the fungal cell wall such as *FLO10* and *FLO1* which both encode flocculin proteins involved in cell-cell adhesion [212], [213](Fig. 6.13).

Together, the results again reflect differences in the types of genes whose levels are upregulated in the two mutants, and show that most genes are upregulated in the absence of *SWI3*.

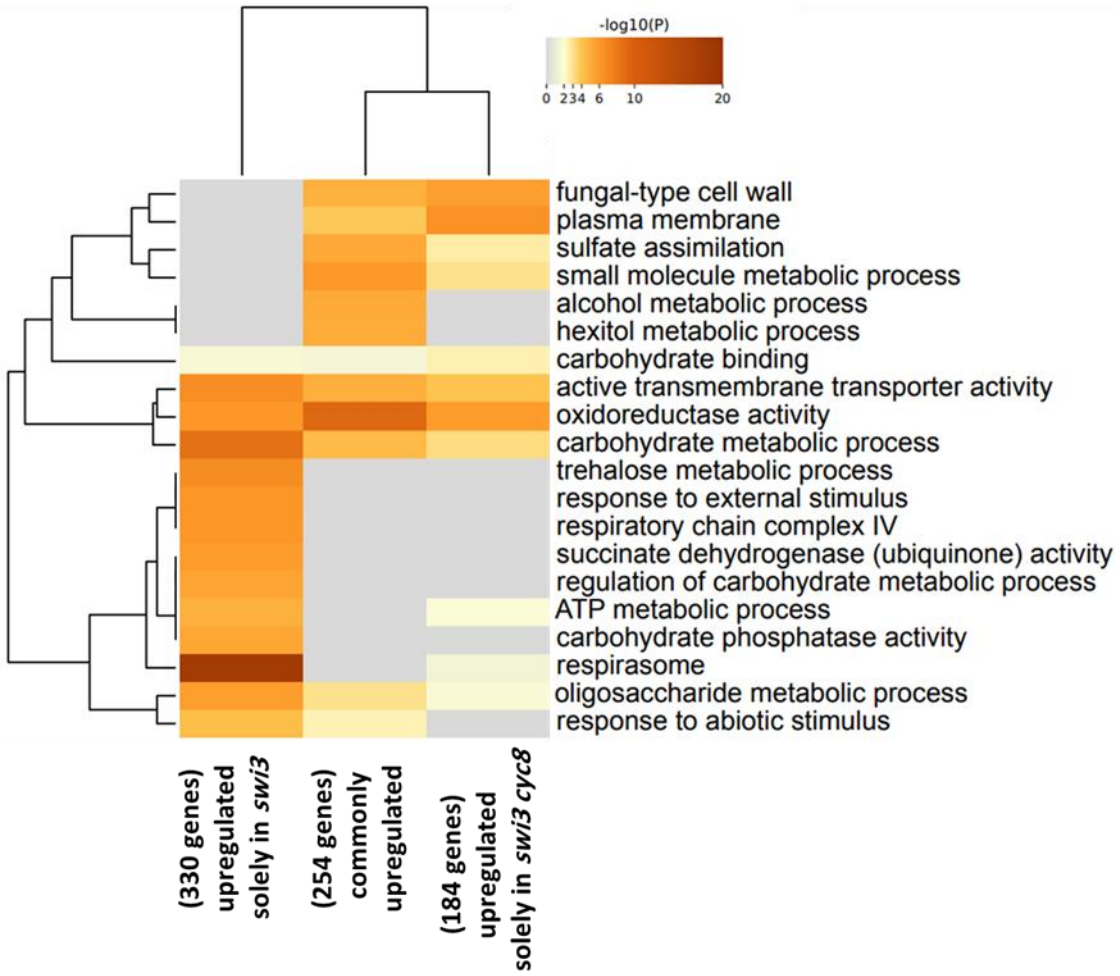

Figure 6. 13: Gene ontology analysis of upregulated genes in the *swi3*, *swi3 cyc8* mutant strain. The heatmap in the first column represents the Go profile for the 330 genes solely upregulated in *swi3.* The second column represents the Go profile for the 254 genes commonly upregulated in the *swi3* and *swi3 cyc8* mutants. The last column represents the Go profile for 184 genes solely upregulated only in the *swi3 cyc8* mutant.

6.3 Comparing the transcriptomes of *swi3*, *cyc8* and *swi3 cyc8* mutants to identify the *SWI3*-dependent gene regulation profile

6.3.1 Comparing the genes downregulated in *swi3*, *cyc8 and swi3 cyc8* mutants

My previous analysis showed differences in the transcriptomes of a *swi3* single mutant and a *swi3 cyc8* double mutant strain. I next wanted to identify those genes that are regulated solely by *SWI3*. I therefore compared the changes in gene transcription in a *cyc8* single mutant strain to the *swi3* and *swi3 cyc8* mutant strains. I began by looking at the genes significantly downregulated in all three mutant strains compared to wt.

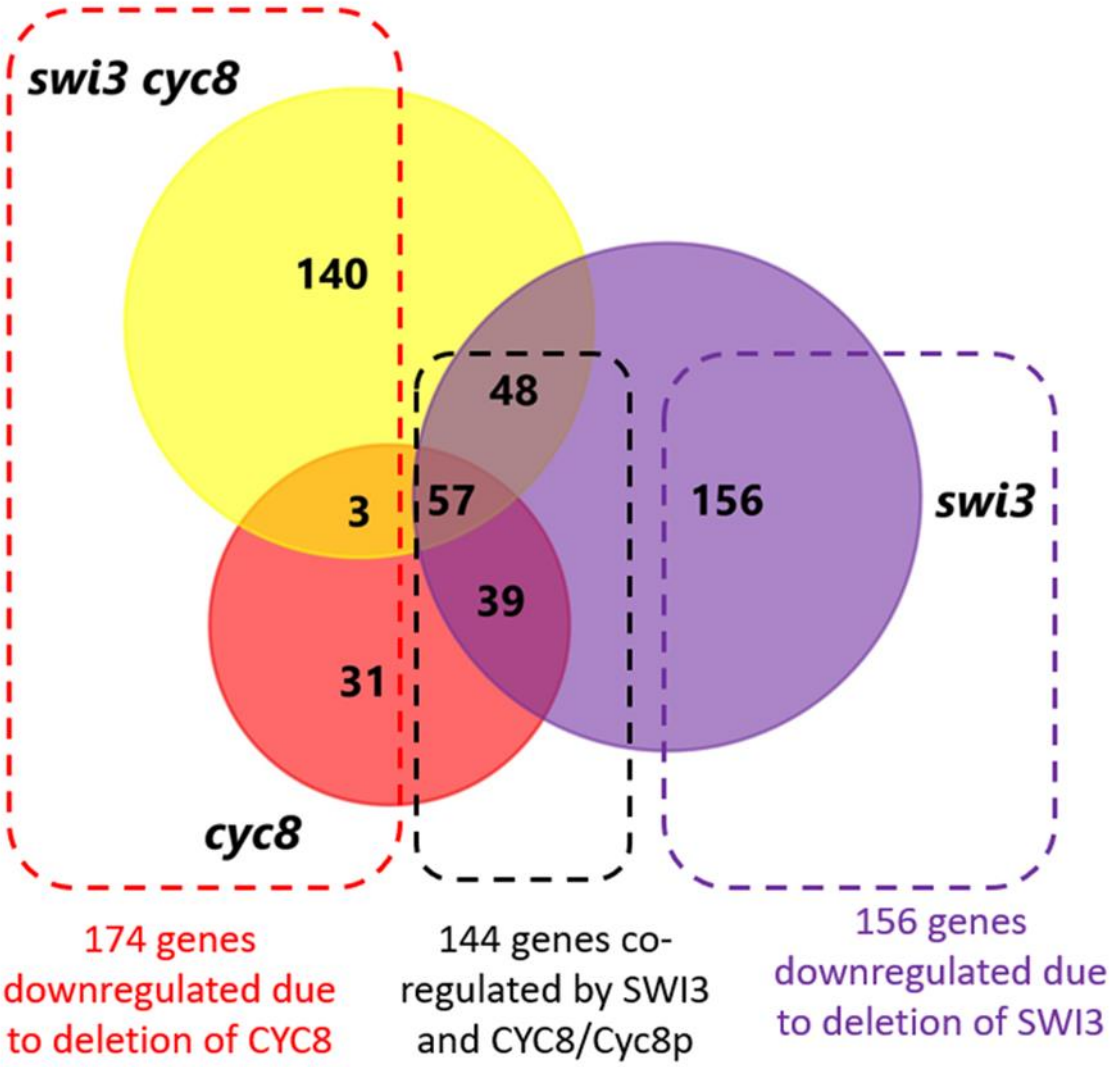

Figure 6. 14: Venn diagram to identify the number of genes downregulated due to deletion of *SWI3.* The number of genes downregulated due to deletion of *SWI3* (156 genes), *CYC8* (174 genes), and both *SWI3* and *CYC8* (144 genes).

A Venn diagram was used to compare the total number of genes downregulated in *swi3*, *cyc8*, and *swi3 cyc8* mutants (Fig. 6.14). The result showed a 57 gene overlap between all mutants. However, a group of 156 genes were downregulated solely in the *SWI3* mutant strain; therefore, this set of genes are regulated solely by *SWI3*. The loss of Cyc8p or *CYC8* does not influence the regulation of this set of genes. Similarly, this

analysis identified 174 genes that were downregulated due to the deletion of *CYC8*. These genes included a group of 31 genes that were downregulated solely in the *cyc8* mutant strain; therefore this set of genes are regulated solely by *CYC8*. There were also 3 genes that were downregulated in both the *cyc8* and *swi3 cyc8* mutant strains, and a group of 140 genes which were downregulated solely in the *swi3 cyc8* double mutant strain.

Interestingly, this analysis identified a group of 144 genes that were downregulated due to co-regulation of *SWI3* and *CYC8* (or Cyc8p).

6.3.2 Comparing the transcription levels of *cyc8*, *swi3* and *swi3 cyc8* downregulated genes

I next looked to see if the downregulated genes in the mutants were regulated to different extents. However, by comparing the average level of transcription of the total number of genes downregulated in each mutant, the data showed there was no significant difference in the average level of gene downregulation in each strain. (Fig. 6.15).

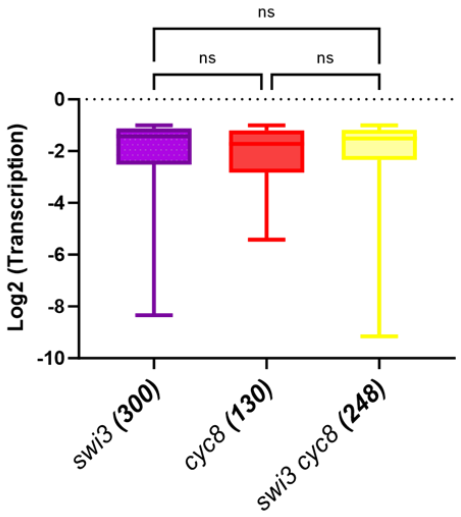

Figure 6. 15: Comparing the transcription level of the total number of genes downregulated in the *swi3*, *cyc8*, and *swi3 cyc8*.

6.3.3 Gene ontology analysis of genes downregulated in the *cyc8, swi3* and *swi3 cyc8* mutant strains

To identify the function of the genes downregulated in the *swi3*, *cyc8*, and *swi3 cyc8* strains*,* gene ontology analysis of the total number of genes downregulated in each strain was performed. (Fig. 6.16). The result revealed that all of the mutants had a strong enrichment of genes involved in DNA integration. Examples of these genes included *ZRT1,* which encodes a zinc transporter [214] and *FAA3* which encodes a long chain fatty acyl-CoA synthetase [215] In the *swi3* deletion mutant, analysis revealed an enrichment of genes involved in rRNA processing, such as rRNA methyltransferases, *BMT5,* and *BMT6* [216]. In the *cyc8* deletion mutant, there was an enrichment of genes involved in the vacuolar transporter chaperone complex such as *VTC1* [217]. Genes downregulated in the *swi3 cyc8* mutant included a large number of fungal cell well type genes such as *AGA1* and *MFA2*, which were as described previously.

Overall, the Go profiles of genes downregulated in each mutant were different, with the *swi3* mutant target gene showing the widest range of functions.

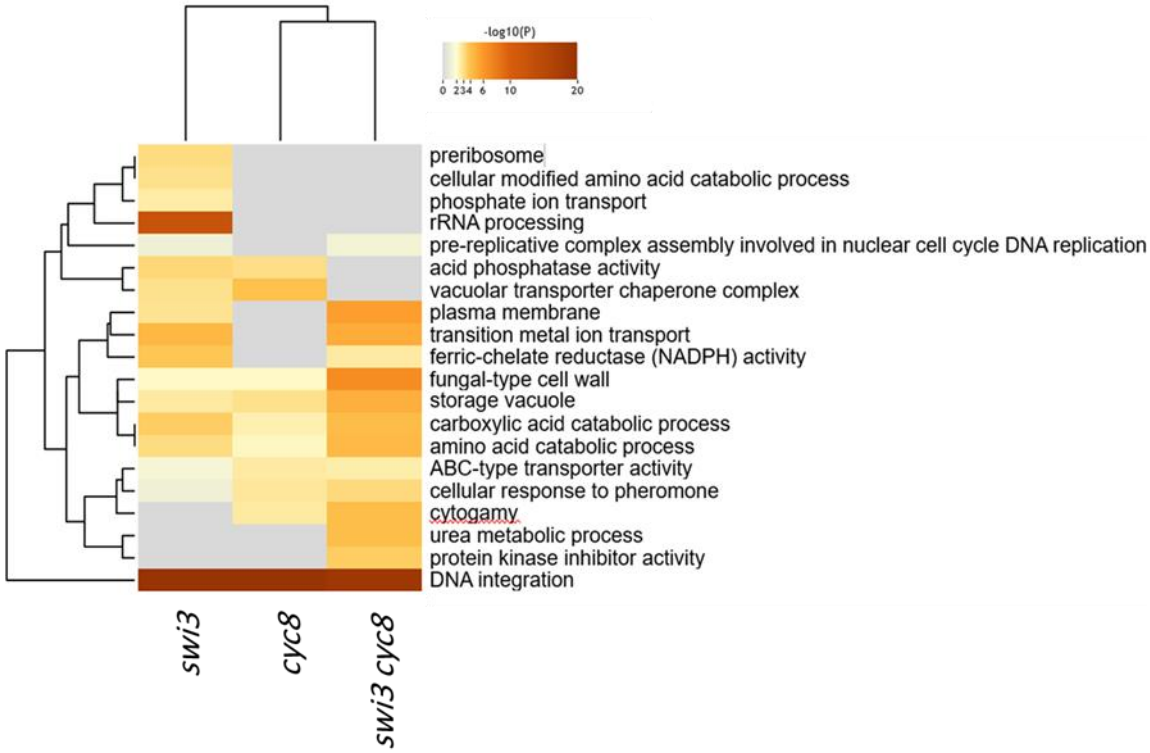

Figure 6. 16: Gene ontology analysis of all genes significantly downregulated in the *swi3*, *cyc8*, and *swi3cyc8* compared to wt. Heat map generated using metascape website. Each Colum represents a mutant strain and each row represents a significant GO term the colour scale indicates the statistical significance of the enrichment of genes assigned to each GO term, darker orange colours indicate more significant. The GO terms are separated into three categories; Molecular Function, Biological Process and Cellular components.

6.3.4 Comparing the genes upregulated in *swi3, cyc8 and swi3 cyc8* mutants

Next, I compared the genes that were significantly upregulated in all three mutant strains compared to wt. Again, the aim was to separate out and identify those genes subject solely to negative regulation by *SWI3* and *CYC8*.

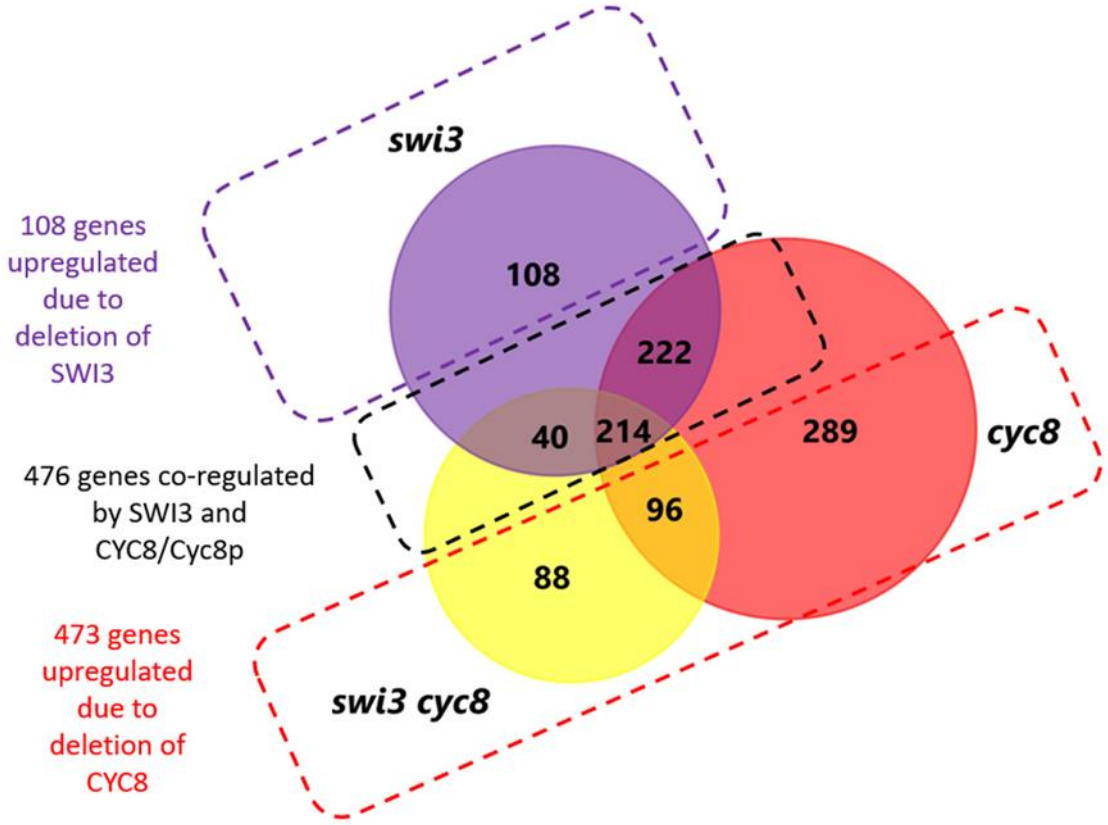

Figure 6. 17: Venn diagram to identify the number of genes upregulated due to deletion of *CYC8 and SWI3*. Analysis to show the number of genes upregulated due to deletion of *SWI3* and *CYC8* and the number of genes co-regulated by *SWI3* and *CYC8.*

A Venn diagram representing the total number of genes upregulated in *swi3*, *cyc8*, and *swi3 cyc8* mutants revealed a large overlap in the number of genes commonly upregulated in each mutant; with 476 genes (Fig. 6.17). A group of 108 genes were upregulated solely in the *swi3* mutant strain, suggesting *SWI3* solely negatively regulates these genes. The data also showed that 289 genes were upregulated solely in the *cyc8* mutant strain, which suggests these genes are subject to unique negative regulation by *CYC8*. 96 genes were upregulated in both the *cyc8* and *swi3 cyc8* mutant strains, and a group of 88 genes were only upregulated in the *swi3 cyc8* mutant strain. The 96 genes upregulated in the *cyc8* and *swi3 cyc8* mutants suggest that Cyc8p is present in the *swi3 cyc8* mutant and is exerting a regulatory role at these genes.

Importantly, the analysis of this data revealed 476 genes co-regulated in the *SWI3* and *CYC8*, which suggests that *SWI3* and *CYC8* can function together to negatively influence target gene transcription.

6.3.5 Comparing the transcription levels of *cyc8*, *swi3* and *swi3 cyc8* up-regulated genes

Comparison of the average level of transcription of the total number of genes upregulated in each mutant showed that there was a significant difference between the mutants (Fig. 6.18). The highest extent of upregulation was in the *cyc8* mutant, followed by the *swi3 cyc8* double mutant, with the least upregulation evident in the *swi3* deletion mutant compared to wt.

In summary, the data has revealed differences in the numbers and levels of target gene de-repression that occurs in the different mutants. This confirms that there were significant differences between the *swi3* single mutant and the *swi3 cyc8* double mutants, and suggests that the *swi3* and *cyc8* single mutants differ also.

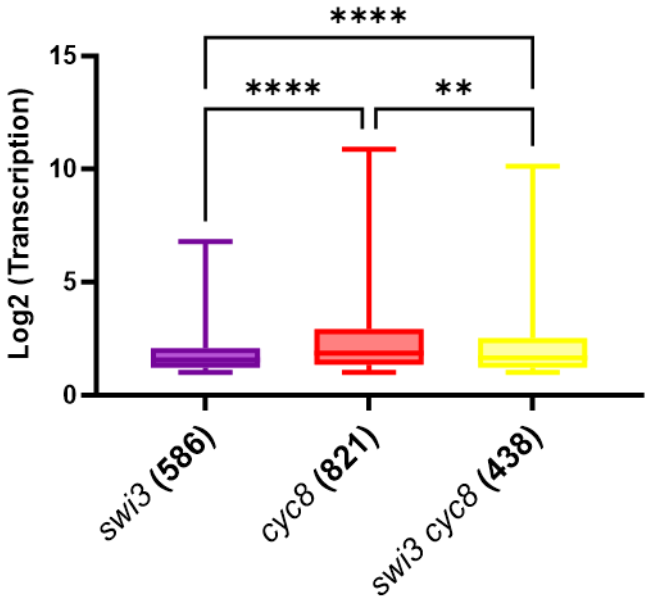

Figure 6. 18: Comparing the average transcription level of the total number of genes upregulated in the *swi3*, *cyc8*, and *swi3 cyc8* strains relative to wt.

6.3.6 Gene ontology analysis of genes upregulated in the *cyc8, swi3*, and *swi3 cyc8* mutants

Gene ontology analysis of the total number of genes upregulated in the 3 mutants was conducted (Fig. 6.19). The analysis showed differences in the gene ontology terms assigned to the genes upregulated in all three mutants.

Firstly, I looked at the genes upregulated in the *swi3* single mutant. The result showed that these genes have a strong role in oxidoreductase activity and included the *COX4*, *COX8,* and *COX9* genes which encode mitochondrial inner membrane electron transport chain 1 [218].

Following the GO profile analysis in the *swi3 cyc8* double mutant, it was seen that many genes play a role in sulfate assimilation. Examples of these genes include *MET1*, *MET3*, *MET5*, and *MET10* [219].

When, I looked at the GO profile in the *cyc8* single mutant, consistent with published studies, genes were enriched that played a role in the cell wall and flocculation, such as the *FLO1*, *FLO5*, *FLO9*, *FLO10*, and *FLO11* genes [220] (Fig. 6.19).

Overall, the results revealed variation in the Go profiles of each mutant, with the biggest difference in target gene functions being found in the *cyc8* single mutant.

In summary, although the *swi3* mutant shows the greatest levels of gene upregulation out of all the SWI-SNF subunit mutants, and the fact that Cyc8p levels cannot be detected in the *swi3* mutant, the transcriptome of a *swi3* mutant is significantly different from that of a *swi3 cyc8* double and a *cyc8* single mutant. Thus, the transcriptome of a *swi3* mutant is unique amongst the Swi-Snf subunit mutants and has little in common with a Tup1-Cyc8 mutant, suggesting a direct role for Swi3p in repressing gene transcription at a significant number of genes.

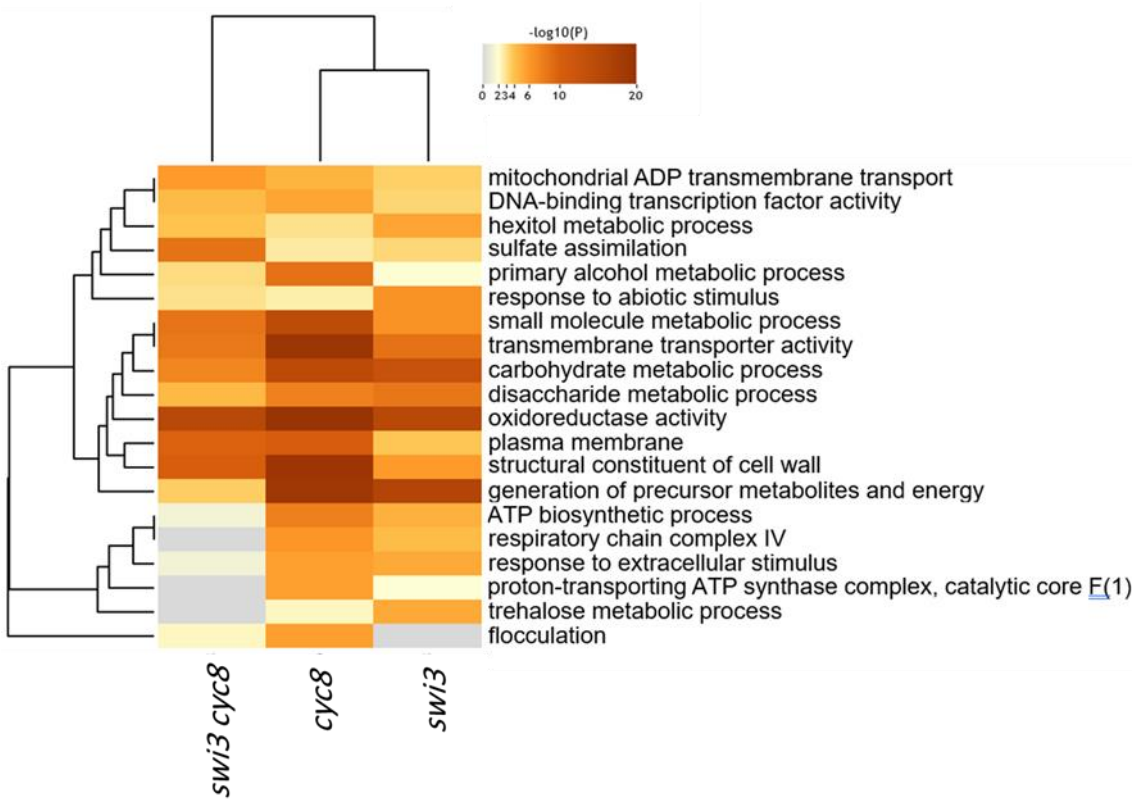

Figure 6. 19: Gene ontology analysis of all genes significantly upregulated in *swi3*, *cyc8*, and *swi3cyc8* compared to wt.

6.4 Investigating a direct interaction between Swi3p and Cyc8p

The previously described Western blot result showed that Cyc8p was not detectable in a *swi3* mutant (Fig. 6.2). However, *CYC8* mRNA levels were the same in the *swi3* mutant as they were in wt (Fig. 6.4A). This suggests that the loss of Cyc8p in the *swi3* mutant is occurring at the protein level and is not a consequence of a failure to transcribe *CYC8* in the absence of Swi3p.

I therefore wanted to test the hypothesis that there might be a direct interaction between Cyc8p and Swi3p which could be essential to maintain Cyc8p stability. The prediction would be that in the absence of this interaction, such as in a *swi3* deletion mutant, Cyc8p would be susceptible to degradation, and would be depleted from the cell.

I therefore performed co-immunoprecipitation to test for a specific protein-protein interaction between Swi3p and Cyc8p in wt cells containing tagged Swi3p and Cyc8p (Swi3-Myc and Cyc8-HA, respectively).

6.4.1 Looking for Swi3p following initial Cyc8p immunoprecipitation

The first co-immunoprecipitation experiment was to pull down Cyc8-HA and probe for the presence of Swi3-Myc in the resultant immunoprecipitated eluate. A Swi3-Myc strain with untagged Cyc8p was used as a negative control (Fig.6.20).

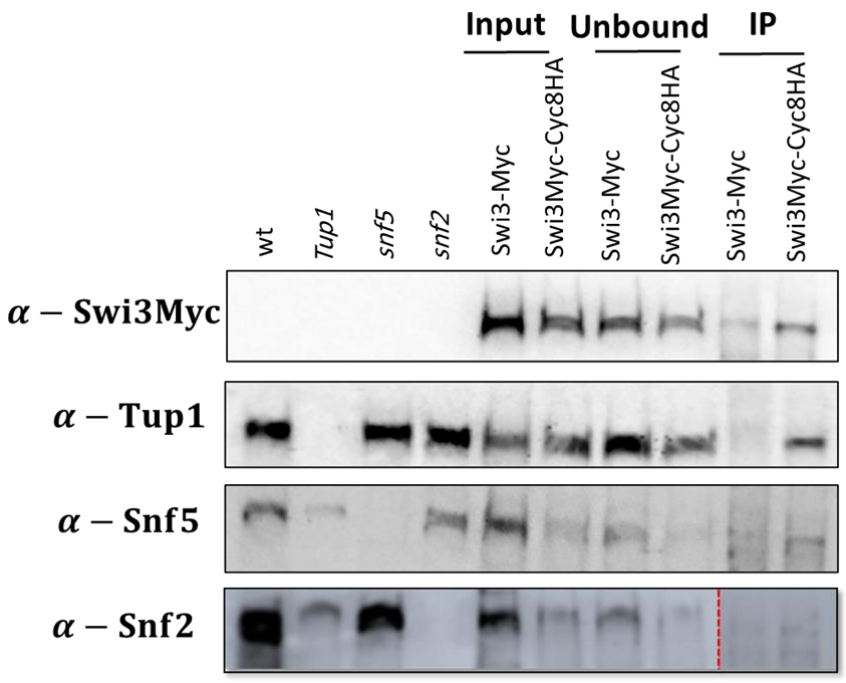

Figure 6. 20: Western Blot analysis for Swi3-myc following the Cyc8-HA pull-down. The yeast strains indicated were grown to log phase. A Cyc8-HA pull down was performed and the eluate analysed for associated proteins; the proteins examined in the eluate were Swi3p (via a Myc-tagged Swi3p construct), Tup1p, Snf5p, and Snf2p. The Swi3-Myc tagged strain (with no Cyc8-HA) acted as a negative control for the Co-immunoprecipitation. Antibodies used were specific to the myc tag, Tup1p, Snf5p, and Snf2p. Protein from wt (lane 1) *tup1* (lane 2), *snf5* (lane 3), and *snf2* strains (lane 4) were included as positive or negative controls for the relevant antibody. The anti-Snf2p result (bottom blot image) was cut (dashed line) and the (IP) lanes were exposed for longer to account for a weaker signal.

As can be seen, following the initial Cyc8-HA pull down, Swi3-Myc could be detected in the subsequent eluate (IP) at significantly higher levels than that detected in the IP using the untagged Cyc8p control strain. This suggests that there is a direct interaction between Swi3p and Cyc8p.

Since Tup1p and Cyc8p form a complex, Tup1p should also be detected following a co-immunoprecipitation experiment using Cyc8-HA pull down. I therefore probed the eluate for Tup1p and found that Tup1p was indeed detected. Importantly, Tup1p was not detected using the control Swi3-Myc strain which did not contain a Cyc8-HA tag.

I then looked for the presence of other subunits of the Swi-Snf complex, Snf5p and Snf2p, in the eluate following the initial Cyc8-HA pull down. In both cases, the proteins were detected in the immunoprecipitate using the Cyc8-HA/ Swi3-Myc strain but were absent in the immunoprecipitate using the control Swi3-Myc strain which did not contain a Cyc8-HA tag (See rows 4 & 5, lane 9, Fig. 6.20).

Together, this suggests that Swi3p does directly interact with Cyc8p, and that this interaction is mediated by these proteins most likely residing within their respective Swi-Snf and Tup1-Cyc8 complexes.

6.4.2 Looking for Cyc8p following initial Swi3-Myc immunoprecipitation

I next performed the reciprocal experiment whereby I used Swi3-Myc as the bait and probed for Cyc8-HA in the eluate. A Cyc8-HA strain with untagged Swi3p was used as a negative control in this experiment (Fig. 6.21). The result clearly showed that Cyc8-HA was detected in the eluate following a Swi3-Myc pull down. Importantly, Cyc8-HA, was not detected in the eluate following immunoprecipitation using the control Cyc8-HA strain in which Swi3p was untagged (See rows 1 & 2, lane 8, Fig. 6.21). This supports the previous result suggesting that Cyc8p and Swi3p directly interact.

As a control, I also probed the eluate following the Swi3-Myc pull down for the Snf5p subunit of the Swi-Snf complex. As expected, the presence of Snf5p was detected in the eluate following the Swi3-Myc pull down.

Together, the co-immunoprecipitation results indicate a direct interaction between Swi3p and Cyc8p when these proteins are potentially residing within the Swi-Snf and Tup1-Cyc8 complexes.

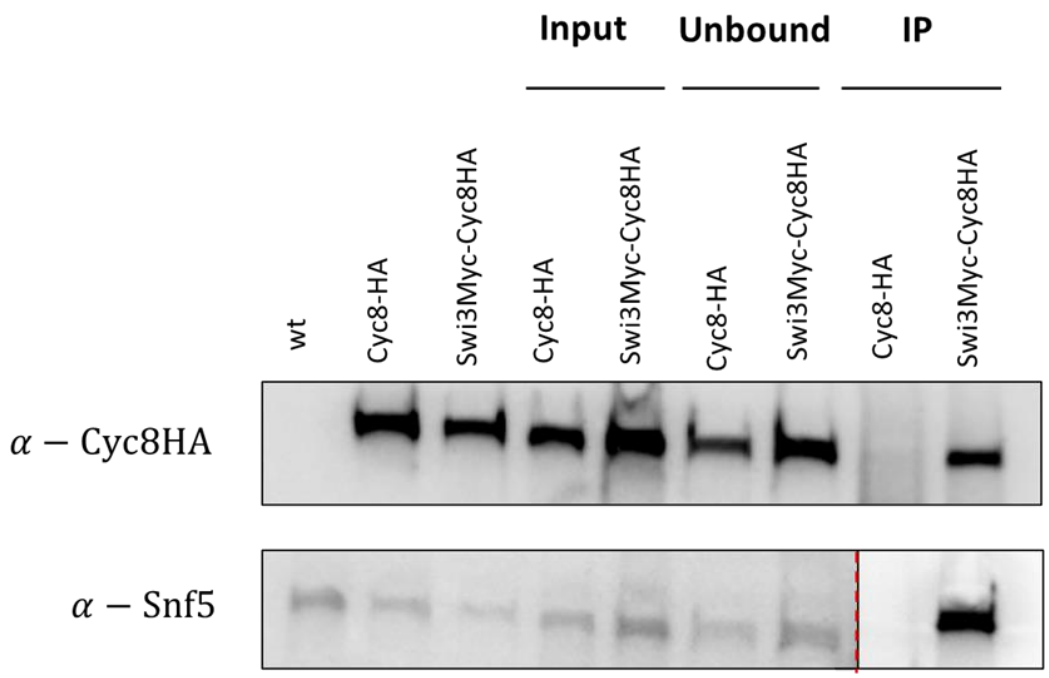

Figure 6. 21: Western Blot analysis for Cyc8p following the Swi3-Myc pull-down. The yeast strains indicated were grown to log phase. For the Co-Ip experiment, the Cyc8-HA tagged strain acted as a negative control for the Co-immunoprecipitation. The antibodies used were specific to the HA tag and Snf5p. The anti-Snf5p result (bottom blot image) was cut and the (IP) lanes were exposed for longer to account for a weak signal.

6.5 Investigating global Swi3p and Cyc8p occupancy

The Co-IP experiments strongly suggest that Cyc8p and Swi3p can directly interact with each other. However, the data does not indicate whether this interaction is taking place on or off chromatin. To get insight into this question, I analysed published data sets of Swi3p and Cyc8p occupancy following ChIP-exo which can map proteins across global chromatin at high resolution [131]. The prediction would be that if the proteins did interact together on chromatin, there should be significant overlap of the occupancy of the Swi3p and Cyc8p proteins. Furthermore, the potential co-occupancy of Swi3p and Cyc8p would be expected to be enriched at those genes I had shown were regulated by both Swi3p and Cyc8p.

The Swi3p and Cyc8p occupancy data was obtained from Rossi *et al*. data, in which they allocated a binding site for each protein with the nearest gene. Their data revealed 844 genes associated with Swi3p and 504 genes associated with Cyc8p (Fig. 6.22A). Importantly, a Venn diagram showed that 315 genes of these genes were assigned as being occupied by both Swi3p and Cyc8p (Fig. 6.22B).

I next compared the 315 genes commonly associated with both Swi3p and Cyc8p occupancy with the 354 genes that I previously showed were up and down-regulated in both the *swi3* and *swi3 cyc8* mutants (Fig. 6.22C). The results revealed an overlap of 26 genes that were occupied by both Swi3p and Cyc8p and whose transcription was altered in the absence of both *SWI3* and *CYC8* (Fig. 6.22C, Table 6.1). Together, these data suggest that these genes are occupied by both Swi3p and Cyc8p and that both factors directly influence the transcription of these genes.

An example of one of these genes at which both Swi3p and Cyc8p can be detected by ChIP exo and which are subject to regulation by both *SWI3* and *CYC8* is the *PDR5* gene (Fig. 6.23).

Figure 6. 22: (A) Comparing the global occupancy sites for Swi3p and Cyc8p [131] 844 sites of Swi3p and 504 sites of Cyc8p. **(B)** Venn diagram to show the overlapping sites of occupancy for Swi3p and Cyc8p. **(C)** Comparing the genes showing Swi3p and Cyc8p co-occupancy (315 genes) with the genes identified as being co-regulated by *SWI3* and *CYC8* (354 genes). Venn diagram to show the 315 co-occupied genes vs genes up and down-regulated in both mutants.

Genes	Description of the protein product
AAC1	ADP/ATP Carrier
ACO1	ACOnitase
ARO9	Aromatic aminotransferase
CMC4	Protein that localizes to the mitochondrial intermembrane space
CWP1	Cell Wall Protein
DIP5	DIcarboxylic amino acid Permease
ENO2	a phosphopyruvate hydratase
ERG25	Methylsterol monoxygenase
GPD1	Glycerol-3-Phosphate Dehydrogenase
HMS2	Protein with similarity to heat shock transcription factors
HSP12	Heat Shock Protein
HXT15	Putative transmembrane polyol transporter
PDR5	Plasma membrane ATP-binding cassette (ABC) transporter Pleiotropic Drug Resistance
PHO84	High-affinity inorganic phosphate (Pi) transporter; also, low-affinity manganese transporter
PRB1	Vacuolar proteinase B yscB with H3 N-terminal endopeptidase activity
PRM5	Pheromone-regulated protein
PTR2	Integral membrane peptide transporter
ROX1	Heme-dependent repressor of hypoxic genes
SOK2	Nuclear protein that negatively regulates pseudohyphal differentiation
TPO1	Polyamine transporter
YFL015C	Uncharacterized protein
YKR041W	Uncharacterized protein
YMR007W	Uncharacterized protein
YNL146W	Uncharacterized protein
YOL085C	Uncharacterized protein
YPR064W	Uncharacterized protein

Table 6. 1: The list of the 26 genes showing shared occupancy with Swi3p and Cyc8p and whose transcription is altered (down or up-regulated) in the *swi3* single and *swi3 cyc8* double mutants.

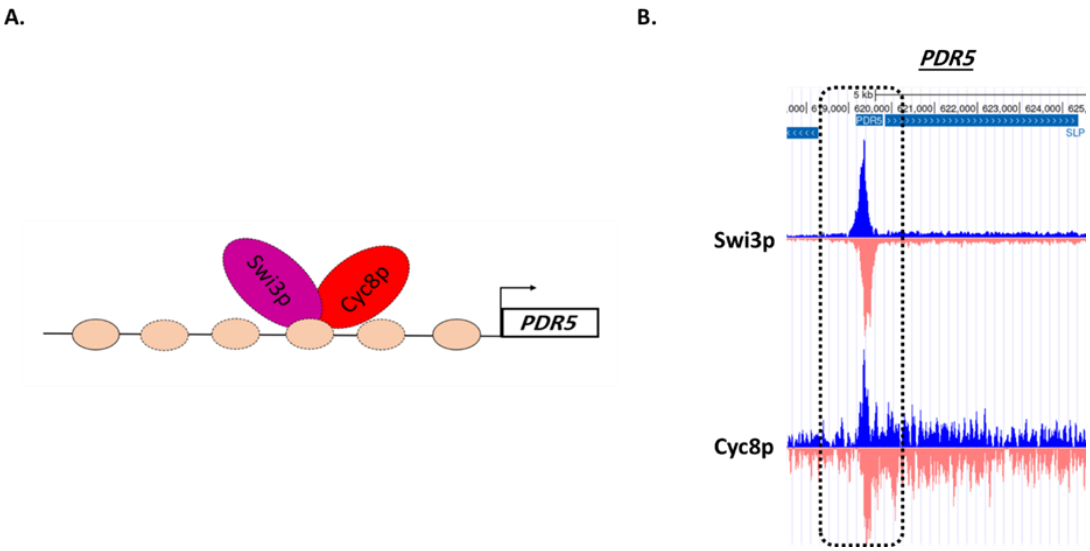

Figure 6. 23: (A) Schematic to show Cyc8p and Swi3p found at the same gene promoter regions. **(B)** J-browse screenshot of the *PDR5* (*YOR153W*) gene as an example of a Swi3p and Cyc8p co-occupied and *SWI3* and *CYC8* co-regulated gene. The blue peaks indicate the location of the *PDR5* gene.

Discussion

The overall aim of this chapter was to investigate the potential interplay between the Swi3p subunit of the Swi-Snf co-activator complex and the Cyc8p subunit of the Tup1-Cyc8 co-repressor complex. The RNA-Seq data in Chapter 4 demonstrated that the Swi3p subunit mutant (*swi3*) showed the most unique changes in its transcriptome compared to the other Swi-Snf subunit mutants. Furthermore, a large number of genes in the *swi3* mutant were upregulated which suggested that the Swi3p subunit of Swi-Snf was unique in that it played a significant role in the negative regulation of gene transcription (i.e. in mediating gene repression).

Interestingly, preliminary data from earlier studies in the lab showed that Cyc8p was undetectable following Western blot analysis of protein lysates from a *swi3* mutant [130](Fig. 6.2). Together, this suggested that a *swi3* mutant, in which Cyc8p cannot be detected, might more resemble a *swi3 cyc8* double mutant, which would explain why *SWI3* (and Swi3p) apparently plays such a large role in regulating gene repression.

When I compared the transcriptome of the *swi3* mutant with the transcriptome of a *swi3 cyc8* double mutant I found that there were significant differences in the number of genes down and upregulated in the *swi3* and *swi3 cyc8* mutants. Most importantly the predicated large overlap in genes up and downregulated in the *swi3* and *swi3 cyc8* mutants was not apparent. Thus, at least at the level of transcription, the *swi3* mutant was not that similar to the *swi3 cyc8* double mutant. Further comparison of the transcriptomes of the *swi3* mutant with the *cyc8* mutant also showed that these mutants were dissimilar (Fig. 6.7). These data therefore confirm that the Swi3p subunit mutant does play a large role in repressing gene transcription, however the repressive role of Swi3p is not being mediated via Cyc8p.

Interestingly, when I compared the average transcription levels of the sets of genes that were upregulated in both mutants, I found that there was a statistically significant

difference between the genes solely upregulated in the *swi3* and *swi3 cyc8* mutant strains (Fig. 6.18). Thus, the loss of both Swi3p and Cyc8p had a greater impact upon repression of these genes than loss of either protein alone, suggesting a level of cooperativity between these proteins can contribute to target gene repression.

Most strikingly, further analysis revealed evidence of a role for *CYC8* in both positively and negatively regulating some *SWI3*-regulated genes. For example, the *FIT1* gene was downregulated in the *swi3* mutant, but was upregulated in the *swi3 cyc8* double mutant. One interpretation of these data is that even though Cyc8p levels in the *swi3* mutant were undetectable, these data suggest that there might be low levels of Cyc8p in the *swi3* mutant cells that are exerting a regulatory role; in this case, *CYC8* is exerting a repressive role at *FIT1* in the *swi3* mutant (Fig.6. 12).

One way to test this hypothesis would be to perform ChIP analysis of Cyc8p in the *swi3* mutant at these apparently co-regulated genes. Even though the levels of Cyc8p in the *swi3* mutant cells are low and are undetectable by western blotting, occupancy of Cyc8p at the potential target genes might be enriched and relatively high. Coupled with the amplification of immunoprecipitated signal employed whilst performing gene-specific ChIP, this technique might allow detection of Cyc8p at these potential target genes, should it be there. Conversely, the formal possibility remains that the apparent influence of Cyc8p upon transcription in the *swi3* mutant could be an indirect effect from a complete loss of Cyc8p in these cells.

In summary, the comparison of the transcriptomes of the *swi3*, *cyc8,* and *swi3 cyc8* mutants revealed that Swi3p is responsible for the repression of a large number of genes and that this regulatory role is not functioning via the significantly reduced levels of Cyc8p in the *swi3* mutant. Indeed, the analysis of the transcriptomes suggests that *CYC8* can influence some gene transcription in the *swi3* mutant, suggesting a low level of Cyc8p might still be present in this mutant which is directly mediating this regulatory role.

I confirmed preliminary data from our lab that Cyc8p levels were undetectable by Western blotting in a *swi3* mutant[130]. The simplest explanation for this result would be that Swi3p, in the context of the Swi-Snf complex, is required for *CYC8* transcription. However, our RNA-seq data revealed that this was not the case; *CYC8* mRNA levels in the *swi3* mutant were the same as in wt (Fig. 64A). This suggests that the loss, or at least significant depletion, of Cyc8p in the *swi3* mutant occurs post-transcriptionally. I therefore hypothesized that an interaction between Swi3p and Cyc8p might be required for Cyc8p stability, such that in the absence of Swi3p, Cyc8p is degraded and is lost from the cell.

I used co-immunoprecipitation to investigate if there was evidence for a possible direct interaction between Swi3p and Cyc8p. The results convincingly showed that a Swi3p and Cyc8p interaction could be detected using co-immunoprecipitation (Fig. 6. 20,21). Furthermore, the data suggested that this interaction might be mediated by Swi3p and Cyc8p whilst residing within the Swi-Snf and Tup1-Cyc8 complexes, respectively.

Although the co-IP experiments convincingly showed a direction interaction between Cyc8p and Swi3p, I did not have time to perform experiments to prove this interaction was required to maintain Cyc8p stability. Had time permitted, it would have been interesting to perform experiments to directly show that Cyc8p is degraded following loss of Swi3p. At least in the first instance, this could have been achieved by using a degron approach to conditionally degrade Swi3p, and then monitor Cyc8p levels over time following Swi3p loss [221].

The evidence of a direct interaction between Swi3p and Cyc8p shown here has not been reported before. However, Swi-Snf and Tup1-Cyc8 are known to co-regulate certain genes such as *SUC2* and *FLO1*[118]. At these genes, the two complexes have been shown to function antagonistically. Tup1-Cyc8 was shown to be required for *FLO1* and *SUC2* repression, whereas Swi-Snf was required for gene activation. The evidence

also suggests that the activity of the complexes functions at the level of chromatin whereby Tup1-Cyc8 establishes an array of strongly positioned, deacteylated nucleosomes over the upstream gene regions which is non-permissive for gene activation [222]. Conversely, Swi-Snf was shown to destabilise this nucleosomal array to enable gene transcription to occur.

The accepted model for the activity of Tup1-Cyc8 and Swi-Snf suggest that they function in a mutually exclusive manner whereby the presence of Tup1-Cyc8, and the associated non-permissive chromatin structure at target genes, blocks the recruitment of Swi-Snf [223]. It is only in the absence of Tup1-Cyc8 that Swi-Snf can be recruited to remodel the promoter chromatin to enable transcription initiation to occur.

The interaction data between the two complexes shown here therefore raises the question as to why the Swi-Snf and Tup1-Cyc8 complexes might be directly interacting. One possible hypothesis is that the current model for the mutual exclusivity between Tup1-Cyc8 and Swi-Snf occupancy and activity is incorrect, and the two complexes can occupy the same target genes, potentially at sites in close proximity, at the same time [131](Fig.6.23). Such co-occupancy could feasibly enable the rapid switching between gene activity and gene repression at co-regulated genes. Evidence of Tup1-Cyc8 persisting at some actively transcribed genes supports this hypothesis [220].

It might be that co-occupancy of these complexes at target genes has been missed due to either a failure to identify all of the genes co-regulated by the two complexes and/or poor detection of the two complexes at target genes due to limitations of the ChIP technique. To start to examine this possibility more decisively, sequential ChIP for the two complexes at known co-regulated genes would need to be performed to directly determine if they can occupy target gene promoters at the same time [129].

Chapter 7

Final Discussion

Discussion

The yeast Swi-Snf complex, the first ATP-dependent remodelling complex discovered, regulates gene expression by modifying chromatin architecture, allowing transcription factors and regulatory proteins to access DNA [194]. While the Snf2p subunit is well-studied, the roles of other Swi-Snf subunits are still not fully understood.

My study aimed to assess Swi-Snf subunit mutants to reveal potential functional differences. Despite extensive efforts, obtaining a *swi1* mutant for analysis proved impossible. This led to speculation that the deletion mutant may be either too debilitated to recover or was nonviable. Literature presents conflicting views on *swi1* mutants' viability, with some suggesting nonviability while others report their use [224]. Based on my strain background, I conclude that a *swi1* mutant is likely nonviable.

Efforts to create a Swi1p anchor-away strain failed, despite the technique's proven utility for gene functional analysis via rapid protein removal from the nucleus upon rapamycin induction [225] Yet, C-terminal tagging may impair Swi1p function, leading to cell death. Thus, obtaining a tagged Swi1p strain was unattainable due to potential lethality. Doubling time measurements for mutants revealed varying growth impacts. *Snf2* and *snf5* mutants exhibited the most prolonged doubling times, underscoring *SNF2* and *SNF5* crucial roles in growth maintenance. These findings highlight specific subunits' significant roles in modulating SWI/SNF complex functionality and yeast cell proliferation.

The *SNF2* gene deletion mutant and the Snf2p catalytic mutant exhibited distinct growth impairments, with differing responses to stressors like HU, caffeine, and NaCl. Unexpectedly, despite both mutants rendering the Swi-Snf complex inactive, the *snf2* deletion mutant displayed more severe defects, suggesting its role in destabilizing the complex [83]. This implies that the structurally intact yet inactive Swi-Snf complex, as seen in the *snf2K798A* catalytic mutant, retains some residual activity independent of ATPase function. Microscopic examination unveiled diverse mutant cell morphology. The *snf2* and *snf5* mutants formed small cell clusters, possibly implicating them in cell

wall remodelling for successful separation. The elongated shapes of the *snf6* mutant hinted at compromised cell wall integrity, supported by their heightened sensitivity to caffeine stress. The enlarged cells of the *taf14* mutant suggested a role in cell size regulation, potentially linked to cell cycle control or protein synthesis upregulation, necessitating further investigation. Despite its pronounced phenotypes, the *taf14* mutant exhibited growth similar to wild-type under standard conditions, indicating its role in temperature stress response and cell size regulation without detriment to routine growth.

When exposed to HU-induced DNA damage, several mutants displayed heightened sensitivity, except *Swp82*, *Snf11*, and *Snf12*, which showed minor sensitivity. This suggests these subunits may not significantly contribute to DNA damage response. The distinct HU sensitivity between the *snf2* deletion and *snf2K798A* mutants challenges the presumed role of Swi-Snf in DNA repair, indicating ATPase activity may not be crucial. These basic experiments highlight the diverse and sometimes unique roles of Swi-Snf subunits in cellular functions like growth regulation, cell size, and DNA damage response, complicating our understanding of their functionality.

Our study on yeast Swi-Snf mutants revealed varied transcriptional regulation changes compared to wild type. Downregulated genes confirm Swi-Snf positive regulation of transcription, while upregulated genes indicate its negative control [226]. Gene regulation in *snf2* and *snf2K798A* mutants aligned, reflecting Snf2p's role in chromatin remodelling (Lin et al., 2020)[20]. The *swi3* mutant showed more upregulated genes, suggesting a stronger negative regulatory function, akin to SWI/SNF's influence in inflammation (Singh et al., 2023) [194]. Heat maps confirmed the *snf2* mutant transcriptomes were comparable, while *swi3* differed markedly, highlighting SWI/SNF subunits distinct gene regulatory roles [226].

Comparative analysis revealed that *snf2* deletion and *snf2K798A* mutants share downregulated genes, aligning with Guo et al. (2022) [227]. Gene ontology highlighted Snf2p's involvement in transporter, catalytic, and DNA-binding activities, suggesting

Snf2p's broad regulatory impact (Guo et al., 2022) [227]. Contrasting with Swi-Snf's known activating role, our data indicates a large *SNF2* repressive function, with 307 and 264 genes upregulated in *snf2* and *snf2K798A* mutants, respectively, including 244 overlapping genes (Fig. 4.7). This supports the dual nature of SWI/SNF as both activator and repressor [226], [227]. The *snf2* deletion mutant exhibited a more robust influence upon transcription than *snf2K798A*, implying a stronger gene expression impact due to *SNF2* absence (Fig. 4.7).

Our research contrasts *snf2* mutants with others, like *snf5*, to understand Swi-Snf's role in gene regulation. The *snf2* mutant uniquely downregulated 224 genes, highlighting its significant transcriptional impact, while *snf5* uniquely downregulated 91 genes (Fig. 4.9), consistent with the pivotal role of Snf2p's ATP-dependent activity in chromatin remodelling (He et al., 2021) [228]. Conversely, *snf2* upregulated 307 genes (234 unique) whilst *snf5* upregulated only 141 genes (68 unique), indicating *SNF2* has a broader repressive role (Fig. 4.12). Interestingly, some *SNF2* and *SNF5* regulated genes, such as *FLO9*, showed opposite expression patterns in the respective *snf2* and *snf5* mutants (Fig. 4.10). This suggests that at genes like *FLO9*, *SNF2* could have a negative role upon transcription whilst *SNF5* had a positive role. At other genes, this behaviour was seen to be reversed. For example at genes such as *ALD3*, *SNF2* had a positive role upon transcription whilst *SNF5* had a negative role. We also observed antagonistic effects between the Snf2p and Swi3p at some target genes, illustrating their complex interactions (Fig. 4.18). For example, the *swi3* and *snf2* mutants demonstrated also antagonistic effects upon transcription at some target genes (Fig. 4.21). Gene ontology analysis also showed distinct regulatory functions for Snf2p, Swi3p and Snf5p. Together, these data reflect that the Snf2p, Swi3p and Snf5p SWI/SNF subunits have diverse, and sometimes opposing, roles in gene regulation [120], [229].

Most interestingly, the *swi3* mutant uniquely upregulated 436 genes, suggesting its significant role in gene repression (Fig. 4.24), consistent with SWI/SNF subunits' diverse regulatory functions [195]. The study enhances our molecular understanding of SWI-SNF's gene regulation, showing the complex's influence on both gene activation and repression. We also found that *SNF2* can repress gene expression to a similar extent as it can activate genes, challenging the view of Swi-Snf as primarily functioning as an activator of transcription. The complex's regulatory scope, with subunits exerting distinct and sometimes opposing effects, highlights the dynamic interplay within SWI-SNF, shaping the transcriptional landscape. These insights are vital for grasping the molecular governance of gene regulation by the SWI-SNF complex.

The genome-wide analysis of the different Swi-Snf subunits revealed their diverse roles in gene regulation. The study challenges the notion of Swi-Snf working as a uniform complex, with Swi3p's presence at 980 genomic sites versus Snf2p being found at far fewer sites, highlighting subunit diversity. This diversity correlates with individual subunit functions in gene expression modulation. Specifically, Snf2p and Taf14p are linked to snRNA transcription regulation, aligning with Szczepanski et al. (2024) [230]. The broad distribution of subunits across transcript types underscores their extensive genomic influence, building on Misato Ohtani (2016) [231] 's work on the Swi-Snf complex's role in gene expression dynamics.

Our study also reveals that Swi-Snf subunits can function independently, with minimal co-occupancy at genomic sites among Swi3p, Snf6p, Swi1p, Snf11p, and Snf2p, indicating unique interactions. Taf14p displays the most distinct occupancy pattern, further highlighting the unique roles of each subunit in transcription and possibly replication and DNA repair.

Swi-Snf complexes are also associated with diseases such as cancer and neurocognitive disorders. The specificity of SWI/SNF subunit binding to chromatin is key for gene regulation, cellular maintenance, and differentiation. The independent binding of SWI/SNF subunits to various sites highlights their varied roles in chromatin remodeling

and gene regulation, which might be relevant to the human Swi-Snf complex's functions and disease implications [194], [226].

The predominant occupancy of Snf2p, Swi3p, and Snf6p across ORFs enhances our grasp of the Swi-Snf complex's gene regulatory roles. Indeed, Snf2p's ORF presence suggests a broader role in gene regulation whereby it might play the most major role during transcription elongation, challenging the notion of its promoter-restricted activity [232]. Swi3p and Snf6p's distribution across promoters and ORFs corroborates their gene expression regulatory function, supported by ChIP and RNA-Seq data [233]. The selective binding of Swi-Snf subunits to coding and promoter regions is crucial for transcription processes. The spatial dynamics of these subunits reveal their varied roles in transcription across different genes, as seen with *SER3* and *UTR5*, where Swi3p and Snf2p show distinct occupancy patterns, indicating the complex's intricate role in chromatin remodelling and gene regulation [226].

The overlap of 270 sites among Swi-Snf subunits suggests coordinated gene expression regulation, aligning with the complex's role in transcriptional activation via chromatin remodeling. Raab et al. (2015) support this with evidence of widespread genomic binding [234]. Swi3p and Snf6p's overlap at 206 genes indicates a functional relationship essential for regulating gene sets, resonating with Xiaofang's (2007) findings on gene regulation synergy. Swi3p and Snf2p's unique occupancy at 184 and 139 sites, respectively, implies independent roles, as discussed by Alfert et al. (2019) [235]. Venn diagram analysis by Chahar et al. (2023) reveals complex subunit interactions, with a core set of 153 ORFs and tRNAs commonly occupied, suggesting a shared regulatory mechanism [236]. This complements Church and Workman's (2024) research on the complex's vital role in metabolism and gene regulation [223].

Snf2p's role in gene regulation is highlighted by its occupancy correlation with mutant transcriptional profiles, indicating both joint and individual SWI/SNF subunit effects. Snf2p is linked to 12.6% of activated down-regulated genes and 10.1% of repressed up-regulated genes, as shown by gene ontology [237]. Novel recruitment mechanisms via

Snf2p's N-terminus and its unacetylatable form at the *INO1* promoter underscore its importance in chromatin remodelling and gene expression [238]. However, overall, Swi-Snf subunits' occupancy poorly correlates with transcriptional changes in *snf2*, *swi3*, and *snf6* mutants, indicating regulation of many of the genes by this complex is indirect.

Swi3p's regulatory role is evident from its occupancy and transcriptional changes in a *swi3* deletion mutant, suggesting roles in both gene activation (13.7% of down-regulated genes) and repression (15.4% of up-regulated genes). This aligns with SWI/SNF complex research, which implicates chromatin remodeling in gene regulation via nucleosome positioning and histone modifications [239], [240], [241]. Swi3p's recruitment to gene promoters affects transcriptional outcomes, with gene ontology analysis showing its broad regulatory influence across various genomic contexts without enrichment in a single category. Swi3p's central role in gene regulation is underscored by its selective control over specific genes, reflecting its diverse regulatory capabilities within the SWI/SNF complex.

The study on Snf6p reveals its nuanced role in the SWI/SNF complex's transcription regulation, with only 10.7% of activated genes and 2.7% of repressed genes directly regulated by Snf6p, indicating this subunit is involved in a more limited regulatory mechanism. This is consistent with Zhang et al.'s findings on Snf6p's limited role in Pol I transcription initiation [242]. He et al.'s insights into the SWI/SNF complex structure suggest that Snf6p and other auxiliary subunits are involved more in targeting the complex to specific genomic loci as opposed to being central to complex activity [228].

We also explored the interaction between the Swi3p subunit of the Swi-Snf co-activator and the Cyc8p subunit of the Tup1-Cyc8 co-repressor complexes. RNA-Seq data revealed that the *swi3* mutant displayed the most distinct transcriptome changes, with many genes being upregulated, indicating Swi3p's significant role in repressing gene transcription [174]. Intriguingly, data showed Cyc8p's absence in *swi3* mutants,

suggesting the swi3 single mutant might be more similar to a *swi3 cyc8* double mutant [174].

Comparing the transcriptomes of the *swi3* mutant and the *swi3 cyc8* double mutant revealed significant differences in gene regulation, contradicting the expected overlap [174]. The *swi3* mutant differed notably from the *cyc8* mutant as well, indicating distinct transcriptional impacts. These findings confirm Swi3p's substantial role in gene repression, independent of Cyc8p's influence [174], [243]. Gene transcription analysis showed a significant difference in upregulation between *swi3* and *swi3 cyc8* mutants, indicating a combined loss of Swi3p and Cyc8p has a stronger repressive effect on these genes (Fig. 6.11) [174]. Additionally, *CYC8* appears to regulate *SWI3*-controlled genes both positively and negatively. Notably, the *FIT1* gene was downregulated in the *swi3* mutant but upregulated in the *swi3 cyc8* double mutant, suggesting a possible repressive role of undetectable Cyc8p levels in the *swi3* mutant cells (Fig. 6. 12).

To investigate the regulatory roles of Swi3p and Cyc8p further, ChIP analysis could reveal Cyc8p's occupancy at co-regulated genes in *swi3* mutants, despite the detection levels[220] Transcriptome comparisons of *swi3*, *cyc8*, and *swi3 cyc8* mutants also indicated Swi3p represses many genes independent of Cyc8p's reduced levels in *swi3* mutants. Together these data suggest a potential low-level presence of Cyc8p directly influencing gene regulation and also suggest a significant repressive role for Swi3p both working synergistically with, and independent of, Cyc8p.

The western blotting showing undetectable Cyc8p levels in *swi3* mutants [244], implied possible post-transcriptional loss of Cyc8p possibly due to a required interaction with Swi3p for stability. Co-immunoprecipitation supported a direct Swi3p-Cyc8p interaction within their respective complexes [Fig. 6. 20,21]. Swi-Snf and Tup1-Cyc8 complexes, known to co-regulate genes like *SUC2* and *FLO1*, function antagonistically at the chromatin level. Tup1-Cyc8 establishes repressive nucleosomal arrays, while Swi-Snf disrupts them for transcription (Fig. 6. 23). The discovery of Swi3p-Cyc8p interaction challenges the mutually exclusive model of these complexes' function, suggesting

possible co-occupancy at gene promoters, allowing rapid transcriptional switches at co-regulated genes. Sequential ChIP could confirm this co-occupancy hypothesis at known co-regulated genes.

In conclusion, our comprehensive study on the Swi-Snf complex and its subunits has illuminated the intricate and multifaceted roles these components play in gene regulation. The findings underscore the complexity of chromatin remodeling and its impact on transcriptional regulation, challenging the traditional view of the Swi-Snf complex both as a uniform entity and as a co-activator.

Key insights from our research include:

- The *swi1* mutant likely nonviability suggests essential roles for *SWI1* in cell viability.
- The *SNF2* and *SNF5* subunits are critical for growth, with their mutants showing prolonged doubling times, indicating their importance in maintaining cellular proliferation.
- The *snf2* deletion mutant exhibited more severe growth defects compared to the Snf2p catalytic mutant, consistent with a destabilizing effect on the Swi-Snf complex and suggesting residual activity of the complex independent of ATPase function.
- Mutant cell morphologies and sensitivities to stressors revealed subunit-specific roles in cell wall integrity, cell size regulation, and DNA damage response.
- RNA-Seq data and gene expression analysis highlighted the dual nature of SWI/SNF as both an activator and repressor, with subunit variability influencing gene regulation.

- The distinct transcriptomic profiles of *snf2* and *swi3* mutants, along with gene ontology findings, emphasized the unique and sometimes opposing regulatory effects of different Swi-Snf subunits.
- The genomic occupancy of Swi-Snf subunits at ORFs as well as at promoters suggests a more extensive role for Swi-Snf in transcription elongation in addition to its more established role at promoters where it is known to function to enable initiation of transcription.
- The direct physical interaction between Swi3p and Cyc8p challenges the mutually exclusive model of Swi-Snf and Tup1-Cyc8 complex activity, suggesting a more intimate association at genes.

Overall, our study provides valuable contributions to the understanding of the SWI-SNF complex's governance of gene regulation, highlighting the need to consider each subunit's unique impact on regulatory mechanisms. The complex's regulatory scope, with subunits exerting distinct and sometimes opposing effects, shapes the transcriptional landscape, offering vital insights into the molecular mechanisms of gene regulation by the SWI-SNF complex.

Appendix

Gene	Description of protein
AGA1	Anchorage subunit of a-agglutinin of a-cells
ATF2	Alcohol acetyltransferase
BAR1	Aspartyl protease secreted to periplasmic space of mating type a cell
BAT2	Cytosolic branched-chain amino acid (BCAA) aminotransferase
CAR2	L-ornithine transaminase (OTAse); catalyzes the second step of arginine degradation
CIS1	Uncharacterized protein
GPX2	Phospholipid hydroperoxide glutathione peroxidase
HMS2	Protein with similarity to heat shock transcription factors
IRC7	Cysteine desulphydrase, enables growth on cysteine as nitrogen source
IZH2	Plasma membrane receptor for plant antifungal osmotic
MNN1	MaNNosyltransferase
MRH1	Protein that localizes primarily to the plasma membrane
NDJ1	Protein that regulates meiotic SPB cohesion and telomere clustering
PHM6	Uncharacterized protein
PHO11	Acid phosphatase
PHO12	Acid phosphatase

Gene	Description of protein
PHO3	Constitutive acid phosphatase
PHO5	Repressible acid phosphatase
PHO8	Repressible vacuolar alkaline phosphatase
PHO81	Cyclin-dependent kinase (CDK) inhibitor
PHO84	Inorganic phosphate transporter PHO84
QDR2	Plasma membrane transporter of the major facilitator superfamily
REE1	Cytoplasmic protein involved in the regulation of enolase (ENO1)
SPL2	Protein with similarity to cyclin-dependent kinase inhibitors
SRD1	Protein involved in the processing of pre-rRNA to mature rRNA
TIP1	Major cell wall mannoprotein with possible lipase activity
VTC3	Regulatory subunit of vacuolar transporter chaperone (VTC) complex
VTC4	Vacuolar membrane polyphosphate polymerase
YAR009C	Retrotransposon TYA Gag and TYB Pol genes; Gag processing produces capsid proteins
YBL005W-B	Retrotransposon TYA Gag and TYB Pol genes; transcribed/translated as one unit
YCL021W-A	Uncharacterized protein

YDR261C-D	Retrotransposon TYA Gag and TYB Pol genes
YDR365W-B	Retrotransposon TYA Gag and TYB Pol genes
YER138C	Retrotransposon TYA Gag and TYB Pol genes
YGR027W-B	Retrotransposon TYA Gag and TYB Pol genes
YGR038C-B	Retrotransposon TYA Gag and TYB Pol genes
YHB1	Nitric oxide oxidoreductase; flavohemoglobin that plays role in oxidative and nitrosative stress responses
YHR214C-B	Retrotransposon TYA Gag and TYB Pol genes
YJR027W	Retrotransposon TYA Gag and TYB Pol genes
YJR029W	Retrotransposon TYA Gag and TYB Pol genes
YLR035C-A	Retrotransposon TYA Gag and TYB Pol genes
YLR227W-B	Retrotransposon TYA Gag and TYB Pol genes
YLR256W-A	Retrotransposon TYA Gag gene co-transcribed with TYB Pol
YML039W	Retrotransposon TYA Gag and TYB Pol genes
YMR317W	Uncharacterized protein
YNL054W-B	TyB Gag-Pol protein; proteolytically processed to make the Gag, reverse transcriptase (RT), protease (PR), and integrase (IN) proteins that are required for retrotransposition
YOL014W	Uncharacterized protein
YOL103W-B	Retrotransposon TYA Gag and TYB Pol genes
YOR142W-B	Retrotransposon TYA Gag and TYB Pol genes

YOR192C-B	Retrotransposon TYA Gag and TYB Pol genes
YPR137C-B	Retrotransposon TYA Gag and TYB Pol genes
YPR158C-D	Retrotransposon TYA Gag and TYB Pol genes
YPR158W-B	Retrotransposon TYA Gag and TYB Pol genes
YRO2	Protein with a putative role in response to acid stress
ZRT1	High-affinity zinc transporter of the plasma membrane

Table S1: The list of 57 genes commonly downregulated in the *snf2*, *swi3*, *snf5,* and *snf6* mutant strain compared to wt.

Gene	Description of protein
AAC1	Mitochondrial inner membrane ADP/ATP translocator
ADR1	Carbon source-responsive zinc-finger transcription factor
ALD4	Mitochondrial aldehyde dehydrogenase
BNA2	Biosynthesis of Nicotinic Acid
DAL1	Allantoinase; converts allantoin to allantoate in the first step of allantoin degradation; expression sensitive to nitrogen catabolite repression
ECM13	Uncharacterized protein
GAP1	General Amino acid Permease
HBN1	Uncharacterized protein
HPF1	Haze-protective mannoprotein
LDS2	Lipid Droplets in Sporulation
MET10	Subunit alpha of assimilatory sulfite reductase; complex converts sulfite into sulfide
MET13	Major isozyme of methylenetetrahydrofolate reductase
MET14	Adenylylsulfate kinase
MET16	3'-phosphoadenylsulfate reductase
MET2	L-homoserine-O-acetyltransferase
MET28	bZIP transcriptional activator in the Cbf1p-Met4p-Met28p complex; participates in the regulation of sulfur metabolism
MET3	ATP sulfurylase; catalyzes the primary step of intracellular sulfate activation, essential for assimilatory reduction of sulfate to sulfide, involved in methionine metabolism; human homolog PAPSS2 complements yeast null mutant
MET5	Sulfite reductase beta subunit; involved in amino acid biosynthesis, transcription repressed by methionine
MET6	Cobalamin-independent methionine synthase; involved in methionine biosynthesis and regeneration; requires a minimum of two glutamates on the methyltetrahydrofolate substrate, similar to bacterial metE homologs
MMP1	High-affinity S-methylmethionine permease; required for utilization of S-methylmethionine as a sulfur source
MND1	Protein required for recombination and meiotic nuclear division
PDC6	Minor isoform of pyruvate decarboxylase; decarboxylates pyruvate to acetaldehyde, involved in amino acid catabolism; transcription is glucose- and ethanol-dependent, and is strongly induced during sulfur limitation
PUT4	Proline permease; required for high-affinity transport of proline; also transports the toxic proline analog azetidine-2-

	carboxylate (AzC); PUT4 transcription is repressed in ammonia-grown cells
ROX1	Heme-dependent repressor of hypoxic genes
SPO20	Meiosis-specific subunit of the t-SNARE complex
STR3	Peroxisomal cystathionine beta-lyase
SUL2	High affinity sulfate permease; sulfate uptake is mediated by specific sulfate transporters Sul1p and Sul2p, which control the concentration of endogenous activated sulfate intermediates
THI12	Protein involved in synthesis of the thiamine precursor HMP
THI4	THIamine metabolism
YGR050C	Uncharacterized protein
YKR041W	Uncharacterized protein
YMR122C	Uncharacterized protein
YMR244W	Uncharacterized protein
YPR064W	Uncharacterized protein
ALG14	Component of UDP-GlcNAc transferase
CSS1	Uncharacterized protein

Table S2: The list of 35 genes commonly upregulated in the *snf2*, *swi3*, *snf5*, and *snf6* mutant strains compared to wt.

References

References

[1] S. Hahn and E. T. Young, “Transcriptional regulation in saccharomyces cerevisiae: Transcription factor regulation and function, mechanisms of initiation, and roles of activators and coactivators,” *Genetics*, vol. 189, no. 3, 2011, doi: 10.1534/genetics.111.127019.

[2] C. Menichelli *et al.*, “Identification of long regulatory elements in the genome of Plasmodium falciparum and other eukaryotes,” *PLoS Comput Biol*, vol. 17, no. 4, Apr. 2021, doi: 10.1371/journal.pcbi.1008909.

[3] M. J. Dunham *et al.*, “Characteristic genome rearrangements in experimental evolution of Saccharomyces cerevisiae,” *Proc Natl Acad Sci U S A*, vol. 99, no. 25, 2002, doi: 10.1073/pnas.242624799.

[4] C. R. Clapier, J. Iwasa, B. R. Cairns, and C. L. Peterson, “Mechanisms of action and regulation of ATP-dependent chromatin-remodelling complexes,” Jul. 01, 2017, *Nature Publishing Group*. doi: 10.1038/nrm.2017.26.

[5] T. Schlick, J. Hayes, and S. Grigoryev, “Toward convergence of experimental studies and theoretical modeling of the chromatin fiber,” Feb. 17, 2012. doi: 10.1074/jbc.R111.305763.

[6] V. Sokolova, S. Sarkar, and D. Tan, “Histone variants and chromatin structure, update of advances,” Jan. 01, 2023, *Elsevier B.V.* doi: 10.1016/j.csbj.2022.12.002.

[7] R. K. Sahu, S. Singh, and R. S. Tomar, “The mechanisms of action of chromatin remodelers and implications in development and disease,” Oct. 01, 2020, *Elsevier Inc.* doi: 10.1016/j.bcp.2020.114200.

[8] A. Finley and R. A. Copeland, “Small molecule control of chromatin remodeling,” Sep. 18, 2014, *Elsevier Ltd*. doi: 10.1016/j.chembiol.2014.07.024.

[9] D. Jiang, T. Li, C. Guo, T. S. Tang, and H. Liu, “Small molecule modulators of chromatin remodeling: from neurodevelopment to neurodegeneration,” Dec. 01, 2023, *BioMed Central Ltd*. doi: 10.1186/s13578-023-00953-4.

[10] C. A. Keleher, M. J. Redd, J. Schultz, M. Carlson, and A. D. Johnson’, “SsnG-Tupl Is a General Repressor of Transbription in Yeast,” 1992.

[11] V. Wood, K. M. Rutherford, A. Ivens, M. A. Rajandream, and B. Barrell, “A re-annotation of the Saccharomyces cerevisiae genome,” *Comp Funct Genomics*, vol. 2, no. 3, pp. 143–154, 2001, doi: 10.1002/cfg.86.

[12] B. Li, M. Carey, and J. L. Workman, “The Role of Chromatin during Transcription,” Feb. 23, 2007. doi: 10.1016/j.cell.2007.01.015.

[13] K. Luger, A. W. Mäder, R. K. Richmond, D. F. Sargent, and T. J. Richmond, “Crystal structure of the nucleosome core particle at 2.8 Å resolution,” *Nature*, vol. 389, no. 6648, 1997, doi: 10.1038/38444.

[14] G. S. Brush, “Evidence that histone H1 is dispensable for proper meiotic recombination in budding yeast,” *BMC Res Notes*, vol. 8, no. 1, 2015, doi: 10.1186/s13104-015-1246-1.

[15] S. C. R. Elgin, “Heterochromatin and gene regulation in Drosophila,” *Curr Opin Genet Dev*, vol. 6, no. 2, 1996, doi: 10.1016/S0959-437X(96)80050-5.

[16] S. Takahata and Y. Murakami, “Opposing Roles of FACT for Euchromatin and Heterochromatin in Yeast,” Feb. 01, 2023, *MDPI*. doi: 10.3390/biom13020377.

[17] A. Juárez-Reyes *et al.*, “Systematic profiling of subtelomeric silencing factors in budding yeast,” *G3: Genes, Genomes, Genetics*, vol. 13, no. 10, Oct. 2023, doi: 10.1093/g3journal/jkad153.

[18] A. Hocher and T. Warnecke, “Nucleosomes at the Dawn of Eukaryotes,” 2024. doi: 10.1093/gbe/evae029.

[19] R. D. Kornberg and Y. Lorch, “Primary Role of the Nucleosome,” Aug. 06, 2020, *Cell Press*. doi: 10.1016/j.molcel.2020.07.020.

[20] A. Lin, Y. Du, and W. Xiao, “Yeast chromatin remodeling complexes and their roles in transcription,” Aug. 01, 2020, *Springer*. doi: 10.1007/s00294-020-01072-0.

[21] A. R. Cutter and J. J. Hayes, “A brief review of nucleosome structure,” 2015. doi: 10.1016/j.febslet.2015.05.016.

[22] I. Cohen, E. Poręba, K. Kamieniarz, and R. Schneider, “Histone modifiers in cancer: Friends or foes?,” 2011. doi: 10.1177/1947601911417176.

[23] B. C. Smith and J. M. Denu, “Chemical mechanisms of histone lysine and arginine modifications,” Jan. 2009. doi: 10.1016/j.bbagrm.2008.06.005.

[24] A. J. Courey and S. Jia, “Transcriptional repression: The long and the short of it,” 2001. doi: 10.1101/gad.939601.

[25] P. B. Talbert and S. Henikoff, “Histone variants at a glance,” *J Cell Sci*, vol. 134, no. 6, 2021, doi: 10.1242/jcs.244749.

[26] H. G. Davies and M. E. Haynes, “Electron microscope observations on cell nuclei in various tissues of a teleost fish: the nucleolus associated monolayer of chromatin structural units,” *J Cell Sci*, vol. 21, no. 2, 1976, doi: 10.1242/jcs.21.2.315.

[27] S. G. Swygert *et al.*, “Local chromatin fiber folding represses transcription and loop extrusion in quiescent cells,” *Elife*, vol. 10, 2021, doi: 10.7554/eLife.72062.

[28] B. V G Allfrey, R. Faulkner, and A. E. Mirsky, “Lindsten, unpublished data. ACETYLATION AND METHYLATION OF HISTONES AND THEIR POSSIBLE ROLE IN THE REGULATION OF RNA SYNTHESIS*,” 1938.

[29] A. Sadakierska-Chudy and M. Filip, “A Comprehensive View of the Epigenetic Landscape. Part II: Histone Post-translational Modification, Nucleosome Level, and Chromatin Regulation by ncRNAs,” Feb. 01, 2015, *Springer Science and Business Media, LLC*. doi: 10.1007/s12640-014-9508-6.

[30] G. J. Narlikar, H. Y. Fan, and R. E. Kingston, “Cooperation between complexes that regulate chromatin structure and transcription,” 2002. doi: 10.1016/S0092-8674(02)00654-2.

[31] Y. Zhang and D. Reinberg, “Transcription regulation by histone methylation: Interplay between different covalent modifications of the core histone tails,” Sep. 15, 2001. doi: 10.1101/gad.927301.

[32] M. Y. Mazina and N. E. Vorobyeva, “Chromatin Modifiers in Transcriptional Regulation: New Findings and Prospects,” *Acta Naturae*, vol. 13, no. 1, pp. 16–30, 2021, doi: 10.32607/actanaturae.11101.

[33] K. A. Janssen, S. Sidoli, and B. A. Garcia, “Recent Achievements in Characterizing the Histone Code and Approaches to Integrating Epigenomics and Systems Biology,” in *Methods in Enzymology*, vol. 586, Academic Press Inc., 2017, pp. 359–378. doi: 10.1016/bs.mie.2016.10.021.

[34] S. Sidoli, L. Cheng, and O. N. Jensen, “Proteomics in chromatin biology and epigenetics: Elucidation of post-translational modifications of histone proteins by mass spectrometry,” Jun. 27, 2012. doi: 10.1016/j.jprot.2011.12.029.

[35] L. Hongs, G. P. Schrothp, H. R. Matthew&, P. Yaus, and E. M. Bradburysliii, “Studies of the DNA Binding Properties of Histone H4 Amino Terminus THERMAL DENATURATION STUDIES REVEAL THAT ACETYLATION MARKEDLY REDUCES THE BINDING CONSTANT OF THE H4 ‘TAIL’ TO DNA* A,” 1993.

[36] J. L. Workman and R. E. Kingston, “ALTERATION OF NUCLEOSOME STRUCTURE AS A MECHANISM OF TRANSCRIPTIONAL REGULATION,” 1998. [Online]. Available: www.annualreviews.org

[37] D. K. Pokholok *et al.*, “Genome-wide map of nucleosome acetylation and methylation in yeast,” *Cell*, vol. 122, no. 4, pp. 517–527, Aug. 2005, doi: 10.1016/j.cell.2005.06.026.

[38] P. A. Grant *et al.*, “Yeast Gcn5 functions in two multisubunit complexes to acetylate nucleosomal histones: characterization of an Ada complex and the SAGA (Spt/Ada) complex.”

[39] M. Arif *et al.*, “Nitric oxide-mediated histone hyperacetylation in oral cancer: Target for a water-soluble HAT inhibitor, CTK7A,” *Chem Biol*, vol. 17, no. 8, pp. 903–913, Aug. 2010, doi: 10.1016/j.chembiol.2010.06.014.

[40] S. Y. Park and J. S. Kim, “A short guide to histone deacetylases including recent progress on class II enzymes,” Feb. 01, 2020, *Springer Nature*. doi: 10.1038/s12276-020-0382-4.

[41] O. J. Rando and F. Winston, “Chromatin and transcription in yeast,” *Genetics*, vol. 190, no. 2, pp. 351–387, Feb. 2012, doi: 10.1534/genetics.111.132266.

[42] Y. X. Niu, J. Bai, and S. Z. Zheng, “The Regulation and Function of Histone Methylation,” Dec. 01, 2018, *Springer New York LLC*. doi: 10.1007/s12374-018-0176-6.

[43] N. E. Oey *et al.*, “A neuronal activity-dependent dual function chromatin-modifying complex regulates arc expression,” *eNeuro*, vol. 2, no. 1, 2015, doi: 10.1523/ENEURO.0020-14.2015.

[44] K. Hyun, J. Jeon, K. Park, and J. Kim, “Writing, erasing and reading histone lysine methylations,” 2017. doi: 10.1038/emm.2017.11.

[45] A. J. Bannister, R. Schneider, and T. Kouzarides, “Histone methylation: Dynamic or static?,” 2002. doi: 10.1016/S0092-8674(02)00798-5.

[46] K. Y. Chou, J. Y. Lee, K. B. Kim, E. Kim, H. S. Lee, and H. Y. Ryu, “Histone modification in Saccharomyces cerevisiae: A review of the current status,” Jan. 01, 2023, *Elsevier B.V.* doi: 10.1016/j.csbj.2023.02.037.

[47] S. D. Briggs *et al.*, “Histone H3 lysine 4 methylation is mediated by Set1 and required for cell growth and rDNA silencing in Saccharomyces cerevisiae,” *Genes Dev*, vol. 15, no. 24, pp. 3286–3295, Dec. 2001, doi: 10.1101/gad.940201.

[48] G. Zardo, “The role of H3K4 trimethylation in CpG islands hypermethylation in cancer,” Feb. 01, 2021, *MDPI AG*. doi: 10.3390/biom11020143.

[49] B. D. Strahl *et al.*, “Set2 Is a Nucleosomal Histone H3-Selective Methyltransferase That Mediates Transcriptional Repression,” *Mol Cell Biol*, vol. 22, no. 5, pp. 1298–1306, Mar. 2002, doi: 10.1128/mcb.22.5.1298-1306.2002.

[50] B. R. Cairns, “Chromatin remodeling: Insights and intrigue from single-molecule studies,” Nov. 2007. doi: 10.1038/nsmb1333.

[51] C. R. Clapier, J. Iwasa, B. R. Cairns, and C. L. Peterson, “Mechanisms of action and regulation of ATP-dependent chromatin-remodelling complexes,” Jul. 01, 2017, *Nature Publishing Group*. doi: 10.1038/nrm.2017.26.

[52] J. A. Martens, P. Y. J. Wu, and F. Winston, “Regulation of an intergenic transcript controls adjacent gene transcription in Saccharomyces cerevisiae,” *Genes Dev*, vol. 19, no. 22, pp. 2695–2704, Nov. 2005, doi: 10.1101/gad.1367605.

[53] S. Buratowski, “Progression through the RNA Polymerase II CTD Cycle,” Nov. 25, 2009. doi: 10.1016/j.molcel.2009.10.019.

[54] N. Bischler, H. Tschochner, P. Schultz, A. Â. Sentenac, C. Carles, and M. Riva, “Ge Â rald Peyroche, Philipp Milkereit.”

[55] P. Aprikian, B. Moorefield, and R. H. Reeder, “New Model for the Yeast RNA Polymerase I Transcription Cycle,” *Mol Cell Biol*, vol. 21, no. 15, pp. 4847–4855, Aug. 2001, doi: 10.1128/mcb.21.15.4847-4855.2001.

[56] K.-J. Armache, H. Kettenberger, P. Cramer, and E. P. Geiduschek, “Architecture of initiation-competent 12-subunit RNA polymerase II.” [Online]. Available: www.pnas.orgcgidoi10.1073pnas.1030608100

[57] M. Werner, P. Thuriaux, and J. Soutourina, “Structure-function analysis of RNA polymerases I and III,” Dec. 2009. doi: 10.1016/j.sbi.2009.10.005.

[58] A. I. Garrido-Godino, F. Gutiérrez-Santiago, and F. Navarro, “Biogenesis of RNA Polymerases in Yeast,” Apr. 28, 2021, *Frontiers Media S.A.* doi: 10.3389/fmolb.2021.669300.

[59] S. Hahn and E. T. Young, “Transcriptional regulation in saccharomyces cerevisiae: Transcription factor regulation and function, mechanisms of initiation, and roles of activators and coactivators,” *Genetics*, vol. 189, no. 3, pp. 705–736, Nov. 2011, doi: 10.1534/genetics.111.127019.

[60] H. E. Mischo and N. J. Proudfoot, “Disengaging polymerase: Terminating RNA polymerase II transcription in budding yeast,” Jan. 2013. doi: 10.1016/j.bbagrm.2012.10.003.

[61] P. B. Becker and J. L. Workman, “Nucleosome remodeling and epigenetics,” *Cold Spring Harb Perspect Biol*, vol. 5, no. 9, Sep. 2013, doi: 10.1101/cshperspect.a017905.

[62] L. Xu, W. Wang, J. Chong, J. H. Shin, J. Xu, and D. Wang, “RNA polymerase II transcriptional fidelity control and its functional interplay with DNA modifications,” *Crit Rev Biochem Mol Biol*, vol. 50, no. 6, pp. 503–519, Nov. 2015, doi: 10.3109/10409238.2015.1087960.

[63] M. Barba-Aliaga, P. Alepuz, and J. E. Pérez-Ortín, “Eukaryotic RNA Polymerases: The Many Ways to Transcribe a Gene,” Apr. 21, 2021, *Frontiers Media S.A.* doi: 10.3389/fmolb.2021.663209.

[64] C. W. M. Roberts and S. H. Orkin, “The SWI/SNF complex - Chromatin and cancer,” 2004, *Nature Publishing Group*. doi: 10.1038/nrc1273.

[65] H. K. Prajapati, J. Ocampo, and D. J. Clark, “Interplay among atp-dependent chromatin remodelers determines chromatin organisation in yeast,” Aug. 01, 2020, *MDPI AG*. doi: 10.3390/biology9080190.

[66] D. P. Ryan, R. Sundaramoorthy, D. Martin, V. Singh, and T. Owen-Hughes, “The DNA-binding domain of the Chd1 chromatin-remodelling enzyme contains SANT and SLIDE

domains," *EMBO Journal*, vol. 30, no. 13, pp. 2596–2609, Jul. 2011, doi: 10.1038/emboj.2011.166.

[67] J. F. Flanagan *et al.*, "Double chromodomains cooperate to recognize the methylated histone H3 tail," *Nature*, vol. 438, no. 7071, pp. 1181–1185, Dec. 2005, doi: 10.1038/nature04290.

[68] C. R. Clapier, J. Iwasa, B. R. Cairns, and C. L. Peterson, "Mechanisms of action and regulation of ATP-dependent chromatin-remodelling complexes," Jul. 01, 2017, *Nature Publishing Group*. doi: 10.1038/nrm.2017.26.

[69] C. R. Clapier and B. R. Cairns, "The biology of chromatin remodeling complexes," 2009. doi: 10.1146/annurev.biochem.77.062706.153223.

[70] C. R. Clapier, "Sophisticated conversations between chromatin and chromatin remodelers, and dissonances in cancer," Jun. 01, 2021, *MDPI*. doi: 10.3390/ijms22115578.

[71] G. Mizuguchi, X. Shen, J. Landry, W. H. Wu, S. Sen, and C. Wu, "ATP-Driven Exchange of Histone H2AZ Variant Catalyzed by SWR1 Chromatin Remodeling Complex," *Science (1979)*, vol. 303, no. 5656, 2004, doi: 10.1126/science.1090701.

[72] D. D. Ruhl *et al.*, "Purification of a human SRCAP complex that remodels chromatin by incorporating the histone variant H2A.Z into nucleosomes," *Biochemistry*, vol. 45, no. 17, 2006, doi: 10.1021/bi060043d.

[73] C. R. Clapier, J. Iwasa, B. R. Cairns, and C. L. Peterson, "Mechanisms of action and regulation of ATP-dependent chromatin-remodelling complexes," 2017. doi: 10.1038/nrm.2017.26.

[74] C. R. Clapier and B. R. Cairns, "The biology of chromatin remodeling complexes," 2009. doi: 10.1146/annurev.biochem.77.062706.153223.

[75] S. K. Hota and B. G. Bruneau, "ATP-dependent chromatin remodeling during mammalian development," Aug. 15, 2016, *Company of Biologists Ltd*. doi: 10.1242/dev.128892.

[76] M. D. Bashyam, S. Animireddy, and P. Bala, "Taming the master: SWI/SNF chromatin remodeller as a therapeutic target in cancer," 2019. doi: 10.18520/cs/v116/i10/1653-1665.

[77] B. Mossink, M. Negwer, D. Schubert, and N. Nadif Kasri, "The emerging role of chromatin remodelers in neurodevelopmental disorders: a developmental perspective," 2021. doi: 10.1007/s00018-020-03714-5.

[78] E. Errichiello *et al.*, "SMARCA4 inactivating mutations cause concomitant Coffin–Siris syndrome, microphthalmia and small-cell carcinoma of the ovary hypercalcaemic type," *Journal of Pathology*, vol. 243, no. 1, 2017, doi: 10.1002/path.4926.

[79] S. Tartey and O. Takeuchi, “Chromatin remodeling and transcriptional control in innate immunity: Emergence of Akirin2 as a novel player,” 2015. doi: 10.3390/biom5031618.

[80] A. Chaudhri, G. Lizee, P. Hwu, and K. Rai, “Chromatin Remodelers Are Regulators of the Tumor Immune Microenvironment,” 2024. doi: 10.1158/0008-5472.CAN-23-2244.

[81] A. Berson, R. Nativio, S. L. Berger, and N. M. Bonini, “Epigenetic Regulation in Neurodegenerative Diseases,” 2018. doi: 10.1016/j.tins.2018.05.005.

[82] J. Côté, J. Quinn, J. L. Workman, and C. L. Peterson, “Stimulation of GAL4 derivative binding to nucleosomal DNA by the yeast SWI/SNF complex,” *Science (1979)*, vol. 265, no. 5168, pp. 53–60, 1994, doi: 10.1126/science.8016655.

[83] A. Dutta *et al.*, “Composition and Function of Mutant Swi/Snf Complexes,” *Cell Rep*, vol. 18, no. 9, pp. 2124–2134, Feb. 2017, doi: 10.1016/j.celrep.2017.01.058.

[84] F. Winston and M. Carlson, “Yeast SNF/SWI transcriptional activators and the SPT/SIN chromatin connection,” *Trends in Genetics*, vol. 8, no. 11, pp. 387–391, Nov. 1992, doi: 10.1016/0168-9525(92)90300-S.

[85] R. G. Dastidar, J. Hooda, A. Shah, T. M. Cao, R. M. Henke, and L. Zhang, “The nuclear localization of SWI/SNF proteins is subjected to oxygen regulation,” *Cell Biosci*, vol. 2, no. 1, Aug. 2012, doi: 10.1186/2045-3701-2-30.

[86] A. A. Reyes, R. D. Marcum, and Y. He, “Structure and Function of Chromatin Remodelers,” Jul. 09, 2021, *Academic Press*. doi: 10.1016/j.jmb.2021.166929.

[87] J. H. M. Soffers and J. L. Workman, “The SAGA chromatin-modifying complex: the sum of its parts is greater than the whole,” 2020, doi: 10.1101/gad.341156.

[88] M. A. Schwabish and K. Struhl, “The Swi/Snf Complex Is Important for Histone Eviction during Transcriptional Activation and RNA Polymerase II Elongation In Vivo,” *Mol Cell Biol*, vol. 27, no. 20, pp. 6987–6995, Oct. 2007, doi: 10.1128/mcb.00717-07.

[89] P. Sudarsanam and F. Winston, “The Swi/Snf family: Nucleosome-remodeling complexes and transcriptional control,” 2000. doi: 10.1016/S0168-9525(00)02060-6.

[90] H. Szerlong, K. Hinata, R. Viswanathan, H. Erdjument-Bromage, P. Tempst, and B. R. Cairns, “The HSA domain binds nuclear actin-related proteins to regulate chromatin-remodeling ATPases,” *Nat Struct Mol Biol*, vol. 15, no. 5, pp. 469–476, May 2008, doi: 10.1038/nsmb.1403.

[91] H. L. Schubert *et al.*, “Structure of an actin-related subcomplex of the SWI/SNF chromatin remodeler,” *Proc Natl Acad Sci U S A*, vol. 110, no. 9, pp. 3345–3350, Feb. 2013, doi: 10.1073/pnas.1215379110.

[92] Z. Nie *et al.*, “Novel SWI/SNF Chromatin-Remodeling Complexes Contain a Mixed-Lineage Leukemia Chromosomal Translocation Partner,” *Mol Cell Biol*, vol. 23, no. 8, pp. 2942–2952, Apr. 2003, doi: 10.1128/mcb.23.8.2942-2952.2003.

[93] D. Reddy, S. Bhattacharya, and J. L. Workman, “(mis)-Targeting of SWI/SNF complex(es) in cancer,” Jun. 01, 2023, *Springer*. doi: 10.1007/s10555-023-10102-5.

[94] T. Bieluszewski, S. Prakash, T. Roulé, and D. Wagner, “The Role and Activity of SWI/SNF Chromatin Remodelers,” 2023, doi: 10.1146/annurev-arplant-102820.

[95] N. Krishnamurthy, S. Kato, S. Lippman, and R. Kurzrock, “Chromatin remodeling (SWI/SNF) complexes, cancer, and response to immunotherapy,” Sep. 02, 2022, *BMJ Publishing Group*. doi: 10.1136/jitc-2022-004669.

[96] Y. Tsurusaki *et al.*, “Mutations affecting components of the SWI/SNF complex cause Coffin-Siris syndrome,” *Nat Genet*, vol. 44, no. 4, pp. 376–378, Apr. 2012, doi: 10.1038/ng.2219.

[97] T. Shorstova *et al.*, “SWI/SNF-Compromised cancers are susceptible to bromodomain inhibitors,” *Cancer Res*, vol. 79, no. 10, pp. 2761–2774, 2019, doi: 10.1158/0008-5472.CAN-18-1545.

[98] C. Kadoch *et al.*, “Proteomic and bioinformatic analysis of mammalian SWI/SNF complexes identifies extensive roles in human malignancy,” *Nat Genet*, vol. 45, no. 6, pp. 592–601, Jun. 2013, doi: 10.1038/ng.2628.

[99] N. Chatterjee, D. Sinha, M. Lemma-Dechassa, S. Tan, M. A. Shogren-Knaak, and B. Bartholomew, “Histone H3 tail acetylation modulates ATP-dependent remodeling through multiple mechanisms,” *Nucleic Acids Res*, vol. 39, no. 19, pp. 8378–8391, Oct. 2011, doi: 10.1093/nar/gkr535.

[100] N. Krishnamurthy, S. Kato, S. Lippman, and R. Kurzrock, “Chromatin remodeling (SWI/SNF) complexes, cancer, and response to immunotherapy,” Sep. 02, 2022, *BMJ Publishing Group*. doi: 10.1136/jitc-2022-004669.

[101] T. Jégu *et al.*, “A SWI/SNF chromatin remodelling protein controls cytokinin production through the regulation of chromatin architecture,” *PLoS One*, vol. 10, no. 10, Oct. 2015, doi: 10.1371/journal.pone.0138276.

[102] G. M. Euskirchen *et al.*, “Diverse roles and interactions of the SWI/SNF chromatin remodeling complex revealed using global approaches,” *PLoS Genet*, vol. 7, no. 3, Mar. 2011, doi: 10.1371/journal.pgen.1002008.

[103] U. S. Varanasi, M. Klis, P. B. Mikesell, and R. J. Trumbly, “The Cyc8 (Ssn6)-Tup1 Corepressor Complex Is Composed of One Cyc8 and Four Tup1 Subunits,” 1996.

[104] R. L. Smitha and A. D. Johnsonb, “Turning genes off by Ssn6-Tup1: A conserved system of transcriptional repression in eukaryotes,” 2000. doi: 10.1016/S0968-0004(00)01592-9.

[105] B. Lee, “Distinct phenotypes and transcriptomes of tup1Δ and cyc8Δ mutants suggest novel roles for TUP1 and CYC8 in Saccharomyces cerevisiae.”

[106] D. Tzamarias and K. Struhl, “Distinct TPR motifs of Cyc8 are involved in recrumng the Cyc8-Tupl corepressor complex to differentially regulated promoters.”

[107] C. Jabet, E. R. Sprague, A. P. Vandemark, and C. Wolberger, “Characterization of the N-terminal Domain of the Yeast Transcriptional Repressor Tup1 PROPOSAL FOR AN ASSOCIATION MODEL OF THE REPRESSOR COMPLEX Tup1Ssn6*,” 2000. [Online]. Available: http://www.jbc.org

[108] D. Tzamarias and K. Struhl, “Functional dissection of the yeast Cyc8-Tupl transcriptional co-repressor complex,” *Nature*, vol. 369, no. 6483, 1994, doi: 10.1038/369758a0.

[109] K. Komachi, M. J. Redd, and A. D. Johnson, “The WD repeats of Tupl interact with the homeo domain protein,” 1994.

[110] R. S. Conlan, N. Gounalaki, P. Hatzis, and D. Tzamarias, “The Tup1-Cyc8 Protein Complex Can Shift from a Transcriptional Co-repressor to a Transcriptional Co-activator*,” 1999. [Online]. Available: http://www.jbc.org

[111] E. J. Parnell, T. J. Parnell, and D. J. Stillman, “Genetic analysis argues for a coactivator function for the Saccharomyces cerevisiae Tup1 corepressor,” *Genetics*, vol. 219, no. 2, Oct. 2021, doi: 10.1093/genetics/iyab120.

[112] J. R. Bone and S. Y. Roth, “Recruitment of the yeast Tup1p-Ssn6p repressor is associated with localized decreases in histone acetylation,” *Journal of Biological Chemistry*, vol. 276, no. 3, pp. 1808–1813, Jan. 2001, doi: 10.1074/jbc.M008668200.

[113] A. B. Fleming, S. Beggs, M. Church, Y. Tsukihashi, and S. Pennings, “The yeast Cyc8-Tup1 complex cooperates with Hda1p and Rpd3p histone deacetylases to robustly repress transcription of the subtelomeric FLO1 gene,” *Biochim Biophys Acta Gene Regul Mech*, vol. 1839, no. 11, pp. 1242–1255, 2014, doi: 10.1016/j.bbagrm.2014.07.022.

[114] A. B. Fleming and S. Pennings, “Antagonistic remodelling by Swi-Snf and Tup1-Ssn6 of an extensive chromatin region forms the background for FLO1 gene regulation,” *EMBO Journal*, vol. 20, no. 18, 2001, doi: 10.1093/emboj/20.18.5219.

[115] K. H. Wong and K. Struhl, “The Cyc8-Tup1 complex inhibits transcription primarily by masking the activation domain of the recruiting protein,” *Genes Dev*, vol. 25, no. 23, pp. 2525–2539, Dec. 2011, doi: 10.1101/gad.179275.111.

[116] Z. Zhang and J. C. Reese, “Redundant mechanisms are used by Ssn6-Tup1 in repressing chromosomal gene transcription in Saccharomyces cerevisiae,” *Journal of Biological Chemistry*, vol. 279, no. 38, pp. 39240–39250, Sep. 2004, doi: 10.1074/jbc.M407159200.

[117] M. Carlson and D. Botstein, “Organization of the SUC Gene Family in Saccharomyces,” 1983.

[118] A. B. Fleming and S. Pennings, “Tup1-Ssn6 and Swi-Snf remodelling activities influence long-range chromatin organization upstream of the yeast SUC2 gene,” *Nucleic Acids Res*, vol. 35, no. 16, pp. 5520–5531, Aug. 2007, doi: 10.1093/nar/gkm573.

[119] C. B. Brachmann *et al.*, “Designer deletion strains derived from Saccharomyces cerevisiae S288C: A useful set of strains and plasmids for PCR-mediated gene disruption and other applications,” *Yeast*, vol. 14, no. 2, pp. 115–132, Jan. 1998, doi: 10.1002/(SICI)1097-0061(19980130)14:2<115::AID-YEA204>3.0.CO;2-2.

[120] J. N. Hirschhorn, S. A. Brown, C. D. Clark, and F. Winston, “Evidence that SNF2/SWI2 and SNF5 activate transcription in yeast by altering chromatin structure,” *Genes Dev*, vol. 6, no. 12, 1992, doi: 10.1101/gad.6.12a.2288.

[121] H. Haruki, J. Nishikawa, and U. K. Laemmli, “The Anchor-Away Technique: Rapid, Conditional Establishment of Yeast Mutant Phenotypes,” *Mol Cell*, vol. 31, no. 6, pp. 925–932, Sep. 2008, doi: 10.1016/j.molcel.2008.07.020.

[122] R. D. Gietz and R. H. Schiestl, “High-efficiency yeast transformation using the LiAc/SS carrier DNA/PEG method,” *Nat Protoc*, vol. 2, no. 1, pp. 31–34, Feb. 2007, doi: 10.1038/nprot.2007.13.

[123] A. I. Wach, A. N. D T Br Ach At, C. R. Istin A Alber Ti-seg U I, C. I. N E R Ebisch U N G, and A. D. Peter Ph Ilippsen, “H eterologous H IS 3 M arker and G F P R eporter M odules for PCR-Targeting in S accharomyces cerevisiae,” John Wiley & Sons, 1997.

[124] M. S. Longtine *et al.*, “Additional modules for versatile and economical PCR-based gene deletion and modification in Saccharomyces cerevisiae,” *Yeast*, vol. 14, no. 10, pp. 953–961, Jul. 1998, doi: 10.1002/(SICI)1097-0061(199807)14:10<953::AID-YEA293>3.0.CO;2-U.

[125] T. W. Christianson, R. S. Sikorski, M. Dante, J. H. Shero, and P. Hieter, “Multifunctional yeast high-copy-number shuttle vectors,” *Gene*, vol. 110, no. 1, pp. 119–122, Jan. 1992, doi: 10.1016/0378-1119(92)90454-W.

[126] M. A. Collart and S. Oliviero, “Preparation of Yeast RNA,” *Curr Protoc Mol Biol*, vol. 23, no. 1, Jul. 1993, doi: 10.1002/0471142727.mb1312s23.

[127] E. P. Szymanski and O. Kerscher, “Budding yeast protein extraction and purification for the study of function, interactions, and post-translational modifications,” *Journal of Visualized Experiments*, no. 80, Oct. 2013, doi: 10.3791/50921.

[128] S. Gallagher, S. E. Winston, S. A. Fuller, and J. G. R. Hurrell, “Immunoblotting and immunodetection,” 2008. doi: 10.1002/0471142727.mb1008s83.

[129] E. Gerace and D. Moazed, “Coimmunoprecipitation of proteins from yeast,” in *Methods in Enzymology*, vol. 541, Academic Press Inc., 2014, pp. 13–26. doi: 10.1016/B978-0-12-420119-4.00002-1.

[130] M. Alhussain, “Investigating chromatin remodelling by the Swi-Snf and Tup1-Cyc8 complexes.”

[131] M. J. Rossi *et al.*, “A high-resolution protein architecture of the budding yeast genome,” *Nature*, vol. 592, no. 7853, pp. 309–314, Apr. 2021, doi: 10.1038/s41586-021-03314-8.

[132] W. Wang *et al.*, “Purification and biochemical heterogeneity of the mammalian SWI-SNF complex,” 1996.

[133] A. Dutta *et al.*, “Swi/Snf dynamics on stress-responsive genes is governed by competitive bromodomain interactions,” *Genes Dev*, vol. 28, no. 20, pp. 2314–2330, Oct. 2014, doi: 10.1101/gad.243584.114.

[134] S. Shivaswamy, A. Bhinge, Y. Zhao, S. Jones, M. Hirst, and V. R. Iyer, “Dynamic remodeling of individual nucleosomes across a eukaryotic genome in response to transcriptional perturbation,” *PLoS Biol*, vol. 6, no. 3, pp. 0618–0630, Mar. 2008, doi: 10.1371/journal.pbio.0060065.

[135] “sudarsanam and winston 2000”.

[136] Z. Zhang *et al.*, “Architecture of SWI/SNF chromatin remodeling complex,” Dec. 01, 2018, *Higher Education Press*. doi: 10.1007/s13238-018-0524-9.

[137] M. Stern, R. Jensen, and I. Herskowitz, “Five SWI genes are required for expression of the HO gene in yeast,” *J Mol Biol*, vol. 178, no. 4, pp. 853–868, Oct. 1984, doi: 10.1016/0022-2836(84)90315-2.

[138] E. V. Soares, “Flocculation in Saccharomyces cerevisiae: A review,” 2011. doi: 10.1111/j.1365-2672.2010.04897.x.

[139] I. Breitenbach-Schmitt, J. Heinisch, H. Schmitt, and F. Zimmermann, “Yeast mutants without phosphofructokinase activity can still perform glycolysis and alcoholic fermentation,” 1984.

[140] J. F. Flanagan and C. L. Peterson, “A role for the yeast SWI/SNF complex in DNA replication,” *Nucleic Acids Res*, vol. 27, no. 9, pp. 2022–2028, May 1999, doi: 10.1093/nar/27.9.2022.

[141] C. Lundin *et al.*, “Methyl methanesulfonate (MMS) produces heat-labile DNA damage but no detectable in vivo DNA double-strand breaks,” *Nucleic Acids Res*, vol. 33, no. 12, pp. 3799–3811, 2005, doi: 10.1093/nar/gki681.

[142] M. Rege, J. L. Feldman, N. L. Adkins, and C. L. Peterson, “SWI/SNF antagonizes SIR heterochromatin to promote transcription of genes expressed 1 during mitotic exit in Saccharomyces cerevisiae 2 3.”

[143] K. Kuranda, V. Leberre, S. Sokol, G. Palamarczyk, and J. Francois, “Investigating the caffeine effects in the yeast Saccharomyces cerevisiae brings new insights into the

connection between TOR, PKC and Ras/cAMP signalling pathways," *Mol Microbiol*, vol. 61, no. 5, pp. 1147–1166, Sep. 2006, doi: 10.1111/j.1365-2958.2006.05300.x.

[144] D. E. Levin, "Cell wall integrity signaling in Saccharomyces cerevisiae.," *Microbiol Mol Biol Rev*, vol. 69, no. 2, pp. 262–91, Jun. 2005, doi: 10.1128/MMBR.69.2.262-291.2005.

[145] Z. Du *et al.*, "Elucidating the regulatory mechanism of Swi1 prion in global transcription and stress responses," *Sci Rep*, vol. 10, no. 1, Dec. 2020, doi: 10.1038/s41598-020-77993-0.

[146] P. Sudarsanam and F. Winston, "The Swi/Snf family: Nucleosome-remodeling complexes and transcriptional control," 2000. doi: 10.1016/S0168-9525(00)02060-6.

[147] I. M. Gavin and R. T. Simpson, "Interplay of yeast global transcriptional regulators Ssn6p-Tup1p and Swi-Snf and their effect on chromatin structure," *EMBO Journal*, vol. 16, no. 20, 1997, doi: 10.1093/emboj/16.20.6263.

[148] J. A. Martens and F. Winston, "Evidence that Swi/Snf directly represses transcription in S. cerevisiae.," *Genes Dev*, vol. 16, no. 17, pp. 2231–6, Sep. 2002, doi: 10.1101/gad.1009902.

[149] J. A. Martens and F. Winston, "Evidence that Swi/Snf directly represses transcription in S. cerevisiae," *Genes Dev*, vol. 16, no. 17, pp. 2231–2236, Sep. 2002, doi: 10.1101/gad.1009902.

[150] Z. Wang, M. Gerstein, and M. Snyder, "RNA-Seq: A revolutionary tool for transcriptomics," Jan. 2009. doi: 10.1038/nrg2484.

[151] D. Winter, A. V Podtelejnikov, M. Mann, and R. Li, "The complex containing actin-related proteins Arp2 and Arp3 is required for the motility and integrity of yeast actin patches." [Online]. Available: http://biomednet.com/elecref/0960982200700519

[152] M. T. McCammon, C. B. Epstein, B. Przybyla-Zawislak, L. McAlister-Henn, and R. A. Butow, "Global transcription analysis of Krebs tricarboxylic acid cycle mutants reveals an alternating pattern of gene expression and effects on hypoxic and oxidative genes," *Mol Biol Cell*, vol. 14, no. 3, pp. 958–972, Mar. 2003, doi: 10.1091/mbc.E02-07-0422.

[153] L. Valente *et al.*, "ARTICLE Infantile Encephalopathy and Defective Mitochondrial DNA Translation in Patients with Mutations of Mitochondrial Elongation Factors EFG1 and EFTu," 2007. [Online]. Available: www.ajhg.org

[154] A. Cohen, N. Perzov, H. Nelson, and N. Nelson, "A novel family of yeast chaperons involved in the distribution of V- ATPase and other membrane proteins," *Journal of Biological Chemistry*, vol. 274, no. 38, pp. 26885–26893, Sep. 1999, doi: 10.1074/jbc.274.38.26885.

[155] E. Reifenberger, E. Boles, and M. Ciriacy, "Kinetic characterization of individual hexose transporters of Saccharomyces cerevisiae and their relation to the triggering

mechanisms of glucose repression," *Eur J Biochem*, vol. 245, no. 2, pp. 324–333, 1997, doi: 10.1111/j.1432-1033.1997.00324.x.

[156] K. Koch *et al.*, "Structure, biochemical and kinetic properties of recombinant Pst2p from Saccharomyces cerevisiae, a FMN-dependent NAD(P)H:quinone oxidoreductase," *Biochim Biophys Acta Proteins Proteom*, vol. 1865, no. 8, pp. 1046–1056, Aug. 2017, doi: 10.1016/j.bbapap.2017.05.005.

[157] L. Pintard, J. M. Bujnicki, B. Lapeyre, and C. Bonnerot, "MRM2 encodes a novel yeast mitochondrial 21s rRNA methyltransferase," *EMBO Journal*, vol. 21, no. 5, 2002, doi: 10.1093/emboj/21.5.1139.

[158] L. J. Martins, L. T. Jensen, J. R. Simons, G. L. Keller, and D. R. Winge, "Metalloregulation of FRE1 and FRE2 homologs in Saccharomyces cerevisiae," *Journal of Biological Chemistry*, vol. 273, no. 37, pp. 23716–23721, Sep. 1998, doi: 10.1074/jbc.273.37.23716.

[159] S. A. Garland, K. Hoff, L. E. Vickery, and V. C. Culotta, "Saccharomyces cerevisiae ISU1 and ISU2: Members of a Well-conserved Gene Family for Iron-Sulfur Cluster Assembly." [Online]. Available: http://www.idealibrary.com

[160] W. Li, A. P. Mitchell, and A. Mitchell, "Proteolytic Activation of Rimlp, a Positive Regulator of Yeast Sporulation and Invasive Growth," 1997.

[161] P. Lesage, X. Yang, and M. Carlson, "Yeast SNF1 Protein Kinase Interacts with SIP4, a C 6 Zinc Cluster Transcriptional Activator: a New Role for SNF1 in the Glucose Response," 1996.

[162] M. R. Felice *et al.*, "Post-transcriptional regulation of the yeast high affinity iron transport system," *Journal of Biological Chemistry*, vol. 280, no. 23, pp. 22181–22190, Jun. 2005, doi: 10.1074/jbc.M414663200.

[163] Y. Yang, Z. Zhang, Y. Li, X. G. Zhu, and Q. Liu, "Identifying cooperative transcription factors by combining ChIP-chip data and knockout data," Nov. 2010. doi: 10.1038/cr.2010.146.

[164] C. Deng and W. Saunders, "RIM4 encodes a meiotic activator required for early events of meiosis in Saccharomyces cerevisiae," *Molecular Genetics and Genomics*, vol. 266, no. 3, pp. 497–504, 2001, doi: 10.1007/s004380100571.

[165] V. Singh, G. K. Azad, S. K. Sariki, and R. S. Tomar, "Flocculation in Saccharomyces cerevisiae is regulated by RNA/DNA helicase Sen1p," *FEBS Lett*, vol. 589, no. 20, pp. 3165–3174, Oct. 2015, doi: 10.1016/j.febslet.2015.09.006.

[166] J. B. Konopkat, "AFR1 Acts in Conjunction with the oc-Factor Receptor To Promote Morphogenesis and Adaptation," 1993.

[167] I. Barta and R. Iggol, "Autoregulation of expression of the yeast Dbp2p 'DEAD-box' protein is mediated by sequences in the conserved DBP2 intron," 1995.

[168] P. G. Kopeckot and R. B. Wickner, “Cloning of the URAl Gene of Saccharomyces cerevisiae,” 1980.

[169] X. J. Chen and G. D. Clark-Walker, “α and β subunits of F1-ATPase are required for survival of petite mutants in Saccharomyces cerevisiae,” *Molecular and General Genetics*, vol. 262, no. 4–5, 1999, doi: 10.1007/s004380051156.

[170] B. Regenberg, L. Duè Ring-Olsen, M. C. Kielland-Brandt, and S. Holmberg, “Substrate speci®city and gene expression of the amino-acid permeases in Saccharomyces cerevisiae.” [Online]. Available: http://genome-www.stanford.edu/saccharomyces

[171] H.-D. Park, S. Scott, R. Rai, R. Dorrington, † And, and T. G. Cooper, “Synergistic Operation of the CAR2 (Ornithine Transaminase) Promoter Elements in Saccharomyces cerevisiae,” 1999.

[172] C. Wang, Z. Guo, X. Zhan, F. Yang, M. Wu, and X. Zhang, “Structure of the yeast Swi/Snf complex in a nucleosome free state,” *Nat Commun*, vol. 11, no. 1, Dec. 2020, doi: 10.1038/s41467-020-17229-x.

[173] S. Blümli *et al.*, “Acute depletion of the ARID1A subunit of SWI/SNF complexes reveals distinct pathways for activation and repression of transcription,” *Cell Rep*, vol. 37, no. 5, Nov. 2021, doi: 10.1016/j.celrep.2021.109943.

[174] M. C. Church, A. Price, H. Li, and J. L. Workman, “The Swi-Snf chromatin remodeling complex mediates gene repression through metabolic control,” *Nucleic Acids Res*, vol. 51, no. 19, pp. 10278–10291, Oct. 2023, doi: 10.1093/nar/gkad711.

[175] Z. Li *et al.*, “UbiNet 2.0: A verified, classified, annotated and updated database of E3 ubiquitin ligase-substrate interactions,” *Database*, vol. 2021, 2021, doi: 10.1093/database/baab010.

[176] V. N. Nguyen, K. Y. Huang, J. T. Y. Weng, K. R. Lai, and T. Y. Lee, “UbiNet: An online resource for exploring the functional associations and regulatory networks of protein ubiquitylation,” *Database*, vol. 2016, 2016, doi: 10.1093/database/baw054.

[177] Z. He, K. Chen, Y. Ye, and Z. Chen, “Structure of the SWI/SNF complex bound to the nucleosome and insights into the functional modularity,” Dec. 01, 2021, *Springer Nature*. doi: 10.1038/s41421-021-00262-5.

[178] W. Fu *et al.*, “Organization, genomic targeting, and assembly of three distinct SWI/SNF chromatin remodeling complexes in Arabidopsis,” *Plant Cell*, vol. 35, no. 7, pp. 2464–2483, Jul. 2023, doi: 10.1093/plcell/koad111.

[179] G. M. Euskirchen *et al.*, “Diverse roles and interactions of the SWI/SNF chromatin remodeling complex revealed using global approaches,” *PLoS Genet*, vol. 7, no. 3, Mar. 2011, doi: 10.1371/journal.pgen.1002008.

[180] Z. T. Beck, S. C. Cloutier, M. J. Schipma, C. J. Petell, W. K. Ma, and E. J. Tran, “Regulation of glucose-dependent gene expression by the RNA helicase Dbp2 in

Saccharomyces cerevisiae," *Genetics*, vol. 198, no. 3, pp. 1001–1014, Nov. 2014, doi: 10.1534/genetics.114.170019.

[181] G. M. Euskirchen *et al.*, "Diverse roles and interactions of the SWI/SNF chromatin remodeling complex revealed using global approaches," *PLoS Genet*, vol. 7, no. 3, Mar. 2011, doi: 10.1371/journal.pgen.1002008.

[182] K. Li, B. Wang, and H. Hu, "Research progress of SWI/SNF complex in breast cancer," Dec. 01, 2024, *BioMed Central Ltd*. doi: 10.1186/s13072-024-00531-z.

[183] H. S. Rhee and B. F. Pugh, "Comprehensive genome-wide protein-DNA interactions detected at single-nucleotide resolution," *Cell*, vol. 147, no. 6, pp. 1408–1419, Dec. 2011, doi: 10.1016/j.cell.2011.11.013.

[184] P. J. Park, "ChIP-seq: Advantages and challenges of a maturing technology," Oct. 2009. doi: 10.1038/nrg2641.

[185] H. S. Rhee and B. F. Pugh, "ChiP-exo method for identifying genomic location of DNA-binding proteins with near-single-nucleotide accuracy," *Curr Protoc Mol Biol*, no. SUPPL.100, 2012, doi: 10.1002/0471142727.mb2124s100.

[186] D. T. Auble, K. E. Hansen, C. G. F. Mueller, W. S. Lane, J. Thorner, and S. Hahn, "Mot l, a global repressor of RNA polymerase II transcription, inhibits TBP binding to DNA by an ATP-dependent mechamsm."

[187] C. L. Smith, R. Horowitz-Scherer, J. F. Flanagan, C. L. Woodcock, and C. L. Peterson, "Structural analysis of the yeast SWI/SNF chromatin remodeling complex," *Nat Struct Biol*, vol. 10, no. 2, pp. 141–145, Feb. 2003, doi: 10.1038/nsb888.

[188] A. Singh, S. B. Modak, M. M. Chaturvedi, and J. S. Purohit, "SWI/SNF Chromatin Remodelers: Structural, Functional and Mechanistic Implications," Jun. 01, 2023, *Springer*. doi: 10.1007/s12013-023-01140-5.

[189] A. V. Feoktistov, S. G. Georgieva, and N. V. Soshnikova, "Role of the SWI/SNF Chromatin Remodeling Complex in Regulation of Inflammation Gene Expression," Apr. 01, 2022, *Pleiades journals*. doi: 10.1134/S0026893322020054.

[190] G. M. Euskirchen *et al.*, "Diverse roles and interactions of the SWI/SNF chromatin remodeling complex revealed using global approaches," *PLoS Genet*, vol. 7, no. 3, Mar. 2011, doi: 10.1371/journal.pgen.1002008.

[191] A. Andrades *et al.*, "SWI/SNF complexes in hematological malignancies: biological implications and therapeutic opportunities," Dec. 01, 2023, *BioMed Central Ltd*. doi: 10.1186/s12943-023-01736-8.

[192] H. Fan *et al.*, "Transcription-Translation coupling: Direct interactions of RNA polymerase with ribosomes and ribosomal subunits," *Nucleic Acids Res*, vol. 45, no. 19, pp. 11043–11055, Nov. 2017, doi: 10.1093/nar/gkx719.

[193] X. Yang, R. Zaurin, M. Beato, and C. L. Peterson, “Swi3p controls SWI/SNF assembly and ATP-dependent H2A-H2B displacement,” *Nat Struct Mol Biol*, vol. 14, no. 6, pp. 540–547, Jun. 2007, doi: 10.1038/nsmb1238.

[194] A. Singh, S. B. Modak, M. M. Chaturvedi, and J. S. Purohit, “SWI/SNF Chromatin Remodelers: Structural, Functional and Mechanistic Implications,” Jun. 01, 2023, *Springer*. doi: 10.1007/s12013-023-01140-5.

[195] A. B. Sanz *et al.*, “Chromatin remodeling by the SWI/SNF complex is essential for transcription mediated by the yeast cell wall integrity MAPK pathway,” *Mol Biol Cell*, vol. 23, no. 14, pp. 2805–2817, Jul. 2012, doi: 10.1091/mbc.E12-04-0278.

[196] C. A. Keleher, M. J. Redd, J. Schultz, M. Carlson, and A. D. Johnson’, “SsnG-Tupl Is a General Repressor of Transbription in Yeast,” 1992.

[197] T. Coche, D. Prozzi, M. Legrain’, F. Hilgerl, and J. Vandenhaute, “Nucleotide sequence of the PHO81 gene involved in the regulation of the repressible acid phosphatase gene in Saccharomyces cerevisiae,” 2176.

[198] J. M. Tkach *et al.*, “Dissecting DNA damage response pathways by analysing protein localization and abundance changes during DNA replication stress,” *Nat Cell Biol*, vol. 14, no. 9, pp. 966–976, Sep. 2012, doi: 10.1038/ncb2549.

[199] D. A. L. And and L. F. Bisson, “The HXT1 Gene Product of Saccharomyces cerevisiae Is a New Member of the Family of Hexose Transporters,” 1991.

[200] C. W. Yun, M. Bauler, R. E. Moore, P. E. Klebba, and C. C. Philpott, “The Role of the FRE Family of Plasma Membrane Reductases in the Uptake of Siderophore-Iron in Saccharomyces cerevisiae,” *Journal of Biological Chemistry*, vol. 276, no. 13, pp. 10218–10223, Mar. 2001, doi: 10.1074/jbc.M010065200.

[201] T. Delaveau, E. Carvajal Julius Subik, C. Jacq, J. Subik, and E. Carvajal, “PDR3, a new yeast regulatory gene, is homologous to PDR1 and controls the multidrug resistance phenomenon,” 1994.

[202] C. Cappellaro2, C. Baldermann2, R. Rachel4, and W. Tanner2’, “Mating type-specific cell-cell recognition of Saccharomyces cerevisiae: cell wall attachment and active sites of a-and x-agglutinin1,” 1994.

[203] F. Gómez-Esquer *et al.*, “CRR1, a gene encoding a putative transglycosidase, is required for proper spore wall assembly in Saccharomyces cerevisiae,” *Microbiology (N Y)*, vol. 150, no. 10, pp. 3269–3280, Oct. 2004, doi: 10.1099/mic.0.27314-0.

[204] M. Riggi, B. Kusmider, and R. Loewith, “The flipside of the TOR coin - TORC2 and plasma membrane homeostasis at a glance,” *J Cell Sci*, vol. 133, no. 9, May 2020, doi: 10.1242/jcs.242040.

[205] M. J. Martinez *et al.*, “Genomic analysis of stationary-phase and exit in Saccharomyces cerevisiae: Gene expression and identification of novel essential genes,” *Mol Biol Cell*, vol. 15, no. 12, pp. 5295–5305, Dec. 2004, doi: 10.1091/mbc.E03-11-0856.

[206] K. Sato and A. Nakano, “Emp47p and its close homolog Emp46p have a tyrosine-containing endoplasmic reticulum exit signal and function in glycoprotein secretion in Saccharomyces cerevisiae,” *Mol Biol Cell*, vol. 13, no. 7, pp. 2518–2532, 2002, doi: 10.1091/mbc.E02-01-0027.

[207] O. Protchenko *et al.*, “Three Cell Wall Mannoproteins Facilitate the Uptake of Iron in Saccharomyces cerevisiae,” *Journal of Biological Chemistry*, vol. 276, no. 52, pp. 49244–49250, Dec. 2001, doi: 10.1074/jbc.M109220200.

[208] E. H. Muller *et al.*, “Thiamine repression and pyruvate decarboxylase autoregulation independently control the expression of the Saccharomyces cerevisiae PDC5 gene,” *FEBS Lett*, vol. 449, no. 2–3, pp. 245–250, Apr. 1999, doi: 10.1016/S0014-5793(99)00449-4.

[209] C. Panozzo *et al.*, “Aerobic and anaerobic NAD+ metabolism in Saccharomyces cerevisiae,” *FEBS Lett*, vol. 517, no. 1–3, pp. 97–102, Apr. 2002, doi: 10.1016/S0014-5793(02)02585-1.

[210] J. Olesen, S. Hahn, and L. Guarente, “Yeast HAP2 and HAP3 Activators Both Bind to the CYC7 Upstream Activation Site, UAS2, in an Interdependent Manner,” 1987.

[211] M. Carlson, J. L. Celenza, and F. J. Eng, “Evolution of the Dispersed SUC Gene Family of Saccharomyces by Rearrangements of Chromosome Telomeres,” 1985.

[212] O. Kobayashi, N. Hayashi, R. Kuroki, and H. Sone, “Region of Flo1 Proteins Responsible for Sugar Recognition,” 1998.

[213] S. E. Van Mulders *et al.*, “Phenotypic diversity of Flo protein family-mediated adhesion in Saccharomyces cerevisiae,” *FEMS Yeast Res*, vol. 9, no. 2, pp. 178–190, Mar. 2009, doi: 10.1111/j.1567-1364.2008.00462.x.

[214] H. Zhao and D. Eide, “The yeast ZRTJ gene encodes the zinc transporter protein of a high-affinity uptake system induced by zinc limitation,” 1996.

[215] D. R. Johnson, L. J. Knoll, D. E. Levin, and J. I. Gordon, “Saccharomyces cerevisiae Contains Four Fatty Acid Activation (FAA) Genes: An Assessment of Their Role in Regulating Protein N-Mydstoylation and Cellular Lipid Metabolism.”

[216] S. Sharma, J. Yang, S. Düttmann, P. Watzinger, P. Kötter, and K. D. Entian, “Identification of novel methyltransferases, Bmt5 and Bmt6, responsible for the m3U methylations of 25S rRNA in Saccharomyces cerevisiae,” *Nucleic Acids Res*, vol. 42, no. 5, pp. 3246–3260, Mar. 2014, doi: 10.1093/nar/gkt1281.

[217] A. Cohen, N. Perzov, H. Nelson, and N. Nelson, “A Novel Family of Yeast Chaperons Involved in the Distribution of V-ATPase and Other Membrane Proteins*,” 1999. [Online]. Available: http://www.jbc.org

[218] B. M. Geier *et al.*, “Kinetic Properties and Ligand Binding of the Eleven-subunit Cytochrome-c Oxidase from Saccharomyces cerevisiae Isolated with a Novel Large-Scale Purification Method,” *Eur J Biochem*, vol. 227, no. 1–2, pp. 296–302, 1995, doi: 10.1111/j.1432-1033.1995.tb20388.x.

[219] D. Thomas, gine Barbey, and Y. Surdin-Kerjang, “Gene-Enzyme Relationship in the Sulfate Assimilation Pathway of Saccharomyces cerevisiae STUDY OF THE 3’-PHOSPHOADENYLYLSULFATE REDUCTASE STRUCTURAL.”

[220] B. Lee, M. Church, K. Hokamp, M. M. Alhussain, A. A. Bamagoos, and A. B. Fleming, “Systematic analysis of tup1 and cyc8 mutants reveals distinct roles for TUP1 and CYC8 and offers new insight into the regulation of gene transcription by the yeast Tup1-Cyc8 complex,” *PLoS Genet*, vol. 19, no. 8 August, Aug. 2023, doi: 10.1371/journal.pgen.1010876.

[221] A. Shetty, N. I. Reim, and F. Winston, “Auxin-Inducible Degron System for Depletion of Proteins in Saccharomyces cerevisiae,” *Curr Protoc Mol Biol*, vol. 128, no. 1, p. e104, Sep. 2019, doi: 10.1002/cpmb.104.

[222] A. B. Fleming, S. Beggs, M. Church, Y. Tsukihashi, and S. Pennings, “The yeast Cyc8-Tup1 complex cooperates with Hda1p and Rpd3p histone deacetylases to robustly repress transcription of the subtelomeric FLO1 gene,” *Biochim Biophys Acta Gene Regul Mech*, vol. 1839, no. 11, pp. 1242–1255, 2014, doi: 10.1016/j.bbagrm.2014.07.022.

[223] M. C. Church and J. L. Workman, “The SWI/SNF chromatin remodeling complex: a critical regulator of metabolism,” *Biochem Soc Trans*, Apr. 2024, doi: 10.1042/BST20231141.

[224] P. Sudarsanam, V. R. Iyer, P. O. Brown, and F. Winston, “Whole-genome expression analysis of snfswi mutants of Saccharomyces cerevisiae.” [Online]. Available: www.pnas.org

[225] X. Fan, J. V. Geisberg, K. H. Wong, and Y. Jin, “Conditional depletion of nuclear proteins by the Anchor Away system,” *Curr Protoc Mol Biol*, no. SUPPL.93, Jan. 2011, doi: 10.1002/0471142727.mb1310bs93.

[226] A. V. Feoktistov, S. G. Georgieva, and N. V. Soshnikova, “Role of the SWI/SNF Chromatin Remodeling Complex in Regulation of Inflammation Gene Expression,” Apr. 01, 2022, *Pleiades journals*. doi: 10.1134/S0026893322020054.

[227] M. Guo *et al.*, “Comparative Expression Profiling of Snf2 Family Genes During Reproductive Development and Stress Responses in Rice,” *Front Plant Sci*, vol. 13, May 2022, doi: 10.3389/fpls.2022.910663.

[228] Z. He, K. Chen, Y. Ye, and Z. Chen, “Structure of the SWI/SNF complex bound to the nucleosome and insights into the functional modularity,” Dec. 01, 2021, *Springer Nature*. doi: 10.1038/s41421-021-00262-5.

[229] L. Neigeborn A N D and M. Carlson, “GENES AFFECTING T H E REGULATION O F SUCZ GENE EXPRESSION BY GLUCOSE REPRESSION IN SACCHAROMYCES CEREVISIAE,” 1984.

[230] A. Szczepanski *et al.*, “A SWI/SNF-dependent transcriptional regulation mediated by POU2AF2/C11orf53 at enhancer,” *Nat Commun*, vol. 15, no. 1, Dec. 2024, doi: 10.1038/s41467-024-46492-5.

[231] M. Ohtani, “Transcriptional regulation of snRNAs and its significance for plant development,” *J Plant Res*, vol. 130, no. 1, pp. 57–66, Jan. 2017, doi: 10.1007/s10265-016-0883-3.

[232] J. R. Raab, J. S. Runge, C. C. Spear, and T. Magnuson, “Co-regulation of transcription by BRG1 and BRM, two mutually exclusive SWI/SNF ATPase subunits,” *Epigenetics Chromatin*, vol. 10, no. 1, Dec. 2017, doi: 10.1186/s13072-017-0167-8.

[233] G. M. Euskirchen *et al.*, “Diverse roles and interactions of the SWI/SNF chromatin remodeling complex revealed using global approaches,” *PLoS Genet*, vol. 7, no. 3, Mar. 2011, doi: 10.1371/journal.pgen.1002008.

[234] J. R. Raab, S. Resnick, and T. Magnuson, “Genome-Wide Transcriptional Regulation Mediated by Biochemically Distinct SWI/SNF Complexes,” *PLoS Genet*, vol. 11, no. 12, 2015, doi: 10.1371/journal.pgen.1005748.

[235] A. Alfert, N. Moreno, and K. Kerl, “The BAF complex in development and disease,” Mar. 21, 2019, *BioMed Central Ltd.* doi: 10.1186/s13072-019-0264-y.

[236] S. Chahar *et al.*, “Transcription induces context-dependent remodeling of chromatin architecture during differentiation,” *PLoS Biol*, vol. 21, no. 12, Dec. 2023, doi: 10.1371/journal.pbio.3002424.

[237] S. Pundhir *et al.*, “The impact of SWI/SNF and NuRD inactivation on gene expression is tightly coupled with levels of RNA polymerase II occupancy at promoters,” *Genome Res*, vol. 33, no. 3, pp. 332–345, Mar. 2023, doi: 10.1101/gr.277089.122.

[238] M. Esposito, G. L. Sherr, A. Esposito, G. Kaluski, F. Ellington, and C. H. Shen, “Accumulation of unacetylatable Snf2p at the INO1 promoter is detrimental to remodeler recycling supply for CUP1 induction,” *PLoS One*, vol. 15, no. 3, 2020, doi: 10.1371/journal.pone.0230572.

[239] T. J. Sarnowski *et al.*, “SWI3 subunits of putative SWI/SNF chromatin-remodeling complexes play distinct roles during Arabidopsis development,” *Plant Cell*, vol. 17, no. 9, pp. 2454–2472, 2005, doi: 10.1105/tpc.105.031203.

[240] X. Yang, R. Zaurin, M. Beato, and C. L. Peterson, “Swi3p controls SWI/SNF assembly and ATP-dependent H2A-H2B displacement,” *Nat Struct Mol Biol*, vol. 14, no. 6, pp. 540–547, Jun. 2007, doi: 10.1038/nsmb1238.

[241] R. Bustos *et al.*, “A central regulatory system largely controls transcriptional activation and repression responses to phosphate starvation in arabidopsis,” *PLoS Genet*, vol. 6, no. 9, Sep. 2010, doi: 10.1371/journal.pgen.1001102.

[242] Y. Zhang *et al.*, “The SWI/SNF Chromatin Remodeling Complex Influences Transcription by RNA Polymerase I in Saccharomyces cerevisiae,” *PLoS One*, vol. 8, no. 2, Feb. 2013, doi: 10.1371/journal.pone.0056793.

[243] S. M. Sauty, K. Shaban, and K. Yankulov, “Gene repression in S. cerevisiae—looking beyond Sir-dependent gene silencing,” Feb. 01, 2021, *Springer Science and Business Media Deutschland GmbH*. doi: 10.1007/s00294-020-01114-7.

[244] L. Aravind and L. M. Iyer, “The SWIRM domain: a conserved module found in chromosomal proteins points to novel chromatin-modifying activities,” 2002. [Online]. Available: http://genomebiology.com/2002/3/8/research/0039.1